ISSN (1230-0322)

2022, Vol. 72, No. 3

Food

Polish Journal of Food and Nutrition Sciences

formerly Acta Alimentaria Polonica

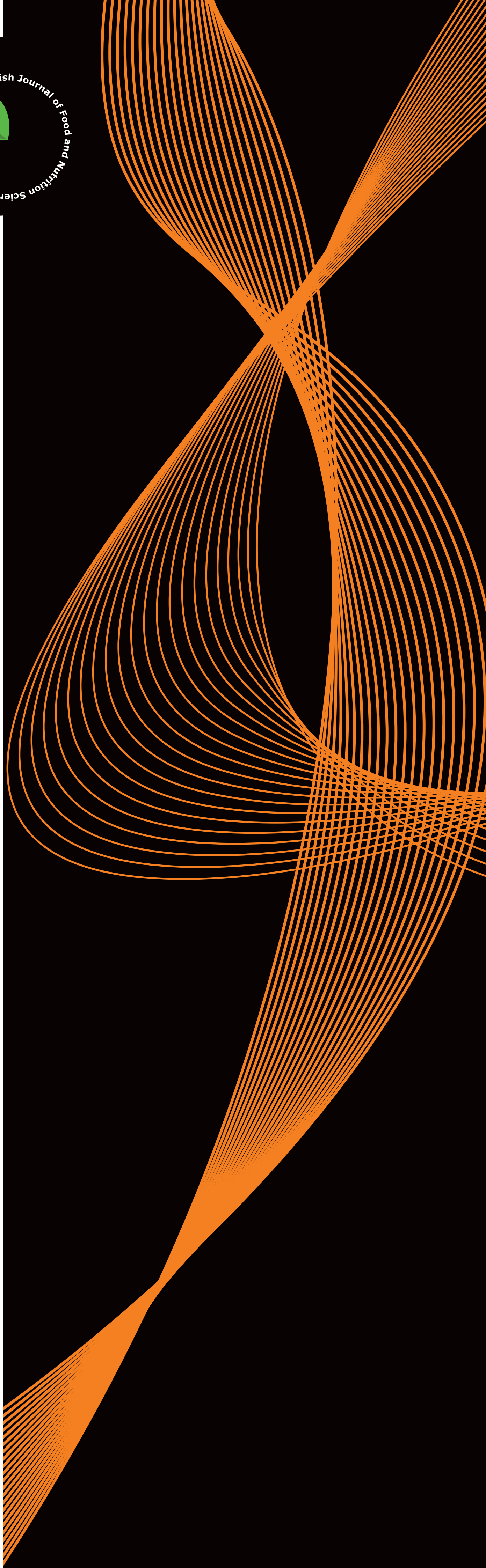

Published

by Institute of Animal
Reproduction and Food
Research of the Polish
Academy of Sciences,
Olsztyn

ISSN (1230–0322)
2022, Vol. 72, No. 3

Polish Journal of Food and Nutrition Sciences

formerly Acta Alimentaria Polonica

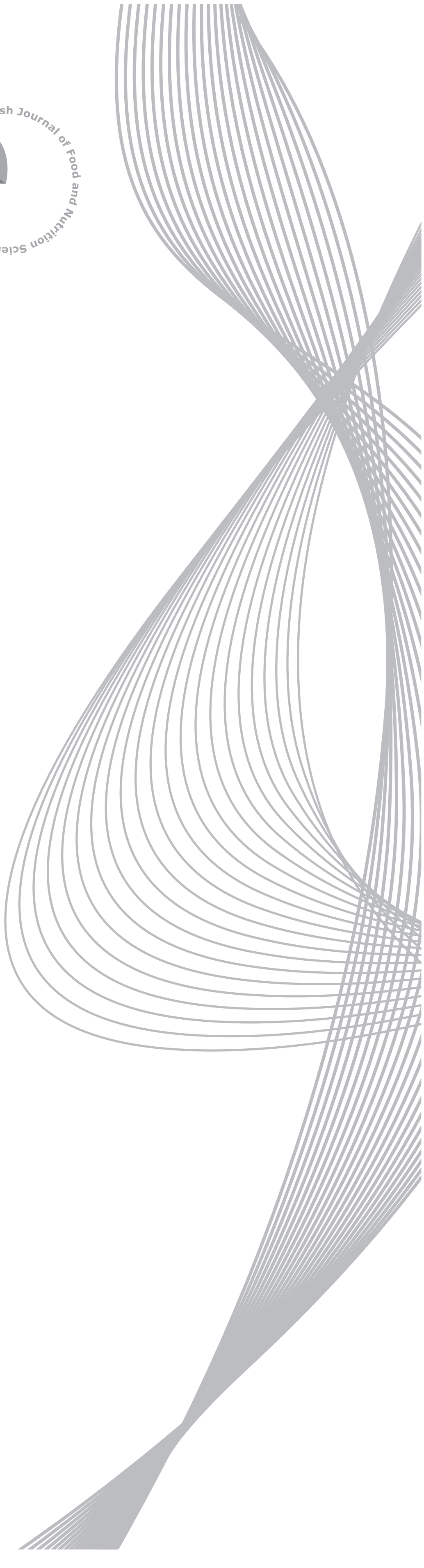

Published
by Institute of Animal
Reproduction and Food
Research of the Polish
Academy of Sciences,
Olsztyn

Pol. J. Food Nutr. Sci. 2022, Vol. 72, No. 3

Advisory Board of PJFNS 2019–2022

Marek Adamczak
University of Warmia and Mazury in Olsztyn, Poland
Huda Al-Kateb
Birmingham City University, Birmingham, UK
Wilfried Andlauer
University of Applied Sciences and Arts Western Switzerland
Valais, Sion, Switzerland
Anna Brzozowska
Warsaw University of Life Sciences, Poland
Zuzana Ciesarova
VUP Food Research Institute, Bratislava, Slovak Republic
Maria Dolores Del Castillo
CSIC-UAM, Madrid, Spain
Juana Frias
Institute of Food Science, Technology and Nutrition
(ICTAN), Madrid, Spain
Liwei Gu
University of Florida, Gainesville, USA
Henryk Jeleń
Poznań University of Life Sciences, Poland
Georgios Koutsidis
Northumbria University, Newcastle-upon-Tyne, UK
Andrzej Lenart
Warsaw University of Life Sciences, Poland
John Lodge
Northumbria University, Newcastle-upon-Tyne, UK
Adolfo J. Martinez-Rodriguez
CSIC-UAM, Madrid, Spain
Francisco J. Morales
CSIC, Madrid, Spain
Zhongli Pan
University of California, Davis, USA;
World Food Center, China
Ron B. Pegg
University of Georgia, Athens, USA
Mariusz K. Piskuła
Institute of Animal Reproduction and Food Research
of the Polish Academy of Sciences in Olsztyn, Poland
Da-Wen Sun
National University of Ireland, Dublin, Ireland
Lida Wądołowska
Warmia and Mazury University, Olsztyn, Poland
Zenon Zduńczyk
Institute of Animal Reproduction and Food Research
of the Polish Academy of Sciences in Olsztyn, Poland
Henryk Zieliński
Institute of Animal Reproduction and Food Research
of the Polish Academy of Sciences in Olsztyn, Poland

POLISH JOURNAL OF FOOD AND NUTRITION SCIENCES

covered by CURRENT CONTENTS/AGRICULTURE, BIOLOGY & ENVIRONMENTAL SCIENCES,
JOURNAL CITATION REPORTS AND SCIENCE CITATION INDEX EXPANDED, BIOSIS, SCOPUS,
IFIS Publishing and CAS abstracts, and AGRO-Librex, FROSTI, PSJC, AGRIS and Index Copernicus data bases

2022, VOL. 72, NO. 3

REVIEW PAPER

ORIGINAL PAPERS

Subscription

2022 – One volume, four issues per volume. Annual subscription rates are: Poland 150 PLN, all other countries 80 EUR. Prices are subject to exchange rate fluctuation. Subscription payments should be made by direct bank transfer to Bank Gospodarki Żywnościowej, Olsztyn, Poland, account No 17203000451110000000452110 SWIFT code: GOPZPLWOLA with corresponding banks preferably. Subscription and advertising offices at the Institute of Animal Reproduction and Food Research of Polish Academy of Sciences, ul. J. Tuwima 10, 10-747 Olsztyn, Poland, tel./fax (48 89) 5234670, fax (48 89) 5240124, e-mail: pjfns@pan.olsztyn.pl; http://journal.pan.olsztyn.pl

Zamówienia prenumeraty: Joanna Molga (e-mail: pjfns@pan.olsztyn.pl)

Wersja pierwotna (referencyjna) kwartalnika PJFNS: wersja papierowa (ISSN 1230–0322)
Nakład: 70 egz.; Ark. wyd. 16; Ark. druk. 16
Skład i druk: Mercurius, www.mercurius.com.pl

Pol. J. Food Nutr. Sci., 2022, Vol. 72, No. 3, pp. 211–228
On-line ISSN: 2083-6007
Print ISSN: 1230-0322
DOI: 10.31883/pjfns/152568
http://journal.pan.olsztyn.pl

Review article
Section: Food Quality and Functionality

Jamun Seed: A Review on Bioactive Constituents, Nutritional Value and Health Benefits

Yamini Tak[1], *Manpreet Kaur*[2], *Mool Chand Jain*[3], *Mahesh Kumar Samota*[4], *Nirmal Kumar Meena*[5], *Gurpreet Kaur*[6], *Rajendra Kumar*[7], *Daisy Sharma*[8], *José M. Lorenzo*[9, 10], *Ryszard Amarowicz*[11]

[1]Department of Biochemistry, Agriculture University, Kota, Rajasthan-324001, India
[2]Department of Biochemistry, Punjab Agricultural University, Ludhiana, Punjab-141004, India
[3]Department of Horticulture, College of Agriculture, Agriculture University, Kota, Rajasthan-324001, India
[4]HCP Division, ICAR-Central Institute of Post-Harvest Engineering & Technology, Abohar-152116, India
[5]Department of Fruit Science, College of Horticulture & Forestry, Jhalawar-326023, Rajasthan, India
[6]Department of Agriculture, Sant Baba Bhag Singh University, Jalandhar-144030, Punjab, India
[7]Department of Entomology, MBDDS Girls College, Siswali, Baran, Rajasthan-334001, India
[8]Department of Food Nutrition and Dietetics, Assam down town University, Panikhaity, Guwahati- 781137, Assam, India
[9]Centro Tecnológico de la Carne de Galicia, Parque Tecnológico de Galicia, 32900 San Cibrao das Viñas, Spain
[10]Área de Tecnología de los Alimentos, Facultad de Ciencias de Ourense, Universidad de Vigo, 32004 Ourense, Spain
[11]Institute of Animal Reproduction and Food Research, Polish Academy of Sciences,
Tuwima Street 10, 10–748 Olsztyn, Poland

Key words: jamun seeds, nutrients, bioactives, extraction and purification, nutraceuticals

Jamun fruit, a member of the Myrtaceae family, is commercially grown in tropical and subtropical areas of the world for its fruits with sweet, sour, and astringent luscious flesh. Seeds of jamun fruits are discarded as trash during the industrial processing of fruit pulp into beverages, jellies, jam, vinegar, wine, and squash. These seeds are a potential source of bioactive compounds including hydrolysable tannins, phenolic acids, flavonoids, other phenolics, terpenoids, phloroglucinol derivatives and saponins, which have been endorsed several biological activities, such as antidiabetic, anticancer, anti-inflammatory, antioxidant, antimicrobial, antihyperlipidemic and antihypercholesterolemic, as well as cardioprotective, hepatoprotective and neuroprotective properties. High contents of carbohydrates, dietary fiber, minerals, and ascorbic acid have also been found in jamun seeds. However, potential utilization of these seeds as innovative implements for health benefits has not yet been fully understood. We aim to compile scientific research and recent advances on jamun seed nutritional profile, bioactive compounds composition, bioactive properties, and their potential as an ingredient in functional food formulation.

INTRODUCTION

Jamun (*Syzygium cumini* or *Syzygium jambolana* or *Eugenia jambolana* or *Eugenia cumini*) is a polyembryonic species of the Myrtaceae family grown for its fruit, timber, and ornamental values. Jamun blossoms in both tropical and subtropical regions and is mostly grown in deep loam and well-drained soils. Jamun, also known as Indian blackberry, Malabar plum, Portuguese plum, Java plum, black plum, or jambolan, is a native to the Indian subcontinent and spread across Southeast Asia, Latin America, and Africa [de Sousa Sabino *et al.*, 2018]. India is ranked second, accounting for around 15.4% of total global production, or 13.5 million tonnes [https://www.agrifarming.in/jamun-farming]. Jamun fruits are small, usually oval-shaped with a pink purple to blue black colour when completely ripe, with a subtly sweet, astringent, and sour flavour, and a firm seed inside [Gajera *et al.*, 2018; de Sousa Sabino *et al.*, 2018; un Din *et al.*, 2020]. At fully ripen stage, jamun pulp contains sugars (glucose, fructose), free amino acids, minerals (Na, K, Ca, Mn, Mg), dietary fiber, ascorbic acid, β-carotene, organic acids [Gajera *et al.*, 2018; Seraglio *et al.*, 2018], phenolic compounds (anthocyanins, flavonols, ellagotannins and gallotannins) [Faria *et al.*, 2011; Lestario *et al.*, 2017], volatile compounds (*trans*-ocimene, *cis*-ocimene, β-myrcene, and α-terpineol), and flavouring compounds (dihydrocarvyl acetate, geranyl butyrate, and terpinyl valerate) [Vijayanand *et al.*, 2001].

Because jamun fruits are highly perishable in nature, most of them are processed. Jam, jelly, vinegar, wine, squash, and non-fermented ready-to-drink beverages are some

---

* Corresponding Author:
E-mail: r.amarowicz@pan.olsztyn.pl (Prof. R. Amarowicz)

Submitted: 17 March 2022
Accepted: 2 August 2022

of the traditional jamun fruit products [de Sousa Sabino *et al*., 2018]. Moreover, the fruit pulp can be dried and used as a food colorant and as a nutritious and health-promoting additive for pasta, ice cream, *etc.* [Lestario *et al*., 2017; Panghal *et al.*, 2019; Shelke *et al.*, 2020; Singh *et al.*, 2019]. However, since only the pulp is used in the processing of the jamun fruit, the rest generate the waste. Seeds are the main post-processing waste product. Their amount is large, because they constitute 10–47% of the total weight of the fruit [Benherlal & Arumughan, 2007; Gajera *et al*., 2018; un Din *et al*., 2020]. The generated waste causes problem for the industry and for the environment, but on the other hand, it has become a challenge for scientists. Jamun fruit waste has the potential to become a valuable by-product and open up avenues for the scientific and research community to assist industry and farmers in generating revenue. Jamun seeds have been utilized to treat diabetes and digestive problems in Ayurveda since ancient times. Currently, the health-promoting properties of jamun seeds are being confirmed and many bioactive compounds responsible for it, including phenolics, terpenoids, phloroglucinol derivatives and saponins, were identified [Liu *et al.*, 2017a,b, 2018; Martin *et al.*, 1998; Omar *et al*., 2012; Thiyagarajan *et al*., 2016]. Intensive research on biological potential is ongoing and the seed extracts, extract fractions and isolated compounds are being tested for antidiabetic, antioxidant, anti-inflammatory, anticancer, antimicrobial, cardioprotective, hepatoprotective, and neuroprotective properties. Moreover, the jamun seeds have been found to contain nutrients. They are rich in carbohydrates, dietary fiber, ascorbic acid, and some minerals [Benherlal & Arumughan, 2007; Ghosh *et al.*, 2017; Kaur *et al.*, 2011]. The nutritional and phytochemical profiles of jamun seeds revealed that they could be a novel source for pharmaceutical and food industries. This review mainly discusses the nutrients and phytochemicals of jamun seeds and recent research into their bioactive potential in the context of the possibility of using this jamun fruit processing by-product in the functional food formulation.

NUTRITIONAL PROFILE OF JAMUN SEEDS

Proximate analysis indicated that moisture content of jamun fruit seeds ranged from 12.45 to 52.4 g/100 g and yielded crude protein, total lipids, total carbohydrates, and ash contents as 4.7–8.2 g/100 g, 0.35–1.28 g/100 g, 70.9–91.0 g/100 g, and 2.0–22.3 g/100 g on a dry matter (dm) basis, respectively [Benherlal & Arumughan, 2007; Ghosh *et al.*, 2017; Indrayan *et al*., 2005].

Carbohydrates

Carbohydrates are the main nutrient of the jamun seeds [Benherlal & Arumughan, 2007; Ghosh *et al.*, 2017; Indrayan *et al*., 2005]. Among digestible carbohydrates, which provide the energy needed to support various metabolic processes in the human body, starch dominates with the content ranging from 23 g/100 g to 60 g/100 g dm of seed [Benherlal & Arumughan, 2007; Gajera *et al.*, 2018]. The content of total soluble sugars is negligible – 0.1–1.4 g/100 g [Gajera *et al.*, 2018; Ghosh *et al.*, 2017]. Moreover, jamun seeds were recognized as the rich source of dietary fiber [Kaur *et al*., 2011], which together with lignin constituted non-digestible carbohydrates and represented nutritionally important, health-promoting food ingredient. The content of total dietary fiber of jamun seeds was evaluated at 27.7 g/100 g and the fraction of insoluble dietary fiber was significantly greater than that of the soluble dietary fiber (24.9 g/100 g and 2.8 g/100 g, respectively) [Kaur *et al*., 2011]. In turn, Pandey & Khan [2002] found water-soluble gums as the main fraction of non-digestible carbohydrates of jamun seeds with the content of 40 g/100 g of fresh matter, fm (moisture content of 5.9 g/100 g). The second non-digestible seed carbohydrate fraction was water-insoluble neutral detergent fiber (15 g/100 g fm) containing cellulose (6.9 g/100 g fm), hemicellulose (5.9 g/100 g fm), lignin (1.0 g/100 g fm), cutin (0.76 g/100 g fm), and silica (0.44 g/100 g fm). The profile of dietary fiber may determine its health benefits. As recently discussed in a review article by Cronin *et al*. [2021], the different type of dietary fiber can modulate the gut microbiota composition in various ways and thus alter the short chain fatty acid production and glucose and lipid metabolism which, if it is abnormal, is associated with a risk of chronic diseases.

Recently, many polysaccharides with biological activity, including antioxidant activity, and α-amylase and α-glucosidase inhibitory properties, have been isolated from various parts of plants [Deng *et al*., 2020; Oh & Yoon, 2018; Tan *et al.,* 2021]. Concerning the jamun seeds, Al-Dhabi & Ponmurugan [2020] isolated the water-soluble polysaccharide fraction free of reducing sugar, uronic acid, and starch. However, the biological activity of these polysaccharides has not been analysed.

Proteins

Proteins constitute up to 8% of jamun seed dm [Benherlal & Arumughan, 2007; Indrayan *et al*., 2005], although some literature reports indicate a much higher protein content – 19.96 g/100 g fm [Santos *et al*., 2020]. In addition to crude protein, free amino acids were reported in *S. cumini* seeds with the content of 4.84–9.90 mg/100 g [Gajera *et al*., 2018], but their profile has not been analysed. Recently, Binita *et al*. [2014] attempted to determine the protein profile of jamun seeds using two-dimensional gel electrophoresis (2D-PAGE) and matrix-assisted laser desorption/ionization time-of-flight mass spectrometry (MALDI-TOF/MS) and identified 15 functional proteins including lactoferrin, chitinase1, sulphate transporter like protein, pectate lyases, β-tubulin, ABC transporter, phosphate binding protein, 1-aminocyclopropane-1-carboxylate oxidase, G protein coupled receptor, ADP-glucose pyrophosphorylase, and glutamate–ammonia ligase adenylyltransferase, which are important in plant defense mechanisms, metabolism, and transport of inorganic salts. Nevertheless, the jamun seed proteins are still very poorly understood and, to the best of our knowledge, there is a lack of data on their nutritional value, amino acid composition, digestibility, and possible use as food. More research is needed in this area.

Lipids

The total lipid content of jamun seed is low (below 1.5 g/100 g) [Benherlal & Arumughan, 2007; Ghosh *et al.*, 2017], nevertheless fatty acid composition of lipids is healthy balanced. The saturated fatty acids (SFA) account for 50% and unsaturated fatty acids (UFA) including monounsaturated fatty acids and polyunsaturated fatty acids for 14% and 36% of total fatty acids, respectively [Bhaskar *et al*., 2021]. Among SFA, lauric acid (12:0; 2.8%), myristic acid (16:0; 31.7%), palmitic acid (16:0; 4.7%), and stearic acid (18:0; 6.5%) were determined. Oleic acid (18:1 *n*-9; 32.2%), linoleic (18:2 *n*-6; 16.1%), and epoxy and cyclopropenoid fatty acids, such as malvalic (1.2%), sterculic (1.8%), and vernolic (1.3%) acids, were also found in the fatty acid profile of jamun seed oil [Daulatabad *et al*., 1988]. In turn, Bhaskar *et al*. [2021] identified a few methyl esters of SFA (myristic acid, pentadecanoic acid, and heptadecanoic acid) and methyl esters of UFA (7,10,13-hexadecatrienoic acid, 8,11-octadecadienoic acid, 7,10-hexadecadienoic acid and 6,9,12,15-docosatetraenoic acid), together with fatty acid relevant compounds (3,7,11,15-tetramethyl-2-hexadecen-1-ol, docosyl acetate, 1-eicosene and 1,4-eicosadiene) in jamun seed oil using the GC–MS analysis. A low content of lipids and a high content of dietary fiber make the nutritional value of jamun seed low, raching only 267 kcal/100 g [Indrayan *et al*., 2005], which can be considered nutritionally beneficial in the context of the current global problem of overweight and obesity in humans.

Micronutrients

Jamun seed contains ascorbic acid and a high amount of minerals, making it an attractive product for nutritionists [Ghosh *et al*., 2017; Indrayan *et al*., 2005].

Concerning the mineral composition of jamun seeds, Ravi *et al*. [2004a] found 9 dietary macro- and microelements. The dominant ones were manganese, potassium, iron, and chromium. Calcium and copper were determined in trace amounts, and sodium, zinc, and magnesium were detected with moderate levels. A similar qualitative profile was reported by Ghosh *et al*. [2017], although the ratios between the elements were different and the decreasing content was found for the following minerals: potassium (606 mg/100 g), calcium (136 mg/100 g), magnesium (112 mg/100 g), sodium (43.9 mg/100 g), iron (4.20 mg/100 g), copper (2.13 mg/100 g), chromium (1.40 mg/100 g), zinc (0.46 mg/100 g), and manganese (0.40 mg/100 g). The differences in the mineral composition may be due to different environmental conditions during plant growth and their soil-climate adaptation, varietal differences as well as harvest time [Granado-Rodríguez *et al*., 2021; Moussa *et al*., 2020]. Seraglio *et al*. [2018] found that the ripening process directly affected the contents of minerals of *S. cumini* fruit pulp and ripe fruits had significantly higher contents of potassium and calcium compared to these in intermediate ripe stage. It can be assumed that a similar phenomenon also applies to seeds, but this issue needs more extensive research.

Among vitamins and pro-vitamins, only ascorbic acid was determined in jamun seeds [Gajera *et al*., 2018; Ghosh *et al*., 2017]. Its content ranged from 90 mg/100 g to 137 mg/100 g for different genotypes and was higher compared to that in fruit pulp of each genotype [Gajera *et al*., 2018]. A slightly lower content of ascorbic acid of jamun seeds was reported by Ghosh *et al*. [2017], which was 49.8 mg/100 g.

Although β-carotene along with other carotenoids has been determined in jamun fruit pulp [Faria *et al*., 2011], its presence (and other fat-soluble vitamins) has not been confirmed in seeds. Gupta & Agrawal [1970] identified only β-sitosterol in the unsaponifiable fraction of the jamun seed oil.

PHYTOCHEMICALS OF JAMUN SEEDS

Jamun seeds contain a variety of phytochemicals belonging to phenolic compounds, terpenes and terpenoids, sterols and saponins. The profile of these bioactive compounds of *S. cumini* seeds is summarised in Table 1.

Phenolic compounds

Phenolic compounds are the most frequently recognised in jamum seeds and they are the most widely represented group of bioactive compounds (Table 1). The total phenolic content (TPC) has been determined as 55.54 mg gallic acid equivalents (GAE)/g dm of jamun seeds and 22.59 mg GAE/g fresh seeds at a moisture content of 62.25 g/100 g [Balyan & Sarkar, 2017; Shrikanta *et al*., 2015]. Lower TPC (26.9 mg GAE/g dried powdered seeds) was found by Aqil *et al*. [2012]. In turn, Mahindrakar & Rathod [2020a, 2020b] and Bajpai *et al*. [2005] reported higher values ranging from 79.89 to 108.7 mg GAE/ g dry seeds. Regarding jamun seed extracts, TPC of an aqueous extract of dried seed powder obtained under optimal extraction conditions (49.2°C, 89.4 min, and liquid-to-solid ratio 51.6:1, mL/g) with a yield 17.3% was 415 mg/g dried extract [Balyan & Sarkar, 2017]. This value was consistent with TPCs recorded for methanolic fractions obtained from seeds of various *S. cumini* genotypes (361.16–496.26 mg/g extract), which were, in turn, 6.0–9.8 times higher than those determined for fruit pulps from the same genotypes [Gajera *et al*., 2017].

Phenolic acids, flavonoids (flavones, flavan-3-ols, flavonols, flavanonols and dihydrochalcones), stilbenoids, coumarins, lignans, hydrolysable tannins, and phloroglucinol derivatives are present in the profile of the phenolic compounds of jamun seeds (Table 1). Among them, two phenolic acids (gallic and ellagic acids), their simple derivatives and their polymeric forms (gallotannins and ellagitannins, respectively) are most often qualified and quantified [Bajpai *et al*., 2005; Balyan & Sarkar, 2017; Bhatia & Bajaj, 1975; Liu *et al*., 2018; Omar *et al*., 2012; Sawant *et al*., 2015]. It was found that tannic acid (gallotannin), gallic acid, and ellagic acid constituted 45.4%, 21.9% and 8.65% of the phenolic compounds of *S. cumini* seed aqueous extract, respectively [Balyan & Sarka, 2017]. The content of gallic acid was determined over a wide range from 0.65 to 6.24 mg/g dm of seeds and 90.8 mg/g extract, and the content of ellagic acid was reported as 0.038 mg/g dm and 36 mg/g extract [Bajpai *et al*., 2005; Balyan & Sarka, 2017; Shrikanta *et al*., 2015]. The use of liquid chromatography with tandem mass spectrometry (LC-MS/MS) and nuclear magnetic resonance (NMR) spectroscopy techniques has allowed to identify 9 gallotannins and 17 ellagitannins and other ellagic acid derivatives of jamun seeds [Bhatia & Bajaj, 1975; Elhawary *et al*., 2022; Liu *et al*., 2018; Omar *et al*., 2012; Sawant *et al*., 2015]. It is well known that hydrolysable tannins have a strong antioxidant

TABLE 1. Bioactive compounds identified in jamun seeds.

Class of compounds	Compound	Reference
Phenolic acids	Protocatechuic acid	Elhawary *et al*. [2022]
	p-Coumaric acid	Shrikanta *et al*. [2015]; Balyan & Sarkar [2017]
	Caffeic acid	Balyan & Sarkar [2017]; Gajera *et al*. [2017]; Abdin *et al*. [2019]; Elhawary *et al*. [2022]
	Ferulic acid	Gajera *et al*. [2017]; Abdin *et al*. [2019]
	Chlorogenic acid	
	Gallic acid	Bhatia & Bajaj [1975]; Bajpai *et al*. [2005]; Omar *et al*. [2012]; Sawant *et al.* [2015]; Shrikanta *et al*. [2015]; Balyan & Sarkar [2017]; Gajera *et al*. [2017]; Liu *et al.* [2018]; Abdin *et al*. [2019]; Elhawary *et al*. [2022]
	Syringic acid	Liu *et al.* [2018]
	5-Hydroxyveratric acid	
	Ellagic acid	Bhatia & Bajaj [1975]; Bajpai *et al*. [2005]; Aqil *et al.* [2012]; Omar *et al*. [2012]; Sawant *et al.* [2015]; Balyan &Sarkar [2017]; Gajera *et al.* [2017]; Liu *et al.* [2018]; Elhawary *et al*. [2022]
Stilbenoids	Resveratrol	Shrikanta *et al.* [2015]
Flavonols	Quercetin	Bhatia & Bajaj [1975]; Bajpai *et al*. [2005]; Sharma *et al.* [2008b]; Jadeja *et al*. [2012]; Balyan & Sarkar, [2017]; Elhawary *et al*. [2022]
	Rutin	Sharma *et al.* [2008b]; Jadeja *et al*. [2012]
	Myricetin	Liu *et al.* [2018]
	Myricetin 3-*O*-glucoside	Elhawary *et al.* [2022]
	Myricitrin	
	Syringetin	
	Syringetin 3-*O*-glucoside	
	Laricitrin	
	Quercitrin	
	Kaempferol	Bajpai *et al*. [2005]; Jadeja *et al*. [2012]; Abdin *et al*. [2019]; Elhawary *et al*. [2022]
Flavanonols	Dihydromyricetin	Elhawary *et al*. [2022]
Flavan-3-ols	(+)-Catechin	Balyan & Sarkar, [2017]; Gajera *et al*. [2017]; Abdin *et al*. [2019]
	(–)-Epicatechin	Shrikanta *et al*. [2015]; Balyan & Sarkar [2017]; Abdin *et al*. [2019]
	(–)-Epigallocatechin	Elhawary *et al*. [2022]
Flavones	Swertisin	Omar *et al*. [2012]
	Schaftoside	Liu *et al.* [2018]
	Apigenin 6,8-di-*C*-β-D-glucopyranoside	
Gallotannins	Tannic acid	Balyan & Sarkar [2017]
	1-Galloyl glucose	Bhatia & Bajaj [1975]
	6-Galloyl glucose	
	1,6-Digalloyl glucose	Elhawary *et al*. [2022]
	1,2,6-Trigalloyl glucose	
	1,2,3,6-Tetragalloyl glucose	
	1,2,3,4,6-Pentagalloyl glucose	
	Valoneic acid dilactone	Omar *et al*. [2012]; Sawant *et al.* [2015]; Liu *et al.* [2018]
	Jamutannin A and B	Omar *et al*. [2012]
Ellagitannins and ellagic acid derivatives	Corilagin	Bhatia & Bajaj [1975]; Elhawary *et al*. [2022]
	Eugeniin	Elhawary *et al*. [2022]
	3,6-Hexahydroxydiphenoyl glucose	Bhatia & Bajaj [1975]
	4,6-Hexahydroxydiphenoyl glucose	
	Iso-oenothein C	Omar *et al*. [2012]; Liu *et al*. [2018]
	Cornusiin B	Omar *et al*. [2012]
	Phyllanthusiin E	
	Rubuphenol	Sawant *et al.* [2015]; Liu *et al.* [2018]
	Eschweilenol A and C	Liu *et al.* [2018]
	Tergallic acid dilactone	
	Ellagic acid 4-*O*-xylopyranoside	
	3’-*O*-Methyl ellagic acid 4-*O*-xylopyranoside	
	3-*O*-Methyl ellagic acid-4’-*O*-α-L-rhamnopyranoside	
	Ellagic acid-4-*O*-β-D-glucopyranoside	
	Decarboxy ellagic acid	
	3,3’,4’-Tri-*O*-methyl ellagic acid	Bhatia & Bajaj [1975]; Liu *et al.* [2018]
	3,3’-Di-*O*-methyl ellagic acid	Bhatia & Bajaj [1975]

TABLE 1 – continued

Class of compounds	Compound	Reference
Coumarins	Brevifolin carboxylic acid	Omar *et al.* [2012]
Dihydrochalcones	Phloridzin	Liu *et al.* [2018]
Lignans	Medioresinol 4”-*O*-β- -glucoside (+)-Pinoresinol *O*-β-glucoside (+)-Syringaresinol *O*-β-glucoside Dihydrodehydrodiconiferyl alcohol 4”-*O*-β-glucoside	Martin *et al.* [1998]
Phloroglucinol derivatives	Jamunones A–O Spiralisone C	Liu *et al.* [2017b]
Monoterpenes	α-Pinene β-Pinene Limonene	Scharf *et al.* [2016]
Monoterpenoids	γ-Terpineol	Scharf *et al.* [2016]; Elhawary *et al.* [2022]
Sesquiterpenes	α-Copaene *E*-Caryophyllene α-Humulene δ-Cadinene α-Selinene Germacrene D	Scharf *et al.* [2016]
Sesquiterpenoids	Jambolanins A−K Sootepdienone Gibberodione Orientalol E Guaianediol Junipediol Cryptomeridiol Litseachromolaevanes A (4*R*)-4-Hydroxy-1,10-seco-muurol-5-ene-1,10-dione (8*R*,9*R*)-Isocaryolane- -8,9-diol Caryolandiol Clovane-2β,9α-diol	Liu *et al.* [2017a]
	Caryophyllenyl alcohol Caryophyllene oxide Caryophylla-4(12), 8(13)-dien-5-ol	Scharf *et al.* [2016]
Norsesquiterpenoids	Jambolanes A and B	Liu *et al.* [2017a]
Triterpenoids	Actinidic acid Oleanolic acid Ursolic acid Corosolic acid Arjunolic acid Asiatic acid	Liu *et al.* [2017a]
	Maslinic acid	Sawant *et al.* [2015]
	Betulinic acid	Elhawary *et al.* [2022]
Saponins	Vitalboside A	Thiyagarajan *et al.* [2016]
Sterols	β-Sitosterol	Gupta & Agrawal [1970]

and antibacterial activities [Karamać, 2009; Puljula *et al*., 2020]. They can also affect the functioning of the digestive tract [Żary-Sikorska *et al*., 2021]. In the case of jamun seeds, it was found that the ellagitannin-rich fraction of these seeds inhibited canonical Wnt signaling pathway in a human 293T cell line, suggesting its potential against colon carcinogenesis [Sharma *et al*., 2010]. Moreover, the *in vitro* antioxidant activity of the jamun seed fraction containing ellagitannins and ellagic acid was reported and it was higher than that of the pulp with anthocyanins as the main component [Aqil *et al*., 2012].

Among phenolic acids, apart from ellagic and gallic acids, also *p*-cumaric, caffeic, ferulic and chlorogenic acids were quantified in seeds of the same *S. cumini* genotypes and their contents were 14.06, 1.02–4.73, 1.50–8.21 and 0.89–6.80 μg/g seed, respectively [Gajera *et al*., 2017; Shrikanta *et al*., 2015]. The presence of protocatechuic acid, syringic acid, and 5-hydroxyveratric acid was confirmed in the studies by Liu *et al*. [2018] and Elhawary *et al*. [2022].

Flavonoids are another class of phenolic compounds that are commonly distributed in plants. In jamun seeds, myricetin and its derivatives have been most widely represented including myricetin glycosides (myricetin 3-*O*-glucoside), *O*-methylated forms (syringetin, syringetin 3-*O*-glucoside, laricitrin), and dihydroxy derivatives (dihydromyricetin) [Elhawary *et al*., 2022; Liu *et al*., 2018]. In turn, (–)-epicatechin (129.20 μg/g dm), quercetin (98 μg/g dm), kaempferol (59 μg/g dm) and (+)-catechin (5.36–16.80 μg/g seed) were reported as the most abundant among flavonoids [Bajpai *et al*., 2005; Gajera *et al*., 2017; Shrikanta *et al*., 2015]. According to Sharma *et al*. [2008a,b] and Jadeja *et al*. [2012], rutin, quercetin and kaempferol present in standardized flavonoid-rich extracts of jamun seeds were responsible for their diverse bioactivity. The hypoglycemic and hypolipidemic effects and anti-atherogenic potential of such extracts were found. Flavone *C*-glycosides (swertisin, schaftoside and apigenin 6,8-di-*C*-β-D-glucopyranoside), that are limited in natural sources, have also been identified in jamun seeds [Liu *et al*., 2018; Omar *et al*., 2012]. Interestingly, jamun seeds do not contain the anthocyanins that are present in the pulp of the fruits [Aqil *et al*., 2012; Benherlal & Arumughan, 2007]. Lestario *et al*. [2017] reported that the content of pulp anthocyanins increased, but contents of flavonols, gallotannins, and ellagitannins decreased by 60%, 35%, and 11%, respectively, throughout fruit maturation. However, it has not been studied so far whether the seed phenolic profile changed during fruit ripening.

Other phenolic compounds detected in jamun seeds include stilbenoids (resveratrol), coumarins (brevifolin carboxylic acid), lignans (medioresinol 4”-*O*-β-glucoside, (+)-pinoresinol *O*-β-glucoside, (+)-syringaresinol *O*-β-glucoside, and dihydrodehydrodiconiferyl alcohol 4”-*O*-β-glucoside) and phloroglucinol derivatives (jamunones A–O and spiralisone C) [Liu *et al*., 2017b; Martin *et al*., 1998; Omar *et al*., 2012; Shrikanta *et al*., 2015]. Among them, only resveratrol was quantified at the level of 34.87 μg/g dm [Shrikanta *et al*., 2015]. In the mentioned publication, the authors suggested that resveratrol contributed significantly to the antioxidant capacity of jamun seeds. In turn, phloroglucinol derivatives of jamun seeds inhibited protein tyrosine phosphatase 1B activity [Liu *et al*., 2017a] and can therefore be considered as anti-diabetes and anti-obesity agents. The bioactivity of jamun seed coumarins and lignans has not been determined so far.

Terpenes and terpenoids

Forty-five terpenes and terpenoids classified as monoterpenes, monoterpenoids, sesquiterpenes, sesquiterpenoids, norsesquiterpenoids and triterpenoids have been identified in jamun seeds [Elhawary *et al*., 2022; Liu *et al*., 2017a; Sawant *et al*., 2015; Scharf *et al*., 2016]. The names of these compounds are listed in Table 1.

Scharf *et al*. [2016] reported that two sesquiterpene hydrocarbons (*E*-caryophyllene and α-humulene) were the major compounds of essential oil of fresh jamun seeds and their contents were 42.5% and 22.2% of the total essential oil, respectively. However, both the total essential oil content of the seeds and the essential oil profile changed during seed storage. The hydrodistillation yield decreased from 0.11% (*w/w*) for fresh seeds to 0.06% (*w/w*) for seeds after two-month storage. A successive decrease in the percentage of sesquiterpene hydrocarbons (from 74.1 to 21.0% after four months storage) and monoterpenes (from 7.8 to 1.3%), and an increase in the contribution of oxidized sesquiterpenes (from 12.3 to 70.5%) were noted in the profile of compounds. The major compounds of fresh seeds were partially oxidized to mainly caryophyllene oxide and humulene epoxide during storage.

Some of the jamun seed sesqutierepenoids were found to be biologically active [Liu *et al*., 2017b]. Among twelve isolated sesqutierepenoids, a mixture of jambolanins D and E as well as sootepdienone, guaianediol, cryptomeridiol, (4*R*)-4-hydroxy-1,10-seco-muurol-5-ene-1,10-dione, caryolandiol, and clovane-2β,9α-diol exhibited antimicrobial activity against *Staphylococcus aureus*. On the other hand, these compounds did not inhibit the proliferation of *Escherichia coli* and *Candida albicans* at the concentration 100 μg/disk. In turn, Sawant *et al*. [2015] did not detect the aldose reductase (AR) inhibitory activity and protein tyrosine phosphatase 1B (PTP1B) inhibitory activity of maslinic acid isolated from jamun seeds when tested at concentration up to 100 μg/mL.

Other phytochemicals

Vitalboside A, a pentacyclic triterpene glycoside (saponin), was identified by NMR techniques and isolated using chromatographic methods from jamun seeds [Thiyagarajan *et al*., 2016]. The content of vitalboside A in the methanolic extract of jamun seeds was 0.8% (*w/w*). The antidiabetic and anti-adipogenic activities of the isolated compound were shown.

Another bioactive phytochemical detected in *S. cumini* seeds is β-sitosterol. It was identified in the unsaponifiable fraction of the jamun seed oil [Gupta & Agrawal, 1970]. Presence of sterol with an unidentified structure in the Sephadex LH-20 fraction of the ethanolic jamun seed extract was reported by Sharma *et al*. [2011a,b]. This fraction exhibited hypolipidemic and antidiabetic activity in alloxan-induced mildly diabetic and severely diabetic rabbits.

EXTRACTION, PURIFICATION AND ISOLATION OF JAMUN SEED BIOACTIVE COMPOUNDS

Extraction is the first and most important step in the recovery of biological molecules from plant material. The solvent extraction with pure or aqueous methanol, ethanol and acetone was most commonly used to extract phenolics from jamun seeds [Liu *et al*., 2018; Elhawary *et al*., 2022; Sawant *et al*., 2015; Shrikanta *et al*., 2015]. Aqueous acetone was used in the first step of isolation of jamun seed sesquiterpenoids and phloroglucinol derivatives [Liu *et al*., 2017a,b], and water to recover polysaccharides with potential bioactivity [Al-Dhabi & Ponmurugan, 2020]. In the last-mentioned study, microwave treatment during extraction was successfully applied to increase extraction yield. In turn, ultrasonic-assisted extraction (UAE) was used to most effectively extract *S. cumini* seed phenolics [Mahindrakar & Rathod, 2020a]. Authors compared UAE with conventional, stirred batch extraction, and found that contents of (+)-catechin, gallic acid, total phenolic and total flavonoid as well as antioxidant activity (DPPH assay) were 3.6, 1.5, 1.3, 1.4 and 1.2 times higher, respectively, for the extract obtained by UAE. Both extractions were carried out under optimal conditions, which were as follows for UAE: 12 min of extraction time, 35°C of temperature, 1:15 of solid material to solvent ratio, 125 W of power, and 60% of duty cycle. The stirred batch extraction required longer extraction time, higher solvent volume and higher temperature than UAE by 8.8, 1.3 and 1.4 times, respectively. Abdin *et al*. [2019] used the response surface methodology (RSM) for optimization UAE of jamun seeds in terms of maximizing total phenolic content and for the inhibition of α-amylase and pancreatic lipase. The effects of extraction time (10–90 min), ethanol concentration (10–90%, *v/v*), and solvent to solid material ratio (10–70 mL/g) were investigated and the optimal UAE conditions were found as 59.8 min – extraction time, 63.1% (*v/v*) – ethanol concentration, and 43.8 mL/g – solvent to solid material ratio. The RSM was also applied to optimize the microwave-assisted extraction of polysaccharides from jamun seeds [Al-Dhabi & Ponmurugan, 2020]. Four-factor, five-step central composite rotary experimental design allowed to state that microwave power of 515 W, pH of 3.2, extraction time of 3.1 min, and solid material to solvent ratio of 1:15 g/mL were the most efficient conditions for the recovery of polysaccharides.

Fractionation of the crude extracts is a common step in the isolation of phytochemicals. Various techniques are used to obtain fractions rich in specific class of compounds, the most common are chromatographic separations. However, fractionation is often preceded by re-extraction of the crude extract with solvents of different polarities. Such a path was followed by Sawant *et al*. [2015], who partitioned methanolic extract of jamun seeds using water, ethyl acetate, and *n*-butanol sequentially to find AR and PTP1B inhibitory active compounds. The most active ethyl acetate extract was then purified by a multi-step column chromatography (with silica gel, Diaion HP-20 and Sephadex LH-20) until the compounds (valoneic acid dilactone, ellagic acid, and rubuphenol) responsible for the activity could be isolated by means of preparative high-performance liquid chromatography (HPLC).

Partition of the methanolic extract of jamun seeds with ethyl acetate and *n*-butanol was deployed to enable isolation of hydrolysable tannins [Omar *et al*., 2012]. In the next step, the *n*-butanol extract was separated by medium pressure liquid chromatography to five fractions and each of them was used to isolate pure compounds using different systems of column chromatography and semipreparative HPLC. In turn, sesquiterpenoids were isolated from a 70% (*v/v*) aqueous acetone extract of jamun seeds, which was partitioned with ethyl acetate and water, and thereafter an ethyl acetate part was fractionated by a combination of MCI gel CHP-20P, silica gel, and Sephadex LH-20 column chromatography, as well as semipreparative HPLC [Liu *et al*., 2017a]. Phloroglucinol derivatives and saponin (vitalboside A) were isolated from jamun seeds by similar techniques, by re-extracting the crude extract and then fractionating it using various chromatographic methods [Liu *et al*., 2017b; Thiyagarajan *et al*., 2016]. Another technique was harnessed by Jasmine *et al.* [2010] who loaded the crude methanolic extract into the silica gel column, from which the compounds were eluted with a gradient system of solvents of increasing polarity. In this way, five fractions were obtained and one of them was active against drug-resistant bacteria. Silica gel (60–120 mesh) column chromatography with 95% ethanol as a mobile phase and Sepahex LH-20 column chromatography with methanol were applied by Sharma *et al*. [2011a,b] to separate fractions rich in bioactive compounds directly from jamun seed methanolic crude extract.

Filtration techniques are another way to purify crude extracts. In the case of jamun seeds, an aqueous extract was subjected to integrated cross flow ultrafiltration (UF) and nanofiltration (NF) [Balyan & Sarkar, 2016]. These membrane processes allowed to clarify the extract and concentrate the phenolic compounds, respectively. UF with a membrane with molecular weight cutoff of 100 kDa under low pressures (below 450 kPa) recovered 65% of total phenolic content, increased DPPH radical scavenging activity from 75.5 to 90.2%, and enhanced the purity by 1.35 times. Furthermore, NF with 250 Da membrane of UF-clarified permeate resulted in about three-fold concentration of phenolic compounds.

BIOLOGICAL ACTIVITIES OF JAMUN SEED EXTRACT

A range of pharmacological properties is possessed by various extracts of jamun which include antidiabetic, antihyperlipidemic, antihypercholesterolemic, anticancer, cardioprotective, hepatoprotective, neuroprotective, anti-inflammatory, antioxidant, and antimicrobial activities (Table 2), as established by scientific studies.

Antidiabetic activity

The antidiabetic effect of many natural products is based on the inhibition of α-amylase and α-glucosidase activities, which slow down starch digestion contributing to the reduction in blood glucose level [Alam *et al*., 2019; Lee & Yoon, 2022]. The extracts of seeds of black jamun landraces inhibited α-amylase activity in the range of 59.1–90.6% [Gajera *et al.*, 2017]. The water extract obtained from jamun seed kernels showed inhibitory activity against α-amylase and α-glucosidase characterized by IC_{50} values of 9.03 and 7.13 μg/mL, respectively [Mahindrakar & Rathod, 2020b]. The same authors, using a three-phase partitioning extraction, reported IC_{50} of 9.33 μg/mL for α-amylase and 7.55 μg/mL for α-glucosidase [Mahindrakar & Rathod, 2021]. In turn, Abdin *et al*. [2019] determined 87.66% α-amylase inhibitory activity of the fraction of jamun seed aqueous ethanol extract containing (+)-catechin, (–)-epicatechin, kaempferol, gallic, chlorogenic, caffeic, and ferulic acids as main phenolics and tested at a concentration of 640 μg/mL. Shinde *et al*. [2008] evaluated inhibitory activity of jamun seed extracts against microbial (*Saccharomyces cerevisiae* and *Bacillus stearothermophilus, in vitro*), and mammalian (*in vivo* on Goto-Kakizaki rat intestine, administration of 250 mg/kg body weight) α-glucosidase. Both acetone and 70% ethanol extracts exhibited inhibitory activity against enzyme of all three sources. Three hydrolysable tannins isolated from jamun seeds were the strong α-glucosidase inhibitors [Omar *et al*., 2012]. Their IC_{50} values were as follows: 8.2 μM (*iso*-oenothein C), 12.2 μM (cornusin B), and 75.1 μM (oenothein C). Liu *et al.* [2018] reported strong α-glucosidase inhibitory activity of phenolic compounds isolated from jamun seeds and elucidated using modern spectroscopic methods. Among 21 isolated compounds, eight (mainly ellagitannins and ellagic acid derivatives) inhibited α-glucosidase better than acarbose – a clinical drug. Tergalic acid dilactone was found as the strongest inhibitor with the IC_{50} value of 5 μM.

In the diabetic state, hyperglycemia increases glucose metabolism *via* the polyol pathway [Alam *et al*., 2019]. Aldose reductase (AR) catalyzes the conversion of glucose to sorbitol. This polyol, generated at high levels, cannot diffuse across cell membranes and either accumulates or is converted to fructose. In turn, protein tyrosine phosphatase B1 (PTP1B) is a negative regulator of the insulin signaling pathway and is associated with risk of both type 1 and 2 diabetes [Alam *et al*., 2019]. Gallic acid, valoneic acid dilactone, rubuphenol, and ellagic acid separated from jamun seeds were found to inhibit AR with IC_{50} values of 0.77, 0.075, 0.165, and 0.12μg/mL, while valoneic acid dilactone, rubuphenol, and ellagic acid inhibited PTP1B with IC_{50} values of 9.37, 28.14, and 25.96μg/mL, respectively [Sawant *et al.,* 2015]. Fourteen phloroglucinol derivatives isolated from jamun seeds inhibited PTP1B activity. The values of IC_{50} were in the range of 0.42–3.2 μM. The strongest inhibitory activity possessed jamunone E ($C_{26}H_{30}O_5$) with 2,5,7-trihydroxy-2,3-dihydrochromone moiety [Liu *et al.* 2017b].

Several *in vivo* studies showed the antidiabetic activity of jamun seeds, their extracts and phytochemicals. Study revealed that jamun seed extract preferably improves various biochemical actions, such as glucose tolerance and glucose uptake, maintains glucose homeostasis in diabetic animals, and exhibits benefits in restoring β-cells [Sharma *et al.,* 2008a]. Addition of defatted jamun seeds as well as water-soluble fiber isolated from this material to the diet of diabetic rats exerted a hypoglycemic effect [Pandey & Khan, 2002]. The ethanolic extract of phenolic compounds obtained from jamun seeds reduced significantly the blood glucose level in rats [Yadav *et al.,* 2010]. The authors reported 41%

TABLE 2. Bioactivities of jamun seed extracts/phytochemicals – last decade studies.

Origin of jamun seeds	Type of extract/Class of compounds	Methods	Bioactivity	Mode of action/Key finding	References
Gir forest western Gujarat, India	Methanol extract	Inhibition of porcine pancreatic α-amylase in DNS assay	Antidiabetic activity	α-Amylase inhibitory activity of 59.1–90.6% (IC$_{50}$ – 12.9 μg/mL)	Gajera *et al.* [2017]
		DPPH assay	Antioxidant activity	DPPH$^{\bullet}$ scavenging activity of 73.8–92.4%	
Konkan region of Maharashtra, India	Aqueous extract obtained by ultrasonic-assisted extraction	DPPH assay	Antioxidant activity	SC$_{50}$ – 10.59 μg/mL	Mahindrakar & Rathod [2020a]
India (industrial waste)	Aqueous extract	DNS assay, assay with *p*-nitrophenyl α-D-glucopyranoside	Antidiabetic activity	IC$_{50}$ for α-amylase and α-glucosidase inhibitory activity – 9.03 and 7.13 mg/mL, respectively	Mahindrakar & Rathod [2020b]
		DPPH assay	Antioxidant activity	SC$_{50}$ – 12.97 μg/mL	
India (industrial waste)	Extract obtained by three-phase (water, 20% ammonium sulfate and tert-butanol) partition	DNS assay, assay with *p*-nitrophenyl α-D-glucopyranoside	Antidiabetic activity	IC$_{50}$ for α-amylase and α-glucosidase inhibitory activity – 9.33 and 7.55 mg/mL, respectively	Mahindrakar & Rathod [2021]
		DPPH assay	Antioxidant activity	SC$_{50}$ – 12.15 μg/mL	
Kafrelshiekh, Egypt	Fraction of aqueous ethanol extract	DNS assay, assay with *p*-nitrophenyl laurate	Antidiabetic and anti-obesity activity	Fraction of JSE inhibited 87.66% (conc. 640 μg/mL) and 86.61% (conc. 1280 μg/mL) of α-amylase and pancreatic lipase activities, respectively	Abdin *et al.* [2019]
		ABTS, DPPH, hydroxyl radical scavenging activity assays	Antioxidant activity	SC$_{50}$ of JSE fraction for ABTS$^{\bullet+}$ – 105.3 μg/mL, for DPPH$^{\bullet}$ – 153.8 μg/mL, for hydroxyl radical – 501.6 μg/mL	
Gujarat, India	Isolated hydrolysable tannins	Assay with *p*-nitrophenyl-α-D-glucopyranoside	Antidiabetic activity	IC$_{50}$ for α-glucosidase inhibitory activity of iso-oenothein C, cornusin B and oenothein C – 8.2, 12.2 and 75.1 μM, respectively	Omar *et al.* [2012]
Gujarat, India	Isolated phenolics	Assay with *p*-nitrophenyl-α-D-glucopyranoside	Antidiabetic activity	Eight isolated phenolics (ellagitannins and ellagic acid derivatives) were very strong α-glucosidase inhibitors (IC$_{50}$ – 5.0–21.2 μM)	Liu *et al.* [2018]
		DPPH assay, inhibition of ROS production in murine RAW264.7 macrophages	Antioxidant activity	Nine most active isolated phenolics: SC$_{50}$ for DPPH – 25.0–87.2 μM, 24–36% inhibition of ROS production in the RAW264.7 macrophages (conc. 20 μM)	
Bangalore, India	Fractions and isolated phenolics	Aldose reductase and PTP1B inhibition assays, *in vitro*	Antidiabetic activity	IC$_{50}$ for aldose reductase: 0.075 μg/mL (valoneic acid dilactone), 0.12 μg/mL (ellagic acid), 0.165 μg/mL (rubuphenol) and for PTP1B: 9.37 μg/mL (valoneic acid dilactone), 25.96 μg/mL (ellagic acid), 28.14 μg/mL (rubuphenol)	Sawant *et al.* [2015]
Gujarat, India	Isolated phloroglucinol derivatives	PTP1B inhibition assays, *in vitro*	Antidiabetic activity	IC$_{50}$ of isolated phloroglucinol derivatives – 0.42–3.2 μM and positive control (synthetic PTP1B inhibitor) – 2.0 μM	Liu *et al.* [2017a]

TABLE 2 – continued

Origin of jamun seeds	Type of extract/Class of compounds	Methods	Bioactivity	Mode of action/Key finding	References
Bangalore, India	Hydro-ethanolic extract	RIN-5F and L6 cells, *in vitro*	Antidiabetic activity	Glucose uptake by L6 myoblast cells was increased (19.91% at 40 μg extract/mL) as compared to vehicle control; JCE showed enhancement of insulin release (2.8-fold at 40 μg/mL)	Assan Aliyar *et al*. [2021]
Local market, Faisalabad, Pakistan	50% (*v/v*) Aqueous ethanol extract	*In vivo* model (male Sprague Dawley hyperglycemic/diabetic rats)	Antihyperglycemic activity	In normal and hyperglycemic mice, JSE lowered glucose by 7.04% and 14.36%, respectively, and increased insulin level by 3.56% and 7.24%, respectively	Raza *et al*. [2017]
Local market, Karnataka, India	80% (*v/v*) Ethanol extract	DPPH assay; assay based on the reduction of Mo(VI) to Mo(V) (total antioxidant capacity)	Antioxidant activity	DPPH$^{\bullet}$ SC$_{50}$ – 0.40 mg/mL and total antioxidant capacity – 3.33 mmol GAE/g extract	Shrikanta *et al*. [2015]
Garden of NIPER, S.A.S. Nagar, India	75% (*v/v*) Aqueous ethanol with 10 mM HCl extract; additionally, hydrolysed with 2M HCl	ORAC, FRAP, DPPH and ABTS assays	Antioxidant activity	SC$_{50}$ for DPPH$^{\bullet}$ – 6.3 and 19.8 μg/mL (crude and hydrolyzed extract respectively) and for ABTS$^{\bullet+}$ – 4.6 μg/mL (both extracts); FRAP (concentration giving 50% reduction of ferric iron) – 23.6 and 24.7 μg/mL (crude and hydrolyzed extract, respectively); ORAC – 3.379±151 μmol TE/g (both extracts)	Aqil *et al*. [2012]
		Human non-small-cell lung carcinoma cell line A549	Antiproliferative activity	Hydrolyzed JSE showed higher antiproliferative activity (IC$_{50}$ of 38 μg/mL) then unhydrolyzed JSE (IC$_{50}$ of 64 μg/mL)	
Santa Maria, Rio Grande do Sul, Brazil	Aqueous extract (powder and nanoparticles)	*Candida albicans*-infected diabetic male albino Wistar rats	Antioxidant activity	JSE in nanoparticle form was more effective than JSE at reducing the oxidative burst induced by diabetes and/or *Candida* infection in rats	Bitencour *et al*. [2017]
Keshav Shristi Bhayandar, Mumbai, India	Fraction of ethanol extract	Human cancer cell lines: breast adenocarcinoma (MCF7), ovarian adenocarcinoma (A2780), prostate carcinoma (PC-3), non-small--cell lung carcinoma (H460)	Anticancer activity	The highest inhibition of cell proliferation by JSE was reported for A2780 cell line (IC$_{50}$ – 49 μg/mL)	Yadav *et al*. [2011]
		Agar cup-plate assay.	Antibacterial activity	JSE showed antibacterial activity against *E. coli, P. aeruginosa, S. aureus, B. subtilis* with zone of inhibition of 20, 11, 17, 15 mm, respectively with 20 and 11 mm, respectively	
Chenai, India	Methanol extract	HepG2 cells, MTT assay	Anticancer activity	JSE. induced apoptosis in HepG2 cells through decrease in MMP and downregulation of HFN-1α	Prakash & Devaraj [2019]
Botanical gardens in Egypt	Methanol extract	Human breast cancer (MCF-7 cell line and MDA-231 cell line), colon cancer (HCT-116 cell line), MTT assay	Anticancer activity	Strong JSE activity against HCT-116 cells, with IC$_{50}$ of 1.24 μg/mL	Elhawary *et al*. [2020]

TABLE 2 – continued

Origin of jamun seeds	Type of extract/Class of compounds	Methods	Bioactivity	Mode of action/Key finding	References
Viçosa, Minas Gerais, Brazil	Mixture of ethanol, methanol and acetone (1:1:1, *v/v/v*) extract	Agar diffusion assay	Antibacterial activity	JSE was active against *A. hydrophila, C. violaceum, E. coli, P. aeruginosa, S. enterica* serovar Typhimurium, *S. marcescens, L. monocytogenes*, and *S. aureus*	Santos *et al.* [2020]
Santa Maria, RS, Brazil	Aqueous extract	Lymphocytes, and ADA, DPP-4, and acetylcholinesterase activities, CD26 expression	Immunomodulatory properties	JSE exhibits immunomodulatory properties probably *via* the pathway of DPP-4–ADA complex	Bellé *et al.* [2013]
India	Methanol extract	Rat heart-derived H9C2 cardiomyoblast cells	Anti-inflammatory activity	JSE decreased glucose-induced cardiac stress, suppressed gelatinase activity in H9C2 cells, gelatinase-B expression and NF-κB nuclear translocation in these cells	Atale *et al.* [2021]
Gujarat, India	70% (*v/v*) Ethanol extract	Hydrogen peroxide induced cytotoxicity in H9C2 cells	Cardioprotective properties	JSE is capable of cardioprotective activity due to lowering intracellular oxidative stress, preventing depletion of cellular antioxidants and improving cell viability	Devkar *et al.* [2012]
Uttar Pradesh, India	Methanol extract	H9C2 cardiomyoblast cells	Cardioprotective properties	Exposure of glucose-stressed H9C2 cells to JSE showed decline in the activity of catalase and superoxide dismutase and collagen content	Atale *et al.* [2013]
Chittagong, Bangladesh	Methanol extract	Alloxan-induced diabetic Wistar albino rats	Cardio- and hepatoprotective properties	JSE at dose of 200 mg/kg reversed cardiac and liver damage caused by alloxan in rats	Nahid *et al.* [2017]
India	Aqueous extract	High fat diet- streptozotocin induced type 2 diabetic rats	Antihyperglycemic and antidyslipidemic activity	JSE at doses of 200 and 400 mg/kg decreased rat serum total cholesterol (by 39.9 and 44.2%, respectively), triglycerides (by 43.1 and 46.7%, respectively), LDL-cholesterol (by 28.3 and 32.9%, respectively) compared to control group	Sharma *et al.* [2017]
India	Ethanol extract	Streptozotocin induced Alzheimer's disease Wistar rats	Neuroprotective properties	JSE at doses of 200 and 400 mg/kg decreased amyloid load, tau phosphorylation and levels of tumor necrosis factor α (TNF-α) and interleukin-1β (IL-1β) in the hippocampus of JSE treated rats compared to negative control group	Kosaraju *et al.* [2014]
Local market, Warangal, India	Methanol extract	Scopolamine induced spatial memory impairments in male albino Wistar rats	Antiamnesic activity	JSE at doses of 200 and 400 mg/kg decreased lipid peroxidation and acetylcholinesterase activity, increased activity of superoxide dismutase and catalase in brain of treated animals, and positively affected short term or working memory compared to control group	Alikatte *et al.* [2012]

ABTS – 2,2'-azinobis-(3-ethylbenzthiazolin-6-sulfonic acid); ADA – adenosine deaminase; DNS – 3,5-dinitrosalicylic acid; DPP-4 – dipeptidyl peptidase 4; DPPH – 2,2-diphenyl-1-picrylhydrazyl; FRAP – ferric--reducing antioxidant power; GAE – gallic acid equivalents; HFN-1α – hepatocyte nuclear factor-1α; IC_{50} – concentration of the compound/extract causing 50% inhibition; JSA – jamun seed extract; MMP – mitochondrial membrane potential; ORAC – oxygen radical absorbance capacity; PTP1B – protein tyrosine phosphatase 1B; ROS – reactive oxygen species; SC_{50} – concentration of the antioxidant causing 50% radical scavenging; TE – Trolox equivalents.

and 44% of the mentioned reduction after oral administration of the extract. For the aqueous extract, the ability for blood glucose reduction was lower – 26% and 27% after 1 and 2 h, respectively. In the experiment with streptozotocin-diabetic rats (15 days, addition of 500 and 1000 mg of powdered jamun seeds per kg body weight to the rat diet) caused positive changes in diabetes markers. Fasting blood glucose was reduced by 75 and 122 mg/dL (in diabetic control it increased by 34 mg/dL). The value of post-treatment fasting and peak blood glucose 38 and 36 mg/dL was much lower than that in diabetic control (78 mg/dL). The positive changes in liver glycogen were reported; involving a decrease by 50 and 52 mg/g of liver in experimental group, and 90 mg/g of liver in normal control [Sridhar *et al*., 2005]. The decreased levels of blood glucose and increased glucose tolerance were found due to administration of jamun seed kernels (100 mg/kg body weight) to streptozotocin-induced diabetic rats [Ravi *et al*., 2004b]. In the same experiment, a decrease in the liver glycogen content was observed. It is worth emphasizing that no hypoglycemic effect was shown when powdered seed coat was used as a dietary ingredient. Ravi *et al*. [2003] reported that the activities of important enzymes for carbohydrate metabolism were returned almost to the normal levels due to administration of jamun seed kernels to diabetic rats. In the study of Raza *et al.* [2017], an aqueous ethanolic extract of jamun seeds caused glucose reduction by 14.36% and increased blood insulin level by 7.24% in hyperglycemic rats. Findings of Sharma *et al.* [2011b] also showed positive properties of jamun seeds including their significant effect on decreasing blood glucose level. The fraction isolated from the crude extract using Sephadex LH-20 column chromatography possessed potent antihyperglycemic activity in experiments with alloxan-induced diabetic rabbits. Phytochemicals present in jamun seeds have a beneficial effect on hypoglycaemic activity by stimulating the glucose uptake (GLUT 4) by skeletal muscle cells [Syama *et al.,* 2018].

A long-run human study conducted for 1 year on 99 patients with type 2 diabetes mellitus who poorly controlled blood sugar level and were administered *S. cumini* seed powder at a dose of 10 g/day showed decrease in fasting plasma glucose and postprandial blood sugar, thus indicating the beneficial role of jamun seed powder in controlling type 2 diabetes mellitus [Sidana *et al.,* 2017]. The study also confirmed the pharmaceutical value of *S. cumini* as a regional, traditional medicine for diabetes management.

Antihyperlipidemic and antihypercholesterolemic activity

The presence of several bioactive compounds in jamun seeds helps to regulate the blood lipid profile. Oral infusion of an alcoholic jamun seed extract (100 mg/kg body weight) in diabetic rats resulted in a significant reduction in serum lipids [Prince *et al*., 2004]. The jamun seed extract also decreased the total serum cholesterol to high-density lipoprotein (HDL) cholesterol ratio, serum low-density lipoprotein (LDL) cholesterol level and 3-hydroxy-3-methyl-glutaryl-coenzyme A (HMG-CoA) reductase activity in alloxan-induced diabetic rabbits and streptozotocin-induced diabetic rats [Sharma *et al*., 2003; 2011a,b; Sridhar *et al*., 2005]. The plasma lipoprotein cholesterol (HDL-, LDL-, and VLDL-C) and fatty acid composition were altered in streptozotocin-induced diabetic rats when administered the ethanolic jamun seed extract [Ravi *et al*., 2005]. In the experiment of Ulla *et al* [2017], the supplementation of the rats high-carbohydrate and high-fat diet with jamun seed powder for 56 days (2.5%, *w/w,* of diet) reduced white adipose tissue (WAT) weights, and plasma lipids, such as total cholesterol, triglyceride, LDL and HDL cholesterol concentration. In experiments of Sharma *et al.* [2017], diabetic rats were treated with a water jamun seed extract (200 and 400 mg/(kg×day)). The authors observed decreased serum levels of total cholesterol (by 39.9 and 44.2%, respectively), triglycerides (by 43.1 and 46.7%, respectively), and LDL-cholesterol (by 28.3 and 32.9%, respectively) compared with diabetic control group. Due to addition of extracts to rat diet, the concentration of HDL-cholesterol increased by 14.6 and 20.2%, respectively.

Parveen *et al.* [2020] demonstrated antihyperlipidemic effect of jamun seeds in a human study. The supplementation of the diet of patients diagnosed with prediabetes with jamun seed capsulated powder (4.5 g/day) significantly improved the level of total cholesterol and LDL-cholesterol from 266 to 216 mg/dL and from 189 to 139 mg/dL, respectively.

Anticancer activity

Jamun seed extract exhibited protection in albino mice against peroxidative damage contributing to skin cancer [Parmar *et al.,* 2010]. The oral intake of extracts (125 mg/kg body weight) reduced tumor burden, number of papilloma cells and their size. In experiments of Arun *et al.* [2011], the jamun seed extract administered orally (500–1500 mg/kg body weight) to mice before the exposure to genotoxic carcinogens (7,12-dimethylbenz(α)anthracene and urethane) prevented the breakage of pBR322 DNA, significantly reduced the chromosomal aberrations in metaphase, and reduced the formation of micronuclei in polychromatic erythrocytes.

Among *in vitro* studies, Yadav *et al.* [2011] examined the cytotoxic activity of the jamun seed extract by MTS assay on various cancer cell lines. The results were expressed as IC_{50} values (the concentration of the extract inhibiting cell proliferation up to 50% of the negative control). With IC_{50} of 49 μg/mL, A2780 (ovarian cancer) cell line was found to be most sensitive while non-small-cell lung carcinoma (H460) proved to be the least sensitive (IC_{50} 165 μg/mL). A very low IC_{50} value (0.06–0.08 μg/mL) was shown by flavopiridol (positive control) on all the cell lines. The induction of apoptosis in human hepatoma cells (HepG2) by the jamun seed extract was reported by Prakash & Devaraj [2019]. In this study, the use of different extract concentrations (10, 20, and 40 μg/mL) decreased the mitochondrial potential as well as down-regulated a hepatocyte nuclear factor-1α (HFN-1α). It was confirmed by western blotting. In turn, Aqil *et al*. [2012] used an MMT assay to evaluate the effect of jamun seed extracts (crude and hydrolyzed) on cancer cell viability. Both extracts exhibited strong antiproliferative activity against human non-small-cell lung cancer A549. The activity of the crude and hydrolyzed extract, expressed as IC_{50}, reached the value of 64 and 38 μg/mL, respectively. The methanolic extract of jamun seeds exhibited cytotoxic activity against colon cancer cell line (HCT-116), with IC_{50} value of 1.24 μg/mL

[Elhawary *et al*., 2022]. According to molecular docking study, myricetin 3-glucoside, myricitrin, reynoutrin, and quercitrin present in the extract were most potential ligands within a protein active site (FIH-1).

Cardio- and hepatoprotective properties

The methanolic jamun seed extract administered to mice at the dose of 200 mg/kg body weight revealed the protective and recovery ability on cardiac tissue due to its capability to decrease myocardial necrosis biomarkers such as aspartate aminotransferase (AST), alanine transaminase (ALT), uric acid, creatine phosphokinase (CPK), and lactate dehydrogenase (LDH) [Nahid *et al.,* 2017]. Atale *et al*. [2013] reported reduction in size of myocyte, lower generation of reactive oxygen species (ROS), and lower accumulation of collagen in response to the administration of the jamun seed extract. According to the study of Devkar *et al* [2012], jamun seeds are potential cardioprotective agents due to a higher content of phenolic compounds, can reduce intracellular oxidative stress, preventing depletion of cellular antioxidants and improving cell viability. The mentioned research investigated hydrogen peroxide-induced cytotoxicity in H9C2 cells.

Hepatoprotective effect of the methanolic seed extract was reported when administered at doses of 100, 200 and 400 mg/kg to Wistar albino rats treated with carbon tetrachloride dosages. The extract significantly reversed the elevated marker enzymes (glutamic oxaloacetic transaminase (GOT), glutamic pyruvic transaminase (GPT), alkaline phosphatase (ALP), acid phosphatase (ACP) and bilirubin), which were comparable even with those of the Liv.52®-treated group. The dose of 400 mg/kg body weight was highly effective against the hepatotoxicity caused by carbon tetrachloride [Sisodia & Bhatnakar, 2009]. Likewise, the methanolic jamun seed extract when administered at a dose of 200 mg/kg body weight to diabetic rats, exhibited hepatoprotective effect by significantly increasing the protein concentration, ALT, AST, ALP and bilirubin levels, and reducing enhanced liver enzymes even more than in the rats treated with the gliclazide (25 mg/kg) [Nahid *et al*., 2017].

Neuroprotective properties

The therapeutic potential of dipeptidyl peptidase-4 (DPP-4) inhibitors in the treatment of Alzheimer's disease (AD) was confirmed in experimental studies [Holscher, 2010]. Because phenolic compounds are known as DPP-4 inhibitors, Kosaraju *et al*. [2017] tested the neuroprotective effect of the jamun seed extract against the streptozotocin-induced AD in a rat model. The administration of jamun seed extract at doses of 200 and 400 mg/kg decreased amyloid load, tau phosphorylation and inflammation in the brain. Levels of tumor necrosis factor α (TNF-α) and interleukin-1β (IL-1β) in the hippocampus of rats from group treated with jamun seed extract was reduced when compared with a negative control group.

The antiamnestic effect of the jamun seed methanolic extract was evaluated in a rat model by Alikatte *et al*. [2012]. The extract administration (200 and 400 mg/kg) exerted positive effects on short-term or working memory and reversed cognitive impairments in rats. In brains of rats treated with extracts, the level of lipid peroxidation was lower and the activities of superoxide dismutase and catalase higher than in the control group. The authors reported also suppression of acetylcholinesterase activity in experimental groups.

Anti-inflammatory activity

Due to the occurrence of several bioactive compounds, jamun seed powder or its extract can act as an anti-inflammatory agent, decreasing both acute and chronic inflammation. It was confirmed by several *in vivo* studies. Bioactive compounds of ethyl acetate and methanol extracts of jamun seeds orally administered to Wistar rats with carrageenan-induced paw edema (200 and 400 mg/kg body weight) elicited anti-inflammatory effect [Kumar *et al*., 2008]. Chaudhuri *et al*. [1990] used the chloroform fraction of jamun seed in a lower dose (100 mg/kg body weight) and also reported the inhibition of carrageenan-induced paw edema in rats. The inhibition of migration of leucocytes into the pleural fluid was noted. In addition, the authors observed the reduction of the weight of cotton pellet-induced granuloma.

The study of Atale *et al*. [2021] demonstrated the anti-inflammatory effect of the jamun seed extract in rats with high-glucose-induced heart-derived H9C2 cardiomyoblasts. The bioactive compounds present in the extract prevented glucose-induced cardiac stress, gelatinase activity in H9C2 cardiomyocytes, gelatinase-B expression and NF-κB nuclear translocation in these cells. The docking studies confirmed a strong interaction between jamun seed phenolic compounds and gelatinase-B.

The results of a study by Bellé *et al.* [2013] indicated that the jamun seed extract can act as an inhibitor of the DPP-4 and adenosine deaminase (ADA) in human lymphocytes. Probably, the bioactive compounds present in extract may interact with DPP-ADA complex and modify the purinergic signaling.

Antioxidant activity

The antioxidant potential of jamun seeds was analyzed by several *in vitro* methods, using various techniques for the extraction of bioactive compounds. The phenolics (gallic acid, ellagic acid, ferulic acid, (+)-catechin, and quercetin) of seeds originated from underutilized indigenous black jamun landraces found in the Gir forest region of India showed significant antiradical activity against $DPPH^{\bullet}$ [Gajera *et al*., 2017]. The $DPPH^{\bullet}$ scavenging activity of extracts of jamun kernel powder obtained using an ultrasonic-assisted aqueous extraction, regular water extraction, and a three-phase partitioning extraction was determined by Mahindrakar & Rathod [2020a,b; 2021]. The concentration of the antioxidant causing 50% radical scavenging (SC_{50}) was 10.59, 12.97, and 12.15 μg/mL, respectively. Much higher SC_{50} values of 105.3, 153.8, and 501.6 μg/mL were found for $ABTS^{\bullet+}$, $DPPH^{\bullet}$ and hydroxyl radical, respectively, by Abdin *et al*. [2019] who determined radical scavenging activity of the chromatographically (D101 resin) purified jamun seed aqueous ethanol extract. In turn, Shrikanta *et al*. [2015] reported a very low SC_{50} value of 0.40 mg/mL for $DPPH^{\bullet}$ scavenging activity of 80% (*v/v*) ethanol extract. The extract was also tested in the assay based on the reduction of Mo(VI) to Mo(V) and its total antioxidant capacity was determined at 3.33 mmol GAE/g extract. Phenolic compounds isolated from jamun seeds with the highest

DPPH$^•$ scavenging activity were ellagitannins and ellagic acid derivatives (SC_{50} values in the range of 25.0–87.2 μM) [Liu *et al*., 2018]. The same compounds also strongly inhibited ROS generation in the RAW264.7 macrophages.

Aqil *et al*. [2012] investigated antioxidant activity of the crude and hydrolyzed extracts of jamun seeds as ferric-reducing antioxidant power (FRAP), oxygen radical absorbance capacity (ORAC), and using antiradical assays (DPPH and ABTS). In the DPPH assay, the crude and hydrolyzed extracts exhibited SC_{50} of 16.3 and 19.8 μg/mL, respectively. For both extracts, results of the ABTS assay were the same – SC_{50} of 4.6 μg/mL. Results of FRAP were expressed by the concentration inducing 50% reduction of the ferric iron, which amounted to 23.6 μg/mL (crude extract) and 24.7 μg/mL (hydrolyzed extract). Both extracts were characterized by the same ORAC value – 3.379 mmol Trolox equivalents/g.

The *in vivo* experiment carried out by Bitencourt *et al*. [2017] demonstrated the antioxidant potential of the jamun seed extract. *Candida albicans*-infected diabetic rats were treated for three weeks with an aqueous seed extract and the same extract in the form of nanoparticles with a daily dose of 100 mg/kg. The crude extract and its nanoparticle form were able to decrease levels of thiobarbituric acid reactive substances (TBARS) in serum, kidney, liver, and pancreas of the treated groups when compared to control animals.

Antimicrobial activity

According to Bag *et al*. [2012], the extract of jamun seeds exhibited the antibacterial potential against multidrug-resistant human bacterial pathogens. The possibility of applying the jamun seed extract as a novel antimicrobial agent was confirmed by means of the agar well diffusion and microbroth dilution assays. Jasmine *et al.* [2010] found that the crude extracts of jamun seeds could act against isolated β-lactamase-producing drug-resistant bacteria. The zone of inhibition was in the range of 14–21 mm and a minimum inhibitory concentration (MIC) was in the range of 31.75–62.5 μg/mL. According to the authors, saponins present in the extract were the active phytochemicals. Eight sesquiterpenoids isolated from jamun seeds were active (100 μg/disk) against *S. aureus.* However, the same compounds at the same concentration caused no effect against *E. coli* and *C. albicans* [Liu *et al*., 2017a]. According to Santos *et al*. [2020], phenolic extracts of jamun seeds were activite against *Aeromonas hydrophila*, *Chromobacterium violaceum*, *E. coli*, *Pseudomonas aeruginosa*, *Salmonella enterica* serovar Typhimurium, *Serratia marcescens*, *Listeria monocytogenes*, and *S. aureus*. The strongest antimicrobial activity was reported in the case of *S. aureus*. The extract used inhibited also violacein production by *C. violaceum.* Inhibition of *E. coli, S. aureus*, and *P. aeruginosa* growth by a fraction isolated from the ethanol extract of jamun seed was also reported by Yadav *et al*. [2011]. The zones of inhibition in agar cup-plate assay were 20, 17 and 11 mm, respectively. Yadav *et al.* [2017], using an agar well diffusion assay, demonstrated the antimicrobial activity of the jamun seed extract against *Bacillus subtilis.* The minimum inhibitory concentration of the methanolic extract was 0.3 mg/mL. The results of flow cytometry showed that antimicrobial activity of compounds present in the extract was related to the induction of membrane permeability in bacterial cells. According to docking analysis, among bioactive compounds of the jamun seed extract, lupeol showed the highest binding energy with DD-carboxypeptidase and LD-carboxypeptidase from *B. subtilis*, and stigmasterol and betasitosterol showed the highest binding energy for class D β-lactamase and β-lactamase.

The research conducted by Chandrasekaran & Venkatesalu [2004] showed antifungal activity of bioactive compounds extracted from jamun seeds using water and methanol. Extracts were active against such dermatophytic fungi as *Candida albicans*, *Tricophyton rubrum*, *T. mentagrophytes, Microsporum gypseum*, and *Aspergillus niger*.

APPLICATION OF JAMUN SEEDS AND THEIR EXTRACT IN THE FOOD INDUSTRY

Jamun seed powder and its infusion are traditionally used in the treatment of diabetes and ulcers. Currently, the application of these seeds to prepare herbal formulations is gaining popularity worldwide. Raza *et al.* [2017] recommended the jamun seed powder as a health-promoting additive to foods due to its antihyperglycemic properties. However, its use in the production of bread, pasta or cookies still requires researches of product safety and quality, and processes conditions optimization. In the case of infusions/extracts, their low storage stability is disadvantageous. Modern techniques, such as ultrafiltration and nanofiltration, show promise in solving this problem [Balyan & Sarkar, 2018]. The cited study estimated parameters of the first-order kinetic model to fit the changes of total phenolic contents and total flavonoid contents of UF and NF fractions of the jamun seed aqueous extract during storage. These parameters can be useful for designing appropriate storage conditions for industrial scale-up of the process. Another possibility of increasing the stability of the jamun seed extract was proposed by Peixoto & Freitas [2013]. The authors spray-dried the aqueous extract using silicon dioxide and cassava starch as carriers. The obtained powder had low hygroscopicity at 43% relative humidity and was characterized by adequate flowability and compactability. Moreover, the antihyperglycemic and antioxidant properties of the spray-dried extract were comparable to those of the lyophilized one.

Whole jamun-based functional confection (WJFC) containing 2% of the jamun seed powder was produced and investigated by Sehwag & Das [2016] and Sehwag *et al*. [2018]. WJFC was characterized by a high content of dietary fiber and a low calorific value. It could be applied as a natural prebiotic, antioxidant or antidiabetic preparation. WJFC as an inhibitor of α-amylase activity helped in maintaining a low blood glucose level.

The study of VenuGopal & Anu-Appaiah [2017] investigated effects of, the addition of jamun seeds during production of wines from jamun fruits. The seeds added to wine increased the content of phenolic compounds at the beginning of fermentation. However, the content of phenolics reduced throughout aging. The presence of phenolic compounds and polysaccharides originating from seeds influenced wine browning. In turn, Singh & Kocher [2020] used response surface methodology to optimize the parameters of the fermentation of *S. cumini* fruits with seed power supplementation. Phenolics (specially tannins) of seeds were responsible for stabilizing sensory attributes and antioxidant potential of stored wines.

Abdin *et al.* [2022] used the jamun seed extract as a component of the edible sodium alginate/gum Arabic films. Such a product, featuring appropriate physicochemical properties, can serve as a good source of antioxidant compounds and can be used in modern food packaging.

CONCLUSION AND FUTURE PROSPECTIVE DIRECTIONS

According to the review, the seed of the jamun fruit has a richly-varied composition of bioactive compounds, including terpenoids, phenolic compounds and saponins with high contents of gallic acid, ellagic acid and hydrolysable tannins. These compounds are responsible for the extensive biological activities of jamun seeds and their extracts. Jamun seeds appear to be a low-cost source of a natural antidiabetic agent, although their antioxidant, anti-inflammatory antimicrobial potential is becoming more and more appreciated. As modern techniques for the extraction, separation and purification of jamun seeds bioactives are developed, it seems that powder, extracts and fractions may soon be harnessed in the production of functional foods and nutraceuticals intended for people at risk of diabetes, cancer, cardiovascular, hepatic and neurodegenerative diseases, and bacterial and microbial infections. Nevertheless, more research is needed to elucidate the molecular mechanisms of the of health-beneficial activities of jamun seed compounds. The biological activity of saponins and lignans from jamun seeds, and the bioavailability of bioactive compounds are still poorly understood. In addition, the nutritional value of jamun seeds seems to be still little known, especially in terms of proteins, their amino acid composition and biological value. Clinical trials of jamun seed-based goods on humans, taking into account all safety concerns, will increase the value of jamun seeds for use in the food and non-food industries.

RESEARCH FUNDING

This study received no external funding.

CONFLICT OF INTERESTS

Authors declare no conflict of interest.

ORCID IDs

R. Amarowicz https://orcid.org/0000-0001-9731-0045
J.M. Lorenzo https://orcid.org/0000-0002-7725-9294
Y. Tak https://orcid.org/0000-0003-3549-0284

REFERENCES

1. Abdin, M., Hamed, Y.S., Akhtar, H.M.S., Chen, D., Mukhtar, S., Wan, P., Riaz, A., Zeng, X. (2019). Extraction optimisation, antioxidant activity and inhibition on α-amylase and pancreatic lipase of polyphenols from the seeds of *Syzygium cumini. International Journal of Food Science and Technology*, *54*(6), 2084–2093. https://doi.org/10.1111/ijfs.14112
2. Abdin, M., El-Beltagy, A.E., El-Sayed, M.E., Naeem, M.A. (2022). Production and characterization of sodium alginate/gum Arabic based films enriched with *Syzygium cumini* seeds extracts for food application. *Journal of Polymers and the Environment*, *30*, 1615–1626. https://doi.org/10.1007/s10924-021-02306-z
3. Alam, F., Shafique, Z., Amjad, S.T., Bin Asad, M.H.H. (2019). Enzymes inhibitors from natural sources with antidiabetic activity: A review. *Phytotherapy Research*, *33*(1), 41–54. https://doi.org/10.1002/ptr.6211
4. Al-Dhabi, N.A., Ponmurugan, K. (2020). Microwave assisted extraction and characterization of polysaccharide from waste jamun fruit seeds. *International Journal of Biological Macromolecules*, *152*, 1157–1163. https://doi.org/10.1016/j.ijbiomac.2019.10.204
5. Alikatte, K.L., Akondi, B.R., Yerragunta, V.G., Veerareddy, P.R., Suresh Palle, S. (2012). Antiamnesic activity of *Syzygium cumini* against scopolamine induced spatial memory impairments in rats. *Brain & Development*, *34*,(10), 844–851. http://doi.org/10.1016/j.braindev.2012.02.008
6. Aqil, F., Gupta, A., Munagala, R., Jeyabalan, J., Kausar, H., Sharma, R.J., Singh, I.P., Gupta, R.C. (2012). Antioxidant and antiproliferative activities of anthocyanin/ellagitannin-enriched extracts from *Syzygium cumini* L. (Jamun, the Indian blackberry). *Nutrition and Cancer*, *64*(3), 428–438. https://doi.org/10.1080/01635581.2012.657766
7. Arun, R., Prakash, M.V.D., Abraham, S.K., Premkumar, K. (2011). Role of *Syzygium cumini* seed extract in the chemoprevention of *in vivo* genomic damage and oxidative stress. *Journal of Ethnopharmacology*, *134*(2), 329–333. https://doi.org/10.1016/j.jep.2010.12.014
8. Assan Aliyar, M., Nadig, P., Bharatam, N. (2021). *In vitro* antidiabetic activity, bioactive constituents, and molecular modeling studies with sulfonylurea receptor1 for insulin secretagogue activity of seed extract of *Syzygium cumini* (L.). *Journal of Herbmed Pharmacology*, *10*(3), 304–312. https://doi.org/10.34172/jhp.2021.35
9. Atale, N., Chakraborty, M., Mohanty, S., Bhattacharya, S., Nigam, D., Sharma, M., Rani, V. (2013). Cardioprotective role of *Syzygium cumini* against glucose-induced oxidative stress in H9C2 cardiac myocytes. *Cardiovascular Toxicology*, *13*(3), 278–289. https://doi.org/10.1007/s12012-013-9207-1
10. Atale, N., Mishra, C.B., Kohli, S., Mongre, R.K., Prakash, A., Kumari, S., Yadav, U.C.S., Jeon, R., Rani, V. (2021). Anti-inflammatory effects of *S. cumini* seed extract on gelatinase-B (MMP-9) regulation against hyperglycemic cardiomyocyte stress. *Oxidative Medicine and Cellular Longevity*, *2021*, art. no. 8839479. https://doi.org/10.1155/2021/8839479
11. Bag, A., Bhattacharyya, S.K., Pal, N.K., Chattopadhyay, R.R. (2012). *In vitro* antibacterial potential of *Eugenia jambolana* seed extracts against multidrug-resistant human bacterial pathogens. *Microbiological Research*, *167*(6), 352- 357. https://doi.org/10.1016/j.micres.2012.02.005
12. Bajpai, M., Pande, A., Tewari, S.K., Prakash, D. (2005). Phenolic contents and antioxidant activity of some food and medicinal

plants. *International Journal of Food Sciences and Nutrition*, *56*(4), 287–291.
https://doi.org/10.1080/09637480500146606

13. Balyan, U., Sarkar, B. (2016). Integrated membrane process for purification and concentration of aqueous *Syzygium cumini* (L.) seed extract. *Food and Bioproducts Processing*, *98*, 29–43.
https://doi.org/10.1016/j.fbp.2015.12.005
14. Balyan, U., Sarkar, B. (2017). Aqueous extraction kinetics of phenolic compounds from jamun (*Syzygium cumini* L.) seeds. *International Journal of Food Properties, 20*(2), 372–389.
https://doi.org/10.1080/10942912.2016.1163266
15. Balyan, U., Sarkar, B. (2018). Ultrafiltration of *Syzygium cumini* (L.) seeds extract: Analysis of flux decline and extract stability. *Asia-Pacific Journal of Chemical Engineering, 13*(2), art. no. e2166.
https://doi.org/10.1002/apj.2166
16. Bellé, L.P., Bitencourt, P.E.R., Abdalla, F.H., de Bona, K.S., Peres, A., Maders, L.D.K., Moretto, M.B. (2013). Aqueous seed extract of *Syzygium cumini* inhibits the dipeptidyl peptidase IV and adenosine deaminase activities, but it does not change the CD26 expression in lymphocytes *in vitro. Journal of Physiology and Biochemistry*, *69*(1), 119–124.
https://doi.org/10.1007/s13105-012-0195-6
17. Benherlal, P.S., Arumughan, C. (2007). Chemical composition and *in vitro* antioxidant studies of *S. cumini* fruit. *Journal of the Science of Food and Agriculture*, *87*(14), 2560–2569.
https://doi.org/10.1002/jsfa.2957
18. Bhaskar, K., Sassykova, L.R., Prabhahar, M., ShebhaPercis, E., Nalini, A., Jenish, T., Jayarajan, J., Sendilvelan, S. (2021). Analysis of *Cymbopogon citratus*, *Pinus sylvestris* and *Syzygium cumini* biodiesel feedstocks for its fatty acid composition. *Materials Today: Proceedings, 45*, Part 7, 5970–5977.
https://doi.org/10.1016/j.matpr.2020.09.254
19. Bhatia, I.S., Bajaj, K.L. (1975). Chemical constituents of the seeds and bark of *Syzygium cumini*. *Planta Medica*, *28*(8), 346–352.
https://doi.org/10.1055/s-0028-1097868
20. Binita, K., Kumar, S., Sharma, V.K., Sharma, V., Yadav, S. (2014). Proteomic identification of *Syzygium cumini* seed extracts by MALDI-TOF/MS. *Applied Biochemistry and Biotechnology*, *172*, 2091–2105.
https://doi.org/10.1007/s12010-013-0660-x
21. Bitencourt, P.E.R., Cargnelutti, L.O., Stein, C.S., Lautenchleger, R., Ferreira, L.M., Sangoi, M., Denardi, L., Borges, R.M., Boligon, A., Moresco, R.N., Cruz, L., Zanette, R.A., Alves, S.H., Moretto, M.B. (2017). Nanoparticle formulation increases *Syzygium cumini* antioxidant activity in *Candida albicans*-infected diabetic rats. *Pharmaceutical Biology*, *55*(1), 1082–1088.
https://doi.org/10.1080/13880209.2017.1283338
22. Chandrasekaran, M., Venkatesalu, V. (2004). Antibacterial and antifungal activity of *Syzygium jambolanum* seeds. *Journal of Ethnopharmacology*, *91*(1), 105–108.
https://doi.org/10.1016/j.jep.2003.12.012
23. Chaudhuri A.K.N., Pal, S., Gomes, A., Bhattacharya, S. (1990). Anti-inflammatory and related actions of *S. cumini* seed extract. *Phytotherepia Research*, *4*(1), 5–10.
https://doi.org/10.1002/ptr.2650040103
24. Cronin, P., Joyce, S.A., O'Toole, P.W., O'Connor, E.M., (2021). Dietary fibre modulates the gut microbiota. *Nutrients*, *13*(5), art. no. 1655.
https://doi.org/10.3390/nu13051655
25. Daulatabad, C.M.J.D., Abdurrazzaque, M., Mirajkar, A.M., Hosamani, K.M., Mulla, G.M.M. (1988). Epoxy and cyclopropenoid fatty acids in Syzygium cuminii seed oil. *Journal of the Science of Food and Agriculture*, *43*(1), 91–94.
https://doi.org/10.1002/jsfa.2740430111
26. De Sousa Sabino, L.B., de Brito, E.S., da Silva I.J., Júnior (2018). Jambolan – *Syzygium jambolanum*. In S. Rodrigues, E. de Oliveira Silva, E.S. de Brito (Eds.), *Exotic Fruits*, Academic Press, London, UK, pp. 251–256.
https://doi.org/10.1016/B978-0-12-803138-4.00032-0
27. Deng, Y., Huang, L., Zhang, C., Xie, P., Cheng, J., Wang, X., Liu, L. (2020). Novel polysaccharide from *Chaenomeles speciosa* seeds: Structural characterization, α-amylase and α-glucosidase inhibitory activity evaluation. *International Journal of Biological Macromolecules 153*, 755–766.
https://doi.org/10.1016/j.ijbiomac.2020.03.057
28. Devkar, R.V., Pandya, A.V., Shah, N.H. (2012). Protective role of *Brassica olerecea* and *Eugenia jambolana* extracts against H_2O_2 induced cytotoxicity in H9C2 cells. *Food & Function*, *3*(8), 837–843.
https://doi.org/10.1039/c2fo00001f
29. Elhawary, S.S.E., kamal Eldin Elmotyam, A., kamel Alsayed, D., Zahran, E.M., Fouad, M.A., Sleem, A.A., Elimam, H., Rashed, M.H., Hayallah, A.M., Anber, F., Mohammed, A.F., Abdelmohsen, U.R. (2022). Cytotoxic and anti-diabetic potential, metabolic profiling and *in silico* studies of *Syzygium cumini* (L.) Skeels belonging to family *Myrtaceae. Natural Product Research*, *36*(4), 1026–1030.
https://doi.org/10.1080/14786419.2020.1843032
30. Faria, A.F., Marques, M.C., Mercadante, A.Z. (2011). Identification of bioactive compounds from jambolão (*Syzygium cumini*) and antioxidant capacity evaluation in different pH conditions. *Food Chemistry*, *126*(4), 1571–1578.
https://doi.org/10.1016/j.foodchem.2010.12.007
31. Gajera, H.P., Gevariya, S.N., Hirpara, D.G., Patel, S.V., Golakiya, B.A. (2017). Antidiabetic and antioxidant functionality associated with phenolic constituents from fruit parts of indigenous black jamun (*Syzygium cumini* L.) landraces. *Journal of Food Science and Technology*, *54*(10), 3180–3191.
https://doi.org/10.1007/s13197-017-2756-8
32. Gajera, H.P., Gevariya, S.N., Patel, S.V., Golakiya, B.A. (2018). Nutritional profile and molecular fingerprints of indigenous black jamun (*Syzygium cumini* L.) landraces. *Journal of Food Science & Technology, 55*(2), 730–739.
https://doi.org/10.1007/s13197-017-2984-y
33. Ghosh, P., Radhan, R.C., Mishra, S., Patel, A.S., Kar, A. (2017). Physicochemical and nutritional characterization of jamun (*Syzygium cuminii*). *Current Research in Nutrition and Food Science Journal, 5*(1), 25–35.
https://doi.org/10.12944/CRNFSJ.5.1.04
34. Granado-Rodríguez, S., Aparicio, N., Matías, J., Pérez-Romero, L.F., Maestro, I., Gracés, I., Pedroche, J.J., Haros, C.M., Fernandez-Garcia, N., del Hierro, J.N., Martin, D., Bolaños, L., Reguera, M. (2021). Studying the impact of different field environmental conditions on seed quality of quinoa: the case of three different years changing seed nutritional traits in Southern Europe. *Frontiers in Plant Science*, *12*, art. no. 649132.
https://doi.org/10.3389/fpls.2021.649132

35. Gupta, D.R., Agrawal, S.K. (1970). Chemical examination of the unsaponifiable matter of the seed fat of *Syzgium cumini*. *Science and Culture*, *36*(5), 298.
36. Holscher, C. (2010). Incretin analogues that have been developed to treat type 2 diabetes hold promise as a novel treatment strategy for Alzheimer's disease. *Recent Patents on CNS Drug Discovery*, *5*(2), 109–117.
https://doi.org/10.2174/157488910791213130
37. Indrayan, A.K., Sharma, S., Durgapaal, D., Kumar, N., Kumar, M. (2005). Determination of nutritive value and analysis of mineral elements for some medicinally valued plants from Uttaranchal. *Current Science*, *89*(7), 1252–1255.
https://www.jstor.org/stable/24110980
38. Jadeja, R.N., Thouaojam, M.C., Sankhari, J.M., Jain, M., Devkar, R.V., Ramachandran, A.V. (2012). Standardized flavonoid-rich *Eugenia jambolana* seed extract retards *in vitro* and *in vivo* LDL oxidation and expression of VCAM-1 and P-selectin in atherogenic rats. *Cardiovascular Toxicilogy*, *12*, 73–82.
https://doi.org/10.1007/s12012-011-9140-0
39. Jamun Farming Information (Indian Black Plum) – AgriFarming.
https://www.agrifarming.in/jamun-farming
40. Jasmine, R., Selvakumar, B.N., Daisy, P.S., Ignacimuthu, S. (2010). Activity of *Eugenia jambolana*, an ethnomedical plant, against drug-resistant bacteria. *Pharmaceutical Biology*, *48*(4), 405–410.
https://doi.org/10.3109/13880200903150401
41. Karamać, M. (2009). *In-vitro* study on the efficacy of tannin fractions of edible nuts as antioxidants. *European Journal of Lipid Science and Technology*, *111*(11), 1063–1071.
https://doi.org/10.1002/ejlt.200900067
42. Kaur, L., Han, K.-S., Bains, K., Singh, H. (2011). Indian culinary plants enhance glucose-induced insulin secretion and glucose consumption in INS-1 β-cells and 3T3-L1 adipocytes. *Food Chemistry*, *129*(3), 1120–1125.
https://doi.org/10.1016/j.foodchem.2011.05.089
43. Kosaraju, J., Madhunapantula, S.R.V., Chinni, S., Khatwal, R.B., Dubala, A., Muthureddy Nataraj, S.K., Basavan, D. (2014). Dipeptydyl peptidase-4 inhibition by *Pterocarpus marsupium* and *Eugenia Jambolana* ameliorates streptozotocin induced Alzheimer's disease. *Behavioural Brain Research, 267*, 55–65.
https://doi.org/10.1016/j.bbr.2014.03.026
44. Kumar, A., Ilavarasan, R., Jayachandran, T., Deecaraman, M., Kumar, R.M., Aravindan, P., Krishan, M.R.V. (2008). Anti-inflammatory activity of *Syzygium cumini* seed. *African Journal of Biotechnology*, *7*(8), 941–943.
http://www.academicjournals.org/AJB
45. Lee, J.J., Yoon, K.Y. (2022). Ultrasound-assisted extractions for improving the recovery of phenolics and charantin from bitter melon and for increasing the antioxidant, antidiabetic and antiobesity activities of its extracts. *Polish Journal of Food and Nutrition Sciences*, *72*(2), 141–150.
https://doi.org/10.31883/pjfns/149434
46. Lestario, L.N., Howard, L.R., Brownmiller, C., Stebbins, N.B., Liyanage, R., Lay, J.O. (2017). Changes in polyphenolics during maturation of Java plum (*Syzygium cumini* Lam.). *Food Research International*, *100*, Part 3, 395–391.
https://doi.org/10.1016/j.foodres.2017.04.023
47. Liu, F., Liu, C., Liu, W., Ding, Z., Ma, H., Seeram, N.P., Xu, L., Mu, Y., Huang, X., Li, L. (2017a). New sesquiterpenoids from *Eugenia jambolana* seeds and their anti-microbial activities. *Journal of Food and Agricultural Chemistry*, *66*, 10214–10222.
https://doi.org/10.1021/acs.jnatprod.6b01073
48. Liu, F., Ma, H., Wang, G., Liu, W., Seeram, N.P., Mu, Y., Xu, Y., Huang, X., Li., L. (2018). Phenolics from *Eugenia jambolana* seeds with advanced glycation endproduct formation and alpha-glucosidase inhibitory activities. *Food & Function, 9*(8), 4246–4254.
https://doi.org/10.1039/C8FO00583D
49. Liu, F., Yuan, T., Liu, W., Ma, H., Seeram, N.P., Li, Y., Xu, L., Mu, Y., Huang, X., Li, L. (2017b). Phloroglucinol derivatives with protein tyrosine phosphatase 1B inhibitory activities from *Eugenia jambolana* seeds. *Journal of Natural Products*, *80*(2), 544–550.
https://doi.org/10.1021/acs.jafc.7b04066
50. Mahindrakar, K.V., Rathod, V.K. (2020a). Ultrasonic assisted aqueous extraction of catechin and gallic acid from *Syzygium cumini* seed kernel and evaluation of total phenolic, flavonoid contents and antioxidant activity. *Chemical Engineering and Processing – Process Intensification, 149*, art. no. 107841.
https://doi.org/10.1016/j.cep.2020.107841
51. Mahindrakar, K.V., Rathod, V.K. (2020b). Antidiabetic potential evaluation of aqueous extract of waste *Syzygium cumini* seed kernel's by *in vitro* α-amylase and α-glucosidase inhibition. *Preparative Biochemistry & Biotechnology*, *51*(6), 589–598.
https://doi.org/10.1080/10826068.2020.1839908
52. Mahindrakar, K.V., Rathod, V.K. (2021). Valorization of waste *Syzygium cumini* seed kernels by three-phase partitioning extraction and evaluation of in vitro antioxidant and hypoglycemic potential. *Preparative Biochemistry & Biotechnology*, *51*(10), 1036–1045.
https://doi.org/10.1080/10826068.2021.1894442
53. Martin, T.S., Ohtani, K., Kasai, R., Yamasaki, K. (1998). Lignan glucoside from *Syzygium cumini. Natural Medicine*, *52*(4), 360–363.
54. Moussa, M.I.D., Alashi, A.M., Sossa-Vihotogbé, C.N., Akponikpè, P.B., Baco, M.N., Djènontin, A.J., Aluko, R.E., Akissoé, N.H. (2020). Proximate composition, mineral profile and trypsin-inhibitory activity of West African leafy vegetables: influence of urea micro-dosing and harvest time. *Polish Journal of Food and Nutrition Sciences*, *70*(2), 179–188.
https://doi.org/10.31883/pjfns/119674
55. Nahid, S., Mazumder, K., Rahman, Z., Islam, S., Rashid, M.H., Kerr, P.G. (2017). Cardio- and hepato-protective potential of methanolic extract of *Syzygium cumini* (L.) Skeels seeds: A diabetic rat model study. *Asian Pacific Journal of Tropical Biomedicine, 7*(2), 126–133.
https://doi.org/10.1016/j.apjtb.2016.11.025
56. Oh, M.H., Yoon, K. (2018). Comparison of the biological activity of crude polysaccharide fractions obtained from *Cedrela sinensis* using different extraction methods. *Polish Journal of Food and Nutrition Sciences, 68*(4), 327–334.
https://doi.org/10.1515/pjfns-2018-0007
57. Omar, R., Li, L., Yuan, T., Seeram, N.P. (2012). α-Glucosidase inhibitory hydrolyzable tannins from *Eugenia jambolana* seeds. *Journal of Natural Products*, *75*(8), 1505–1509.
https://doi.org/10.1021/np300417q

58. Pandey, M., Khan, A. (2002). Hypoglycaemic effect of defatted seeds and water soluble fibre from the seeds of *Syzygium cumini* (Linn.) skeels in alloxan diabetic rats. *Indian Journal of Experimental Biology, 40*(10), 1178–1182.
59. Panghal, A., Kaur, R., Janghu, S., Sharma, P., Sharma, P., Chhikara, N. (2019). Nutritional, phytochemical, functional and sensorial attributes of *Syzygium cumini* L. pulp incorporated pasta. *Food Chemistry*, *289*, 723–728. https://doi.org/10.1016/j.foodchem.2019.03.081
60. Parmar, J., Sharma, P., Verma, P., Goyal, P.K. (2010). Chemopreventive action of *Syzygium cumini* on DMBA-induced skin papillomagenesis in mice. *Asian Pacific Journal of Cancer Prevention*, *11*(1), 261–265.
61. Parveen, S., Khan, A.A., Khan, Q.A. (2020). Antihyperlipidemic effect of seeds of jamun (*Eugenia jambolana*) in subjects of intermediate hyperglycemia: A pilot study. *Traditional and Integrative Medicine, 5*(4), 191–197. https://doi.org/10.18502/tim.v5i4.5164
62. Peixoto, M.P.G., Freitas, L.A.P. (2013). Spray-dried extracts from *Syzygium cumini* seeds: Physicochemical and biological evaluation. *Revista Brasileira de Farmacognosia, 23*(1), 145–152. https://doi.org/10.1590/S0102-695X2012005000124
63. Prakash, A.K.S., Devaraj, E. (2019). Cytotoxic potentials of *S. cumini* methanolic seed kernel extract in human hepatoma HepG2 cells. *Environmental Toxicology*, *34*(12), 1313–1319. https://doi.org/10.1002/tox.22832
64. Prince, P.S.M., Kamalakkannan, N., Menon, V.P. (2004). Antidiabetic and antihyperlipidaemic effect of alcoholic *Syzigium cumini* seeds in alloxan induced diabetic albino rats. *Journal of Ethnopharmacology, 91*(2–3), 209–213. https://doi.org/10.1016/j.jep.2003.11.001
65. Puljula, E., Walton, G., Woodward, M.J., Karonen, M. (2020). Antimicrobial activities of ellagitannins against *Clostridiales perfringens*, *Escherichia coli*, *Lactobacillus plantarum* and *Staphylococcus aureus. Molecules*, *25*, art. no. 3714. https://doi.org/10.3390/molecules25163714
66. Ravi, K., Sekar, D., Subramanian, S. (2004a). Hypoglycemic activity of inorganic constituents in *Eugenia jambolana* seed on streptozotocin-induced diabetes in rats. *Biological Trace Element Research*, *99*, 145–155. https://doi.org/10.1385/BTER:99:1-3:145
67. Ravi, K., Sivagnanam, K., Subramanian, S. (2004b). Anti-diabetic activity of *Eugenia jambolana* seed kernels on streptozotocin-induced diabetic rats. *Journal of Medicinal Food*, *7*(2), 187–191. https://doi.org/10.1089/1096620041224067
68. Ravi, K., Rajasekaran, S., Subramanian, S. (2005). Antihyperlipidemic effect of *Eugenia jambolana* seed kernel on streptozotocin-induced diabetes in rats. *Food and Chemical Toxicology*, *43*(9), 1433–1439. https://doi.org/10.1016/j.fct.2005.04.004
69. Ravi, K., Rajasekaran, S., Subramanian, S. (2003). Hypoglycemic effect of *Eugenia jambolana* seed kernels on streptozotocin-induced diabetes in rats. *Pharmaceutical Biology*, 41(8), 598–603. https://doi.org/10.1080/13880200390501929
70. Raza A., Butt, M.S., Iahtisham-Ul-Haq, Suleria, H.A.R. (2017). Jamun (*Syzygium cumini*) seed and fruit extract attenuate hyperglycemia in diabetic rats. *Asian Pacific Journal of Tropical Biomedicine, 7*(8), 750–754. https://doi.org/10.1016/j.apjtb.2017.07.006
71. Santos, C.A., Almeida, F.A., Quecán, B.X.V., Pereira, P.A.P., Gandra, M.M.B., Cunha, L.R., Pinto, U.M. (2020). Bioactive properties of *Syzygium cumini* (L.) Skeels pulp and seed phenolic extracts. *Frontiers in Microbiology*, *11*, art. no. 990. https://doi.org/10.3389/fmicb.2020.00990
72. Sawant, L., Singh, V.K., Dethe, S., Bhaskar, A., Balachandran, J., Mundkinajeddu, D., Agarwal, A. (2015). Aldose reductase and protein tyrosine phosphatase 1B inhibitory active compounds from *Syzygium cumini* seeds. *Pharmaceutical Biology*, *53*(8), 1176–1182. https://doi.org/10.3109/13880209.2014.967784
73. Scharf, D.R., Simionatto, E.L., Kassuya, C.A.L., Stefanello, M.E.A. (2016). Essential oil from *Eugenia jambolana* seeds: Chemical composition and changes during storage. *Journal of Essential Oil Bearing Plants, 19*(8), 2077–2082. https://doi.org/10.1080/0972060X.2016.1232608
74. Sehwag, S., Das, M. (2016). Composition and functionality of whole jamun based functional confection. *Journal of Food Science and Technology, 53*(6), 2569–2579. https://doi.org/10.1007/s13197-016-2219-7
75. Sehwag, S., Upadhyay, R., Das, M. (2018). Optimization and multivariate accelerated shelf life testing (MASLT) of a low glycemic whole jamun (*Syzygium cumini* L.) confection with tailored quality and functional attributes. *Journal of Food Science and Technology*, *55*(12), 4887–4900. https://doi.org/10.1007/s13197-018-3423-4
76. Seraglio, S.K.T., Schulz, M., Nehring, P., Betta, F.D., Valese, A.C., Daguer, H., Gonzaga, L.V., Fett, R., Costa, A.C.O. (2018). Nutritional and bioactive potential of *Myrtaceae* fruits during ripening. *Food Chemistry, 239,* 649–656. https://doi.org/10.1016/j.foodchem.2017.06.118
77. Sharma, B., Balomajumder, C., Roy, P. (2008a). Hypoglycemic and hypolipidemic effects of flavonoid rich extract from *Eugenia jambolana* seeds on streptozotocin induced diabetic rats. *Food and Chemical Toxicology*, *46*(7), 2376–2383. https://doi.org/10.1016/j.fct.2008.03.020
78. Sharma, B., Viswanath, G., Salunke, R., Roy, P. (2008b). Effects of flavonoid-rich extract from seeds of *Eugenia jambolana* (L.) on carbohydrate and lipid metabolism in diabetic mice. *Food Chemistry*, *110*(3), 697–705. https://doi.org/10.1016/j.foodchem.2008.02.068
79. Sharma, M., Li, L., Celver, J., Killian, C., Kovoor, A., Seeram, N.P., (2010). Effects of fruit ellagitannin extracts, ellagic acid, and their colonic metabolite, Urolithin A, on Wnt signaling. *Journal of Agricultural and Food Chemistry*, *58*(7), 3965–3969. https://doi.org/10.1021/jf902857v
80. Sharma, S., Pathak, S., Gupta, G., Sharma, S.K., Singh, L., Sharma, R.K., Mishra, A., Dua, K. (2017). Pharmacological evaluation of aqueous extract of *Syzigium cumini* for its antihyperglycemic and antidyslipidemic properties in diabetic rats fed a high cholesterol diet—Role of PPARγ and PPARα. *Biomedicine & Pharmacotherapy*, *89*, 447–453. https://doi.org/10.1016/j.biopha.2017.02.048
81. Sharma, S.B., Nasir, A., Prabhu, K.M., Murthy, P.S., Dev, G. (2003). Hypoglycaemic and hypolipidemic effect of ethanolic extract of seeds of *Eugenia jambolana* in alloxan-induced diabetic rabbits. *Journal of Ethnopharmacology, 85*(2–3), 201–206. https://doi.org/10.1016/S0378-8741(02)00366-5

82. Sharma, S.B., Rajpoot, R., Nasir, A., Prabhu, K.M., Murthy, P.S. (2011a). Ameliorative effect of active principle isolated from seeds of *Eugenia jambolana* on carbohydrate metabolism in experimental diabetes. *Evidence-Based Complementary and Alternative Medicine*, *2011*, art. no. 789871.
https://doi.org/10.1093/ecam/nep233
83. Sharma, S.B., Tanwar, R.S., Nasir, A., Prabhu, K.M. (2011b). Antihyperlipidemic effect of active principle isolated from seed of *Eugenia jambolana* on alloxan-induced diabetic rabbits. *Journal of Medicinal Food, 14*(4), 353–359.
https://doi.org/10.1089/jmf.2010.1227
84. Shelke, G., Kad, V., Yenge, G., Desai, S., Kakde, S. (2020). Utilization of jamun pomace as functional ingredients to enhance the physico-chemical and sensory characteristics of ice cream. *Journal of Food Processing and Preservation*, *44*(10), art. no. e14736.
https://doi.org/10.1111/jfpp.14736
85. Shinde, J., Taldone, T., Barletta, M., Kunaparaju, N., Hu, B., Kumar, S., Placido, J., Zito, S.W. (2008). α-Glucosidase inhibitory activity of *Syzygium cumini* (Linn.) Skeels seed kernel *in vitro* and in Goto–Kakizaki (GK) rats. *Carbohydrate Research*, *343*(7), 1278–1281.
https://doi.org/10.1016/j.carres.2008.03.003
86. Shrikanta, A., Kumar, A., Govindaswamy, V. (2015). Resveratrol content and antioxidant properties of underutilized fruits. *Journal of Food Science and Technology*, *52*(1), 383–390.
https://doi.org/10.1007/s13197-013-0993-z
87. Sidana, S., Singh, V.B., Meena, B.L., Beniwal, S., Singh, K., Kumar, D., Singla, R. (2017). Effect of *Syzygium cumini* (jamun) seed powder on glycemic control: A double–blind randomized controlled trial. *Journal of Medical Society*, *31*(3), 185–189.
https://doi.org/10.4103/jms.jms_62_16
88. Singh, C.S., Paswan, V.K., Rai, D.C. (2019). Process optimization of spray dried jamun (*Syzygium cumini* L.) pulp powder. *LWT – Food Science and Technology*, *109*, 1–6.
https://doi.org/10.1016/j.lwt.2019.04.011
89. Singh, A., Kocher, G.S. (2020). Standardization of seed and peel infused *Syzygium cumini* – wine fermentation using response surface methodology. *LWT – Food Science and Technology*, *134*, art. no. 109994.
https://doi.org/10.1016/j.lwt.2020.109994
90. Sisodia, S.S., Bhatnagar, M. (2009). Hepatoprotective activity of *Eugenia jambolana* Lam. in carbon tetrachloride treated rats. *Indian Journal of Pharmacology, 41*(1), 23–27.
https://doi.org/10.4103/0253-7613.48888
91. Sridhar, S.B., Sheetal, U.D., Pai, M.R., Shastri, M.S. (2005). Preclinical evaluation of the antidiabetic effect of *Eugenia jambolana* seed powder in streptozotocin-diabetic rats. *Brazilian Journal of Medicinal and Biological Research, 38*(3), 463–468.
https://doi.org/10.1590/S0100-879X2005000300018
92. Syama, H.P., Arun, K.B., Sinumol, G., Dhanya, R., Anusree, S.S., Nisha, P., Shankar, L.R., Sundaresan, A., Jayamurthy, P. (2018). *Syzygium cumini* seed exhibits antidiabetic potential via multiple pathways involving inhibition of α-glucosidase, DPP-IV, glycation, and ameliorating glucose uptake in L6 cell lines. *Journal of Food Processing and Preservation, 42*(2), art. no. e13464.
https://doi.org/10.1111/jfpp.13464
93. Tan, M., Zhao, Q., Zhao, B. (2021). Physicochemical properties, structural characterization and biological activities of polysaccharides from quinoa (*Chenopodium quinoa* Willd.) seeds. *Journal of Biological Macromolecules, 193*, Part B, 1635–1644.
https://doi.org/10.1016/j.ijbiomac.2021.10.226
94. Thiyagarajan, G., Muthukumaran, P., Kumar, B.S., Muthusamy, V.S., Lakshmi, B.S. (2016). Selective inhibition of PTP1B by vitalboside A from *Syzygium cumini* enhances insulin sensitivity and attenuates lipid accumulation via partial agonism to PPARc: *In vitro* and *in silico* investigation. *Chemical Biology & Drug Design*, *88*(2), 302–312.
https://doi.org/10.1111/cbdd.12757
95. Ud Din, S., Jaskani, M.J., Naqvi, S.A., Awan, F.S. (2020). Diversity and divergence in domesticated and wild jamun (*Syzygium cumini*) genotypes of Pakistan. *Scientia Horticulturae*, *273*, art. no. 109617.
https://doi.org/10.1016/j.scienta.2020.109617
96. Ulla, A., Alam, M.A., Sikder, B., Sumi, F.A., Rahman, M.M., Habib, Z.F., Mohammed, M.K., Subhan, N., Hossain, H., Reza, H.M. (2017). Supplementation of *Syzygium cumini* seed powder prevented obesity, glucose intolerance, hyperlipidemia and oxidative stress in high carbohydrate high fat diet induced obese rats. *BMC Complementary and Alternative Medicine*, *17*(1), art. no. 289.
https://doi.org/10.1186/s12906-017-1799-8
97. VenuGopal, K.S., Anu-Appaiah, K.A. (2017). Seed incorporation during vinification and its impact on chemical and organoleptic properties in *Syzygium cumini* wine. *Food Chemistry*, *237*, 693–700.
https://doi.org/10.1016/j.foodchem.2017.05.160
98. Vijayanand, P., Jagan Mohan Rao, L., Narasimham, P. (2001). Volatile flavour components of jamun fruit (*Syzygium cumini* L). *Flavour and Fragrance Journal, 16* (1), 47–49.
https://doi.org/10.1002/1099-1026(200101/02)16:1<47::AID-FFJ944>3.0.CO;2-L
99. Yadav, M., Lavania, A., Tomar, R., Prasad, G.B.K.S., Jain, S., Yadav, H. (2010). Complementary and comparative study on hypoglycemic and antihyperglycemic activity of various extracts of *Eugenia jambolana* seed, *Momordica charantia* fruits, *Gymnema sylvestre*, and *Trigonella foenum graecum* seeds in rats. *Applied Biochemistry and Biotechnology*, *160*, 2388–2400.
https://doi.org/10.1007/s12010-009-8799-1
100. Yadav, S.S., Meshram, G.A., Shinde, D., Patil, R.C., Manohar, S.M., Upadhye, M.V. (2011). Antibacterial and anticancer activity of bioactive fraction of *Syzygium cumini* L. seeds. *HAYATI Journal of Biosciences*, *18*(3), 118–122.
https://doi.org/10.4308/hjb.18.3.118
101. Yadav, A.K., Saraswat, S., Sirohi, P., Rani, M., Srivastava, S., Singh, M.P., Singh, N.K. (2017). Antimicrobial action of methanolic seed extracts of *Syzygium cumini* Linn. on *Bacillus subtilis*. *AMB Express*, *7*, art. no. 196.
https://doi.org/10.1186/s13568-017-0500-4
102. Żary-Sikorska, E., Fotschki, B., Kosmala, M., Milala, J., Matusevicius, P., Rawicka, A., Juśkiewicz, J. (2021). Strawberry polyphenol-rich fractions can mitigate disorders in gastrointestinal tract and liver functions caused by a high-fructose diet in experimental rats. *Polish Journal of Food and Nutrition Sciences*, *71*(4), 423–440.
https://doi.org/10.31883/pjfns/143057

Pol. J. Food Nutr. Sci., 2022, Vol. 72, No. 3, pp. 229–238
On-line ISSN: 2083-6007
Print ISSN: 1230-0322
DOI: 10.31883/pjfns/151750
http://journal.pan.olsztyn.pl

Original article
Section: Nutritional Research

Effect of Chromium Picolinate and Chromium Nanoparticles Added to Low- or High-Fat Diets on Chromium Biodistribution and the Blood Level of Selected Minerals in Rats

Anna Stępniowska[1], *Jerzy Juśkiewicz*[2]*, *Krzysztof Tutaj*[1], *Joanna Fotschki*[3], *Bartosz Fotschki*[2], *Katarzyna Ognik*[1]

[1]*Department of Biochemistry and Toxicology, Faculty of Animal Science and Bioeconomy,*
University of Life Sciences in Lublin, Akademicka 13, 20–950 Lublin, Poland
[2]*Department of Biological Functions of Food, Division of Food Science,*
Institute of Animal Reproduction and Food Research of the Polish Academy of Sciences, Tuwima 10, 10–748 Olsztyn, Poland
[3]*Department of Immunology and Food Microbiology, Division of Food Science,*
Institute of Animal Reproduction and Food Research of the Polish Academy of Sciences, Tuwima 10, 10–748 Olsztyn, Poland

Key words: minerals, chromium, nanoparticles, high-fat diet

The metabolism of chromium (Cr), calcium (Ca), phosphorus (P), iron (Fe), copper (Cu), and zinc (Zn) is interconnected, and their deficiency or excessive accumulation may lead to various disturbances, including anemia and diabetes. The current research was undertaken to determine whether low-fat or high-fat diets with the Cr(III) addition in the form of picolinate (CrPic) or nanoparticles (CrNPs) have an interactive effect on the retention and accumulation of this element in organs and the content of P, Ca, Fe, Cu and Zn in the blood plasma of rats. The experiment was performed using 48 outbred male Wistar rats fed a low-fat or high-fat semi-purified rat diet with dietary addition of chromium at a dose of 0.3 mg/kg body weight. The obtained results point to the paramount importance of the dietary Cr form on the excretion pattern of this microelement. It has been found that CrNPs were to a greater extent excreted from the rat's body *via* urine and feces in comparison to CrPic, as indicated by the values of the Cr retention index (44.4 *vs.* 65.9%, respectively). The additional dietary Cr, irrespective of its form and diet type, was not accumulated in the analyzed internal organs, *i.e.* brain, spleen, kidneys, liver, thigh bone, and thigh muscle. It should be stressed that dietary CrPic, unlike CrNPs, added to the high-fat diet adversely reduced plasma concentration of vital minerals in comparison to the levels observed in rats fed the low-fat diet, *i.e.* Zn (60.5 *vs.* 69.9 μM), Cu (13.6 *vs.* 15.7 μM), and P (1.12 *vs.* 1.30 μM). In turn, the CrNPs, but not CrPic, added to the high-fat diet decreased plasma Fe level (1.41 *vs.* 2.43 μM).

INTRODUCTION

The available literature provides ample evidence that trivalent chromium (Cr(III)) is an important micromineral actively involved in the metabolic fate of carbohydrates, lipids, and proteins [Dworzański *et al*., 2020, 2021; Inanç *et al*., 2006; Ognik *et al*., 2021; Sahin *et al*., 2011; Suksomboon *et al*., 2014; Tuzcu *et al*., 2011]. On the other hand, there are many unanswered questions about Cr(III) supplementation as there are also articles questioning its importance [Stearns, 2000]. Chromium's advantage is that its safety was confirmed by no detrimental health consequences of dietary inclusion of trivalent Cr in animal experiments [Pechova & Pavlata, 2007]. In the released opinion of the European Food Safety Authority (EFSA), Cr(III) should not be considered as an essential nutrient [EFSA, 2014], but it is currently deemed a stock supplementary ingredient.

The intestinal tract is the main route of Cr(III) entering the internal tissues. In rodents, its most active absorption processes occur in the jejunum; while its absorption is less effective in the ileum and duodenum [Pechova & Pavlata, 2007]. Chromium is absorbed from the intestine to a little extent, with the absorption rate ranging from 0.4% to 2.0%. The retention rate of Cr from inorganic and organic species has been reported at less than 3% for the former and ten times higher for the latter [Lyons, 1994]. It should be stressed that the literature *in vivo* data describing the Cr accumulation in internal tissues and organs is relatively scarce [Anderson *et al*., 1996; Chang *et al*., 1992; Lindemann *et al*., 2008; Şahin *et al*., 2001; Staniek *et al*., 2013].

High blood insulin level was shown as a diminishing factor in regard to Cr cycled in the body as chromium is incorporated to insulin-dependent cells *via* the low molecular weight chromium-binding substance (LMWCr) [Davis, 1997].

---

* Corresponding Author:
E-mail: j.juskiewicz@pan.olsztyn.pl (J. Juśkiewicz)

Submitted: 30 May 2022
Accepted: 30 June 2022
Published on-line: 27 July 2022

Król *et al*. [2014] found that the administration of a high-fat diet caused elevated insulin levels in rat serum, regardless of Cr dietary application (applied doses of 10 or 50 mg Cr propionate per kg diet). It is worth noting that hepatic Cr accumulation may be enhanced under conditions of insulin-related disturbances. Studies on Cr distribution in rat tissues have demonstrated its highest content in the kidneys [Prescha *et al*., 2014]. Previous studies addressing the impact of dietary Cr on tissue levels of other mineral components have shown a significant interaction of Cr with Fe [Anderson *et al*., 1996; Lindemann *et al*., 2008; Yoshida *et al*., 2010]. Dietary Cr(III) has been reported to affect the metabolism of other macro- and micro-elements, for instance increased Zn level and diminished that of Cu [Vlizlo *et al*., 2014]. The maintenance of the right, balanced physiological status of trace minerals, *i.e.* Fe, Zn, Cu, and Cr, seems to be of paramount importance. Undoubtedly, the metabolic fate of Fe, Cr, Cu, and Zn is mutually dependent and the body's mineral status and may greatly affect the occurrence of several physiological and metabolic disturbances, *e.g.* diabetes, anemia, or insulin-resistance.

The current research was undertaken to determine whether low-fat or high-fat diets with the addition of Cr in the form of chromium picolinate or nanoparticles have an interactive effect on the retention and accumulation of this element in organs and the contents of other minerals (P, Ca, Fe, Cu and Zn) in the blood plasma of rats.

MATERIAL AND METHODS

Chromium used in experiments

Chromium in the two forms was used as the additive to rat diets: chromium nanoparticles (CrNPs) and chromium picolinate (CrPic). CrNPs powder (with spherical morphology) was characterized by high purity (999 g/kg), large surface area (6–8 m^2/g), bulk density of 0.15 g/mL, and true density of 8.9 g/mL and was acquired in SkySpring Nanomaterials Inc. (Houston, TX, USA). CrPic was purchased in Merck Co. (Darmstadt, Germany). Its purity was also high, >980 g/kg.

Animals

The experiment was performed using 48 outbred male Wistar rats (Cmdb:Wi CMDB) fed a low-fat or high-fat semi-purified rat diet (LFD and HFD, respectively) with dietary addition of chromium nanoparticles or chromium picolinate. The study schema consisted of two periods, *i.e.* initial and experimental, each of 9 weeks. During the initial 9-wk period, the rats aged 6-wk were fed a HFD. After the initial period, the high-fat rats were randomly divided into 4 groups with $n=12$ per group and fed, for the subsequent 9-wk, the following dietary treatments: the LFD-CrPic group was fed a standard low-fat diet supplemented with chromium picolinate; the LFD-CrNPs group – a standard low-fat diet supplemented with chromium nanoparticles; the HFD-CrPic group – a high-fat diet supplemented with chromium picolinate; and the HFD-CrNPs group – a high-fat diet supplemented with nanoparticle chromium (Table 1). The rats were administered chromium in a daily dose of 0.3 mg/kg of body weight (BW proposed by the EFSA NDA Panel [2014] as a highly safe dose without any harmful side-effects. In order to maintain a safe and comparable regimen while preparing the diets, both sources of Cr were added along with rapeseed oil and not in the mineral mix.

TABLE 1. Composition of low-fat diet (LFD) and high-fat diet (HFD) with chromium picolinate (CrPic) and chromium nanoparticles (CrNPs) used in the experiment (g/kg).

	LFD-CrPic	HFD-CrPic	LFD-CrNPs	HFD-CrNPs
Casein[1]	148	148	148	148
DL-Methionine	2	2	2	2
Cellulose[2]	80	30	80	30
Choline chloride	2	2	2	2
Cholesterol	3	3	3	3
Vitamin mix[3]	10	10	10	10
Mineral mix[4]	35	35	35	35
Maize starch[5]	640	520	640	520
Rapeseed oil	80 (with Cr-Pic)[6]	80 (with Cr-Pic)[6]	80 (with Cr-NP)[6]	80 (with Cr-NP)[6]
Lard	0	170	0	170

[1] Casein preparation: crude protein 89.7 g/100 g, crude fat 0.3 g/100 g, ash 2.0 g/100 g, and water 8.0 g/100 g.

[2] α-Cellulose (SIGMA, Poznan, Poland), main source of dietary fibre.

[3] AIN-93G-VM [Reeves, 1997], mix (g/kg): 3.0 nicotinic acid, 1.6 Ca pantothenate, 0.7 pyridoxine-HCl, 0.6 thiamine-HCl, 0.6 riboflavin, 0.2 folic acid, 0.02 biotin, 2.5 vitamin B_{12} (cyanocobalamin, 0.1% in mannitol), 15.0 vitamin E (all-*rac*-α-tocopheryl acetate, 500 IU/g), 0.8 vitamin A (all-*trans*-retinyl palmitate, 500,000 IU/g), 0.25 vitamin D_3 (cholecalciferol, 400,000 IU/g), 0.075 vitamin K_1 (phylloquinone), 974.655 powdered sucrose.

[4] Mineral mix, mix (g/kg): 357 calcium carbonate anhydrous, 196 dipotassium phosphate, 70.78 potassium citrate, 74 sodium chloride, 46.6 potassium sulfate, 24 magnesium oxide, 18 microelement mixture, 213.62 starch (to 1 kg). Microelement mixture, mix (g/kg): 31 iron (III) citrate (16.7% Fe), 4.5 zinc carbonate (56% Zn), 23.4 manganese (II) carbonate (44.4% Mn), copper carbonate (55.5% Cu), 0.04 potassium iodide, citric acid to 100 g.

[5] Maize starch preparation: crude protein 0.6 g/100 g, crude fat 0.9 g/100 g, ash 0.2 g/100 g, total dietary fibre 0 g/100 g, and water 8.8 g/100 g.

[6] The dosage of CrPic or CrNPs: 0.3 mg/kg body weight.

The *in vivo* protocol including all manipulations planned to be performed on living rats was in compliance with regulations and ordinances in force in Poland, and Directive 2010/63/EU for animal use in research and education. The application for conducting *in vivo* experiment was accepted by the National Ethics Committee for Animal Experiments (Approval No. 73/2021).

Throughout the study, all animals were kept individually in stainless steel cages in an animal laboratory room with proper for the rodents inside temperature (22±1°C), relative humidity 60±5%, a 12-h day-night regimen, and an air exchange rate of 15 changes per 60 min. The rats were thoroughly scrutinized by the well-trained staff and the veterinarian towards a proper behaviour and health status. All humane endpoints in animal research mentioned in Directive 2010/63/EU were tailored strictly in the present study. The superordinate and the veterinarian were informed daily in the case of any sign of rat distress or pain. For 18 weeks (9-wk of the initial and 9-wk of the experimental period), the animals were provided with free access to tap water and daily amount of semipurified diets in order to keep the experimental dosage of additional dietary chromium. The diets constructed from well-known ingredients were stored at 4°C in plastic tubes for food and perishables during all the feeding period. The experimental dietary treatments for rats were constructed according to the rules described by Reeves [1997] and approved by the American Institute of Nutrition. The diets were based on casein as the main protein source, rapeseed oil as a fat source (oil was coupled with lard in the high-fat diets), and maize starch as a carbohydrate source. The experimental calculations and analyses of biological animal material were performed individually for each rat.

On day 28, the rats were relocated to the balance cages in order to conduct the Cr balance trial which enabled calculations of the Cr digestibility and retention (utilization) coefficients. The construction of the cages (TECNIPLAST S.p.A., Buguggiate, Italy) facilitates an exact collection of feces and urine excreted by an animal. The balance test consisted of a preliminary period lasting 10 days as well as a relevant balance 5-day period during which all excreted feces and urinated liquid were collected to special tubes kept then in the fridge environment. During the relevant balance days, the amounts of ingested diets and drank water were also recorded for each rat. All collected samples, *i.e.* fecal, urinal, dietary, and water ones, were analyzed for Cr content as described below.

The Cr digestibility was expressed as a percentage of the mineral ingested:

$$Cr\ digestibility\ (\%) = \frac{Cr\ intake - Cr\ excreted\ in\ feces}{Cr\ intake} \times 100 \qquad (1)$$

The Cr retention (utilization) was calculated as follows:

$$Cr\ retention\ (\%) = \frac{Cr\ intake - Cr\ excreted\ in\ feces\ and\ urine}{Cr\ intake} \times 100 \qquad (2)$$

During the entire feeding experiment, the rats were individually monitored for body weight and diet consumed. Before the termination of the rats, they were deprived of feed for 12 h but still had full access to tap water. On termination day, the animals were anesthetized with the mixture of ketamine (Ke) and xylazine (X) in 0.9% NaCl (Ke, 100 mg/kg BW; X, 10 mg/kg BW) according to the anaesthesia and euthanasia guidelines for laboratory rodents. The unconscious (a painless state) rats were then laparotomized, and their blood was collected from *caudal vena cava* into heparinized tubes in order to obtain blood plasma *via* centrifugation (350×*g*, 10 min, 4°C). Plasma samples were kept frozen at –70°C until assayed. After blood collection, the rats were euthanized by cervical dislocation in order to confirm the death. The selected internal organs and tissues (liver, kidneys, brain, spleen, thigh muscle, thigh bones) were cut off, weighed if needed, frozen in liquid nitrogen (–196°C), and stored in the low-temperature freezers at –70°C.

Mineral analysis

The concentration of minerals (Cr, P, Ca, Mg, Fe, Cu, and Zn) in the blood plasma samples (0.25 mL) and Cr content in feces, urine, water, diet, and tissue samples (0.5 g, 0.25 mL, 0.25 mL, 0.5 g and 0.5 g, respectively) were determined by flame atomic absorption spectrometry (FAAS) with the aid of a Perkin-Elmer M 5000 atomic absorption spectrometer coupled with an HGA 500 graphite furnace (PerkinElmer Life and Analytical Sciences Co., Shelton, CT, USA). The furnace program was applied to Cr determination in diets, feces, and tissues with a wavelength of 357.9 nm, drying at 110°C, ashing at 1200°C, atomization and cleaning at 2700°C. In the case of the remaining minerals, the microwave oven (Milestone MLS 1200 MEGA, Milestone, Italy) digestion with HNO_3 was applied at three subsequent periods (5 min each) with the heating power of 210, 420, and 560 W, respectively. The FAAS instrument setting and conditions followed the manufacturers' recommendations. The calibration procedure was done with the aid of the Certipure multi-element standard solution (Merck KGaA, Darmstadt, Germany). The air-acetylene oxidizing flame was used in the FAAS procedure, whereas a D_2 lamp was used for background corrections in the case of Cr, Ca, Fe and Zn determination.

Statistical analysis

In tables, the results are presented as means with standard error of the mean (SEM), the latter calculated as standard deviations (SD) divided by square root of the number of rats ($n=48$). The two-way ANOVA was applied in order to assess *p*-values for the two main effects, namely the dietary Cr form (Cr; CrPic and CrNPs) and the diet type (D; LFD and HFD) as well as for the occurrence of a significant interaction between the two main factors (Cr×D). In the case of a significant Cr×D interaction ($p<0.05$), the post-hoc Duncan's test was applied to assess statistical differences among all four experimental groups. The two-way ANOVA requires the normal distribution of samples, so the data were checked for normality *via* the Shapiro-Wilk test. The STATISTICA ver. 12.0 software (StatSoft Corp., Krakow, Poland) was used in the analysis.

RESULTS AND DISCUSSION

Long-term use of an ill-balanced diet leads to many metabolic disorders, including obesity, caused by chronic consumption of a diet rich in saturated fats [Nascimento *et al*., 2013; Orhan *et al*., 2019; Żary-Sikorska *et al*., 2021]. An increased level of dietary fat may additionally disturb the mineral homeostasis in the body [Meli *et al*., 2013; Qi *et al*., 2020; Stępniowska *et al*., 2022]. The present research showed that the total level of Cr in the HFD was higher than in the LFD, regardless of Cr form ($p<0.001$; Table 2). In turn, the calculated intake of Cr during the balance test was higher in rats fed the HFD supplemented with CrNPs than in those fed the LFD (see the significant Cr×D interaction). The aforementioned results may be partly ascribed to the formation of adducts composed of Cr nanoparticles and high levels of saturated fatty acids in the HFD treatment [Muller *et al*., 2017]. Irrespective of diet type, higher urinary Cr excretion was noted when dietary chromium was in the CrNPs form in comparison to that added as CrPic ($p=0.001$). Two-way ANOVA showed the Cr×D interaction also for fecal Cr excretion ($p<0.001$), total Cr excretion ($p<0.001$), Cr digestibility ($p<0.001$),

TABLE 2. Chromium excretion patterns in the digestibility and retention test in rats fed experimental diets.

	Cr content of diet (mg/kg)	Cr intake from diet (mg/5 d)	Excretion of Cr in feces (mg/5 d)	Excretion of Cr in urine (mg/5 d)	Total Cr excretion (mg/5 d)	Cr digestibility (%)	Cr retention (%)
LFD-CrPic	5.55	0.475^{ab}	0.097^{b}	0.011	0.108^{b}	79.6^{a}	77.2^{a}
HFD-CrPic	6.60	0.513^{a}	0.224^{a}	0.009	0.233^{a}	56.3^{b}	54.5^{b}
LFD-CrNPs	5.30	0.442^{b}	0.260^{a}	0.015	0.276^{a}	40.9^{c}	37.5^{c}
HFD-CrNPs	6.90	0.498^{a}	0.227^{a}	0.012	0.239^{a}	53.6^{b}	51.3^{b}
SEM	*0.22*	*0.017*	*0.012*	*0.001*	*0.012*	2.6	2.2
Diet type (D)							
LFD	4.16^{b}	0.351	0.138	0.011	0.150	59.0	55.3
HFD	5.60^{a}	0.422	0.174	0.008	0.182	60.9	59.0
Cr addition (Cr)							
Cr-Pic	6.08	0.494	0.160	0.010^{b}	0.170	67.9	65.9
Cr-NPs	6.10	0.470	0.244	0.014^{a}	0.257	47.3	44.4
p-Value							
D effect	<0.001	<0.001	0.008	0.078	0.016	0.542	0.254
Cr effect	0.101	<0.001	<0.001	0.001	<0.001	<0.001	<0.001
Cr×D interaction	0.102	<0.001	<0.001	0.924	<0.001	<0.001	<0.001

The LFD-CrPic group was fed a standard low-fat diet with supplementation of chromium picolinate; the HFD-CrPic group was subjected to a high-fat diet with chromium picolinate supplementation; the LFD-CrNPs group was fed a standard low-fat diet with supplementation of chromium nanoparticles; the HFD-CrNPs group was fed a high-fat diet with nanoparticle chromium supplementation. The amount of chromium administered to each rat was 0.3 mg/kg body weight. SEM, standard error of the mean (n=48). ^{a,b}Mean values within a column with unlike superscript letters differ significantly ($p<0.05$); differences among the groups (LFD-CrPic, HFD-CrPic, LFD-CrNPs, HFD-CrNPs) are indicated with superscripts only in the case of a statistically significant interaction Cr×D ($p<0.05$). The Cr intake from the diet was the same as total Cr intake (tap water provided to rats contained no Cr).

and Cr retention ($p<0.001$). The nature of the Cr×D interaction for fecal and total Cr excretion was in significantly lower amounts of Cr removed from the body, mainly *via* the fecal route, in the rats administered LFD-CrPic as compared to the remaining three dietary treatments ($p<0.05$ *vs*. HFD-CrPic, LFD-CrNPs, and HFD-CrNPs). The Cr×D interaction showed that the highest percentage of Cr digestibility and retention indices followed the dietary treatments with LFD-CrPic, while the lowest values of these indices were noted in the rats fed LFD-CrNPs (in both cases $p<0.05$ *vs*. all other groups). It has been reported that Cr nanoparticles are better absorbed from the gastrointestinal tract than their organic counterparts [Stępniowska *et al*., 2022]. Indeed, in the present study, CrNPs were well absorbed in the intestine but at the same time that Cr form was not efficiently retained in the body's tissues and organs, as indicated by considerably diminished Cr retention (utilization) percentage. That process was clearly depicted under the standard low-fat dietary treatment by the highest and lowest retention values for CrPic and CrNPs, respectively. The addition of chromium in the form of CrPic to the high-fat diet resulted in decreased digestibility and retention of Cr in the rats, which corroborates our previous findings on the effect of dietary high-fat environment on the mineral utilization in the body [Stępniowska *et al*., 2022]. Chromium picolinate has been shown to exhibit hydrophobic properties and, therefore, to be easily absorbed from the gastrointestinal tract in comparison to other forms of Cr, nicotinate or chloride, available in popular mineral supplements [DiSilvestro & Dy, 2007]. Moreover, it has been found relatively stable in human gastric juice for over three hours, requiring a high concentration of acid (0.1 M) to break the bonds between Cr and picolinic acid [Lamson & Plaza, 2002]. The relatively high stability of chromium picolinate may also partly explain the lesser excretion of dietary CrPic from the rat's body as compared to the novel dietary form of chromium, *i.e.* CrNPs. In the present experiment, regardless of diet type, a greater urinal Cr excretion followed the dietary treatment with CrNPs *vs.* rats administered dietary CrPic (Table 2). Wang *et al.* [2012], who administered Cr in the form of CrPic or CrNPs at a dietary dose of 200 μg/kg to pigs, did not observe different fecal and urinal excretion pattern between those two forms of chromium. In turn, Stępniowska *et al.* [2022] noted a similar amount of chromium excreted with urine in rats fed diets supplemented with different chromium forms, *i.e.* picolinate, chromium-methionine, and as nanoparticles. At the same time, the rats fed diets with Cr nanoparticles excreted considerably more Cr in comparison to the animals subjected to dietary treatments with chromium picolinate or chromium-methionine.

The dietary treatments tested, *i.e.* HFD or LFD with the addition of Cr in the form of CrNPs or CrPic, did not differ among each other with respect to the Cr accumulation in the brain, spleen, kidney, liver, bones, and muscle of rats (Table 3). Jamal *et al.* [1991] observed that Cr was easily

TABLE 3. Chromium content in selected tissues of rats fed experimental diets (μg/g).

	Brain	Spleen	Kidney	Liver	Bones	Muscle
LFD-CrPic	0.133	0.563	1.03	0.438	0.311	0.169
HFD-CrPic	0.131	0.560	1.03	0.448	0.310	0.166
LFD-CrNPs	0.133	0.564	1.03	0.439	0.313	0.168
HFD-CrNPs	0.130	0.562	1.04	0.439	0.311	0.169
SEM	*0.001*	*0.002*	*0.004*	*0.002*	*0.001*	*0.001*
Diet type (D)						
LFD	0.132	0.564	1.03	0.440	0.312	0.169
HFD	0.130	0.560	1.03	0.443	0.310	0.167
Cr addition (Cr)						
Cr-Pic	0.132	0.561	1.03	0.443	0.310	0.167
Cr-NPs	0.131	0.563	1.03	0.439	0.312	0.169
p-Value						
D effect	0.219	0.376	0.870	0.540	0.106	0.331
Cr effect	0.950	0.938	0.917	0.718	0.499	0.670
Cr×D interaction	0.938	0.965	0.525	0.584	0.491	0.235

The LFD-CrPic group was fed a standard low-fat diet with supplementation of chromium picolinate; the HFD-CrPic group was subjected to a high-fat diet with chromium picolinate supplementation; the LFD-CrNPs group was fed a standard low-fat diet with supplementation of chromium nanoparticles; the HFD-CrNPs group was fed a high-fat diet with nanoparticle chromium supplementation. The amount of chromium administered to each rat was 0.3 mg/kg body weight. SEM, standard error of the mean ($n=48$).

accumulated in the kidneys of chickens fed diets containing potassium chromate. In our previous study on Wistar rats subjected to dietary treatments with nano-copper, those small nanoparticles were accumulated in the brain tissue, while such an effect was not observed in the case of $CuCO_3$ added to a mineral mixture [Ognik *et al*., 2020]. An interesting observation was made by Staniek [2019] in female rats fed diets containing low (1 mg/kg), medium (50 mg/kg) and high (500 mg/kg) contents of chromium(III) without (recommended level 45 mg/kg) or with dietary excess (180 mg/kg) of iron. The author scrutinized the effects of the aforementioned treatments on Cu and Zn status in laboratory animals and found decreased Zn contents in the liver, spleen, and kidneys followed Cr(III) addition, especially when Cr(III) was provided at higher dosages. It was quite surprising that there was no interaction between the dietary chromium and the excessive supply of iron on the Cu and Zn status in the rat organism. The two-way ANOVA showed that, irrespective of the dietary additional Cr form, the HFD treatment resulted in a decrease in blood plasma Ca concentration ($p<0.05$ *vs*. LFD; Table 4). A significant Cr×D interaction was observed with respect to the plasma levels of Zn ($p=0.008$), Cu ($p=0.001$), P ($p=0.024$), and Fe ($p=0.014$). In the case of plasma Zn, Cu, and P concentrations, the nature of the interaction was that the LFD-CrPic group excelled significantly the HFD-CrPic one and such differences were not observed between both dietary CrNPs counterparts. Apart from the aforementioned differences between LFD-CrPic and HFD-CrPic groups, the latter animals had additionally a significantly lower plasma Cu level than both CrNPs groups and a lower plasma P level than the LFD-CrNPs rats. The Cr×D effect showed the lowest plasma Fe concentration in the rats administered HFD-CrNPs in comparison to all other groups.

It has been reported that different dietary doses and forms of additional chromium may further affect the retention and tissue distribution of other macro- and microelements [Chang *et al*., 1992; Dogukan *et al*., 2009; Staniek *et al*., 2013]. It should be noted that those effects of dietary chromium might be modulated by the ingested diet type. Indeed, in the present study, the HFD considerably diminished the plasma Ca level compared to LFD. It has been reported that long-term consumption of diets dense in energy derived from fats resulted in reduced gastrointestinal Ca absorption by creating hardly soluble Ca soaps in the intestinal contents [Wang *et al*., 2016]. In addition, the ingestion of a high-fat diet may reduce the expression of genes related to calcium transport, *i.e*. calbindin-D9K, plasma membrane calcium ATPase (PMCA1b), Na-Ca exchanger [Xiao *et al*., 2010]. High-fat diets, which are typically high in saturated fatty acids, have been shown to negatively affect bone mineral density in growing rats [Macri *et al*., 2012]. McCarty [1995] observed that depressed excretion of calcium and hydroxyproline in older (postmenopausal) women followed the supplementary consumption of chromium in the form of picolinate and that this effect might be the cause for elevated bone resorption processes in those patients. The body's calcium management is closely related to the metabolism of phosphorus. The present experiment showed that blood plasma P concentration was substantially ($p<0.05$)

TABLE 4. Concentration of selected minerals in blood plasma of rats fed experimental diets.

	Zn (μM)	Cu (μM)	Mg (mM)	Ca (mM)	P (mM)	Fe (μM)
LFD-CrPic	69.9^{a}	15.7^{a}	0.549	2.26	1.30^{a}	2.73^{a}
HFD-CrPic	60.5^{b}	13.6^{b}	0.558	2.31	1.12^{b}	2.86^{a}
LFD-CrNPs	65.1^{ab}	16.0^{a}	0.604	2.32	1.35^{a}	2.43^{a}
HFD-CrNPs	64.4^{ab}	16.2^{a}	0.561	2.17	1.17^{ab}	1.41^{b}
SEM	*1.2*	*0.6*	*0.007*	*0.03*	*0.02*	*0.11*
Diet type (D)						
LFD	63.7	16.9	0.563	2.33^{a}	1.26	2.83
HFD	63.1	18.6	0.550	2.21^{b}	1.16	2.19
Cr addition (Cr)						
Cr-Pic	65.2	14.7	0.554	2.29	1.21	2.80
Cr-NPs	64.8	16.1	0.583	2.25	1.26	1.92
p-Value						
D effect	0.785	0.085	0.364	0.026	0.024	<0.001
Cr effect	0.136	<0.001	0.121	0.825	0.249	<0.001
Cr×D interaction	0.008	0.001	0.298	0.064	0.024	0.014

The LFD-CrPic group was fed a standard low-fat diet with supplementation of chromium picolinate; the HFD-CrPic group was subjected to a high-fat diet with chromium picolinate supplementation; the LFD-CrNPs group was fed a standard low-fat diet with supplementation of chromium nanoparticles; the HFD-CrNPs group was fed a high-fat diet with nanoparticle chromium supplementation. The amount of chromium administered to each rat was 0.3 mg/kg body weight. SEM, standard error of the mean (n=48). ^{a,b}Mean values within a column with unlike superscript letters differ significantly ($p<0.05$); differences among the groups (LFD-CrPic, HFD-CrPic, LFD-CrNPs, HFD-CrNPs) are indicated with superscripts only in the case of a statistically significant interaction Cr×D ($p<0.05$).

decreased in the rats fed the high-fat diet supplemented with CrPic as compared not only to the rats fed the LFD-CrPic but also to those administered LFD-CrNPs. Our recent research on growing rats revealed blood depletion of Ca, P, Mg, and Zn under the treatment with a diet rich in saturated fats (lard) [Stępniowska *et al*., 2022]. Interestingly, among three sources of additional chromium (chromium picolinate, chromium methionine, chromium nanoparticles) analyzed in that study, the greatest depletion effect of blood P concentration was upon Cr picolinate and the lowest one (insignificant compared to the control non-supplemented group) when the chromium-methionine was applied. The aforementioned effect should be ascribed to the lower consumption of a high-energy diet and elevated P fecal excretion in rats fed HFD [Stępniowska *et al*., 2022]. Nevertheless, additional research is needed in order to explain the exact mechanism of that phenomenon. Our previous work on growing chickens revealed that Cr picolinate added to a diet at 3 mg/kg, but not at 6 mg/kg dietary dose, significantly reduced blood plasma P concentration as compared to the control non-supplemented group [Stępniowska *et al*., 2020].

It has been reported that, when ingested, minerals (Cr and Fe) contest over transferrin as a transport protein in the metabolic pathways [Quarles *et al*., 2010]. A study by Sun *et al*. [1999] showed that the form of dietary Cr seemed to be of paramount importance in its final effects on Fe metabolism. In that study, the dietary addition of $[\mathrm{Cr_3O(O_2CCH_2CH_3)_6(H_20)_3}]^+$ had no effect on the hepatic content of Fe in rats, while the dietary LMWCr did otherwise and caused a drop in liver Fe content. The mutual action of Cr and Fe in the body as well as their metabolism might be affected by different agents, *e.g.* the physiological state of tested animals as well as the physical and chemical structure of Cr added to a diet. In our research, a considerable decrease in blood plasma Fe concentration followed the dietary application of CrNPs to HFD, and that effect was noted compared to all other three dietary treatments. It is well known that the blood Fe concentration largely depends on its absorption rate in the duodenum and that this element is absorbed into enterocytes mainly by divalent metal transporter 1 (DMT1) [Szabo *et al*., 2021]. According to Jiang *et al*. [2018], DMT1 levels might be reduced significantly in the duodenum of rats following the feeding regimen on diets rich in saturated fats, pointing at DMT1 as the factor reducing duodenal iron absorption. In our very recent work, the rats receiving dietary chromium nanoparticles had a higher iron blood concentration compared to the animals administered chromium in the picolinate form, irrespective of low- or high-fat dietary regimen [Stępniowska *et al*., 2022]. The difference in Fe blood concentration in relation to the present work was probably due to the fact that the rats in the previous study were younger and not subjected to the preliminary high-fat dietary feeding period. In addition, in the present study, a higher dietary intake of Cr was reported in the rats from the HFD-CrNPs group than in those from the LFD-CrNPs group (Table 4). Iron and chromium(III) share the transportation route to the tissues *via* a similar vehicle, namely transferrin protein consisting of two C and N lobes. The binding of Fe(III) to the former lobe is about 20 times higher than to the latter one. Deng *et al*. [2016] observed that Cr(III) distrained two Fe(III) binding sites of apotransferrin. It may be speculated that in the case of relatively high dietary supplementation of Cr, as in the present experiment, the binding sites for Fe in transportation and gripping proteins might be taken by chromium. Such possibilities of the diminishing effects of dietary chromium on the potency of transferrin and apotransferrin to capture Fe(III) have been proposed by other authors [Quarles *et al*., 2011; Staniek & Krejpcio, 2017; Vincent & Love, 2012]. Considering blood Ca concentration, its chronically low level is considered as a potent detrimental factor leading to impeded muscle contractility [Moe, 2005], while a decreased Fe pool in the body may impair the redox status and erythropoiesis intensification [Robach *et al*., 2007]. The available literature shows some discrepancies with regard to mutual iron and chromium competition, like in the case of transporting proteins [Quarles *et al*., 2010, 2011; Vincent & Love 2012] or possible synergistic effect of those minerals against anemia [Angelova *et al*., 2014]. But there is no doubt that the level of iron in the internal tissues, including blood, plays the main/important role in the metabolic fate of other trace elements, *e.g.* Zn and Cu. Our research showed that feeding rats with the HFD-CrPic compared to LFD-CrPic resulted in decreased levels of Cu and Zn in their blood plasma and that this effect was not dependent on the Fe blood concentration (Table 4). According to de Luis *et al*. [2013], obese patients suffer serum zinc depletion in comparison to the consumers with normal BW mass. A recent study on mild-diabetic rats showed that dietary addition of chromium (0.75 mg/kg BW) as Cr(III)-glycinate or Cr(III)-picolinate redressed the Cu/Zn balance in blood and selected tissues, *i.e.* kidneys and heart [Król *et al*., 2020].

Experiments conducted on laboratory animals with undisturbed [Anderson *et al*., 1996; Chang *et al*., 1992; Zha *et al*., 2007] and disturbed metabolism [Król & Krejpcio, 2010] have shown that kidneys are very sensitive organs to Cr dietary supplementation. In the present study, there were no side-effects in kidneys followed the dietary treatments with 0.3 mg/kg BW of Cr in the form of picolinate or nanoparticles (Table 3). It should be stressed that a simple comparison between different research could lead to invalid conclusions, and thus a deep insight in the subject must be done before the final claim would be drawn. It is not possible to determine the actual metabolic action of dietary chromium without considering differences in Cr administration time, dose, and form, and health condition in consumers (animals and humans). It should be noted that our study found no interactive effect of feeding rats with a low-fat or high-fat diet with the addition of CrPic or CrNPs chromium at a dose of 0.3 mg/kg BW on the accumulation of this element in internal organs. The results achieved with other type of nanoparticles presented by our research team showed that, in comparison to the commonly used $CuCO_3$, dietary copper nanoparticles to a greater extent were absorbed from the rat intestine, heavily accumulated in the brain tissue, and at the higher dose (6.5 *vs*. 3.25 mg/kg) caused damages to the rat liver [Cholewińska *et al*., 2018]. There is no doubt that more research is needed regarding dietary nanoparticle use in humans and caution is suggested when providing to public pros about a "new promising" source of trace elements in our diet.

CONCLUSIONS

Irrespective of the diet type, *i.e.* high-fat or low-fat, an enhanced excretion of chromium from the rat's body followed the dietary addition of CrNPs as compared to CrPic. It is worth noting that both sources of additional dietary chromium did not cause its accumulation in the analyzed internal organs, *e.g.* brain, spleen, liver, thigh bone, and kidneys. It should be stressed that both CrPic and CrNPs negatively modulated the mineral status of blood plasma when added to the high-fat diet, namely: the dietary CrPic reduced Zn, Cu and P concentrations while CrNPs diminished plasma Fe level.

RESEARCH FUNDING

This work was supported by the National Science Centre, Grant No. 2020/39/B/NZ9/00674.

CONFLICT OF INTERESTS

The authors have no competing interests.

ORCID IDs

B. Fotschki https://orcid.org/0000-0002-9727-7481
J. Fotschki https://orcid.org/0000-0002-0116-0909
J. Juśkiewicz https://orcid.org/0000-0003-0068-5970
K. Ognik https://orcid.org/0000-0003-4393-4092
A. Stępniowska https://orcid.org/0000-0003-2424-8935
K. Tutaj https://orcid.org/0000-0002-3742-3715

REFERENCES

1. Anderson, R.A., Bryden, N.A., Polansky, M.M., Gautschi, K. (1996). Dietary chromium effects on tissue chromium concentrations and chromium absorption in rats. *Journal of Trace Elements in Experimental Medicine*, *9*(1), 11–25. https://doi.org/10.1002/(SICI)1520-670X(199607)9:1%3C11::AID-JTRA2%3E3.0.CO;2-K
2. Angelova, M.G., Petkova-Marinova, T.V., Pogorielov, M.V., Loboda, A.N., Nedkova-Kolarova, V.N., Bozhinova, A.N. (2014). Trace element status (iron, zinc, copper, chromium, cobalt, and nickel) in iron deficiency anaemia of children under 3 years. *Anemia*, *2014*, art. no. 718089. https://doi.org/10.1155/2014/718089
3. Chang, X., Mowat, D.N., Spiers, G.A. (1992). Carcass characteristics and tissue-mineral contents of steers fed supplemental chromium. *Canadian Journal of Animal Science*, *72*(3), 663–668. https://doi.org/10.4141/cjas92-077
4. Cholewińska, E., Ognik, K., Fotschki, B., Zduńczyk, Z., Juśkiewicz, J. (2018). Comparison of the effect of dietary copper nanoparticles and one copper (II) salt on the copper biodistribution and gastrointestinal and hepatic morphology and function in a rat model. *PLoS ONE*, *13*(5), art. no. e0197083. https://doi.org/10.1371/journal.pone.0197083

5. Davis, C.M., Vincent, J.B. (1997). Chromium in carbohydrate and lipid metabolism. *Journal of Biological Inorganic Chemistry*, *2*, 675–679.
https://doi.org/10.1007/s007750050183
6. de Luis, D.A., Pacheco, D., Izaola, O., Terroba, M.C., Cuellar, L., Cabezas, G. (2013). Micronutrient status in morbidly obese women before bariatric surgery. *Surgery for Obesity and Related Diseases*, *9*(2), 323–327.
https://doi.org/10.1016/j.soard.2011.09.015
7. Deng, G., Dyroff, S.L., Lockart, M., Bowman, M.K., Vincent, J.B. (2016). The effects of the glycation of transferrin on chromium binding and the transport and distribution of chromium *in vivo*. *Journal of Inorganic Biochemistry*, *164*, 26–33.
https://doi.org/10.1016/j.jinorgbio.2016.08.008
8. Directive 2010/63/EU of the European Parliament and of the Council of 22 September 2010 on the protection of animals used for scientific purposes (2010). *Official Journal of the European Union*, L 276, 20.10.2010, pp. 33–79.
http://data.europa.eu/eli/dir/2010/63/oj
9. DiSilvestro, R.A., Dy, E. (2007). Comparison of acute absorption of commercially available chromium supplements. *Journal of Trace Elements in Medicine and Biology*, *21*(2), 120–124.
https://doi.org/10.1016/j.jtemb.2007.01.004
10. Dogukan, A., Sahin, N., Tuzcu, M., Juturu, V., Orhan, C., Onderci, M., Komorowski, J., Sahin, K. (2009). The effects of chromium histidinate on mineral status of serum and tissue in fat-fed and streptozotocin-treated type II diabetic rats. *Biological Trace Elements Research*, *131*, 124–132.
https://doi.org/10.1007/s12011-009-8351-8
11. Dworzański, W., Cholewińska, E., Fotschki, B., Juśkiewicz, J., Listos, P., Ognik, K. (2020). Assessment of DNA methylation and oxidative changes in the heart and brain of rats receiving a high-fat diet supplemented with various forms of chromium. *Animals*, *10*(9), art. no. 1470.
https://doi.org/10.3390/ani10091470
12. Dworzański, W., Sembratowicz, I., Cholewińska, E., Tutaj, K., Fotschki, B., Juśkiewicz, J., Ognik, K. (2021). Effects of different chromium compounds on hematology and inflammatory cytokines in rats fed high-fat diet. *Frontiers in Immunology*, *12*, art. no. 614000.
https://doi.org/10.3389/fimmu.2021.614000
13. EFSA. European Food Safety Authority (2014). Scientific opinion on dietary reference values for chromium. *EFSA Journal*, *12*(7), art. no. 3759.
https://doi.org/10.2903/j.efsa.2014.3759
14. Inanç, N., Uyanik, F., Sahin, H., Yaman, H., Erdem, O. (2006). Effects of chromium supplementation on body composition, leptin, ghrelin levels and selected biochemical parameters in obese women. *Trace Elements and Electrolytes*, *23*, 128–133.
https://doi.org/10.5414/TEP23128
15. Jamal, Z.M., Vjekoslav, S., Jelena, P.G., Emil, S. (1991) Distribution of chromium in the internal organs of potassium chromate treated chicks. *Veterinary and Human Toxicology*, *33*(3), 223–225.
PMID: 1858300
16. Jiang, S., Yan, K., Sun, B., Gao, S., Yang, X., Ni, Y., Ma, W., Zhao, R. (2018). Long-term high-fat diet decreases hepatic iron storage associated with suppressing TFR2 and ZIP14 expression in rats. *Journal of Agricultural and Food Chemistry*, *66*(44), 11612–11621.
https://doi.org/10.1021/acs.jafc.8b02974
17. Król, E., Krejpcio, Z. (2010). Chromium(III) propionate complex supplementation improves carbohydrate metabolism in insulin resistance rat model. *Food Chemistry and Toxicology*, *48*(10), 2791–2796.
https://doi.org/10.1016/j.fct.2010.07.008
18. Król, E., Krejpcio, Z., Iwanik, K. (2014). Supplementary chromium(III) propionate complex does not protect against insulin resistance in high-fat-fed rats. *Biological Trace Elements Research*, *157*, 147–155.
https://doi.org/10.1007%2Fs12011-013-9877-3
19. Król, E., Krejpcio, Z., Okulicz, M., Śmigielska, H. (2020). Chromium(III) glycinate complex supplementation improves the blood glucose level and attenuates the tissular copper to zinc ratio in rats with mild hyperglycaemia. *Biological Trace Element Research*, *193*, 185–194.
https://doi.org/10.1007/s12011-019-01686-7
20. Lamson, D.W., Plaza, S.M. (2002). The safety and efficacy of high-dose chromium. *Alternative Medicine Review*, *7*(3), 218–235.
PMID: 12126463
21. Lindemann, M.D,, Cromwell, G.L., Monegue, H.J., Purser, K.W. (2008). Effect of chromium source on tissue concentration of chromium in pigs. *Journal of Animal Science*, *86*(11), 2971–2978.
https://doi.org/10.2527/jas.2008-0888
22. Lyons, T.P. (1994). Biotechnology in the feed industry: 1994 and beyond. In: *Proceedings of Alltech's 10th Annual Symposium, Biotechnology in the Feed Industry*. P. Lyons, K.A. Jacques (Eds.), Nottingham University Press, UK, pp. 1–50.
23. Macri, E.V., Gonzales Chaves, M.M., Rodriguez. P.N., Mandalunis, P., Zeni, S., Lifshitz, F., Friedman, S.M. (2012). High-fat diets affect energy and bone metabolism in growing rats. *European Journal of Nutrition*, *51*, 399–406.
https://doi.org/10.1007/s00394-011-0223-2
24. McCarty, M.F. (1995). Anabolic effects of insulin on bone suggest a role for chromium picolinate in preservation of bone density. *Medical Hypotheses*, *45*(3), 241–246.
https://doi.org/10.1016/0306-9877(95)90112-4
25. Meli, R., Mattace Raso, G., Irace, C., Simeoli, R., Di Pascale, A., Paciello, O., Pagano, T.B., Calignano, A., Colonna, A., Santamaria, R. (2013). High fat diet induces liver steatosis and early dysregulation of iron metabolism in rats. *PLoS ONE*, *8*(6), art. no. e66570.
https://doi.org/10.1371/journal.pone.0066570
26. Moe, S.M. (2005). Disorders of calcium, phosphorus, and magnesium. *American Journal of Kidney Diseases*, *45*(1), 213–218.
https://doi.org/10.1053/j.ajkd.2004.10.014
27. Muller, L., Baldwin, K., Barbacci, D.C., Jackson, S.N., Roux, A., Balaban, C.D., Brinson, B.E., McCully, M.I., Lewis, E.K., Schultz, J.A., Woods, A.S. (2017). Laser desorption/ionization mass spectrometric imaging of endogenous lipids from rat brain tissue implanted with silver nanoparticles. *Journal of The American Society for Mass Spectrometry*, *28*(8), 1716–1728.
https://doi.org/10.1007%2Fs13361-017-1665-4
28. Nascimento, A.R., Machado, M., de Jesus, N., Gomes, F., Lessa, M.A., Bonomo, I.T., Tibiriçá, E. (2013). Structural and functional microvascular alterations in a rat model of metabolic syndrome induced by a high-fat diet. *Obesity*, *21*(10), 2046–2054.
https://doi.org/10.1002/oby.20358

29. Ognik, K., Cholewińska, E., Tutaj, K., Cendrowska-Pinkosz, M., Dworzański, W., Dworzańska, A., Juśkiewicz, J. (2020). The effect of the source and dosage of dietary Cu on redox status in rat tissues. *Journal of Animal Physiology and Animal Nutrition*, *104*(1), 352–361.
https://doi.org/10.1111/jpn.13207
30. Ognik, K., Dworzański, W., Sembratowicz, I., Fotschki, B., Cholewińska, E., Listos, P., Juśkiewicz, J. (2021). The effect of the high-fat diet supplemented with various forms of chromium on rats body composition, liver metabolism and organ histology Cr in liver metabolism and histology of selected organs. *Journal of Trace Elements in Medicine and Biology*, *64*, art. no. 126705.
https://doi.org/10.1016/j.jtemb.2020.126705
31. Orhan, C., Kucuk, O., Tuzcu, M., Sahin, N., Komorowski, J.R., Sahin, K. (2019). Effect of supplementing chromium histidinate and picolinate complexes along with biotin on insulin sensitivity and related metabolic indices in rats fed a high-fat diet. *Food Science & Nutrition*, *7*(1), 183–194.
https://doi.org/10.1002/fsn3.851
32. Pechova, A., Pavlata, L. (2007). Chromium as an essential nutrient: a review. *Veterinarni Medicina*, *52* (1), 1–18.
https://doi.org/10.17221/2010-VETMED
33. Prescha, A., Krzysik, M., Zabłocka-Słowińska, K., Grajeta, H. (2014). Effects of exposure to dietary chromium on tissue mineral contents in rats fed diets with fiber. *Biological Trace Elements Research*, *159*, 325–331.
https://doi.org/10.1007/s12011-014-9973-z
34. Qi, Y., Zhang, Z., Liu, S., Aluo, Z., Zhang, L., Yu, L., Li, Y., Song, Z., Zhou, L. (2020). Zinc supplementation alleviates lipid and glucose metabolic disorders induced by a high-fat diet. *Journal of Agricultural and Food Chemistry*, *68*(18), 5189–5200.
https://doi.org/10.1021/acs.jafc.0c01103
35. Quarles, C.D,, Brumaghim, J.L., Marcus, R.K. (2010). Instrumental comparison of the determination of Cr3+ uptake by human transferrin. *Metallomics*, *2*(12), 792–799.
https://doi.org/10.1039/c0mt00032a
36. Quarles, C.D., Marcus, R.K., Brumaghim, J.L. (2011). Competitive binding of Fe3+, Cr3+, and Ni2+ to transferrin. *Journal of Biological Inorganic Chemistry*, *16*, 913–921.
https://doi.org/10.1007/s00775-011-0792-9
37. Reeves, P.G. (1997). Components of the AIN-93 diets as improvements in the AIN-76A diet. *Journal of Nutrition*, *127*(5), 838S-841S.
https://doi.org/10.1093/jn/127.5.838S
38. Robach, P., Cairo, C., Gelfi, C., Bernuzzi, F., Pilegaard, H., Vigano, A., Santambrogio, P., Cerretelli, P., Calbet, J.A.L., Moutereau, S., Lundby, C. (2007). Strong iron demand during hypoxia-induced erythropoiesis is associated with down-regulation of iron-related proteins and myoglobin in human skeletal muscle. *Blood*, *109*(11), 4724–4731.
https://doi.org/10.1182/blood-2006-08-040006
39. Şahin, K., Şahin, N., Gűler, T., Ertaş, O.N. (2001). The effect of supplemental dietary chromium on performance, some blood parameters and tissue chromium contents of rabbits. *Turkish Journal of Veterinary and Animal Sciences*, *25*, 217–221.
40. Sahin, K., Tuzcu, M., Orhan, C., Agca, C.A., Sahin, N., Guvenc, M., Krejpcio, Z., Staniek, H., Hayirli, A. (2011). The effects of chromium complex and level on glucose metabolism and memory acquisition in rats fed high-fat diet. *Biological Trace Elements Research*, *143*, 1018–1030.
https://doi.org/10.1007/s12011-010-8905-9
41. Staniek, H. (2019). The combined effects of Cr(III) propionate complex supplementation and iron excess on copper and zinc status in rats. *Journal of Trace Elements in Medicine and Biology*, *53*, 49–54.
https://doi.org/10.1016/j.jtemb.2019.01.011
42. Staniek, H., Krejpcio, Z. (2017). The effects of supplementary Cr3 (chromium (III) propionate complex) on the mineral status in healthy female rats. *Biological Trace Elements Research*, *180*, 90–99.
https://doi.org/10.1007/s12011-017-0985-3
43. Staniek, H., Rhodes, N.R., Di Bona, K.R., Deng, G., Love, S.T., Pledger, L.A., Blount, J., Gomberg, E., Grappe, F., Cernosek, C., Peoples, B., Rasco, J.F., Krejpcio Z., Vincent, J.B. (2013). Comparison of tissue metal concentrations in Zucker lean, Zucker obese, and Zucker diabetic fatty rats and the effects of chromium supplementation on tissue metal concentrations. *Biological Trace Elements Research*, *151*, 373–383.
https://doi.org/10.1007/s12011-012-9565-8
44. Stearns, D.M. (2000). Is chromium a trace essential metal? *Biofactors*, *11*(3), 149–162.
https://doi.org/10.1002/biof.5520110301
45. Stępniowska, A., Tutaj, K., Drażbo, A., Kozłowski, K., Ognik, K., Jankowski, J. (2020). Estimated intestinal absorption of phosphorus and its deposition in chosen tissues, bones and feathers of chickens receiving chromium picolinate or chromium nanoparticles in diet. *PLoS ONE*, *15*(11), art. no. e0242820.
https://doi.org/10.1371/journal.pone.0242820
46. Stępniowska, A., Tutaj, K., Juśkiewicz, J., Ognik, K. (2022). Effect of a high-fat diet and chromium on hormones level and Cr retention in rats. *Journal of Endocrinological Investigation*, *45*, 527–535.
https://doi.org/10.1007/s40618-021-01677-3
47. Suksomboon, N., Poolsup, N., Yuwanakorn, A. (2014). Systematic review and meta-analysis of the efficacy and safety of chromium supplementation in diabetes. *Journal of Clinical Pharmacy and Therapeutics*, *39*(3), 292–306.
https://doi.org/10.1111/jcpt.12147
48. Sun, Y., Mallya, K., Ramirez, J., Vincent, J.B. (1999). The biomimetic $[Cr_3O(O_2CCH_2CH_3)_6(H_2O)_3]^+$ decreases cholesterol and triglycerides in rats: towards chromium-containing therapeutics. *Journal of Biological Inorganic Chemistry*, *4*, 838–845.
https://doi.org/10.1007/s007750050357
49. Szabo, R., Bodolea, C., Mocan, T. (2021). Iron, copper, and zinc homeostasis: Physiology, physiopathology, and nanomediated applications. *Nanomaterials*, 11, art. no. 2958.
https://doi.org/10.3390/nano11112958
50. Tuzcu, M., Sahin, N., Orhan, C., Agca, C.A., Akdemir, F., Tuzcu, Z., Komorowski, J., Sahin, K. (2011). Impact of chromium histidinate on high fat diet induced obesity in rats. *Nutrition & Metabolism*, *8*, art. no. 28.
https://doi.org/10.1186/1743-7075-8-28
51. Vincent, J.B., Love, S. (2012). The binding and transport of alternative metals by transferrin. *Biochimica Biophysica Acta*, *1820*(3), 362–378.
https://doi.org/10.1016/j.bbagen.2011.07.003
52. Vlizlo, V., Iskra, R., Maksymovych, I., Lis, M.W., Niedziółka, J.W. (2014). Disturbance of antioxidant protection and natural resis-

tance factors in rats with different availabilities of trivalent chromium. *Turkish Journal of Veterinary & Animal Sciences*, *38*(2), 138–144.
https://doi.org/10.3906/vet-1305-44

53. Wang, Y., Dellatore, P., Douard, V., Qin, L., Watford, M., Ferraris, R.P., Lin, T., Shapses, S.A. (2016). High fat diet enriched with saturated, but not monounsaturated fatty acids adversely affects femur, and both diets increase calcium absorption in older female mice. *Nutrition Research*, *36*(7), 742–750.
https://doi.org/10.1016/j.nutres.2016.03.002
54. Wang, M.Q., Li, H., He, Y.D., Wang, C., Tao, W.J., Du, Y.J. (2012). Efficacy of dietary chromium (III) supplementation on tissue chromium deposition in finishing pigs. *Biological Trace Element Research*, *148*, 316–321.
https://doi.org/10.1007/s12011-012-9369-x
55. Xiao, Y., Cui, J., Shi, Y.H., Sun, J., Wang, Z.P., Le, G.W. (2010). Effects of duodenal redox status on calcium absorption and related genes expression in high-fat diet-fed mice. *Nutrition*, *26*(11–12), 1188–1194.
https://doi.org/10.1016/j.nut.2009.11.021
56. Yoshida, M., Hatakeyama, E., Hosomi, R., Kanda, S., Nishiyama, T., Fukunaga, K. (2010). Tissue accumulation and urinary excretion of chromium in rats fed diets containing graded levels of chromium chloride or chromium picolinate. *Journal of Toxicological Sciences*, *35*(4), 485–491.
https://doi.org/10.2131/jts.35.485
57. Zha, L.Y., Wang, M.Q., Xu, Z.R., Gu, L.Y. (2007). Efficacy of chromium(III) supplementation on growth, body composition, serum parameters, and tissue chromium in rats. *Biological Trace Elements Research*, *119*, 42–50.
https://doi.org/10.1007/s12011-007-0042-8
58. Żary-Sikorska, E., Fotschki, B., Kosmala, M., Milala, J., Matusevicius, P., Rawicka, A., Juśkiewicz, J. (2021). Strawberry polyphenol-rich fraction can mitigate disorders in gastrointestinal tract and liver functions caused by a high-fructose diet in experimental rats. *Polish Journal of Food and Nutrition Sciences*, *71*(4), 423–440.
https://doi.org/10.31883/pjfns/143057

Pol. J. Food Nutr. Sci., 2022, Vol. 72, No. 3, pp. 239–247
On-line ISSN: 2083-6007
Print ISSN: 1230-0322
DOI: 10.31883/pjfns/152434
http://journal.pan.olsztyn.pl

Original article
Section: Nutritional Research

Effects of Long-Term Dietary Administration of Kale (*Brassica oleracea* L. var. *acephala* DC) Leaves on the Antioxidant Status and Blood Biochemical Markers in Rats

Katarzyna Papierska[1]*, *Ewa Ignatowicz*[1], *Jadwiga Jodynis-Liebert*[2], *Małgorzata Kujawska*[2], *Róża Biegańska-Marecik*[3]

[1]*Department of Pharmaceutical Biochemistry, Poznan University of Medical Sciences,*
4 Święcickiego Str., 60–781 Poznań, Poland
[2]*Department of Toxicology, Poznan University of Medical Sciences, 30 Dojazd Str., 60–631 Poznań, Poland*
[3]*Department of Food Technology of Plant Origin, Poznan University of Life Sciences,*
31 Wojska Polskiego Str., 60–624 Poznan, Poland

Key words: antioxidant status, dietary antioxidants, functional food, kale

Kale (*Brassica oleracea* L. var. *acephala* DC) is a leafy green vegetable which belongs to the Brassicaceae family, one of the most commonly cultivated and consumed edible plants. The aim of this study was to investigate the potential adverse effects and antioxidant properties of freeze-dried kale leaves in 90-day dietary experiment on Wistar rats. The kale leaf powder was added to a diet at levels: 10, 30, and 60 g/kg feed. The standard blood biochemical and hematological markers, antioxidant enzyme activities, level of lipid peroxidation, reduced glutathione content, and damage to DNA in the liver were measured. Antioxidant potential in serum was measured and expressed as Trolox equivalents antioxidant capacity (TEAC). The kale leaf phytochemicals, *i.e.*, glucosinolates, phenolic acids and flavonols, were quantified. Major glucosinolates were glucoiberin (164.6 mg/100 g d.w.) and glucobrassicin (130.6 mg/100 g d.w.), whereas kaempferol (159.1 mg/100 g d.w.), quercetin (119.6 mg/100 g d.w.), and sinapic acid (73.8 mg/100 g d.w.) dominated among phenolics. The lowest dose of kale leaves augmented the activity of catalase by 34% in males and by 44% in females. The highest applied dose increased activities of glutathione reductase by 31%, superoxide dismutase by 27%, and glutathione *S*-transferase by 24% in males only. Kale administration did not affect the activities of glutathione peroxidase and paraoxonase 1, glutathione concentration, lipid peroxidation level, and the level of DNA damage in the liver and the whole blood leukocytes. TEAC increased upon all doses of kale leaves by 30–90% in males and by 40–90% in females. The diet with kale did not affect blood biochemical and hematological markers. Results confirm no adverse effects of dried kale leaves used in model rat's diet up to 60 g/kg for 90 days. The changes in hepatic antioxidant enzymes and plasma TEAC suggest beneficial effect of kale leaves on the antioxidant status in rats. Interestingly, these changes were more pronounced in male *versus* female animals.

INTRODUCTION

Nutrient- and non-nutrient phytochemical diet components of diverse chemical structures and ways of action contribute to health preservation, *e.g.* antioxidants are capable of preventing and/or attenuating inflammation-dependent pathological conditions (cardiovascular and neurodegenerative diseases, cancer, and aging impairments) [Pizzino *et al.*, 2017; Zhang *et al.*, 2015] and glucosinolates are particularly active in the prevention of breast cancer [Soundararajan & Kim, 2018]. The contribution of edible phytochemicals to human wellbeing resulted in the development of the concept of functional foods, which are dietary products with the additional function apart from their basic nutritional value and which exert a beneficial effect on human health [Aronson, 2017]. Kale (*Brassica oleracea* L. var *acephala* DC), which is examined in the current study, belongs to the group of *Brassica* vegetables. These edible plants exert chemopreventive activity, resulting primarily from the content of glucosinolates (GLS), including aliphatic (*e.g.*, glucoiberin, glucoraphanin) and indolic (*e.g.*, glucobrassicin) GLS found in various proportions [Šamec *et al.,* 2019]. The absorption, bioavailability, and biological activity of these organic sulfur derivatives depend on the initial stage of metabolism, namely hydrolysis with myrosinase (β-thioglucosidase) [Yagishita *et al.*, 2019]. As a result of this breakdown, a variety of products appear, among which isothiocyanates (sulforaphane and phenethyl isothiocyanate) and indoles (indole-3-carbinol and 3,3'-diindolylmethane) have been studied for their chemopreventive potential [Soundararajan & Kim, 2018]. Various products of GLS hydrolysis have been found to affect diverse pathways: they induce drug-metabolizing

---

* Corresponding Author:
Tel.+48 61 854 66 20;
E-mail: kpapierska@ump.edu.pl (K. Papierska)

Submitted: 15 May 2022
Accepted: 27 July 2022

enzymes [James *et al.*, 2012]; induce apoptosis by the p53, bax, and bcl-2 signaling pathways [Soundararajan & Kim, 2018]; and reduce transcription and increase degradation of an estrogen receptor or arrest the breast cancer cell cycle [Cheng *et al.*, 2019].

Next to GLS, phenolics of diverse structures are components of kale, where flavonoids including kaempferol and its derivatives are dominant [Schmidt *et al.,* 2010]. The majority of reports have demonstrated that dietary polyphenols protect the body against the effects of reactive oxygen species (ROS) and exert anticarcinogenic, anti-inflammatory, hepatoprotective, atheroprotective, and neuroprotective effect, as well as maintain gut microbiota homeostasis [Qu *et al.,* 2018]. However, there are data presenting adverse, pro-oxidant and toxic effects of high doses/concentrations of phenolics used in diverse experimental models, *e.g.* green tea polyphenols have been implicated in inducing hepatotoxicity, carcinogenesis and nephrotoxicity in animals. Moreover, some flavonoids (*e.g.* quercetin or kaempferol) could be converted into genotoxic derivatives [Qu *et al.*, 2018]. Sakr *et al.* [2013] described a genotoxic effect caused by grapefruit juice polyphenols in rats. Also isolated flavonoids, such as silymarin, myricetin, quercetin, kaempferol, rutin, and kaempferol 3-rutinoside, appeared genotoxic to human lymphocytes and sperm [Anderson *et al.*, 1997]. Hence, before the development of functional foods or supplements, safe levels of intake should be established.

The number of *in vivo* biological studies of kale is very limited. Its antioxidant and anticarcinogenic activities have been proved in *in vitro* experiments [Šamec *et al.,* 2019]. Beneficial effects of kale on gastric ulcer and inflammatory bowel disease have been demonstrated in rodents which might be associated with its antimicrobial activity against *Helicobacter pylori.* Moreover, kale suppressed cognitive decline in a mouse model of accelerated senescence. It has been found in intervention study that kale consumption reduced the risk of coronary disease in men. Drinking kale leaf juice for 24 months resulted in bone mass stabilization in postmenopausal women. Inhibition of acetylcholinesterase might suggest that kale seeds can be used in therapy of neurodegenerative diseases [Šamec *et al.,* 2019].

Health-beneficial properties of kale have been widely investigated, but its potential adverse effects have not been studied because it is considered a safe food. No data referring to the long-term ingestion of kale preparations in a natural food matrix were found in the available literature. Therefore, the aim of this study was to assess the antioxidant and potential adverse effects of 90-day dietary administration of freeze-dried kale leaves to rats.

MATERIALS AND METHODS

Chemicals

The normal melting point agarose for comet assay was Prona Plus Agarose (Madrid, Spain). Triton X-100 was obtained from PS PARK Scientific Ltd. (Northampton, Great Britain). Sodium acetate was from Chempur (Piekary Śląskie, Poland), whereas glucotropaeolin was purchased at Roth (Karlsruhe, Germany). Other chemicals were from Sigma Aldrich Chemie GmbH (Steinheim, Germany) and Polish Chemical Reagents Company (Gliwice, Poland). Reagents for the determinations of blood biochemical markers were purchased from Biosystems (Barcelona, Spain).

Materials

Leaves of kale (*Brassica oleracea* L. var. *acephala* DC) of Reflex F1 variety were obtained from the Organic Horticultural Farm in Pamiątkowo near Poznań, Poland. Freeze-dried kale leaves were prepared and analyzed at the Institute of Food Technology of Plant Origin, Poznań University of Life Sciences, Poznań, Poland. The raw material was washed, shredded into pieces, and deep frozen at –50°C. The freeze-drying process was performed at Celico S.A. company (Poznań, Poland) in a tunnel continuous freeze dryer with a separate freezing chamber and ice condensers. The following freeze-drying parameters were applied: pressure of 0.03 mbar, drying temperature of 5°C (shelf temperature), forced drying (conduction drying) temperature of 30°C, freezing chamber temperature of –50°C, and total drying time of 30 h. Freeze-dried kale was packed in plastic bags (OPA/PE), vacuum-sealed (A-300, Multivac, Wolfertschwenden, Germany), and stored at 6°C until use. The freeze-dried kale powder was added to the certified laboratory feed (Labofeed H, ISO 22 000, Animal Fodder Producer Morawski, Kcynia, Poland), thoroughly mixed with the feed to produce pellets with freeze-dried kale leaf levels: 10, 30, and 60 g/kg feed.

Analysis of kale leaf phytochemicals

In order to determine the phenolic compound composition, 2 g of freeze-dried kale leaves were extracted with 70% (*w/v*) methanol (50 mL) at room temperature by sequentially homogenization (Ultra Turrax T-25 homogenizer, IKA-WERKER, Staufen, Germany), shaking for 15 min (Water Bath Shaker 357, Elpan, S.C., Lubawa, Poland), and centrifugation for 30 min at 4,000×*g* (MPW-351R centrifuge, MPW, Warsaw, Poland). The procedure was performed twice. The supernatants were combined and vacuum-evaporated at 40°C (Büchi R-205, BÜCHI Labortechnik, Flawil, Switzerland). The volume of the aqueous residue was adjusted to 25 mL in water [Vallejo *et al.*, 2002]. The phenolic analysis was performed by an Agilent Technologies 1200 rapid resolution liquid chromatography (RRLC) system equipped with a 1260 diode-array detector and a Zorbax SB-C18 (4.6×150 mm, 5 μm) column (Agilent Technologies, Santa Clara, CA, USA). Briefly, the mobile phase consisted of 6% (*v/v*) acetic acid in 2 M sodium acetate (solvent A) and 100% acetonitrile (solvent B), which were used in the following gradient program: 0–15% B for 15 min, 15–30% B for 10 min, 30–50% B for 5 min and 50–100% B for 5 min. The flow rate of the mobile phase was 1 mL/min and the total run time was 40 min [Tsao & Yang, 2003]. The phenolic compounds were detected based on the maximum wavelength of UV-Vis absorption, *i.e.*, hydroxycinnamic acid derivatives at 320 nm and flavanols at 360 nm. Chlorogenic acid, quercetin, and kaempferol were used as external standards. The calibration curve of each standard was used for its quantification. The results were expressed in mg/100 g dry weight (d.w).

Prior to the analysis of glucosinolates, the kale leaf powder was supplemented with glucotropaeolin as an internal standard, extracted with methanol, and the procedure followed the steps described in the official method ISO 9167–1:1992. Glucosinolate separation was carried out with the same LC Agilent Technologies equipment and chromatographic column which were mentioned above to determine phenolic compounds. The total running time of separation was 30 min and the mobile phase was used in the gradient system which was changed as follows: 100% A (water)/0% B (acetonitrile in water, 20:80, *v/v*) for 1 min, then to 100% B over 22 min and isocratically 100% B over 5 min, after which the column was equilibrated at 100% A for 2 min. Absorbance was read out at 229 nm. The peaks were identified by comparison with data obtained from the literature [Verkerk *et al.,* 2001]. The quantity of GLS was determined based on the internal standard (glucotropaeolin) and expressed as mg/100 g d.w.

Trolox equivalent antioxidant capacity (TEAC) of kale leaves was evaluated based on 2,2'-azino-bis-(3-ethylbenzothiazoline-6-sulphonic acid radical cation ($ABTS^{\bullet+}$) scavenging activity of extract, which was determined according to Re *et al.* [1999] method. The $ABTS^{\bullet+}$ was produced by reacting 7 mM ABTS water solution with 2 mM potassium persulphate. The 70% (*w/v*) methanol extract of leaves prepared as described above (50 μL) was added to 5 mL of the $ABTS^{\bullet+}$ solution, which was then incubated at 30°C for 6 min, and afterward absorption was measured at 734 nm. The results were expressed as TEAC of kale leaves based on the calibration curve plotted for Trolox and shown as μmol Trolox/100 g d.w.

In order to determine the ascorbic acid content, the freeze-dried powdered leaves (2 g) were homogenized with metaphosphoric acid (10 g/L) using an Ultra Turrax T-25 homogenizer (IKA-WERKER), then the suspension was shaken (Water Bath Shaker 357, Elpan, S.C.) and centrifuged at 4,000×*g* (MPW-351R centrifuge). The procedure was performed twice. The supernatants were combined and an aliquot of 1 mL was transferred to a volumetric flask. Then, 1 mL of a dithiothreitol solution (50 g/L) was added and the mixture was adjusted to 10 mL with metaphosphoric acid. This solution was analyzed using an LC Agilent Technologies 1200 RRLC system, equipped with a Zorbax SB-C18 column (4.6×150 mm, 5 μm; Agilent Technologies). To elute the ascorbic acid, a mobile phase with a flow rate of 0.7 mL/min in a gradient system of methanol (solvent A) and 5 mM KH_2PO_4 at pH 2.6 (solvent B) was used according to the following program: linear increment from 5% A to 22% over 6 min, then a return to the initial conditions over 9 min. The eluate was detected using a DAD set to 245 nm [Kurilich *et al.*, 1999]. The ascorbic acid was identified by comparing its retention time with that of standard.

Animals

Wistar rats used in the current study were bred at the Breeding Facility of the Department of Toxicology, Poznań University of Medical Sciences, Poznań, Poland. Male (184±47 g) and female (135±22 g) rats were housed in polycarbonate cages (30×20×25 cm; 4≤rats/cage) containing hardwood chip bedding and kept in a 12-h light/dark cycle at an average temperature and humidity of 21°C and 50%, respectively and in the controlled circulation of air. Animals had unlimited access to food and drinking water.

Experimental design

Thirty-two male and thirty-two female rats were divided randomly, each sex, into 4 groups, 8 animals each: controls and rats given pellets containing kale leaves (10, 30, 60 g/kg feed). The experiment lasted 90 days. The animals were monitored throughout the experiment for changes in their health status. Their body weight was recorded once a week and feed intake was measured daily. The daily dose levels (g/kg b.w.) were calculated using the nominal content of preparation tested in the diet, the mean daily feed consumption, and the body weight for a week. The calculated mean daily intake of kale leaves was 0.38±0.04, 1.10±0.16, and 2.19±0.23 g/kg b.w., respectively.

On the 91st day of the experiment, rats were anesthetized with ketamine and xylazine (100/7.5 mg/kg b.w., i.p.), and the blood was withdrawn from the heart to obtain samples for comet assay and aliquots for plasma and serum separation. The livers were excised, a needle was inserted to the portal vein and ice-cold 1.15% KCl was injected until the liver had blanched. The portions of the liver were dissected and stored at –80°C for the determination of biochemical markers. Comet assay in the liver was performed in a portion of the tissue shortly after collection.

The animal experiment followed the animals welfare regulation according to EU Directive 201/63/EU, and was approved by the Local Ethics Committee for Animal Experimentation in Poznań, Poland (protocol No 28/2012).

Blood biochemical markers

Biochemical markers assayed in serum included alanine aminotransferase, aspartate aminotransferase, alkaline phosphatase, total protein, total cholesterol, chloride, inorganic phosphorus, glucose, creatinine, blood urea, potassium, sodium, and calcium. The markers were determined using a chemistry analyzer XL 300 (Erba Diagnostics, Mannheim, Germany).

Hematological markers were determined using an automated hematology analyzer Cell-Dyn 3700 (Abbott Laboratories, Chicago, IL, USA) and included: red blood cells count, white blood cells count, and differential leukocyte count (neutrophils, lymphocytes, monocytes, eosinophils, and basophils), hemoglobin concentration, and platelet count.

Parameters of antioxidant status

In the liver, cytosol superoxide dismutase (SOD) activity was measured on the basis of the inhibition of spontaneous epinephrine oxidation, catalase (CAT) assay was based on monitoring the rate of hydrogen peroxide reduction, glutathione peroxidase (GPx) activity was determined with hydrogen peroxide as a substrate, the rate of NADPH depletion at 340 nm was a measure of the enzyme activity, whereas glutathione reductase (GR) activity was analyzed by measuring NADPH oxidation with oxidized glutathione as a substrate.

In the liver homogenate, the measurement of thiobarbituric acid reactive substances (TBARS) was used to assay lipid peroxidation, and Ellman's reagent was applied to determine reduced glutathione (GSH) content. The above-mentioned methods were described in detail in our previous article by Jodynis-Liebert *et al.* [2009].

Glutathione-*S*-transferase (GST) assay in the liver cytosol was based on the reaction of the reduced glutathione with 1-chloro-2,4-dinitrobenzene (CDNB) [Krajka-Kuźniak *et al.*, 2011]. Protein concentrations in the liver cytosol and homogenate were determined by the routine method with phenolic reagent using bovine serum albumin as the standard. Paraoxonase-1 (PON-1) in rat serum was analyzed with phenylacetate as a substrate, and the rate of generated phenol was measured at 270 nm [Kumru *et al.*, 2004]. Antioxidant potential was measured in the rat plasma using the ABTS assay and expressed as TEAC [Re *et al.*, 1999].

Statistical analysis

The mean values and standard deviations (SD) were calculated separately for males and females. One-way analysis of variance (ANOVA) followed by the Student-Newman-Keuls test for multiple comparisons was used (GraphPad InStat software, San Diego, CA, USA), and $p<0.05$ was considered the limit of significance.

RESULTS AND DISCUSSION

Kale has been recently gaining interest as a crop of a great nutritional value and health-promoting properties resulting from its components, mainly glucosinolates, phenolics, and vitamins. Kale is represented by numerous botanical varieties which differ in chemical composition depending on the cultivar, growing region, agricultural practices employed, and geo-climatic conditions [Sarıkamış *et al.,* 2008; Satheesh & Workneh Fanta, 2020].

Results of the quantification of glucosinolates in the freeze-dried kale leaves are presented in Table 1. Total GLS content in kale leaves was 487.1 mg/100 g d.w. Aliphatic GLS accounted for 60.8%, and indolic GSL for 39.1% of total GLS, which is consistent with literature data [Cieślik *et al.*, 2007; Korus *et al.*, 2014]. Glucoiberin, glucoraphanin, and synigrin were found as major aliphatic glucosinolates of fresh kale juice, while glucobrassicin prevailed in the group of indolic GLS [Korus *et al.*, 2014; Sasaki *et al.*, 2012; Velasco *et al.,* 2007]. Our data corroborate these findings (Table 1): the major GLS turned out to be glucoiberin (164.6 mg/100 g d.w.). The kale leaves were also rich in glucoraphanin (73.8 mg/100 g d.w.) and glucobrassicin (130.6 mg/100g d.w.), the precursor molecules of the biosynthesis of sulforaphane and indole-3-carbinol, respectively, which are known for their anticarcinogenic and antioxidant potential [Cheng *et al.*, 2019; Fuentes *et al.*, 2015; Satheesh & Workneh Fanta, 2020; Soundararajan & Kim, 2018]. The effect of cultivation condition on kale GLS composition was presented in the report of Sarıkamış *et al.* [2008], which showed that the content of glucobrassicin, the major indolic GLS, in kale grown in Turkey depended on the year of cultivation (range from 2094.56 to 2184.05 mg/100 g d.w.), and that aliphatic glucoraphanin and glucoiberin were present in minor quantities, *i.e.* 32.42 to 37.45 mg/100 g d.w. and 8.87 to 120.6 mg/100 g d.w., respectively. The authors have suggested that temporarily high temperatures during the cultivation period boosted up the indole GLS synthesis.

TABLE 1. The content of glucosinolates in freeze-dried kale leaves.

Glucosinolates		Content (mg/100 g d.w.)
Aliphatic	Glucoiberin	164.6±2.2
	Progoitrin	17.9±0.6
	Sinigrin	29.1±0.1
	Glucoraphanin	73.8±1.2
	Gluconapin	10.9±0.0
Indolic	4-Hydroxyglucobrassicin	31.2±0.8
	Glucobrassicin	130.6±2. 9
	4-Methoxyglucobrassicin	12.4±0.6
	Neoglucobrassicin	16.6±0.1
Sum of glucosinolates		487.1± 8.5

Results are presented as mean±standard deviation (n=6); d.w. – dry weight.

Phenolic compounds of kale leaves are represented by various phenolic acids and flavonols, including quercetin and kaempferol, that have been extensively examined for their strong biological activities and health effects [Qu *et al*., 2018; Satheesh & Workneh Fanta, 2020]. The phenolic profile of the freeze-dried kale leaves used in our study is shown in Table 2. Contents of kaempferol and quercetin were 159.1 and 119.6 mg/100 g d.w., respectively. Satheesh & Workneh Fanta [2020] presented a review of data where kaempferol content ranged from 537 to 343 mg/100 g d.w. and that of quercetin from 272 mg/100 g d.w. to 319 mg/100 g d.w. in kale leaves, which was higher than the results obtained in our study. However, our values and these cited data show that kaempferol was the major flavonoid of kale leaves. In turn, Schmidt *et al.* [2010] identified a total of 71 flavonoid glycosides of kale by high-performance liquid chromatography/mass spectrometry and among them kaempferol glycosides (32 compounds) were found to prevail.

The content of ascorbic acid in freeze-dried kale leaves equaled 319.3±6.1 mg/100 g d.w. Literature data demonstrate that vitamin C content in kale has been quantified in the range of 62–969 mg/100 g and that it is higher than in other salad vegetables [Satheesh & Workneh Fanta, 2020]. The recommended daily allowance (RDA) value is 90–120 mg/day [Aly *et al*., 2010].

The TEAC of kale leaves was 9241±5.2 μmol Trolox/100 g d.w. This value was higher than that quantified by other authors for fresh kale leaves, namely: 1175–3620 μmol of Trolox/100 g d.w. [Šamec *et al.*, 2018].

It is known that in some circumstances, certain phenolics can paradoxically behave as pro-oxidants [Qu *et al.*, 2018]. Hence, we examined the effects of freeze-dried kale leaves on parameters of the antioxidant status in rats. The impact exerted by kale leaves administration on the activity of antioxidant enzymes is presented in Table 3. The activity of SOD was increased by 27% only upon the intake of the highest dose of kale leaves in males, whereas in other groups of animals,

TABLE 2. The content of phenolic compounds in freeze-dried kale leaves.

Phenolic compound	Content (mg/100 g d.w.)
Caffeoyloquinic acid	49.3±2.2
Ferulic acid	21.4±0.6
Caffeic acid	22.7±0.2
Sinapic acid	73.8±0.9
Other hydroxycinnamic acids	5.9±0.03
Quercetin	119.6±1.3
Kaempferol	159.1±2.1
Sum of phenolic compounds	451.8±7.3

Results are presented as mean±standard deviation (n=6); d.w. – dry weight.

no significant differences were found in comparison to controls. The activity of CAT was raised in males and females receiving the lowest dose of kale leaves, by 34% and 44%, respectively. The activity of GPx was changed in none of the experimental groups. There was no response of GR to the intake of kale leaves except for the 31% increase in the highest-dose males. A 24% increase in the GST activity was found in males receiving the highest dose, whereas no changes were observed in female rats. Our results indicate that changes in the antioxidant enzymes activities occurred in single groups of animals treated with kale leaves. The only consistency was observed in the response of SOD, GR, and GST, whose activities were elevated in males administered the highest dose.

The increase in the activity of enzymes involved in GSH metabolism, GR and GST, is in contrast with literature data and our previous observations. It has been found that multiple flavonoids can inhibit the activity of isolated GR [Güller *et al.*, 2021]. A decrease in the GR activity was observed in rat hepatocytes cultured with delphinidin, (−)epicatechin, kaempferol, quercetin, luteolin, naringenin, and apigenin [Galvez *et al.*, 1995]. Breinholt and co-workers reported on the GR activity diminishment in the liver of rats treated with flavonoids (quercetin and genistein) [Breinholt *et al.*, 1999]. A decrease in the GR activity was also noticed in our previous similarly designed experiment, where Wistar rats were administered feed containing freeze-dried chokeberry juice rich in anthocyanins and proanthocyanidins for 90 days [Jodynis-Liebert *et al.*, 2009]. GST is a phase II enzyme that detoxifies xenobiotics and potential carcinogens by conjugation with glutathione and, as such, modulates the cellular response to the exposure to electrophiles and oxidants [Krajka-Kuźniak *et al.*, 2011]. Boušová & Skálová [2012] reported on the inhibition of the purified enzyme by multiple flavonoids. Similarly, a decrease in GST activity has been found in rats fed a diet enriched in quercetin and (+)-catechin [Wiegand *et al.*, 2009].

The impact of glucosinolates on antioxidant enzymes in animals was studied by Vang *et al.* [1995], who treated rats for one week with broccoli cultivated at various fertilizer concentrations. Their experiment proved that even a short period of cruciferous vegetable administration upregulated SOD, GR, and GPx in the liver, kidney, and colon. Hence, it could be suggested that the inducing effect of glucosinolates present in kale on antioxidant enzymes prevails over inhibiting the action of kale phenolic compounds.

In our study, kale administration to rats caused a modest increase in the GST activity only in the highest-dose male group (Table 3). However, in the experiment reported by Krajka-Kuźniak *et al.* [2011], after 30 days of cabbage juice

TABLE 3. Antioxidant enzyme activities in the liver and serum of rats fed a diet with freeze-dried kale leaves for 90 days.

Parameter	Sex	Content of kale leaves in feed (g/kg)			
		0	10	30	60
Superoxide dismutase (SOD) (U/mg protein)	M	26.0±1.9	29.2±5.2	21.9±3.4	33.0±2.4* [↑27%]
	F	25.4±4.1	30.6±4.6	27.3±4.2	30.1±2.4
Catalase (CAT) (U/mg protein)	M	4.72±0.76	6.33±1.13* [↑34%]	5.53±0.91	6.01±0.75
	F	3.20±0.42	4.61±0.43* [↑44%]	3.20±0.38	3.36±0.51
Glutathione peroxidase (GPx) (nmol NADPH / (min×mg protein))	M	627±59	630±86	595±72	771±100
	F	920±67	1048±117	854±89	965±71
Glutathione reductase (GR) (nmol NADPH/ (min×mg protein))	M	68.9±8.3	69.7±7.1	62.1±7.7	89.9±6.7* [↑31%]
	F	54.6±8.5	63.1±7.7	55.5±5.8	66.1±6.8
Glutathione *S*-transferase (GST) (nmol CDNB/(min×mg protein))	M	589±65	610±53	584±58	729±57* [↑24%]
	F	486±27	504±57	457±32	517±31
Paraoxonase 1 (PON-1) in serum (U/mL)	M	55.7±5.5	55.5±6.7	55.4±4.8	59.1±5.8
	F	66.8±2.1	66.2±3.8	61.7±6.2	63.1±8.7

Results are presented as mean±standard deviation of 8 values corresponding to 8 animals, in each gender group, each value being the mean of quadruplicate assays; NADPH – nicotinamide adenine dinucleotide phosphate equivalent; CDNB-1-chloro-2,4-dinitrobenzene equivalent; M – males; F – females; *$p<0.05$ for statistical difference *vs*. control.

TABLE 4. Oxidative stress parameters in the liver and whole blood leukocytes of rats fed a diet with freeze-dried kale leaves for 90 days.

Parameter	Sex	Content of kale leaves in feed (g/kg)			
		0	10	30	60
TBARS (nmol MDA/mg protein)	M	17.6±1.8	14.6±4.6	15.8±4.5	19.2±2.8
	F	16.4±2.3	20.7±5.2	15.2±1.8	14.6±0.8
Reduced glutathione (μmol/g liver)	M	5.22±0.81	5.13±0.88	4.98±0.82	5.17±0.96
	F	3.72±0.55	3.40±0.89	2.81±0.55* [↓24%]	3.56±0.60
DNA damage in hepatocytes (arbitrary points)	M	73±5	71±10	71±6	74±7
	F	68±8	69±7	69±8	70±10
DNA damage in the whole blood leukocytes (arbitrary points)	M	70±9	72±8	69±7	68±7
	F	70±10	72±11	73±7	70±10

Results are presented as mean±standard deviation of 8 values corresponding to 8 animals, in each gender group, each value being the mean of quadruplicate assays; TBARS – thiobarbituric acid reactive substances; MDA – malondialdehyde equivalent; M – males; F – females; *$p<0.05$ for statistical difference *vs*. control.

administration to rats, a distinct rise in the enzyme activity was found, which corroborates the capability of glucosinolates and their derivatives to induce the enzyme. Accordingly, after a 21-day administration of sprout extract of Tuscan black cabbage to Sprague-Dawley rats, a significant induction of GST was only noticed when enzymatic decomposition of GLS to isothiocyanates occurred [Melega *et al.*, 2013]. Thus, the differences in the impact of various *Brassica* products on the GST activity might result from the technology of juice/extract preparation, conservation of myrosinase function, and different composition of phytochemicals. Moreover, another reason for these discrepancies may be attributable to various doses applied and experiment duration.

PON-1 is a calcium-dependent enzyme synthesized in the liver and released into plasma, where it associates with high density lipoproteins (HDL). It protects low density lipoproteins (LDL) and HDL molecules against oxidation through breaking up ester bonds in phospholipid peroxides and thus is considered an anti-atherogenic factor. PON-1 strongly depends on the exogenous conditions: (dietary) antioxidants strengthen, whereas toxic xenobiotics diminish its protective activity [Lou-Bonafonte *et al.*, 2015]. In our experiment, the administration of kale leaves to male and female rats did not affect PON-1 activity (Table 3).

Effects of the kale leaves intake on oxidative stress parameters in rats are presented in Table 4. Freeze-dried kale leaves did not affect the TBARS level, an index of lipid peroxidation. The concentration of reduced glutathione was diminished by 24% in females receiving kale leaves in the dose of 30 g/kg feed. In other experimental groups, no changes were observed in comparison to results from related controls.

We included the comet assay in the set of parameters tested because there are some reports referring to the DNA-damaging properties of phenolic compounds. The comet assay detects strand breaks resulting from oxidative DNA damage and is a common method of genotoxicity testing. Lesions appear at sites of oxidized purines and pyrimidines. Background radiation and basal levels of ROS in aerobic organisms contribute to endogenous, steady-state DNA damage [Møller *et al.*, 2004]. In our experiment, no significant changes were found in the extent of DNA damage, both in blood leukocytes and in the liver, in rats consuming kale-enriched feed (Table 4). However, the report of Sakr *et al.* [2013] describes an increase in the genotoxicity range measured by the comet assay in blood lymphocytes of rats treated for five weeks with a grapefruit juice which is a rich source of flavonoids and other phenolics. Isolated flavonoids, including silymarin, myricetin, quercetin, kaempferol, rutin, and kaempferol 3-rutinoside, incubated with human lymphocytes, and sperm cells appeared genotoxic. Nevertheless, in combination with the food mutagens, these compounds showed protective effects since DNA damage was reduced in the lymphocytes [Anderson *et al.*, 1997]. On the other hand, Møller *et al.* [2004] showed that in a 3-week controlled parallel intervention study with volunteers consuming blackcurrant juice or anthocyanin-enriched drink, there were no differences between controls and treated participants in DNA damage markers. The authors concluded that even ingestion of large amounts of dietary antioxidants did not decrease the steady-state levels of oxidative DNA damage and suggested that protective effect might be only observed in subjects exposed to the oxidative stress. Similarly, no effect on the steady-state DNA damage was found when human lymphocytes were incubated with the Brussels sprout extract containing glucosinolates, whereas this extract provided protection against DNA strand breaks in cells exposed to hydrogen peroxide [Zhu & Loft, 2001].

The effect of freeze-dried kale leaves on the antioxidant potential measured in rat plasma as TEAC is presented in Figure 1. TEAC values in rats consuming feed with freeze-dried kale leaves revealed a statistically significant increase compared to the control group value. However, the dose-response relationship was different in both sexes. Whereas in males, the highest TEAC was found in the group fed with 60 g of kale/kg of feed, in females, inversely, the highest TEAC was observed in the lowest dose group. In males, statistically significant differences were observed between 10 g/kg and 30 g/kg dose-group *vs.* 60 g/kg dose-group. In females, such differences were found between all dose-groups ($p<0.05$).

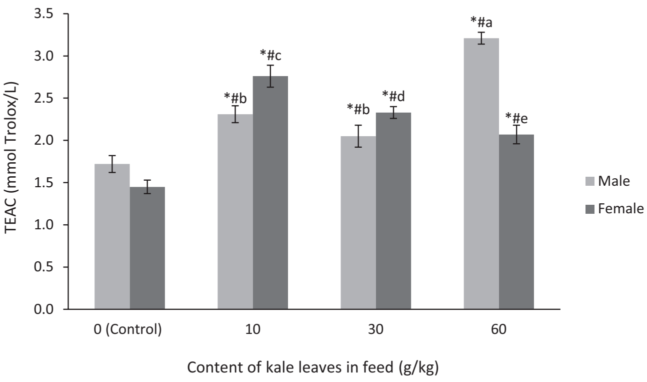

FIGURE 1. Trolox equivalent antioxidant capacity (TEAC) of plasma of rats fed kale leaves. Each column represents mean±standard deviation of 8 values corresponding to 8 animals, each value being the mean of quadruplicate assays. *$p<0.05$ for statistical difference *vs*. control; #$p<0.05$ for male *vs*. female group; different letters over the bar mean statistically significant differences ($p<0.05$) between dose-groups within each sex.

It has been shown that female rats have a higher basal level of antioxidant capacity in tissues than males [Katalinic *et al.*, 2005]. This difference is due to various factors, for example, higher activities of some antioxidant enzymes, and greater levels of endogenous antioxidants in females or the protective effect of estrogen [Massafra *et al.*, 2000; Tiidus *et al.*, 1999; Yamamoto *et al.*, 2002]. Our findings might suggest that this difference is enhanced by the ingestion of natural antioxidants present in kale leaves; however, only in a limited range of doses because the response to the highest dose was much weaker. The observed increase in TEAC values correlates with the results of the antioxidant status analysis in humans consuming *Brassica rapa* L. [Gul *et al.*, 2013]. A relatively high level of TEAC was probably due to the specificity of the preparation production: a low temperature applied for drying kale leaves prevented the loss of antioxidants, including vitamin C and phenolics [Korus & Lisiewska, 2011].

There were no statistically significant differences in the final body weight and mean feed intake between controls and rats administered freeze-dried kale leaves (data not shown).

In contrast, some differences were found in the hematological and biochemical markers between control and treated rats (Tables S1 and S2 in Supplementary Materials). The observed changes were not comprehensive, occurred in single groups of animals or in one sex only, and were not dose-related. The majority of these changes were not extensive.

The highest daily dose of kale leaves tested on animals, 2.16 g/kg b.w., which was safe, corresponds approximately to a daily freeze-dried kale portion of 153.3 g for an individual of 70 kg b.w. This amount is much higher than a likely intake of kale leaves in an everyday human diet or in dietary supplements.

The presented results reflect the response of animals to chemically diverse active ingredients present in the feed. It must be herein underlined that the antioxidant phytochemicals of foods are poorly absorbed in the intestine, rapidly metabolized by the intestinal flora, and excreted. Their absorption may be affected by fiber content, accelerating the intestinal passage, as well as modulation of specific transport mechanisms. Bioavailability, stability, and metabolism of these phytochemicals might be some of the key factors regulating their influence on the antioxidant status [Pizzino *et al*., 2017; Zhang *et al.*, 2015]. The observed effects might also be affected by *in vivo* interactions of active substances with the nutritional matrix. Thus, the antioxidant effects found in plasma and/or tissues might depend mostly on the stimulating impact of these compounds on the endogenous systems of antioxidant defense [Phan *et al.*, 2018]. Further studies, including the impact of active phytochemicals on other physiological functions and disease prevention in animals and humans, are necessary to elucidate the involved mechanisms.

CONCLUSIONS

Results of the current study confirm the safety of a diet enriched in freeze-dried kale leaves applied for 90 days to rat males and females. No toxicologically relevant changes were found in hematological and biochemical markers. The tested material did not enhance the hepatic level of lipid peroxidation and the basic range of DNA damage in the liver and leukocytes. Antioxidant defense system of rats treated with kale leaves was fortified as evidenced by the increase in hepatic activities of catalase, superoxide dismutase, glutathione reductase, and glutathione *S*-transferase as well as by the enhanced antioxidant potential in plasma.

SUPPLEMENTARY MATERIALS

Supplementary data related to this article can be found at http://journal.pan.olsztyn.pl/Effects-of-Long-Term-Dietary-Administration-of-Kale-Brassica-oleracea-L-var-acephala,152434,0,2.html. Table S1: Biochemical parameters in blood of rats fed diet with kale leaves for 90 days. Table S2: Hematology parameters in rats fed diet with kale leaves for 90 days.

RESEARCH FUNDING

This work was supported by the UE Project POIG 01.01.02–00–061/09 Bioactive Food.

CONFLICT OF INTEREST

The authors declare that they have no conflict of interest.

INSTITUTIONAL REVIEW BOARD STATEMENT

The animal experiment followed the animal welfare regulation according to EU Directive 201/63/EU, and was approved by the Local Ethics Committee for Animal Experimentation (protocol No 28/2012).

ORCID IDs

R. Biegańska-Marecik https://orcid.org/0000-0002-3734-4806
E. Ignatowicz https://orcid.org/0000-0002-8128-0408
J. Jodynis-Liebert https://orcid.org/0000-0002-5008-4877

M. Kujawska https://orcid.org/0000-0002-5306-9904
K. Papierska https://orcid.org/0000-0002-5301-7944

REFERENCES

1. Aly, N., El-Gendy, K., Mahmoud, F., El-Sebae, A.K. (2010). Protective effect of vitamin C against chlorpyrifos oxidative stress in male mice. *Pesticide Biochemistry and Physiology, 97*(1), 7–12. https://doi.org/10.1016/j.pestbp.2009.11.007
2. Anderson, D., Dobrzyńska, M., Yu, T.W. (1997). Modulating effects of silymarin and myricetin on food mutagens and doxorubicin in assays with different genetic endpoints. *Journal of Environmental Pathology, Toxicology and Oncology, 16*, 313–327.
3. Aronson, J.K. (2017). Defining ‘nutraceuticals’: neither nutritious nor pharmaceutical: defining ‘nutraceuticals.’ *British Journal of Clinical Pharmacology, 83*(1), SI, 8–19. https://doi.org/10.1111/bcp.12935
4. Boušová, I., Skálová, L. (2012). Inhibition and induction of glutathione *S*-transferases by flavonoids: possible pharmacological and toxicological consequences. *Drug Metabolism Reviews, 44*(4), 267–286. https://doi.org/10.3109/03602532.2012.713969
5. Breinholt, V., Lauridsen, S.T., Dragsted, L.O. (1999). Differential effects of dietary flavonoids on drug metabolizing and antioxidant enzymes in female rat. *Xenobiotica, 29*(12), 1227–1240. https://doi.org/10.1080/004982599237903
6. Cheng, A.C., Shen, C.J., Hung, C.M., Hsu, Y.C. (2019). Sulforaphane decrease of SERTAD1 expression triggers G1/S arrest in breast cancer cells. *Journal of Medicinal Food, 22*(5), 444–450. https://doi.org/10.1089/jmf.2018.4195
7. Cieślik, E., Leszczyńska, T., Filipiak-Florkiewicz, A., Sikora, E., Pisulewski, P.M. (2007). Effects of some technological processes on glucosinolate contents in cruciferous vegetables. *Food Chemistry, 105*(3), 976–981. https://doi.org/10.1016/j.foodchem.2007.04.047
8. Fuentes, F., Paredes-Gonzalez, X., Kong, A.N.T. (2015). Dietary glucosinolates sulforaphane, phenethyl isothiocyanate, indole-3-carbinol/3,3’-diindolylmethane: antioxidative stress/inflammation, Nrf2, epigenetics/epigenomics and in vivo cancer chemopreventive efficacy. *Current Pharmacology Reports, 1*, 179–196. https://doi.org/10.1007/s40495-015-0017-y
9. Galvez, J., Cruz, J.P. de la, Zarzuelo, A., Cuesta, F.S. de la (1995). Flavonoid inhibition of enzymic and nonenzymic lipid peroxidation in rat liver differs from its influence on the glutathione-related enzymes. *Pharmacology, 51*(2), 127–133. https://doi.org/10.1159/000139325
10. Gul, S., Ahmed, S., Gul, H., Shad, K.F., Zia-Ul-Haq, M., Badiu, D. (2013). The antioxidant potential of *Brassica* rapa L. on glutathione peroxidase, superoxide dismutase enzymes and total antioxidant status. *Revista Romana de Medicina de Laborator, 21*(2), 161–169. https://doi.org/10.2478/rrlm-2013-0008
11. Güller, P., Karaman, M., Güller, U., Aksoy, M., Küfrevioğlu, Ö.İ. (2021). A study on the effects of inhibition mechanism of curcumin, quercetin, and resveratrol on human glutathione reductase through *in vitro* and *in silico* approaches. *Journal of Biomolecular Structure and Dynamics, 39*(5), 1744–1753. https://doi.org/10.1080/07391102.2020.1738962
12. ISO 9167–1:1992 Rapeseed and rapeseed meals – Determination of glucosinolates content – Method using high-performance liquid chromatography [accessed on 28 February 2022]. https://www.iso.org/cms/render/live/en/sites/isoorg/contents/data/standard/01/67/16763.html
13. James, D., Devaraj, S., Bellur, P., Lakkanna, S., Vicini, J., Boddupalli, S. (2012). Novel concepts of broccoli sulforaphanes and disease: induction of phase Ii antioxidant and detoxification enzymes by enhanced-glucoraphanin broccoli. *Nutrition Reviews, 70*(11), 654–665. https://doi.org/10.1111/j.1753-4887.2012.00532.x
14. Jodynis-Liebert, J., Adamska, T., Ewertowska, M., Bylka, W., Matławska, I. (2009). *Aquilegia vulgaris* extract attenuates carbon tetrachloride-induced liver fibrosis in rats. *Experimental and Toxicologic Pathology, 61*(5), 443–451. https://doi.org/10.1016/j.etp.2008.10.007
15. Katalinic, V., Modun, D., Music, I., Boban, M. (2005). Gender differences in antioxidant capacity of rat tissues determined by 2,2’-azinobis (3-ethylbenzothiazoline 6-sulfonate; ABTS) and ferric reducing antioxidant power (FRAP) assays. *Comparative Biochemistry and Physiology Part C: Toxicology and Pharmacology, 140*(1), 47–52. https://doi.org/10.1016/j.cca.2005.01.005
16. Korus, A., Lisiewska, Z. (2011). Effect of preliminary processing and method of preservation on the content of selected antioxidative compounds in kale (*Brassica oleracea* L. var. *acephala*) leaves. *Food Chemistry, 129*(1), 149–154. https://doi.org/10.1016/j.foodchem.2011.04.048
17. Korus, A., Słupski, J., Gebczyński, P., Banaś, A. (2014). Effect of preliminary processing and method of preservation on the content of glucosinolates in kale (*Brassica oleracea* L. var. *acephala*) leaves. *LWT – Food Science and Technology, 59*(2), Part 1, 1003–1008. https://doi.org/10.1016/j.lwt.2014.06.030
18. Krajka-Kuźniak, V., Szaefer, H., Bartoszek, A., Baer-Dubowska, W. (2011). Modulation of rat hepatic and kidney phase II enzymes by cabbage juices: comparison with the effects of indole-3-carbinol and phenethyl isothiocyanate. *British Journal of Nutrition, 105*(6), 816–826. https://doi.org/10.1017/S0007114510004526
19. Kumru, S., Aydin, S., Gursu, M.F., Ozcan, Z., 2004. Changes of serum paraoxonase (an HDL-cholesterol-associated lipophilic antioxidant) and arylesterase activities in severe preeclamptic women. *European Journal of Obstetrics and Gynecology and Reproductive Biology, 114*(2), 177–181. https://doi.org/10.1016/j.ejogrb.2003.10.023
20. Kurilich, A.C., Tsau, G.J., Brown, A., Howard, L., Klein, B.P., Jeffery, E.H., Kushad, M., Wallig, M.A., Juvik, J.A. (1999). Carotene, tocopherol, and ascorbate contents in subspecies of *Brassica oleracea*. *Journal of Agricultural and Food Chemistry, 47*(4), 1576–1581. https://doi.org/10.1021/jf9810158
21. Lou-Bonafonte, J.M., Gabás-Rivera, C., Navarro, M.A., Osada, J. (2015). PON1 and mediterranean diet. *Nutrients, 7*(6), 4068–4092. https://doi.org/10.3390/nu7064068
22. Massafra, C., Gioia, D., De Felice, C., Picciolini, E., De Leo, V., Bonifazi, M., Bernabei, A. (2000). Effects of estrogens and androgens on erythrocyte antioxidant superoxide dismutase, catalase and glutathione peroxidase activities during the menstrual cycle. *Journal of Endocrinology, 167*(3), 447–452. https://doi.org/10.1677/joe.0.1670447

23. Melega, S., Canistro, D., Pagnotta, E., Iori, R., Sapone, A., Paolini, M. (2013). Effect of sprout extract from Tuscan black cabbage on xenobiotic-metabolizing and antioxidant enzymes in rat liver. *Mutation Research/Genetic Toxicology and Environmental Mutagenesis, 751*(1), 45–51. https://doi.org/10.1016/j.mrgentox.2012.10.013
24. Møller, P., Loft, S., Alfthan, G., Freese, R. (2004). Oxidative DNA damage in circulating mononuclear blood cells after ingestion of blackcurrant juice or anthocyanin-rich drink. *Mutation Research/Fundamental and Molecular Mechanisms of Mutagenesis, Nutrition and Carcinogenesis, 551*(1–2), 119–126. https://doi.org/10.1016/j.mrfmmm.2004.02.020
25. Phan, M.A.T., Paterson, J., Bucknall, M., Arcot, J. (2018). Interactions between phytochemicals from fruits and vegetables: Effects on bioactivities and bioavailability. *Critical Reviews in Food Science and Nutrition, 58*(8), 1310–1329. https://doi.org/10.1080/10408398.2016.1254595
26. Pizzino, G., Irrera, N., Cucinotta, M., Pallio, G., Mannino, F., Arcoraci, V., Squadrito, F., Altavilla, D., Bitto, A. (2017). Oxidative stress: harms and benefits for human health. *Oxidative Medicine and Cellular Longevity, 2017*, 8416763. https://doi.org/10.1155/2017/8416763
27. Qu, G., Chen, J., Guo, X. (2018). The beneficial and deleterious role of dietary polyphenols on chronic degenerative diseases by regulating gene expression. *BioScience Trends, 12*(6), 526–536. https://doi.org/10.5582/bst.2018.01172
28. Re, R., Pellegrini, N., Proteggente, A., Pannala, A., Yang, M., Rice-Evans, C. (1999). Antioxidant activity applying an improved ABTS radical cation decolorization assay. *Free Radical Biology and Medicine, 26*(9–10), 1231–1237. https://doi.org/10.1016/S0891-5849(98)00315-3
29. Sakr, S.A., Zoil, M.E., El-shafey, S.S. (2013). Ameliorative effect of grapefruit juice on amiodarone–induced cytogenetic and testicular damage in albino rats. *Asian Pacific Journal of Tropical Biomedicine, 3*(7), 573–579. https://doi.org/10.1016/S2221-1691(13)60116-1
30. Šamec, D., Urlić, B., Salopek-Sondi, B. (2019). Kale (*Brassica oleracea* var. acephala) as a superfood: review of the scientific evidence behind the statement. *Critical Reviews in Food Science and Nutrition, 59*(15). https://doi.org/10.1080/10408398.2018.1454400
31. Sarıkamış, G., Balkaya, A., Yanmaz, R. (2008). Glucosinolates in kale genotypes from the Blacksea region of Turkey. *Biotechnology and Biotechnological Equipment, 22*(4), 942–946. https://doi.org/10.1080/13102818.2008.10817584
32. Sasaki, K., Neyazaki, M., Shindo, K., Ogawa, T., Momose, M. (2012). Quantitative profiling of glucosinolates by LC-MS analysis reveals several cultivars of cabbage and kale as promising sources of sulforaphane. *Journal of Chromatography B: Analytical Technologies in the Biomedical and Life Sciences, 903*, 171–176. https://doi.org/10.1016/j.jchromb.2012.07.017
33. Satheesh, N., Workneh Fanta, S. (2020). Kale: Review on nutritional composition, bio-active compounds, anti-nutritional factors, health beneficial properties and value-added products. *Cogent Food and Agriculture, 6*(1), art. no. 1811048. https://doi.org/10.1080/23311932.2020.1811048
34. Schmidt, S., Zietz, M., Schreiner, M., Rohn, S, Kroh, L.W. Krumbein, A. (2010). Identification of complex, naturally occurring flavonoid glycosides in kale (*Brassica oleracea* var. *sabellica*) by high-performance liquid chromatography diode-array detection/electrospray ionization multi-stage mass spectrometry. *Rapid Communications. Mass Spectrometry, 24*(14), 2009–2022. https://doi.org/10.1002/rcm.4605
35. Soundararajan, P., Kim, J.S. (2018). Anti-carcinogenic glucosinolates in cruciferous vegetables and their antagonistic effects on prevention of cancers. *Molecules, 23*(11), art. no. 2983. https://doi.org/10.3390/molecules23112983
36. Tiidus, P.M., Bombardier, E., Hidiroglou, N., Madere, R. (1999). Gender and exercise influence on tissue antioxidant vitamin status in rats. *Journal of Nutritional Science and Vitaminology, 45*(6), 701–710. https://doi.org/10.3177/jnsv.45.701
37. Tsao, R., Yang, R. (2003). Optimization of a new mobile phase to know the complex and real polyphenolic composition: towards a total phenolic index using high-performance liquid chromatography. *Journal of Chromatography A, 1018*(1), 29–40. https://doi.org/10.1016/j.chroma.2003.08.034
38. Vallejo, F., Tomás-Barberán, F.A., García-Viguera, C. (2002). Potential bioactive compounds in health promotion from broccoli cultivars grown in Spain. *Journal of the Science of Food and Agriculture, 82*(11), 1293–1297. https://doi.org/10.1002/jsfa.1183
39. Vang, O., Rasmussen, B.F., Sørensen, H., Clausen, J., Andersen, O. (1995). Effects of dietary broccoli on antioxidant enzymes. *Clinical Chemistry, 41*(12), 1910–1911. https://doi.org/10.1093/clinchem/41.12.1910
40. Velasco, P., Cartea, M.E., Gonzalez, C., Vilar, M., Ordas, A. (2007). Factors affecting the glucosinolate content of kale (*Brassica oleracea acephala* Group). *Journal of Agricultural and Food Chemistry, 55*(3), 955–962. https://doi.org/10.1021/jf0624897
41. Verkerk, R., Dekker, M., Jongen, W.M.F. (2001). Post-harvest increase of indolyl glucosinolates in response to chopping and storage of *Brassica vegetables*. *Journal of the Science of Food and Agriculture, 81*(9), SI, 953–958. https://doi.org/10.1002/jsfa.854
42. Wiegand, H., Boesch-Saadatmandi, C., Regos, I., Treutter, D., Wolffram, S., Rimbach, G. (2009). Effects of quercetin and catechin on hepatic glutathione-*S* transferase (GST), NAD(P)H quinone oxidoreductase 1 (NQO1), and antioxidant enzyme activity levels in rats. *Nutrition and Cancer, 61*(5), 717–722. https://doi.org/10.1080/01635580902825621
43. Yagishita, Y., Fahey, J.W., Dinkova-Kostova, A.T., Kensler, T.W. (2019). Broccoli or sulforaphane: is it the source or dose that matters? *Molecules, 24*(19), art. no. 3593. https://doi.org/10.3390/molecules24193593
44. Yamamoto, T., Ohkuwa, T., Itoh, H., Sato, Y., Naoi, M. (2002). Effect of gender differences and voluntary exercise on antioxidant capacity in rats. *Comparative Biochemistry and Physiology Part C: Toxicology and Pharmacology, 132*(4), 437–444. https://doi.org/10.1016/S1532-0456(02)00097-2
45. Zhang, Y.-J., Gan, R.Y., Li, S., Zhou, Y., Li, A.N., Xu, D.P., Li, H.B. (2015). Antioxidant phytochemicals for the prevention and treatment of chronic diseases. *Molecules, 20*(12), 21138–21156. https://doi.org/10.3390/molecules201219753
46. Zhu, C.Y., Loft, S. (2001). Effects of Brussels sprouts extracts on hydrogen peroxide-induced DNA strand breaks in human lymphocytes. *Food and Chemical Toxicology, 39*(12), 1191–1197. https://doi.org/10.1016/S0278-6915(01)00061-8

Pol. J. Food Nutr. Sci., 2022, Vol. 72, No. 3, pp. 249–261
On-line ISSN: 2083-6007
Print ISSN: 1230-0322
DOI: 10.31883/pjfns/151566
http://journal.pan.olsztyn.pl

Original article
Section: Food Technology

Modification in Physicochemical, Structural and Digestive Properties of Potato Starch During Heat-Moisture Treatment Combined with Microwave Pre- and Post-Treatment

Chunli Deng[1,2], *Oksana Melnyk*[2], *Tatyana Marenkova*[2], *Yanghe Luo*[1]*

[1]*College of Food and Biological Engineering, Hezhou University, 542899, Hezhou, China*
[2]*Food Technology Department, Sumy National Agrarian University, 40021 Sumy, Ukraine*

Key words: heat-moisture treatment, microwave treatment, physicochemical properties, structural properties, digestibility, potato starch

The objective of this study was to investigate the effects of modification by heat-moisture treatment (HMT) combined with microwave pre- and post-treatment (MW) on the physicochemical, structural and digestive properties of potato starch. The light microscopy, scanning electron microscopy (SEM), Fourier transform infrared spectroscopy (FT-IR) and X-ray diffraction (XRD) were used to determine the structural properties of starch. FT-IR and XRD spectra implied that MW and HMT destroyed the double helices and crystalline structure of potato starch. The relative crystallinity of modified starch granules (15.17–18.17%) was lower than that of native starch (19.39%). In the case of physicochemical properties, the modified starches had higher pasting temperature (68.8–93.0°C) and setback viscosity (807–3168 cP), but lower peak viscosity (1315–3662 cP) and breakdown viscosity (17.3–78.3 cP) than that of native potato starch, which were 68.5°C, 496 cP, 6598 cP and 2526 cP, respectively. The HMT and MW modifications significantly increased the content of slowly digestible starch and resistant starch. The resistant starch content of starch obtained by HMT combined with MW post-treatment was significantly higher than that of starch obtained by HMT combined with MW pre-treatment and single HMT. These results may promote good understanding of the effects of HMT combined with MW pre- and post-treatment on physicochemical properties and digestibility of potato starch, and wide utilization of microwave and heat-moisture techniques in starch modification.

INTRODUCTION

As the fourth largest crop in world production after corn, rice and wheat, potato is the largest non-cereal food crop widely cultivated around the world, containing about 75% starch by dry weight [Santos *et al.*, 2016; Zhang *et al.*, 2017]. Potato starch has larger particle size, higher swelling capacity, transparency and viscosity than rice starch or maize starch [Cao & Gao, 2020; Singh *et al.*, 2016], and it is widely used as food thickener, stabilizer or carrier for bioactive compounds in food and industrial products [Singh *et al*., 2003].

However, the properties of low shear, heat sensitivity and easy retrogradation of native potato starch limit its use in some industrial fields [Singh *et al.*, 2004]. Therefore, in order to overcome the shortcomings and achieve desired properties, starch can be modified by physical, chemical and enzymatic methods [Colussia *et al.*, 2020; Gałkowska & Juszczak, 2019; Zhang *et al.*, 2019]. Heat-moisture treatment (HMT) is currently the most studied physical modification method of starch, in which starch granules are treated at high temperature (90–120°C) with certain moisture content (10–35%) for certain time (15 min–16 h) [Wang *et al.*, 2016; Zavareze & Dias, 2011]. Samples are stored in an airtight container before HMT to keep moisture at a constant level. The increased pressure of the sealed environment generated by heating is conducive to increase thermal energy, which is constantly transformed into kinetic energy through the motion of water molecules. This leads to massive segmental movements and the glassy state of amorphous regions of starch can be shifted to a more flexible state, thus HMT makes it possible to control the movement of molecules at high temperatures, monitoring the water concentration [Schafranski *et al.*, 2021; Wang *et al.*, 2021]. HMT alters the interactions of polymer chains in starch by destroying crystalline and helical structures. The structure of starch chains within the amorphous and crystalline granules is reorganized during heat-moisture treatment, resulting in expansion of starch granules, changes in crystallinity, leaching of amylose, and changes in other properties such as gelatinization, retrogradation and thermal stability [Arns *et al.*, 2015; Chung *et al.*, 2010; Tan *et al.*, 2017]. HMT also could partially convert rapidly digested starch (RDS) into slowly digested starch (SDS) and/or resistant starch (RS), resulting in increased content of SDS and/or RS [Uzizerimana *et al.*, 2021]. SDS and RS could interfere with suppressing metabolic diseases due to relatively low glycemic response, thus SDS and RS consumption could

---

* Corresponding Author:
E-mail: luoyanghe@tsinghua.org.cn (Yanghe Luo)

Submitted: 25 March 2022
Accepted: 23 June 2022
Published on-line: 27 July 2022

present health benefits [Wang *et al.*, 2017]. Starch modified by HMT can be used in sauces, candies, canned food, pasta and other foods, as well as an ingredient to increase SDS and RS content [Kaur & Singh, 2019].

Microwave is an electromagnetic radiation in the frequency ranging from 300 MHz to 300 GHz. During microwave treatment (MW), electromagnetic energy is converted into heat energy by triggering high-frequency movement of molecules [Singh *et al.*, 2012]. MW becomes another appealing physical modification method of starch for its uniform heating, high heating rates and environmental protection [Braşoveanu & Nemţanu, 2014]. Many investigations have evidenced that microwave irradiation can change morphology, alter molecular structure, rearrange the structural order and crystalline regions of starch, which consequently affects its physicochemical properties, such as absorption ability, swelling power, gelatinization, retrogradation and digestablity [Chen *et al.*, 2021a; Kumar *et al.*, 2020; Wang *et al.*, 2019].

The effects of single HMT and MW on functionalities and structural properties of starch have been investigated by many researchers as reviewed by Schafranski *et al.* [2021] and Oyeyinka *et al.* [2021]. However, the mechanism of dual modification combined with HMT and MW is far from being fully understood. Therefore, the purpose of this research was to evaluate the effects of HMT assisted by MW pre- and post-treatment on the morphological, physicochemical and *in vitro* digestion properties of potato starch. This research presented a comprehensive understanding of the effects of HMT and MW bi-directional modifications on functional and digestibility properties of starch, as well as the related mechanism, which would provide a useful theoretical basis for further studies on improving the application of microwave technology in starch modification.

MATERIALS AND METHODS

Potato starch extraction

Potato tubers of Favorita variety sold locally in Hezhou city (Guangxi, China) were selected as raw materials, and native potato starch was extracted according to the procedure described by Deka & Sit [2016]. Potato tubers were washed, peeled and cut into cubes before being ground by a high-speed laboratory blender (Joyoung, JYL-C19V, Joyoung Company Limited, Jinan, Shandong, China) for 3 min. The slurry was mixed with distilled water (1:10, *v/v*), and then was filtered with multiple-layer absorbent gauze. The filtered slurry was kept for 4–5 h for sedimentation, then the liquid was poured off, distilled water was added to wash the sediment, and the above process was repeated several times until the liquid was clarified. The final sediment was laid flat in a tray and dried in a hot-air oven (DH411C, Yamato, Tokyo, Japan) at 45°C for 24 h. The dried starch was pulverized with a universal pulverizer (FW100, Tianjin City Taisite Instrument Co., Ltd., Tianjin, China) and passed through an 80-mesh sieve to obtain native potato starch. Native potato starch was kept in airtight polyethylene bags for further analysis. The composition of potato starch was determined as following: total starch 82.38±0.87 g/100 g dry matter (d.m.), lipid 0.12±0.07 g/100 g d.m., protein 0.35±0.10 g/100 g d.m., moisture 10.83±0.18 g/100 g. Total starch was determined using the Megazyme starch assay kit based on AOAC International 996.11 method [AOAC, 2005]. The GB 5009.6–2016, GB 5009.5–2016 and GB 5009.3–2016 methods of China National Standard for Food Safety [China National Standard for Food Safety, 2016] were used to determine content of lipid, protein and moisture, respectively.

Heat-moisture treatment of starch

The heat-moisture treatment (HMT) of native potato starch was carried out according to the procedure described by Deng *et al*. [2021a, b]. The moisture content of native potato starch was measured before HMT. Then, 70 g of four parallel native potato starch samples were weighed into different 500-mL Duran laboratory bottles, and a certain amount of ultrapure water was added into each bottle to adjust the moisture content to 25 g/100 g. The mixtures were equilibrated at 25°C for 24 h to achieve moisture balance. When equilibration had finished, the samples were subjected to HMT at 90°C for 1.5 h, 4 h, 8 h and 12 h, respectively, in a DH411C hot-air oven. After HMT, the treated starch samples were dried at 45°C for 24 h using the same hot-air oven, so that the starch moisture was less than 12 g/100 g. The dried potato starch was intermittently pulverized for 50 s (pulverized for 5 s, stopped for 5 s to avoid too high temperature of starch caused by pulverization) using an FW100 pulverizer (Tianjin City Taisite Instrument Co., Ltd.). The pulverized starch was sieved through an 80-mesh sieve, then hermetically packaged in polyethylene bags, and stored in a glass desiccator for further studies. According to the duration of HMT, the prepared dry starch powder samples were named as HMT1.5, HMT4, HMT8 and HMT12, respectively.

Microwave treatment of starch

The moisture content of native potato starch was adjusted to 25 g/100 g as described above and the starch mixture was equilibrated at 25°C for 24 h. So prepared starch was subjected to MW according to the previous research method described by Deng *et al*. [2021b]. Briefly, the moisture-balanced starch was placed flat into a lab dish (18 cm in diameter), covered with microwave-specific plastic wrap, and 10 holes were evenly pierced with toothpicks. Then, the lab dish with starch was placed in a microwave oven (G80F20CN2L-B8(RO), Guangdong Galanz Microwave Appliance Manufacturing Co., LTD, Foshan, Guangdong, China) for 5 min at 400 W power (increasing the power or time of microwave heating will cause the starch granules to burn). The treated starch samples were dried and stored according to the method mentioned above in single HMT. The prepared starches were named MWS.

Dual modification of starch

Potato starch modifications by HMT in combination with microwave pre-treatment (MW-HMT) and by HMT in combination with microwave post-treatment (HMT-MW) were performed [Deng *et al*., 2021b]. Briefly, the moisture-balanced MWS samples (25 g/100 g) were subjected to HMT at 90°C for 1.5 h, 4 h, 8 h and 12 h, next, dried and stored according to the procedure described above for single HMT. The prepared starches were named as MW-HMT1.5, MW-HMT4, MW-HMT8 and MW-HMT12, respectively. To obtain HMT-MW starches, the moisture content of HMT1.5, HMT4, HMT8 and HMT12 samples was adjusted to 25 g/100 g. After equilibration at 25°C for 24 h, the starch mixtures were subjected to MW according to the description above for single MW. The starch samples were dried and named as HMT1.5-MW, HMT4-MW, HMT8-MW and HMT12-MW, respectively.

Scanning electron microscopy (SEM)

An SU8100 scanning electron microscope (Hitachi Ltd., Tokyo, Japan) was used at an acceleration voltage of 2.0 KV to observe the microstructure of starch granules. The dried starch samples were deposited on the specimen holder by using double-sided adhesive tape and sputter-coated with gold.

Light microscopy

A small amount of each starch sample was placed on a microscope slide with 1–2 drops of glycerol with a distilled water mixture (1:1, *v/v*) to disperse the starch evenly, then the starch was covered with coverslip and placed on the objective table of the microscope (BX53, Olympus Corporation, Tokyo, Japan). The normal light microscopic images and polarized light microscopic images of starch samples were observed and captured under normal light mode and polarized light mode, respectively, with the magnification of ×400.

Determination of pasting properties

A rapid visco-analyzer (RVA Starch Master2, Perten Instruments, Stockholm, Sweden) was used to evaluate the pasting and paste properties of the starch according to the methods described by Sui *et al*. [2015] with slight modifications. A 2.5-g portion of each starch (corrected to moisture content of 14 g/100 g) was mixed with 25 mL of distilled water and kept in the test slot of the equipment. The temperature gradient was as follows: equalization at 50°C for 1 min, increased from 50°C to 95°C within 3.75 min and maintaining at 95°C for 2.5 min, and then decreased to 50°C in 3.75 min and maintaining at 50°C for 2 min.

Determination of swelling power and solubility

Swelling power and solubility of starch samples were determined in triplicate according to the method of Guo *et al.* [2015]. A 0.60 g portion (dry basis) of starch sample was placed into a pre-weighed 50-mL centrifuge tube with 30 mL of distilled water. The starch was completely dispersed in the distilled water by oscillating with a turbine mixer (XW-80A, Haimen Kylin-Bell Lab Instruments Co., Ltd., Haimen, Jiangsu, China) for 5 s. After that, all the centrifuge tubes with starch samples were placed in a water bath oscillator with the speed of 200 rpm for 30 min at 55, 65, 75, 85, and 95°C. The samples were cooled to room temperature before being centrifuged at 2150×*g* for 20 min with an L550 centrifuge (Hunan Xiangyi Laboratory Instrument Development Ltd. Co., Changsha, Hunan, China). The supernatants were poured into pre-weighed aluminum specimen boxes and dried to a constant weight in a DH411C hot-air oven at 105°C, while sediments were immediately weighed. The swelling power (SP, g/g, on dry weight basis) and solubility (S, %) were calculated as follows:

$$Solubility\ (S) = \frac{Weight\ of\ dried\ supernatant}{Weight\ of\ dried\ starch\ sample} \times 100 \tag{1}$$

$$Swelling\ power\ (SP) = \frac{Weight\ of\ sediment}{Weight\ of\ dried\ starch\ sample\left(1 - {}^{Solubility}\!/_{100}\right)} \tag{2}$$

Fourier transform infrared spectroscopy (FT-IR) analysis

The starch samples were placed directly on to sampling unit of an FT-IR spectrophotometer (Spectrum, Perkin Elmer, Waltham, MA, USA) to determine the FT-IR spectra with a scanning spectral range from 4000 cm^{-1} to 400 cm^{-1} at 25°C.

X-Ray diffraction analysis

X-Ray diffraction (XRD) analysis of starch samples was carried out by an X-ray diffractometer (Rigaku Ultima IV, Ultima IVTM, Tokyo, Japan) equipped with a goniometer at 40 kV (target voltage) and 40 mA (tube current). The measurement diffraction angle (2θ) ranged from 4° to 40° at a scanning rate of 4°/min with a step size of 0.02°. MDI Jade 6 software was used to calculate the relative crystallinity (%) of each starch sample according to the following equation:

$$Relative\ crystallinity = \frac{Area\ of\ crystalline\ peaks}{Total\ area\ of\ crystalline\ and\ amorphous\ peaks} \times 100 \tag{3}$$

In vitro digestibility analysis

The contents of rapidly digested starch (RDS, starch which was digested within the first 20 min), slowly digested starch (SDS, starch which was digested between 20 and 120 min) and resistant starch (RS, the residual starch which was digested after 120 min) in native potato starch and treated starch were determined according to the method previously described by Han *et al.* [2021] with some modifications. In brief, 200 mg of starch samples with 10 mL of a sodium acetate buffer solution (0.1 M, pH 5.2) were added to a flask and heated in boiling water for 30 min to completely gelatinize starch. Afterwards, tubes were cooled in a water bath at 37°C and incubated for 30 min with 160 rpm shaking. Then, the enzyme solution of 5 mL of α-amylase from porcine pancreas (300 U/mL, Shanghai Yuanye Bio-Technology Co., Ltd, Shanghai, China) and 2 mL of amyloglucosidase from *Aspergillus niger* (225 U/mL, Shanghai Yuanye Bio-Technology Co., Ltd) were added to each sample tube, and incubation was continued in a water bath at 37°C with 190 rpm shaking. Then, 1 mL of the digestion solution was pipetted into a test tube with 20 mL of anhydrous alcohol to stop the enzyme reaction at intervals of 20 and 120 min, and then centrifuged at 2810×*g* for 10 min in an L550 centrifuge. The released glucose concentration in the supernatant was measured with the glucose oxidase/peroxidase (GOPOD) assay kit (Megazyme, International Ltd. Co., Wicklow, Ireland). The glucose content multiplied by a factor of 0.9 was used to calculate the percentage of hydrolyzed starch and the following formulas were used to calculate the contents of RDS (%), SDS (%), and RS (%):

$$RDS = G20 \times 0.9/TS \quad (4)$$

$$SDS = (G120 - G20) \times 0.9/TS \quad (5)$$

$$RS = 100 - RDS - SDS \quad (6)$$

where: G20 and G120 are the glucose contents after 20 min and 120 min of hydrolysis, respectively; TS is the total starch content of each sample.

Statistical analysis

All the measurements were performed three times unless otherwise stated, and the data were recorded as means± standard deviation (SD). One-way analysis of variance (one-way ANOVA) with post-hoc Duncan's test was performed by Data Processing System (7.05 for Windows, Hangzhou Ruifeng Info-technology Co., Hangzhou, Zhejiang, China). Differences were considered significant at $p<0.05$. Microsoft Office Excel 365 (Microsoft Corp., Redmond, WA, USA) and Origin Pro 8 (OriginLab Corp., Northampton, MA, USA) were used to report the data.

RESULTS AND DISCUSSION

Morphological properties

The surface structural characteristics of native potato starch and modified potato starch samples observed by SEM are presented in Figure 1. The native potato starch granules showed oval or spherical-like shape with no obvious fissures and grooves on the smooth surface. This result was consistent with previous findings reported by Xu *et al*. [2018]. Although there were no noteworthy changes in the structure of starch after the MW, HMT and dual MW and HMT, the surface of treated starch granules became rougher with a different degree of pitting and indentation compared with native starch (Figure 1). Similar results were obtained for millet starch and rice starch modified by MW and HMT, respectively [Li *et al*., 2019a; Wang *et al.*, 2018]. Dual MW and HMT modification made the surface of starch granules rougher with more serious depressions or scallops than single MW or HMT modification, especially in the case of the double modified starch granules *via* HMT assisted by MW pre-treatment (Figure 1).

For HMT-treated starch, the changes on starch granules surface can be attributed to the partial gelatinization caused by pressure and thermal energy, consequently leading to inconsistent swelling and/or aggregation/fusion of starch particles and rough surface, or even to concavities on the granules surface [Wang *et al*., 2018]. For MW-treated starch, the surface roughness and deformation were mainly related to the penetration of microwave energy. When the microwave energy was high enough, the molecular chains that constituted the starch granule structure would break, eventually resulting in pore formation and possible collapse in starch granules [Chen *et al.*, 2021b].

Light microscopy

The micrographs of native potato starch and modified potato starch granules observed under normal light microscopy are shown in Figure 2 and the micrographs of all the starch samples observed under polarized light microscopy are shown in Figure 3. The normal light microscopy image of native starch (Figure 2) exhibited hilum structure with smooth surface, while all treated starch granules showed obvious hollow structure at hilum. The hilum is located in the amorphous zone with relatively fragile structure [Li *et al.*, 2020]. Due to this fragile structure, coupled with partial swelling and disruption of starch granules caused by the MW, HMT and dual modification, the large hollow structure appeared at the umbilicus section of starch granules (Figure 2). Because of the penetration of microwave irradiation, single MW modification had greater effects on hollow structure at the hilum of starch granules than single HMT. Compared with single modified starch, this phenomenon was more obvious in double modified starch, especially in the HMT starch pretreated by MW.

Although the polarized light microscopy of native potato starch granules (Figure 3) and all the modified starches showed a typical Maltese cross with black polarization cross or birefringence, the contour of the Maltese cross of all the modified starches became distorted and fuzzy after MW, HMT and dual modification, and the black zone in the center of the cross became relatively larger than that of native potato starch. These results were similar to those from the previous research of HMT

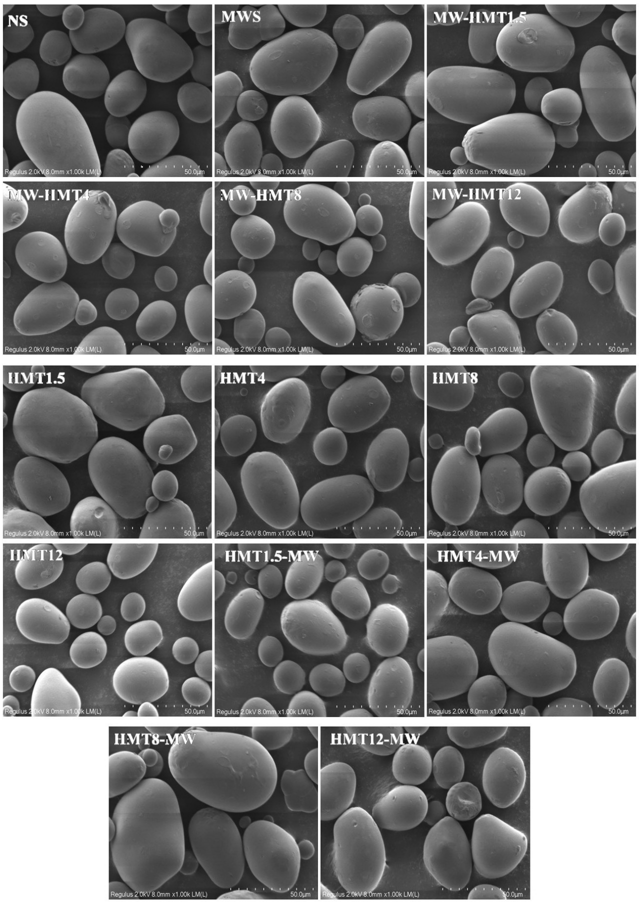

FIGURE 1. Scanning electron microscopy (SEM) micrographs (×1000) of native (NS) and modified potato starches: MWS: single microwave treatment; MW-HMT: heat-moisture treatment combined with microwave pre-treatment; HMT-MW: heat-moisture treatment combined with microwave post-treatment; 1.5, 4, 8, 12 mean the heating duration of HMT (h).

lily starch [Li *et al.*, 2020]. Thermal and microwave energy generated by HMT and MW might induce changes in radial orientation of double helices and amylopectin chains, and eventually changed intensity of birefringence [Ji & Yu, 2018].

Pasting properties

The pasting properties of native and modified potato starch are listed in Table 1 and the rapid viscosity analysis (RVA) pasting profiles are illustrated in Figure 4. The RVA pasting profiles and the pasting properties of potato starch were significantly changed by single MW, single HMT and HMT combined with MW pre- and post-treatment. The peak viscosity of native potato starch was 6598 cP, which was higher than that of all the treated starch samples. The pasting temperature of native potato starch was 68.5°C, which was significantly increased to 73.5–93.0°C after MW and HMT except for the MWS (68.8°C) and the HMT1.5 (71.0°C). Higher pasting temperature indicated interactions between starch chains enhanced by MW and HMT, and more energy was required to destroy the enhanced starch structure during gelatinization process. All the MW-treated starch samples and HMT-treated starch samples showed lower peak viscosity, holding viscosity and breakdown viscosity than that of native potato starch. Similar results were reported for HMT mango kernel starch and MW millet starch [Bharti *et al.*, 2019; Li *et al.*, 2019a]. The decrease in peak viscosity of the sample may be attributed to the recombination and rearrangement in starch granules after MW, HMT, MW-HMT and HMT-MW, which limited the leaching of starch components from granules into the medium, consequently resulting in a decreased peak viscosity. Reduction in holding viscosity representing starch degradation upon application of high temperature and shear, indicated a decrease in peak viscosity [Kaur & Singh, 2019; Li *et al.*, 2019a]. The low breakdown viscosity indicated high thermal stability, resistance development against shear exerted from heating and lower deterioration tendency [Kumar *et al.*, 2020]. Compared with native potato starch setback viscosity (496 cP), all the treated starch samples had higher setback viscosity ranging from 807 to 3168 cP, with the highest values noted for HMT1.5-MW and HMT1.5, and the lowest one for MW-HMT12 (Table 1). Additionally, the duration of HMT affected the pasting properties. The peak viscosity, hold viscosity and final viscosity of HMT modified starch decreased successively with the extension of HMT duration. Moreover, HMT combined with MW pre- and post-treatment resulted in lower peak viscosity than that of starch modified by single MW or

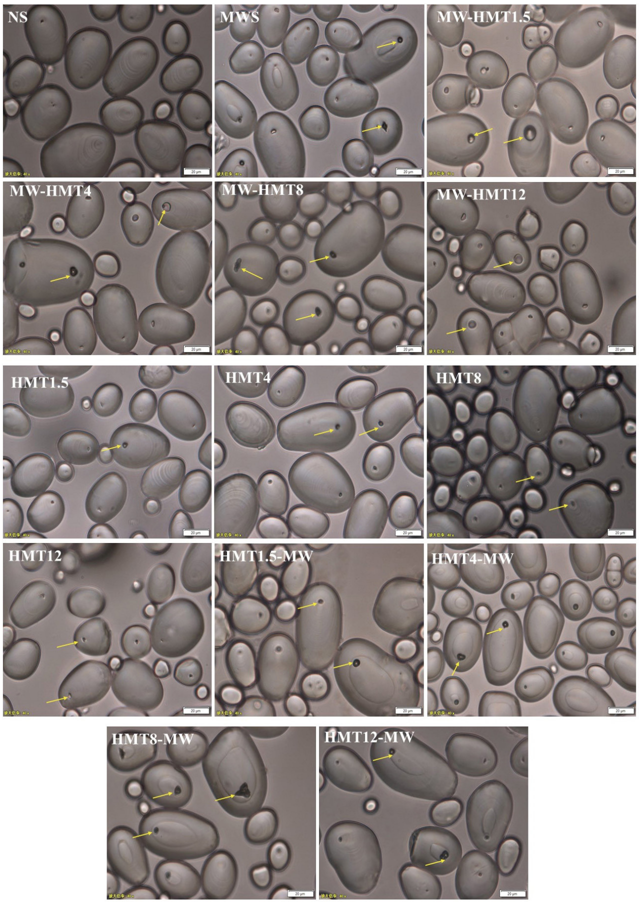

FIGURE 2. Normal light micrographs (×400) of native (NS) and modified potato starches: MWS: single microwave treatment; MW-HMT: heat-moisture treatment combined with microwave pre-treatment; HMT--MW: heat-moisture treatment combined with microwave post-treatment; 1.5, 4, 8, 12 mean the heating duration of HMT (h). The arrows illustrate the treated starch granules showing obvious hollow structure at hilum.

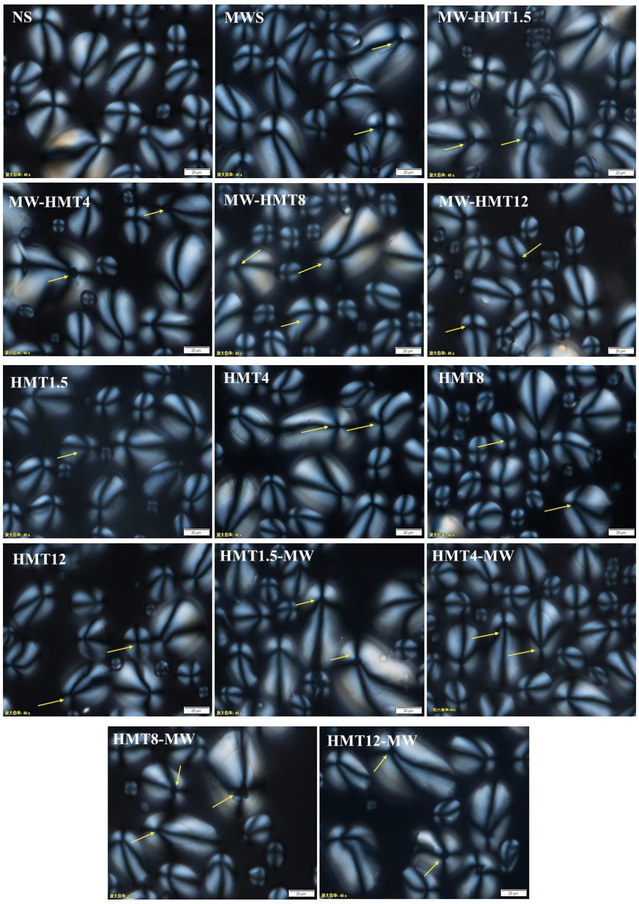

FIGURE 3. Polarized light micrographs (×400) of native (NS) and modified potato starches: MWS: single microwave treatment; MW-HMT: heat-moisture treatment combined with microwave pre-treatment; HMT--MW: heat-moisture treatment combined with microwave post-treatment; 1.5, 4, 8, 12 mean the heating duration of HMT (h). The arrows illustrate the treated starch granules showing obvious hollow structure at hilum.

TABLE 1. Pasting properties of native and modified potato starches.

Starch	Pasting temperature (°C)	Peak viscosity (cP)	Hold viscosity (cP)	Final viscosity (cP)	Breakdown viscosity (cP)	Setback viscosity (cP)
NS	68.5±0.2^{f}	6598±73^{a}	4072±25^{a}	4567±37^{c}	2526±47^{a}	496±12^{j}
MWS	68.8±0.1^{f}	3662±27^{b}	3597±31^{b}	6644±13^{a}	65.7±3.5^{bc}	3047±42^{b}
MW-HMT1.5	80.8±1.5^{bc}	2145±9^{e}	2090±9^{e}	4559±88^{c}	54.3±1.5^{bcde}	2439±39^{c}
MW-HMT4	88.50±1.0^{a}	1591±22^{g}	1548±18^{g}	3027±56^{e}	42.3±3.8^{cdef}	1479±40^{e}
MW-HMT8	92.9±2.0^{a}	1339±6^{jk}	1309±2^{k}	2290±26^{h}	30.3±6.4^{ef}	985±50^{h}
MW-HMT12	93.0±0.6^{a}	1315±18^{k}	1256±19^{l}	2064±18^{i}	58.3±1.5^{bcd}	807±4^{i}
HMT1.5	71.0±0.4^{ef}	3522±8^{c}	3443±11^{c}	6553±88^{a}	78.3±3.5^{b}	3110±79^{ab}
HMT4	80.5±5.6^{bc}	2173±58^{e}	2111±56^{e}	4528±150^{c}	61.7±2.1^{bcd}	2417±98^{c}
HMT8	76.5±1.5^{cd}	1582±21^{g}	1545±18^{g}	3019±14^{e}	38.0±5.6^{def}	1474±17^{e}
HMT12	76.8±0.4^{cd}	1433±2^{hi}	1416±16^{i}	2573± 23^{g}	17.3±14.6^{f}	1157±27^{g}
HMT1.5-MW	73.5±2.7^{de}	2591±24^{d}	2516±23^{d}	5684±91^{b}	75.3±2.1^{b}	3168±102^{a}
HMT4-MW	81.9±5.3^{b}	1854±16^{f}	1799±15^{f}	3696±48^{d}	55.0±2.0^{bcde}	1936±50^{d}
HMT8-MW	75.5±2.0^{de}	1475±58^{h}	1457±36^{g}	28033±97^{f}	55.0±8.9^{bcde}	1345±67^{f}
HMT12-MW	82.4±3.7^{b}	1392±8^{ij}	1373±13^{j}	2465±9^{g}	18.7±11.6^{f}	1092±22^{g}

All values are the mean of triplicate determinations± standard deviation. The means within the same column with different letters are significantly different ($p<0.05$). NS: native potato starch; MWS: single microwave treatment; HMT: heat-moisture treatment; MW: microwave treatment; MW-HMT: heat-moisture treatment combined with microwave pre-treatment; HMT-MW: heat-moisture treatment combined with microwave post-treatment; 1.5, 4, 8, 12 mean the heating duration of HMT (h).

single HMT. Starch modified by HMT combined with MW pre-treatment had lower peak viscosity, hold viscosity and final viscosity than the starch modified by HMT combined with MW post-treatment or the starch modified by single HMT, indicating that MW-HMT starch had lower resistance to heat and shear than HMT-MW starch or HMT starch.

Swelling power and solubility

Differences in cohesive force within starch granules can be characterized by differences in swelling and solubility. The swelling power of native and modified potato starches is shown in Table 2 and the solubility of native and modified potato starches is shown in Table 3. With an increase in test temperature, the swelling power of native starch and modified starches increased. The modified starch showed lower swelling power than native starch when the test temperature was 65°C, 75°C and 85°C, while opposite results were obtained at 95°C, and the MWS sample showed the highest swelling power (21.58%) at 95°C. MWS had the higher swelling power than MW-HMT modified starch at the same test temperature;

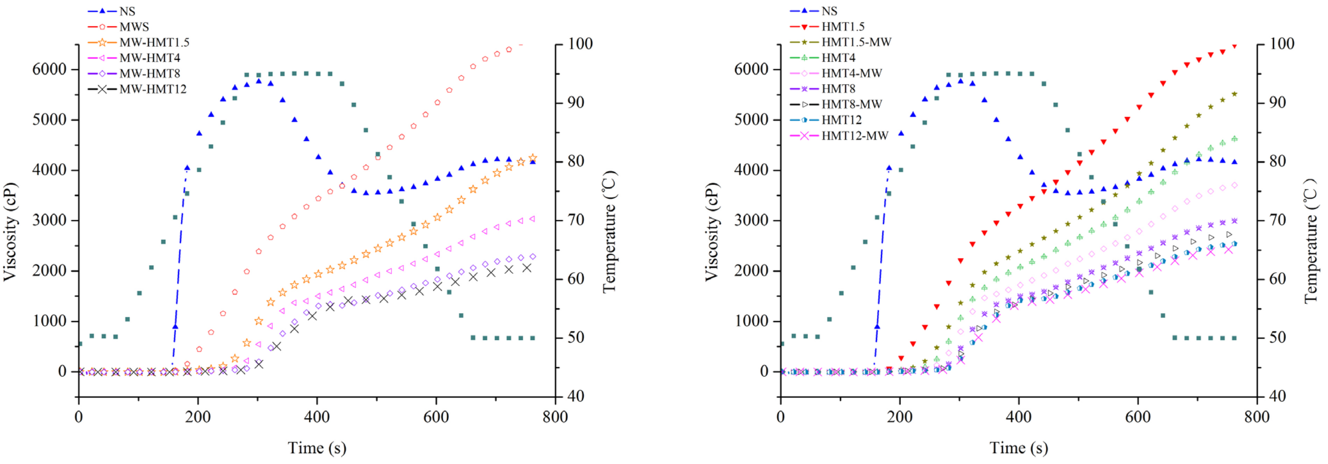

FIGURE 4. Rapid viscosity analysis pasting profiles of native (NS) and modified potato starches: MWS: single microwave treatment; MW-HMT: heat-moisture treatment combined with microwave pre-treatment; HMT-MW: heat-moisture treatment combined with microwave post-treatment; 1.5, 4, 8, 12 mean the heating duration of HMT (h).

TABLE 2. Swelling power of the native and modified potato starches.

Starch	Swelling power (%)				
	55°C	65°C	75°C	85°C	95°C
NS	2.28 ± 0.03^{h}	12.13 ± 0.79^{a}	14.14 ± 0.16^{a}	17.10 ± 0.12^{a}	13.29 ± 0.57^{f}
MWS	4.02 ± 0.23^{a}	12.94 ± 0.19^{b}	12.59 ± 0.20^{c}	15.74 ± 0.26^{b}	21.58 ± 0.04^{a}
MW-HMT1.5	3.05 ± 0.01^{b}	11.20 ± 0.17^{c}	12.31 ± 0.32^{cd}	$12.92\pm0.11d^{ef}$	16.37 ± 0.14^{c}
MW-HMT4	2.84 ± 0.05^{c}	9.58 ± 0.19^{ef}	11.65 ± 0.55^{e}	12.90 ± 0.09^{def}	14.27 ± 0.14^{e}
MW-HMT8	2.63 ± 0.07^{ef}	9.04 ± 0.24^{fgh}	10.56 ± 0.16^{fgh}	11.27 ± 0.23^{g}	14.12 ± 0.83^{e}
MW-HMT12	2.52 ± 0.02^{fg}	8.69 ± 0.23^{h}	10.70 ± 0.02^{fg}	11.19 ± 0.12^{g}	14.35 ± 0.38^{e}
HMT1.5	2.46 ± 0.10^{g}	11.13 ± 0.39^{cd}	13.28 ± 0.64^{b}	13.76 ± 0.70^{c}	18.27 ± 0.31^{b}
HMT4	2.48 ± 0.06^{g}	10.00 ± 0.03^{e}	12.36 ± 0.19^{cd}	13.35 ± 0.16^{cd}	16.36 ± 0.09^{b}
HMT8	2.47 ± 0.04^{g}	9.18 ± 0.15^{fgh}	11.56 ± 0.03^{e}	13.16 ± 0.25^{de}	15.53 ± 0.25^{d}
HMT12	2.47 ± 0.02^{g}	8.85 ± 0.30^{h}	10.89 ± 0.30^{f}	12.58 ± 0.08^{f}	15.20 ± 0.18^{d}
HMT1.5-MW	2.79 ± 0.00^{cd}	10.61 ± 0.25^{d}	11.84 ± 0.31^{de}	13.08 ± 0.01^{def}	18.34 ± 0.03^{b}
HMT4-MW	2.69 ± 0.04^{de}	9.95 ± 0.11^{e}	10.25 ± 0.33^{gh}	12.85 ± 0.20^{def}	16.39 ± 0.06^{c}
HMT8-MW	2.42 ± 0.02^{g}	9.45 ± 0.11^{efg}	10.04 ± 0.13^{h}	12.73 ± 0.11^{ef}	16.81 ± 0.40^{c}
HMT12-MW	2.41 ± 0.08^{g}	8.99 ± 0.32^{gh}	$9..95\pm0.09^{i}$	12.56 ± 0.16^{f}	16.56 ± 0.20^{c}

All values are the mean of triplicate determinations± standard deviation. The means within the same column with different letters are significantly different ($p<0.05$). NS: native potato starch; MWS: single microwave treatment; HMT: heat-moisture treatment; MW: microwave treatment; MW-HMT: heat-moisture treatment combined with microwave pre-treatment; HMT-MW: heat-moisture treatment combined with microwave post-treatment; 1.5, 4, 8, 12 mean the heating duration of HMT (h).

TABLE 3. Solubility of native and modified potato starches.

Starch	Solubility (%)				
	55°C	65°C	75°C	85°C	95°C
NS	4.29 ± 0.44^{a}	4.69 ± 0.31^{a}	2.11 ± 0.17^{j}	2.70 ± 0.17^{i}	7.70 ± 0.31^{g}
MWS	3.59 ± 0.47^{b}	3.24 ± 0.21^{b}	2.77 ± 0.27^{i}	5.64 ± 0.63^{f}	7.27 ± 0.13^{g}
MW-HMT1.5	0.77 ± 0.06^{g}	3.29 ± 0.07^{b}	2.73 ± 0.07^{i}	5.94 ± 0.33^{f}	8.70 ± 0.30^{f}
MW-HMT4	1.53 ± 0.15^{f}	3.18 ± 0.11^{b}	2.98 ± 0.03^{i}	6.70 ± 0.24^{e}	9.94 ± 0.37^{e}
MW-HMT8	2.37 ± 0.02^{de}	3.09 ± 0.06^{bc}	3.51 ± 0.31^{h}	7.29 ± 0.19^{d}	11.36 ± 0.46^{b}
MW-HMT12	2.29 ± 0.04^{e}	3.02 ± 0.04^{bc}	2.32 ± 0.13^{j}	7.18 ± 0.05^{de}	13.54 ± 0.02^{b}
HMT1.5	2.40 ± 0.08^{de}	2.80 ± 0.14^{cd}	5.63 ± 0.15^{f}	4.59 ± 0.11^{g}	7.35 ± 0.30^{g}
HMT4	2.32 ± 0.00^{e}	3.08 ± 0.18^{bc}	6.91 ± 0.25^{d}	4.70 ± 0.15^{g}	11.28 ± 0.31^{b}
HMT8	2.38 ± 0.07^{de}	2.65 ± 0.11^{d}	8.35 ± 0.08^{b}	5.86 ± 0.09^{f}	14.05 ± 0.18^{b}
HMT12	2.66 ± 0.11^{cd}	2.70 ± 0.15^{d}	6.14 ± 0.31^{e}	3.57 ± 0.30^{h}	8.69 ± 0.28^{f}
HMT1.5-MW	3.75 ± 0.17^{b}	3.11 ± 0.07^{bc}	3.01 ± 0.13^{i}	7.14 ± 0.47^{de}	8.43 ± 0.39^{f}
HMT4-MW	2.94 ± 0.06^{c}	3.09 ± 0.08^{bc}	4.42 ± 0.12^{g}	8.09 ± 0.13^{c}	10.53 ± 0.36^{d}
HMT8-MW	1.63 ± 0.12^{f}	4.68 ± 0.14^{a}	7.64 ± 0.21^{c}	15.28 ± 0.13^{b}	13.69 ± 0.14^{b}
HMT12-MW	1.37 ± 0.10^{f}	4.94 ± 0.34^{a}	15.66 ± 0.39^{a}	34.83 ± 0.33^{a}	15.65 ± 0.18^{a}

All values are the mean of triplicate determinations± standard deviation. The means within the same column with different letters are significantly different ($p<0.05$). NS: native potato starch; MWS: single microwave treatment; HMT: heat-moisture treatment; MW: microwave treatment; MW-HMT: heat-moisture treatment combined with microwave pre-treatment; HMT-MW: heat-moisture treatment combined with microwave post-treatment; 1.5, 4, 8, 12 mean the heating duration of HMT (h).

moreover, the swelling power of HMT modified starch (HMT, MW-HMT and HMT-MW) generally decreased with the treatment time when test temperature was the same. The decrease in starch swelling power can be attributed to the enhancement of molecular interactions between amylose and amylopectin, and the amylose-lipid complexes formed during MW and HMT [Han *et al.*, 2021]. Moreover, the swelling power of starch granules can also be affected by starch granules physical destruction, starch molecule rearrangement or/and starch chains re-associations induced by MW and HMT [Li *et al.*, 2019a].

The leaching of soluble molecules of starch granules, such as amylose, sugars can be characterized by solubility. Modified potato starch showed generally higher solubility than native starch when the test temperature was >75°C, and the solubility of starch samples increased respectively with the increase in test temperature from 75°C to 95°C (Table 3). This indicates that temperature increase could induce the leaching of amylose or sugars from starch granules. MW, HMT, HMT combined with MW pre- and post-treatment could cause depolymerization of starch molecules, resulting in a higher ratio of short chains which had greater tendency to hydration than native starch molecules [Han *et al.*, 2021]. At the same test temperature, the solubility of HMT and HMT-MW starch increased with the length of heating time, which indicated that long time heat-moisture treatment could enhance the molecular depolymerization of starch. The MW, HMT and HMT combined with MW pre- and post-treatment can cause the weathering of starch granules, which consequently leads to the improvement of solubility [Deka & Sit, 2016]. However, high gelatinization temperature of modified starch could lead to low solubility at low test temperature. The modified starch had not been gelatinized at low temperature, and the soluble substances cannot be leached out from the starch granules, resulting in low solubility.

FT-IR analysis

FT-IR is used to monitor the appearance, type and the strength of hydrogen bonds, which reflect the changes in starch molecule structure [Li *et al.*, 2021]. The ratio of crystalline regions to amorphous regions of starch granules can be indicated by the absorbance ratio of 1047/1022 cm^{-1}, while the short-range order can be indicated by the absorbance ratio of 1047/1035 cm^{-1} [Zhang *et al.*, 2021]. A higher absorbance ratio of 1047/1022 cm^{-1} indicates larger crystalline region and a higher absorbance ratio of 1047/1035 cm^{-1} indicates a higher short-range order of starch. The FT-IR spectra of native potato starch and modified potato starch are shown in Figure 5 and their corresponding absorbance ratios of 1047/1022 cm^{-1} and 1047/1035 cm^{-1} are summarized in Table 4. As shown in Figure 5, absorption peaks of characteristic groups of all starch granules had similar position and shape, indicating that there was no new absorption peak observed in the spectra, which indicated that any of the modification treatments (single MW, single HMT and HMT combined with MW pre- and post-treatment) neither created new functional groups nor altered the primary structure of the potato starch.

All modified starch granules had lower absorbance ratios of 1047/1022 cm^{-1} than that of native starch, and HMT combined with MW pre- and post-treatment had stronger effects on the decrease in the absorbance ratios than single MW or single HMT. What is more, with the increase in HMT duration, the ratios of 1047/1022 cm^{-1} of single HMT starch samples and HMT starch samples post-treated by MW decreased to different extents, while opposite results were observed for HMT starch samples pre-treated by MW. The ratios of 1047/1035 cm^{-1} of all the starch samples had the same variation trend as that of 1047/1022 cm^{-1}. These results indicated that microwave irradiation and heat-moisture treatment might have destroyed the double helix structure and crystal region of starch granules [Li *et al.*, 2019b]. Under different treatment conditions, the changing trend of the ratios of 1047/1022 cm^{-1} and 1047/1035 cm^{-1} was consistent with the changing trend of relative crystallinity analyzed by XRD (Table 4), which further confirmed that single MW, single HMT and HMT combined with MW pre- and post- treatment destroyed the crystal structure of potato starch.

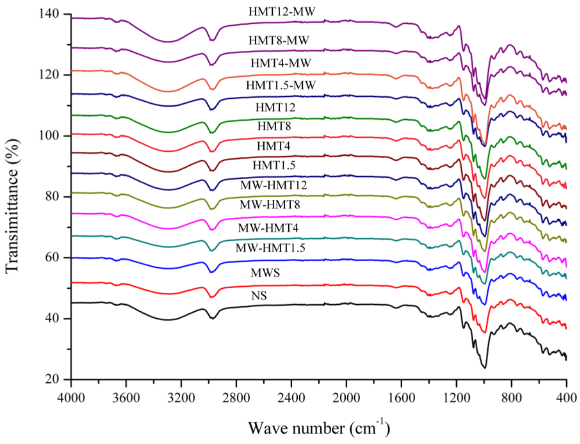

FIGURE 5. Fourier transform infrared spectroscopy spectra of native (NS) and modified starches: MWS: single microwave treatment; MW-HMT: heat-moisture treatment combined with microwave pre-treatment; HMT-MW: heat-moisture treatment combined with microwave post-treatment; 1.5, 4, 8, 12 mean the heating duration of HMT (h).

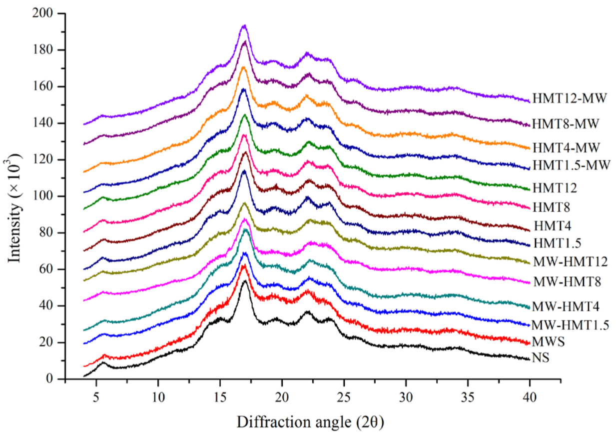

FIGURE 6. X-ray diffraction pattern of native (NS) and modified potato starches. MWS: single microwave treatment; MW-HMT: heat-moisture treatment combined with microwave pre-treatment; HMT-MW: heat-moisture treatment combined with microwave post-treatment; 1.5, 4, 8, 12 mean the heating duration of HMT (h).

TABLE 4. Fourier transform infrared spectroscopy intensity ratios, relative crystallinity and digestibility properties of the native and modified potato starches.

Starch	1047/1022 cm^{-1}	1047/1035 cm^{-1}	Relative crystallinity (%)	Digestibility properties		
				RDS (%)	SDS (%)	RS (%)
NS	1.0361 ± 0.0001^{a}	1.0083 ± 0.0001^{a}	19.39 ± 0.04^{a}	31.14 ± 0.10^{a}	55.17 ± 0.17^{bc}	13.69 ± 0.10^{h}
MWS	1.0150 ± 0.0001^{h}	0.9992 ± 0.0000^{e}	15.35 ± 0.07^{h}	29.14 ± 0.10^{de}	55.90 ± 0.37^{b}	14.97 ± 0.43^{fg}
MW-HMT1.5	1.0099 ± 0.0001^{k}	0.9965 ± 0.0001^{i}	15.55 ± 0.00^{fg}	28.91 ± 0.10^{ef}	55.23 ± 0.34^{bc}	15.86 ± 0.38^{f}
MW-HMT4	1.0100 ± 0.0002^{k}	0.9957 ± 0.0000^{j}	15.65 ± 0.02^{e}	28.43 ± 0.10^{gh}	52.17 ± 0.09^{d}	19.40 ± 0.16^{e}
MW-HMT8	1.0180 ± 0.0001^{f}	0.9980 ± 0.0002^{f}	15.74 ± 0.01^{d}	27.66 ± 0.60^{i}	50.05 ± 1.02^{f}	22.29 ± 0.53^{c}
MW-HMT12	1.0176 ± 0.0000^{g}	0.9978 ± 0.0001^{g}	15.83 ± 0.01^{c}	28.54 ± 0.10^{fg}	57.25 ± 0.68^{a}	14.21 ± 0.78^{gh}
HMT1.5	1.0268 ± 0.0000^{b}	1.0008 ± 0.0000^{c}	18.17 ± 0.04^{b}	28.11 ± 0.31^{h}	57.87 ± 0.35^{a}	14.02 ± 0.38^{gh}
HMT4	1.0232 ± 0.0002^{c}	1.0002 ± 0.0002^{d}	15.80 ± 0.06^{cd}	29.41 ± 0.10^{d}	54.57 ± 0.44^{c}	16.02 ± 0.42^{f}
HMT8	1.0217 ± 0.0000^{d}	0.9992 ± 0.0001^{e}	15.60 ± 0.02^{ef}	29.80 ± 0.20^{c}	47.36 ± 0.93^{g}	22.85 ± 0.72^{c}
HMT12	1.0206 ± 0.0000^{e}	0.9981 ± 0.0001^{f}	15.17 ± 0.04^{i}	30.23 ± 0.10^{b}	47.33 ± 1.20^{g}	22.44 ± 1.10^{c}
HMT1.5-MW	1.0235 ± 0.0000^{c}	1.0042 ± 0.0000^{b}	15.64 ± 0.03^{e}	29.52 ± 0.10^{cd}	51.43 ± 0.01^{de}	19.05 ± 0.09^{e}
HMT4-MW	1.0205 ± 0.0003^{e}	1.0003 ± 0.0000^{d}	15.50 ± 0.01^{g}	28.16 ± 0.10^{gh}	50.75 ± 1.37^{ef}	21.09 ± 1.47^{d}
HMT8-MW	1.0135 ± 0.0000^{i}	0.9969 ± 0.0000^{h}	15.39 ± 0.03^{h}	28.88 ± 0.26^{ef}	43.29 ± 0.32^{h}	27.83 ± 0.47^{a}
HMT12-MW	1.0130 ± 0.0005^{j}	0.9957 ± 0.0000^{j}	15.35 ± 0.04^{h}	29.12 ± 0.10^{de}	46.37 ± 0.33^{g}	24.50 ± 0.37^{b}

All values are the mean of triplicate determinations± standard deviation. The means within the same column with different letters are significantly different ($p<0.05$). RDS: rapidly-digestible starch; SDS: slowly-digestible starch; RS: resistant starch; NS: native potato starch; MWS: single microwave treatment; HMT: heat-moisture treatment; MW: microwave treatment; MW-HMT: heat-moisture treatment combined with microwave pre-treatment; HMT-MW: heat-moisture treatment combined with microwave post-treatment; 1.5, 4, 8, 12 mean the heating duration of HMT (h).

X-Ray diffraction analysis

X-Ray diffraction (XRD) analysis is an important technique used to evaluate changes in starch structure. The patterns of native starch and modified starch analyzed by XRD are shown in Figure 6 and the corresponding relative crystallinity was listed in Table 4. Native potato starch exhibited a B-type of X-ray diffraction pattern, which was characterized with a small peak at 5.6° 2θ, a peak at 17° 2θ, and a doublet at 22° 2θ and 24° 2θ [Juansang *et al*., 2017; Li *et al.*, 2020]. There were some significant changes in the intensities of peaks between native potato starch and modified potato starch. Similar reduction in peak intensities of taro starch after HMT and MW was observed by Deka & Sit [2016]. Significant changes in the XRD patterns of all the modified starches were observed (Figure 6). The diffraction peak at 15° 2θ of all the MW-HMT starch and MWS became smooth, the diffraction peaks at 19.5° 2θ gradually disappeared and the double peaks at 22° 2θ and 24° 2θ merged into a broad peak. Similar changes were observed between HMT and HMT-MW starch, the diffraction peak at 19.5° 2θ, and the double peaks at 22° 2θ and 24° 2θ gradually became smooth with the prolongation of heat-moisture treatment time. These results indicate that the X-ray diffraction of potato starch could be changed from B-type to a mixture of A+B type after HMT or/and MW modification. Similar results were obtained by Li *et al.* [2020] regarding lily starch modification by HMT. Thirty six water molecules in a central channel of the B-unit cell vaporized during the modification process of MW, HMT, MW-HMT and HMT-MW, and then a pair of double helices moved into the central channel which was originally occupied by the vaporized water molecules, leading to the change of crystalline orientation and destruction of crystalline regions, which eventually induced changes in the XRD pattern of potato starch (B→A+B) [Gunaratne & Hoover, 2002; Li *et al.*, 2020].

All modified potato starch granules had lower relative crystallinity than that of native starch, which was 19.39% (Table 4). The relative crystallinity of MWS, MW-HMT1.5, MW-HMT4, MW-HMT8, MW-HMT12 was 15.35%, 15.55%, 15.65%, 15.74% and 15.83% respectively, which indicated that the relative crystallinity of MW-HMT starch increased with the prolongation of heat-moisture treatment time. Moreover, HMT-MW starch had lower relative crystallinity than that of the single HMT starch at the same heat moisture treatment condition. The reduction of relative crystallinity of microwave-irradiated millet starch was also observed by Li *et al.* [2019a]. The source of starch and HMT conditions affected the changes observed in starch crystallinity. The results of this research showed that the effect of HMT on potato starch relative crystallinity was consistent with the previous study on the effect of HMT on that of normal maize starch and waxy maize starch [Sui *et al.*, 2015]. HMT disrupted the amylopectin crystallites and induced the instability of the lamellar arrangement of starch granules, which made the relative crystallinity of HMT starch lower than that of native potato starch [Colussia *et al.*, 2020]. The decrease in crystallinity of the MW starch attributed to the vibrational motion of the polar molecules induced by the microwave radiation directly impacted the crystalline lamellae inside the granule and destroyed their radial crystalline structure [Palav & Seetharaman, 2006; Mollekopf *et al.*, 2011]. What is more, under the combined effect of thermal energy, microwave radiation and moisture, irreversible damage occurred in crystalline regions of starch granules, inducing the growth of the amorphous or semi-crystalline regions, and consequently reducing the relative crystallinity of starch [Khunae *et al.*, 2007].

In vitro digestibility

Based on the rate and degree of *in vitro* digestion, starch is commonly classified into three categories: RDS, SDS and RS, among which SDS and RS are considered to be beneficial to human health [Xu *et al.*, 2019]. The contents of RDS, SDS and RS in native potato starch were 32.14%, 55.17% and 13.69%, respectively (Table 4), which were inconsistent with the results of previous research reported by Wang *et al.* [2019] showing RDS, SDS and RS contents in native potato starch at 22.5%, 12.8% and 64.7% respectively. The unusual results of RDS, SDS and RS contents in native potato starch might be attributed to the method of *in vitro* digestion. Gelatinized and non-gelatinized starch samples showed different *in vitro* digestibility, which was confirmed by Ji & Yu [2018] and by Piecyk & Domian [2021], while the results of Chen's [2020] research directly indicated that gelatinized and non-gelatinized potato starch showed different contents of RDS, SDS and RS. The gelatinized starch showed higher RDS content than non-gelatinized starch for their granular structure had been already disrupted during the cooking process and thus became more susceptible to enzymatic hydrolysis [Li *et al.*, 2020].

The RDS content of all modified potato starches was significantly ($p<0.5$) lower than that of native potato starch, while the RS content was generally higher (Table 4). When the heating time of HMT was less than 12 h, the RS content increased successively with the prolongation of heat-moisture treatment time. Previous studies have reported that HMT could increase the content of RS and the total content of SDS and RS in maize starch [Sui *et al.*, 2015] and sweet potato starch [Trung *et al.*, 2017], while MW also increased the content of RS and the total content of SDS and RS in *Canna edulis* Ker starch [Zhang *et al.*, 2010] and debranched mung-bean starch [Huong *et al.*, 2021]. Amylopectin in starch was partly degraded, the hydrogen bonds between starch molecules were broken, and the molecular chains in starch granules were separated by microwave heating, all these resulting in swelling and gelatinization of starch particles. HMT further rearranged the molecular structures, transformed some RDS fractions into SDS and/or RS fractions and increased the resistance of starch to enzymatic hydrolysis [Li *et al.*, 2018; Liu *et al.*, 2019]. Furthermore, dual modification of HMT and MW increased the total content of SDS and RS but decreased the content of RDS in potato starch (Table 4). It was worth mentioning that under the same HMT heating time, the RS content of HMT-MW starch was higher than that of HMT starch, *e.g.*, the RS content of HMT1.5-MW (19.05%) was higher than that of HMT1.5 (14.02%). Additionally, HMT-MW starch also had a higher RS content than that of MW-HMT starch under the same HMT heating time, *e.g.*, the RS content of HMT1.5-MW (19.05%) was higher than that of MW-HMT1.5 (15.86%). All these results indicated that dual starch modification *via* HMT and MW had greater effects on starch digestion than single MW or HMT, and the sequence of dual modification also affected starch digestibility.

CONCLUSIONS

HMT, MW and HMT combined with MW pre- and post-treatment had significant effects on the microstructure, crystalline and structural properties and digestibility of potato starch. As can be observed from the scanning electron microscopy, normal light and polarized light microscopy, some depressions or potholes appeared on the surface of starch granules after modification, and the center of polarized cross structure slowly expanded. Dual starch modification *via* MW and HMT made the surface of its granules rougher and caused more serious depressions or scallops than single modification with MW or HMT, especially in the case of HMT-MW. All the treatments increased the pasting temperature and setback viscosity but decreased peak viscosity and breakdown viscosity of starch. Modified starch showed lower swelling power than that of native starch when the test temperature was 65–85°C, while opposite results were obtained at 95°C. Modified starch samples showed higher solubility than that of native starch when test temperature was 75–95°C. The FT-IR and XRD spectra implied that HMT and MW destroyed the double helices and crystalline structure of potato starch. All treatments increased the content of RS but reduced the content RDS of potato starch. Under the same HMT heating duration, the RS content of starch modified by HMT combined by with MW post-treatment was significantly higher than that of starch modified by HMT combined by MW pre-treatment and single HMT. The information obtained in this paper might be beneficial to the industrial applications of microwave and heat-moisture techniques deployed to modify starch and eventually produce new starch materials satisfying the potential consumer requirements.

ACKNOWLEDGEMENTS

The authors would like to thank Guangxi Key Laboratory of Health Care Food Science and Technology for providing laboratory facilities and technical assistance during the study.

RESEARCH FUNDING

This study was financially supported by the Middle aged and Young Teachers' Basic Ability Promotion Project of Guangxi (2021KY0710).

CONFLICT OF INTERESTS

Authors declare no conflict of interests.

ORCID IDs

Chunli Deng https://orcid.org/0000-0003-1116-7407
Oksana Melnyk https://orcid.org/0000-0002-9201-7955
Yanghe Luo https://orcid.org/0000-0003-2705-1505

REFERENCES

1. Arns, B., Bartz, J., Radunz, M., Evangelho, J.A.d., Pinto, V.Z., Zavareze, E.d.R., GuerraDias, A.R. (2015). Impact of heat--moisture treatment on rice starch, applied directly in grain paddy rice or in isolated starch. *LWT – Food Science and Technology*, *60*(2), Part 1, 708–713. https://doi.org/10.1016/j.lwt.2014.10.059
2. AOAC, 2005. Oficial Methods of Analysis, 18th ed. Association of Oficial Analytical Chemists, Gaithersburg, MD. https://www.eoma.aoac.org/
3. Bharti, I., Singh, S., Saxena, D.C. (2019). Exploring the influence of heat moisture treatment on physicochemical, pasting, structural and morphological properties of mango kernel starches from Indian cultivars. *LWT – Food Science and Technology*, *110*, 197–206. https://doi.org/10.1016/j.lwt.2019.04.082
4. Braşoveanu, M., Nemţanu, M.R. (2014). Behaviour of starch exposed to microwave radiation treatment. *Starch-Stärke*, *66*(1–2), 3–14. https://doi.org/10.1002/star.201200191
5. Cao, M., Gao, Q. (2020). Effect of dual modification with ultrasonic and electric field on potato starch. *International Journal of Biological Macromolecules*, *150*, 637–643. https://doi.org/10.1016/j.ijbiomac.2020.02.008
6. China National Standard for Food Safety (2016). Determination of Moisture in Food (GB 5009.3). http://down.foodmate.net/standard/sort/3/49325.html
7. China National Standard for Food Safety (2016). Determination of Protein in Food (GB 5009.5). http://down.foodmate.net/standard/sort/3/50381.html
8. China National Standard for Food Safety (2016). Determination of Lipid in Food (GB 5009.6). http://down.foodmate.net/standard/sort/3/50382.html
9. Chen, X., Liu, Y., Xu, Z., Zhang, C., Liu, X., Sui, Z., Corke, H. (2021a). Microwave irradiation alters the rheological properties and molecular structure of hull- less barley starch. *Food Hydrocolloids*, *120*(2), art. no. 106821. https://doi.org/10.1016/j.foodhyd.2021.106821
10. Chen, X., Luo, J., Liang, Z., Zhu, J., Li, L., Wang, Q. (2020). Structural and physicochemical/digestion characteristics of potato starch-amino acid complexes prepared under hydrothermal conditions. *International Journal of Biological Macromolecules*, *145*, 1091–1098. https://doi.org/10.1016/j.ijbiomac.2019.09.202
11. Chen, X., Ma, M., Liu, X., Xu, Z., Zhang, C., Sui, Z., Corke, H. (2021b). Microwave treatment alters the fine molecular structure of waxy hull-less barley starch. *International Journal of Biological Macromolecules*, *193*, Part B, 1086–1092. https://doi.org/10.1016/j.ijbiomac.2021.11.007
12. Chung, H.J., Liu, Q., Hoover, R. (2010). Effect of single and dual hydrothermal treatments on the crystalline structure, thermal properties, and nutritional fractions of pea, lentil, and navy bean starches. *Food Research International*, *43*(2), 501–508. https://doi.org/10.1016/j.foodres.2009.07.030
13. Colussia, R., Kringel, D., Kaur, L., Zavareze, E.d.R., Dias, A.R.G., Singh, J. (2020). Dual modification of potato starch: Effects of heat-moisture and high pressure treatments on starch structure and functionalities. *Food Chemistry*, *318*, art. no. 126475. https://doi.org/10.1016/j.foodchem.2020.126475
14. Deka, D., Sit, N. (2016). Dual modification of taro starch by microwave and other heat moisture treatments. *International Journal of Biological Macromolecules*, *92*, 416–422. https://doi.org/10.1016/j.ijbiomac.2016.07.040
15. Deng, C., Melnyk, O., Luo, Y. (2021a). The effect of heat-moisture treatment conditions on the structure properties and functionalities of potato starch. *Potravinarstvo Slovak Journal of Food Sciences*, *15*, 824–834. https://doi.org/10.5219/1647
16. Deng, C., Melnyk, O., Luo, Y. (2021b). Effects of microwave and heat-moisture treatments on color characteristics, particle size and water distribution of potato starch. *Ukrainian Journal of Food Science, 9*(2), 156–166. https://doi.org/10.24263/2310-1008-2021-9-2-4
17. Gałkowska, D., Juszczak, L. (2019). Effects of amino acids on gelatinization, pasting and rheological properties of modified potato starches. *Food Hydrocolloids*, *92*, 143–154. https://doi.org/10.1016/j.foodhyd.2019.01.063
18. Gunaratne, A., Hoover, R. (2002). Effect of heat–moisture treatment on the structure and physicochemical properties of tuber and root starches. *Carbohydrate Polymers*, *49*(4), 425–437. https://doi.org/10.1016/S0144-8617(01)00354-X
19. Guo, Z., Zeng, S., Lu, X., Zhou, M., Zheng, M., Zheng, B. (2015). Structural and physicochemical properties of lotus seed starch treated with ultra-high pressure. *Food Chemistry*, *186*, 223–230. https://doi.org/10.1016/j.foodchem.2015.03.069
20. Han, L., Cao, S., Yu, Y., Xu, X., Cao, X., Chen, W. (2021). Modification in physicochemical, structural and digestive properties of pea starch during heat-moisture process assisted by pre- and post-treatment of ultrasound. *Food Chemistry*, *360*, art. no. 129929. https://doi.org/10.1016/j.foodchem.2021.129929
21. Huong, N.T.M., Hoa, P.N., Hung, P.V. (2021). Effects of microwave treatments and retrogradation on molecular crystalline structure and *in vitro* digestibility of debranched mung-bean starches. *International Journal of Biological Macromolecules*, *190*, 904–910. https://doi.org/10.1016/j.ijbiomac.2021.09.032
22. Ji, Y., Yu, J. (2018). *In vitro* digestion and physicochemical characteristics of corn starch mixed with amino acid modified by heat-moisture treatment. *Food Hydrocolloids*, *77*, 720–725. https://doi.org/10.1016/j.foodhyd.2017.11.013
23. Juansang, J., Puncha-arnon, S., Uttapap, D., Puttanlek, C., Rungsardthong, V., Watcharatewinkul, Y. (2017). Concentration of plasticizers applied during heat–moisture treatment affects properties of the modified canna starch. *Food Chemistry*, *221*, 1587–1594. https://doi.org/10.1016/j.foodchem.2016.10.134
24. Kaur, M., Singh, S. (2019). Influence of heat-moisture treatment (HMT) on physicochemical and functional properties of starches from different Indian oat (*Avena sativa* L.) cultivars. *International Journal of Biological Macromolecules*, *122*, 312–319. https://doi.org/10.1016/j.ijbiomac.2018.10.197
25. Khunae, P., Tran, T., Sirivongpaisal, P. (2007). Effect of heat--moisture treatment on structural and thermal properties of rice starches differing in amylose content. *Starch – Starke*, *59*(12), 593–599. https://doi.org/10.1002/star.200700618

26. Kumar, Y., Singh, L., Sharanagat, V.S., Patel, A., Kumar, K. (2020). Effect of microwave treatment (low power and varying time) on potato starch: Microstructure, thermo-functional, pasting and rheological properties. *International Journal of Biological Macromolecules*, *155*, 27–35.
https://doi.org/10.1016/j.ijbiomac.2020.03.174
27. Li, H., Wang, R., Liu, J., Zhang, Q., Li, G., Shan, Y., Ding, S. (2020). Effects of heat-moisture and acid treatments on the structural, physicochemical, and *in vitro* digestibility properties of lily starch. *International Journal of Biological Macromolecules*, *148*, 956–968.
https://doi.org/10.1016/j.ijbiomac.2020.01.181
28. Li, H., Zhai, F., Li, J., Zhu, X., Guo, Y., Zhao, B., Xu, B. (2021). Physicochemical properties and structure of modified potato starch granules and their complex with tea polyphenols. *International Journal of Biological Macromolecules*, *166*, 521–528.
https://doi.org/10.1016/j.ijbiomac.2020.10.209
29. Li, Y., Hu, A., Wang, X., Zheng, J. (2019a). Physicochemical and *in vitro* digestion of millet starch: Effect of moisture content in microwave. *International Journal of Biological Macromolecules*, *134*, 308–315.
https://doi.org/10.1016/j.ijbiomac.2019.05.046
30. Li, Y., Hu, A., Zheng, J., Wang, X. (2019b). Comparative studies on structure and physiochemical changes of millet starch under microwave and ultrasound at the same power. *International Journal of Biological Macromolecules*, *141*, 76–84.
https://doi.org/10.1016/j.ijbiomac.2019.08.218
31. Li, Y., Xu, T., Xiao, J., Zong, A., Qiu, B., Jia, M., Liu, L., Liu, W. (2018). Efficacy of potato resistant starch prepared by microwave–toughening treatment. *Carbohydrate Polymers*, *192*, 299–307.
https://doi.org/10.1016/j.carbpol.2018.03.076
32. Liu, K., Zhang, B., Chen, L., Li, X., Zheng, B. (2019). Hierarchical structure and physicochemical properties of highland barley starch following heat moisture treatment. *Food Chemistry*, *271*, 102–108.
https://doi.org/10.1016/j.foodchem.2018.07.193
33. Mollekopf, N., Treppe, K., Dixit, O., Bauch, J., Führlich, T. (2011). Simultaneous drying and modification of properties of starch using vacuum microwave treatment. *Drying Technology*, *29*(5), 599–605.
https://doi.org/10.1080/07373937.2010.519839
34. Oyeyinka, S.A., Akintayo, O.A., Adebo, O.A., Kayitesi, E., Njobeh, P.B. (2021). A review on the physicochemical properties of starches modified by microwave alone and in combination with other methods. *International Journal of Biological Macromolecules*, *176*, 87–95.
https://doi.org/10.1016/j.ijbiomac.2021.02.066
35. Palav, T., Seetharaman, K. (2006). Mechanism of starch gelatinization and polymer leaching during microwave heating. *Carbohydrate Polymers*, *65*(3), 364–370.
https://doi.org/10.1016/j.carbpol.2006.01.024
36. Piecyk, M., Domian, K. (2021). Effects of heat-moisture treatment conditions on the physicochemical properties and digestibility of field bean starch (*Vicia faba* var. minor). *International Journal of Biological Macromolecules*, *182*, 425–433.
https://doi.org/10.1016/j.ijbiomac.2021.04.015
37. Santos, T.D., Leonel, M., Garcia, É., Carmo, E.D., Franco, C. (2016). Crystallinity, thermal and pasting properties of starches from different potato cultivars grown in Brazil. *International Journal of Biological Macromolecules*, *82*, 144–149.
https://doi.org/10.1016/j.ijbiomac.2015.10.091
38. Schafranski, K., Ito, V.C., Lacerda, L.G. (2021). Impacts and potential applications: A review of the modification of starches by heat-moisture treatment (HMT). *Food Hydrocolloids*, *117*, art. no. 106690.
https://doi.org/10.1016/j.foodhyd.2021.106690
39. Singh, J., Colussi, R., McCarthy, O.J., Kaur, L. (2016). Potato starch and its modification. Chapter 8, In J. Singh, L. Kaur (Eds.), *Advances in Potato Chemistry and Technology*, 2nd edition, Academic Press, San Diego, pp. 195–247.
https://doi.org/10.1016/B978-0-12-800002-1.00008-X
40. Singh, J., Kaur, L., Singh, N. (2004). Effect of acetylation on some properties of corn and potato starches. *Starch – Starke*, *56*(12), 586–601.
https://doi.org/10.1002/star.200400293
41. Singh, N., Singh, J., Kaur, L., Sodhi, N.S., Gill, B.S. (2003). Morphological, thermal and rheological properties of starches from different botanical sources. *Food Chemistry*, *81*(2), 219–231.
https://doi.org/10.1016/S0308-8146(02)00416-8
42. Singh, V., Kumar, P., Sanghi, R. (2012). Use of microwave irradiation in the grafting modification of the polysaccharides – A review. *Progress in Polymer Science*, *37*(2), 340–364.
https://doi.org/10.1016/j.progpolymsci.2011.07.005
43. Sui, Z., Yao, T., Zhao, Y., Ye, X., Kong, X., Ai, L. (2015). Effects of heat–moisture treatment reaction conditions on the physicochemical and structural properties of maize starch: Moisture and length of heating. *Food Chemistry*, *173*, 1125–1132.
https://doi.org/10.1016/j.foodchem.2014.11.021
44. Tan, X., Li, X., Chen, L., Xie, F., Li, L., Huang, J. (2017). Effect of heat-moisture treatment on multi-scale structures and physicochemical properties of breadfruit starch. *Carbohydrate Polymers*, *161*, 286–294.
https://doi.org/10.1016/j.carbpol.2017.01.029
45. Trung, P.T.B., Ngoc, L.B.B., Hoa, P.N., Tien, N.N.T., Hung, P.V. (2017). Impact of heat-moisture and annealing treatments on physicochemical properties and digestibility of starches from different colored sweet potato varieties. *International Journal of Biological Macromolecules*, *105*, Part 1, 1071–1078.
https://doi.org/10.1016/j.ijbiomac.2017.07.131
46. Uzizerimana, F., Dang, K., Yang, Q., Hossain, M.S., Gao, S., Bahati, P., Mugiraneza, N.G., Yang, P., Feng, B. (2021). Physicochemical properties and *in vitro* digestibility of tartary buckwheat starch modified by heat moisture treatment: A comparative study. *NFS Journal*, *25*, 12–20.
https://doi.org/10.1016/j.nfs.2021.09.001
47. Wang, H., Liu, Y., Chen, L., Li, X., Wang, J., Xie, F. (2018). Insights into the multi-scale structure and digestibility of heat-moisture treated rice starch. *Food Chemistry*, *242*, 323–329.
https://doi.org/10.1016/j.foodchem.2017.09.014
48. Wang, H., Wang, Z., Li, X., Chen, L., Zhang, B. (2017). Multi-scale structure, pasting and digestibility of heat moisture treated red adzuki bean starch. *International Journal of Biological Macromolecules*, *102*, 162–169.
https://doi.org/10.1016/j.ijbiomac.2017.03.144
49. Wang, H., Zhang, B., Chen, L., Li, X. (2016). Understanding the structure and digestibility of heat-moisture treated starch. *International Journal of Biological Macromolecules*, *88*, 1–8.
https://doi.org/10.1016/j.ijbiomac.2016.03.046

50. Wang, M., Sun, M., Zhang, Y., Chen, Y., Wu, Y., Ouyang, J. (2019). Effect of microwave irradiation-retrogradation treatment on the digestive and physicochemical properties of starches with different crystallinity. *Food Chemistry*, *298*, art. no. 125015. https://doi.org/10.1016/j.foodchem.2019.125015
51. Wang, Q., Li, L., Zheng, X. (2021). Recent advances in heat-moisture modified cereal starch: Structure, functionality and its applications in starchy food systems. *Food Chemistry*, *344*, art. no. 128700. https://doi.org/10.1016/j.foodchem.2020.128700
52. Xu, M., Saleh, A.S., Gong, B., Li, B., Jing, L., Gou, M., Jiang, H., Li, W. (2018). The effect of repeated *versus* continuous annealing on structural, physicochemical, and digestive properties of potato starch. *Food Research International*, *111*, 324–333. https://doi.org/10.1016/j.foodres.2018.05.052
53. Xu, X., Chen, Y., Luo, Z., Lu, X. (2019). Different variations in structures of A- and B-type starches subjected to microwave treatment and their relationships with digestibility. *LWT – Food Science and Technology*, *99*, 179–187. https://doi.org/10.1016/j.lwt.2018.09.072
54. Zavareze, E.d.R., Dias, A.R.G. (2011). Impact of heat-moisture treatment and annealing in starches: A review. *Carbohydrate Polymers*, *83*(2), 317–328. https://doi.org/10.1016/j.carbpol.2010.08.064
55. Zhang, H., Wang, R., Chen, Z., Zhong, Q. (2019). Enzymatically modified starch with low digestibility produced from amylopectin by sequential amylosucrase and pullulanase treatments. *Food Hydrocolloids*, *95*, 195–202. https://doi.org/10.1016/j.foodhyd.2019.04.036
56. Zhang, H., Xu, F., Wu, Y., Hu, H., Dai, X. (2017). Progress of potato staple food research and industry development in China. *Journal of Integrative Agriculture*, *16*(12), 2924–2932. https://doi.org/10.1016/S2095-3119(17)61736-2
57. Zhang, J., Chen, F., Liu, F., Wang, Z. (2010). Study on structural changes of microwave heat-moisture treated resistant *Canna edulis* Ker starch during digestion *in vitro*. *Food Hydrocolloids*, *24*(1), 27–34. https://doi.org/10.1016/j.foodhyd.2009.07.005
58. Zhang, K., Zhao, D., Guo, D., Tong, X., Zhang, Y., Wang, L. (2021). Physicochemical and digestive properties of A- and B-type granules isolated from wheat starch as affected by microwave--ultrasound and toughening treatment. *International Journal of Biological Macromolecules*, *183*, 481–489. https://doi.org/10.1016/j.ijbiomac.2021.04.180

Pol. J. Food Nutr. Sci., 2022, Vol. 72, No. 3, pp. 263–272
On-line ISSN: 2083-6007
Print ISSN: 1230-0322
DOI: 10.31883/pjfns/152667
http://journal.pan.olsztyn.pl

Original article
Section: Food Technology

Effect of Electrolyzed Cassava Starch-Gelatin Coating on Biochemical Properties and Ripening of Banana (*Musa acuminata L.*) Fruits

Thanh Tung Pham[1], Thuy Linh Nguyen[2], Le Phuong Lien Nguyen[1,3], László Baranyai[1], Khanh Son Trinh[4]*

[1]*Institute of Food Science and Technology, Hungarian University of Agriculture and Life Sciences, Hungary*
[2]*Faculty of Fisheries, Nong Lam University, Ho Chi Minh City, Vietnam*
[3]*Institute of Biotechnology and Food Technology, Industrial University of Ho Chi Minh City, Vietnam*
[4]*Faculty of Chemical and Food Technology, Ho Chi Minh City University of Technology and Education, Ho Chi Minh City, Vietnam*

Key words: climacteric fruit, starch, electrolysis, respiration, thin coating

In this study, cassava starch oxidized by the electrolysis was used as an edible coating to improve the shelf life of banana fruits. The effects of coating in solutions of electrolyzed starch with 1, 2 and 3% (*w/v*) gelatin and without gelatin addition on respiratory rate and biochemical properties of banana during 8 days of storage at room temperature (75–80% relative humidity) were evaluated. The micrographs of scanning electron microscopy showed very thin coating layers (<25.2 mm) with continuous network topology and no cracks. During the storage period, a significant reduction in respiration rate and weight loss of coated bananas compared to uncoated fruits was noted. Furthermore, the change in titratable acidity and contents of soluble solids, total carbohydrates and reducing sugars of coated bananas were slower. Increasing the gelatin content in the coating had a beneficial effect on delaying the ripening of bananas. The oxidized starch coating formulation with 3% (*w/v*) of gelatin demonstrated the highest efficiency as it delayed the respiratory peak 4 days more than in the uncoated bananas. This study results suggest that electrolyzed starch-gelatin coating could be a potential material to extend the shelf life of fruits.

INTRODUCTION

In recent decades, postharvest technology has been developed, in which modified atmosphere packaging and cold are widely exploited [Kudachikar *et al.,* 2011; Le Nguyen *et al.,* 2020; Radziejewska-Kubzdela *et al.,* 2007]. However, packaging made of synthetic polymers is harmful to the environment while the low temperature may cause chilling injury symptoms on fruits [Salehi, 2020; Zsom *et al.,* 2018]. Along with customer interest in biodegradable and eco-friendly materials, the edible coating is a suitable alternative to increase fruit shelf life, with the same effect as storage in a modified atmosphere [Chiumarelli & Hubinger, 2014; Karaca *et al.,* 2014; Kokoszka & Lenart, 2007].

Cassava (*Manihot esculenta* C.) starch is commonly used for fruit coating because it can be produced in large quantities at a low cost. Additionally, it is safe for human consumption and has a good gas barrier [Aguilar-Méndez *et al.,* 2008; Kim *et al.,* 2015]. However, due to the retrogradation mechanism and hydrophilicity property of starch, cassava starch-based coating becomes brittle and has a less efficient water vapor barrier [Cortés-Rodríguez *et al.,* 2020; Kim *et al.,* 2015]. Therefore, the electrolysis method is used to oxidize cassava starch to improve the physical-mechanical properties of the coating. By forming cross-linking, electrolyzed cassava starch improves the water-oxygen barrier [Trinh & Dang, 2019]. The water solubility of electrolyzed cassava starch is four times higher than that of the native cassava starch [Trinh & Dang, 2019]. Moreover, the electrolysis method also yields a higher water solubility of starch than other modification methods, which is advantageous for coating applications since it prevents coating brittleness [Basiak *et al.,* 2017; Trinh & Dang, 2019]. Furthermore, electrolyzed cassava starch is whiter in comparison with native cassava starch and the difference in color can be recognized by human eyes [Trinh & Dang, 2019]. Along with being odorless and tasteless, coating transparency is an important property that has a direct influence on consumer decisions [Agarwal, 2021]. Importantly, the electrolysis method is cheap, safe and easy to perform as chlorine can be easily washed out from cassava starch, whereas other oxidation methods may present residues of NaClO and H_2O_2 in food, or use harmful reagents such as $(NH_4)_2SO_4$, $NaBrO_3$, and $KMnO_4$ [Pranoto *et al.,* 2021; Trinh & Dang, 2019]. Gelatin is added to the polymer

---

* Corresponding Author:
E-mail: tungpt@hcmute.edu.vn (Dr. T.T. Pham)

Submitted: 22 June 2022
Accepted: 8 August 2022
Published on-line: 2 September 2022

matrix as a reinforcement to improve the physical-mechanical properties of coating [Podshivalov *et al.,* 2020]. Gelatin is a water-soluble material that is more stable in structure and less moisture-sensitive than starch. Furthermore, the addition of glycerol and sorbitol is necessary to enhance flexibility and maintain the coating integrity [Al-Hassan & Norziah, 2012; Fakhouri *et al.,* 2012]. In the starch-gelatin matrix, glycerol and sorbitol can act as plasticizers as well as compatibilizers [Podshivalov *et al.,* 2017].

Banana is a popular tropical fruit with an abundant world production [FAO, 2021]. Bananas are typically collected before fully mature and stored at room temperature. However, their shelf life is relatively short because the metabolism related to respiration and ethylene production still continues at a rapid rate after harvest [Neelam *et al.,* 2003]. There is currently a lack of studies evaluating the effectiveness of electrolyzed cassava starch coating in fruit preservation. Therefore, the purpose of this research was to develop edible coatings based on electrolyzed cassava starch, gelatin, and blends of glycerol and sorbitol as plasticizers, in order to extend the shelf life of banana during storage at 30±2°C (75–80% relative humidity, RH). The effectiveness of electrolyzed coating was assessed by determining respiration rate, weight loss, and contents of total soluble solids, organic acids, reducing sugars, total carbohydrates, and starch.

MATERIALS AND METHODS

Materials

Banana (*Musa acuminata L.*) was purchased uniformly without any physical damage. The ripeness of bananas was selected at stage 2 based on the scale of Kader [2005]. Fruits were bought at Thu Duc wholesale market, Ho Chi Minh, Vietnam after 12–14 h harvesting.

Cassava starch powder was bought from Fococev Vietnam JointStock Company, Hochiminh, Vietnam (the purity was ≥98%, in dry basis). Gelatin (the purity was ≥99%) and glycerol (the purity was ≥99%) were purchased from Xilong Chemical Industry Incorporated Co. Ltd., Shantou, China. Sorbitol (the purity was ≥99%) was obtained from HiMedia Laboratories Pvt. Ltd. Mumbai, India.

Starch modification procedure

Starch oxidation was performed according to the method of Trinh & Dang [2019]. Cassava starch was added to 3.0% (*w/v*) NaCl solution to form a 10% suspension (*w/v*). The reaction was carried out in an electrolysis tank at room temperature for 60 min. After that, pH of the starch slurry was adjusted to 7.0 by 1 M HCl. The starch slurry was then washed by distilled water (5 times) and centrifuged (3000×*g*, 15 min). Finally, the starch precipitate was collected and dried in a convection dryer (50°C, 48 h).

Edible coating preparation

Before coating, banana fruits were washed with a 0.01% NaClO solution for 3 min to eliminate microorganisms on the surface and drained at room temperature (30°C) [Hossain & Iqbal, 2016]. Fruits were randomly divided into five sample groups (*n*=800). Bananas of four groups (G0-G3) were coated with the solutions the preparation of which was described below, and the fifth group was the control (bananas without coating).

Oxidized cassava starch slurry (8.0%, *w/v*) was completely gelatinized at 95°C in 30 min. Gelatin was hydrated (concentrations of 5%, 10% and 15%, *w/v*) for 1 h at room temperature, then the gelation solutions were heated (70°C, 30 min). To obtain a gelatin-starch based coating solutions (to coat G1, G2 and G3 samples, respectively), gelatinized starch and gelatin solutions were mixed well in ratios 4:1 (*v/v*), thus the final concentration of gelatin in the coating solution was 1%, 2% and 3% (*w/v*), respectively. Parallel, coating solution starch-base only (without gelatin) was prepared to coat G0 samples. Then, plasticizers (sorbitol and glycerol) were added to all coating solutions to reach the final concentration of 1.0% (*w/v*) each. The coating solutions were cooled to room temperature before use.

Banana coating and storage experiment

Banana fruits were washed with water and dried at room temperature then dipped in the coating solution for 1 min. The coated and control samples were stored at 30±2°C (75–80% RH). All samples were analyzed every day during 8 days of storage.

Microscopic analysis of coating surface

Coating layer micrographs were taken using a scanning electron microscope (SEM) to evaluate its microstructure, homogeneity, and thickness. To prepare SEM images, fruits from each treatment was randomly selected and imaged after the coating had dried. JSM 5410 LV scanning electron microscope (JEOL Ltd., Tokyo, Japan) was used at 10 kV and magnification of 1000×.

Respiration rate analysis

The respiration rate of banana fruit was determined by the method of Bailey [1940] using a closed respirometer. Glass containers were assembled following Figure 1. Compressed air, with a constant flow rate (3.5 L/min), was blown throughout the system. Firstly, the air was passed through two containers (#3, containing a saturated KOH solution, 300 mL/container) to completely remove CO_2. Secondly, the CO_2-free air was dehumidified by passing through a container (#4, containing 200 mL of H_2SO_4). Then, CO_2-released from the banana (in #5 container) was absorbed in two containers (#6, containing 300 mL of 0.2 M $Ba(OH)_2$ with drops of phenolphthalein as a color indicator). This measurement proceeded for 60 min. The generated CO_2 was determined by titrating the remaining $Ba(OH)_2$ solution (10 mL) against HCl, and respiration rate (mL CO_2/(kg sample×h)) was calculated by a formula:

$$Respiration\ rate = \frac{30 \times (3V_d - \sum V_c) \times C_M \times M_{CO_2}}{2 \times m \times d \times 10^{-3} \times t}$$

where: V_d – volume of 0.1 M HCl (mL) used for titration without sample in #5 container, V_c – volume of HCl (mL) used for titration with sample in #5 container, C_M – concentration of HCl solution(M), M_{CO_2} molecular weight of CO_2 (g/mol), m – mass of sample (g), d – density of CO_2 (kg/kL), t – time of respiration measurement (h).

Weight loss determination

Banana weight loss was estimated during storage by a 2-digit balance (CP2P-F, Sartorius Ltd., Getynga, Germany). The weight loss (%) was calculated following a previous study [Soradech *et al.,* 2017]:

$$Weight\ loss\ = \frac{W_0 - W_1}{W} \times 100$$

where: W_0 – weight of sample (g) at 0 day (day of storage) and W_1 – weight of banana (g) taken on each interval of storage.

Determination of soluble solid content and titratable acidity

Soluble solid content (SSC) and titratable acidity (TA) of bananas were determined during storage following methods described by Mehdi *et al.* [2011]. Banana fruit pulp (10 g) and distilled water (40 mL) were blended well. The mixture was then centrifuged at 5000×*g* for 5 min and then filtered through a Whatman filter paper. After that, the supernatant was measured by a refractometer (Atago Co., Ltd., Tokyo, Japan) to determine SSC as degree Brix (°Bx). In addition, the supernatant (5.0 mL) was titrated by 0.1 M NaOH with drops of phenolphthalein as a color indicator to determine TA. The result was expressed as g of malic acid equivalent per 100 g of banana pulp fresh weight (FW).

Determination of total carbohydrate and reducing sugar contents

To determine contents of total carbohydrates and reducing sugars of stored bananas, banana pulp (2.0 g) was hydrolyzed by 2.5 M HCl (5.0 mL) for 3 h in a boiling water bath and cooled to room temperature. The mixture was then neutralized by Na_2CO_3 until the effervescence ceases. Distilled water was added to this mixture for making up to 100 mL, and the mixture was centrifuged at 12,000×*g* for 15 min. Total carbohydrate content was determined by the phenol-sulfuric acid method [DuBois *et al.,* 1956]. Absorbance readings were taken at 490 nm using a spectrophotometer (Halo VIS-20, Dynamica Scientific Ltd., UK). Glucose was used as a standard and total carbohydrate content was calculated using a standard curve. Results were expressed as g glucose equivalent per 100 g of banana pulp FW.

Reducing sugar content in supernatant was estimated using dinitrosalicylic acid (DNS) method [Horwitz, 1960]. Results were expressed in mg glucose/g banana pulp, based on the fresh matter.

Starch content

The starch content of stored bananas was determined by the iodine dipping method [Blankenship *et al.,* 1993]. The cross-section of the banana was dyed with an iodine solution (1% KI with 0.1% I_2 in distilled water). The sample was immersed in I_2/KI solution (5 mm of depth, 30 s). Then, the color change (dark blue) was visually observed and scored [Thakur *et al.,* 2019]. The image of color change was estimated at the rate of black-blue point using the ImageJ software (Wayne Rasband, National Institutes of Health, Bethesda, MD, USA). The results were expressed as percentage ratio (%) of black-blue area (starch) to cross-section area.

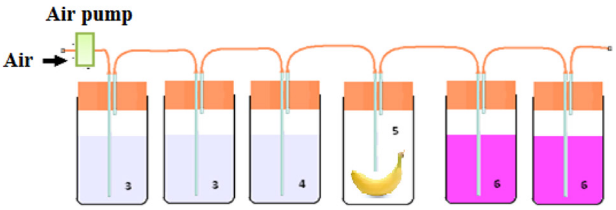

FIGURE 1. A closed respirometer for the respiration rate measurement.

Description of containers is provided in the “Respiration rate analysis subsection” of the “Materials & Method” section.

Statistical analysis

Each measurement was made for 20 banana fruits and was repeated 3 times. Data were statistically analyzed by using one-way analysis of variance (ANOVA). The significance level at $p<0.05$ was used throughout the study. The results were ranked according to Fisher’s least significant difference (LSD) test using Statgraphics statistical analysis software version 15 (Statgraphics Technologies, Inc., The Plains, VA, US).

RESULTS AND DISCUSSION

Coating layers microstructure

The SEM micrographs of the coating layer of bananas are presented in Figure 2. The coating cross-section showed that the G0 sample had a dense and homogeneous polymer network with no pores. The results indicated that the starch granules were totally disrupted and well mixed with the plasticizers in the polymer network during the heating process. This structure promoted the barriers of gases and moisture [Chiumarelli & Hubinger, 2014]. Basiak *et al.* [2017] observed that native starch-based films had a heterogeneous structure, which resembled a fiber network. Ávila-Martín *et al.* [2020] also reported that the microstructure of achira starch-based film presented the cracks in the structure. The differences compared to electrolyzed starch coating layer in our study could be explained by the attribution of plasticizers, which formed strong bonds in the amorphous phase of starch due to its less ordered structure. Thus, the integrity of the coating was maintained by preventing the formation of pores or cracks [Basiak *et al.,* 2018].

Furthermore, as it is shown in Figure 2, adding gelatin thickened the coating layer without causing phase separation. The presence of phase separation and cracks in the structure was observed in gelatin-starch film and gelatin-glycerol film [Al-Hassan & Norziah, 2012; De Carvalho & Grosso, 2004; Moreno *et al.,* 2017]. The authors stated the heterogeneous structure of coating reduced its mechanical properties while increasing gas permeability. Interestingly, Acosta *et al.* [2015] worked on gelatin-cassava starch film and they observed the heterogeneous structures and fibrous regions.

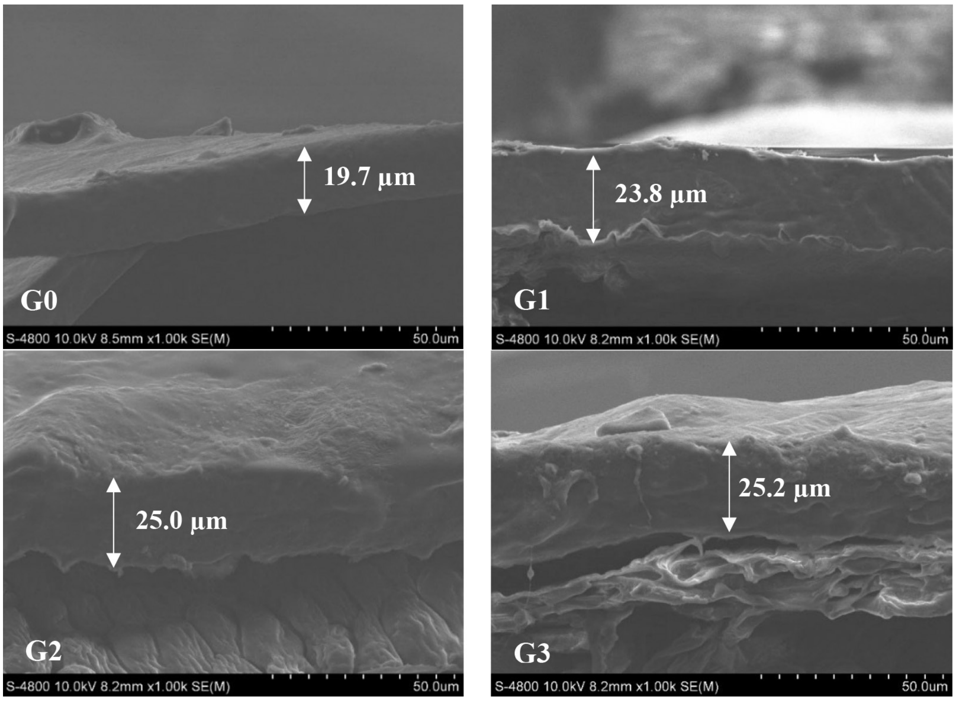

FIGURE 2. Scanning electron micrographs of coating layers of bananas coated in solutions of electrolyzed cassava starch (G0) and electrolyzed cassava starch with 1, 2 and 3% (*w/v*) gelatin (G1, G2 and G3, respectively).

Phase separation occurred even though the hydrophilic properties were similar. However, these results contrasted with the homogeneous structure of electrolyzed cassava starch-gelatin coating layer shown in Figure 2. Thus, starch oxidation by the electrolysis seems to be effective in enhancing the interaction between starch with the gelatin and plasticizers. Theoretically, coating thickness was an important parameter affecting the permeability [Cisneros-Zevallos & Krochta, 2006]. The average thickness of the G0 sample was the lowest (19.7 μm) whilst G1, G2 and G3 samples were about 23.8, 25.0 and 25.2 μm, respectively. The orientation of the starch molecules as well as the compatibility of the polymers, could explain the differences in thickness [Kumar *et al.,* 2019]. Moreover, the increase of gelatin content caused the increase in dry mass and viscosity of the solution [Fakhouri *et al.,* 2015].

Respiration rate

Respiration rate was an important indicator of fruit shelf life [Mehdi *et al.,* 2011]. In climacteric fruits, the rapid increase in the respiration rate along with a strong metabolism was an indicator of the ripening process [Wills & John, 2016].

The respiration rate of the control sample reached its peak on the 3rd day of storage (Figure 3). Interestingly, the use of coatings consisting of G0, G1, G3, and G4 samples delayed the peak of respiration until the 5th, 6th, 6th and 7th day of storage, respectively. This result was in agreement with the SEM results (Figure 3) showing the homogeneous structure of the coating layer, which limited gas dispersion [Khalil *et al.,* 2019]. G0 sample delayed the respiration rate by up to 2 days compared to control sample (Figure 3). This could be explained by the formation of cross-linking in the coating layer that reduced the presence of free hydroxyl groups, resulting in an improved gas barrier [Lawal *et al.,* 2005]. Besides, the addition of gelatin showed a benefit in reducing the ripening rate of bananas. According to Mohsen *et al.* [2017], gelatin was a good barrier to oxygen transfer. This could be explained by a crosslinking action and close packing of the components resulting from the mixing of starch-protein [Jagannath *et al.,* 2003]. It could be a small percentage of the starch and protein in the amorphous phase transformed to the crystalline phase, which was resistant to oxygen transfer in the biopolymer [Shen *et al.,* 2010]. Thus, a coating made from electrolyzed cassava starch and gelatin was strongly affected by the respiration rate of the banana. In general, climacteric fruit started the ripening by a rapid rise in respiration rate. However, when the amount of oxygen in the atmosphere falls to 2%, the fermentation occurs instead of respiration, causing unpleasant flavors and premature aging. Besides, the failure of fruit ripeness caused not only bad flavor but also internal spoilage [Emragi *et al.,* 2022]. This phenomenon was not observed in our treated samples, indicating that the coating kept appropriate low inner O_2 and high CO_2 partial pressures for fruit preservation.

Weight loss

The weight loss is related to water evaporation combined with the loss of water retention, resulting in the wrinkling of fruit [Gol & Rao, 2014]. In addition, respiratory activity also contributed to the reduction in the fruit mass due to the breakdown of sugars, such as glucose, into CO_2 and water [Santi & Jung, 1992].

It was shown in Figure 4 that the treated samples had lower weight loss than the control samples up to 5 days of storage ($p<0.05$). Generally, the results claimed that the coating reduced gas permeability in fruit surfaces, resulting in a reduction of respiration rate, which could account for the lower weight loss. This result is in agreement with the research of Chiumarelli & Hubinger [2014], in which the edible coatings could prevent fruits from dehydration due to their moisture barrier. There was a significant difference ($p<0.05$) in weight loss between the control and treated samples at the beginning of storage, but the G0, G1 and G2 samples showed no significant difference ($p \geq 0.05$) with the control samples from the 6th day of storage, although the values for G3 still were significantly lower than for the control (Figure 4). The weight loss was lower by increasing the content of gelatin in the coating formula and this result was in agreement with Gol & Rao [2014] and Aguilar-Méndez *et al.* [2008]. Thereby, this coating could reduce moisture loss and prolong the shelf life of fruit.

Soluble solid content

The SSC of control, electrolyzed starch and electrolyzed starch-gelatin coated banana fruits during storage is shown in Figure 5. The SSC increased along with fruit ripening. It was probably due to respiration rate, degradation of polysaccharides, or water evaporation [Moreira *et al.,* 2021]. After 8 days of storage, the SSC of the control sample was higer compared with the coated samples (Figure 5). Generally, SSC of coated samples was lower than that of the control during ripening because the hydrolysis of starches and carbohydrates into soluble sugars was delayed [Dwivany *et al.,* 2020].

A layer of coating on the surface of the fruit changed the intrinsic atmosphere and concentration of O_2 and CO_2. In other words, the coating delayed the ripening reflected by lower SSC of banana fruits. For the coated samples, the SSC of the G3 sample was the lowest from the 4th day of storage (Figure 5). Obviously, the content of gelatin had a significant impact on the SSC of the samples. SSC decreased when the amount of gelatin in the coating formula increased. This result was in agreement with Moreira *et al.* [2021], who reported gelatin-starch coated guavas had lower SSC during storage than the control sample.

Titratable acidity

The organic acids were oxidized by the respiration process in climacteric fruits. As a result, the TA was decreased during storage time [Moreira *et al.,* 2021]. The results showed that TA of the samples increased gradually until it reached the peak and then sharply decreased with fruit maturation (Figure 6).

Many organic acids such as malic (a principle acid), citric, oxalic, and tartaric acids are present in banana fruit. Oxalic acid caused astringent taste whilst malic and citric contributed to the tartness of banana fruits [Seymour, 1993]. The content of these acids decreased during ripening due to their use as substrates for respiratory enzyme reactions [Seymour, 1993]. This phenomenon may have occurred in our experiment since TA and respiration correlated significantly (Figure 3 and Figure 6). The results agreed with the finding of Márquez Cardozo *et al.* [2015] showing that TA was related to the respiratory rate. Interestingly, the coating showed a reduction in the respiration rate, therefore delaying the decline in acidity. Furthermore, the higher the gelatin content in the coating solution was, the longer it took to reach the TA peak and the lower the TA reduction of banana fruits (Figure 6).

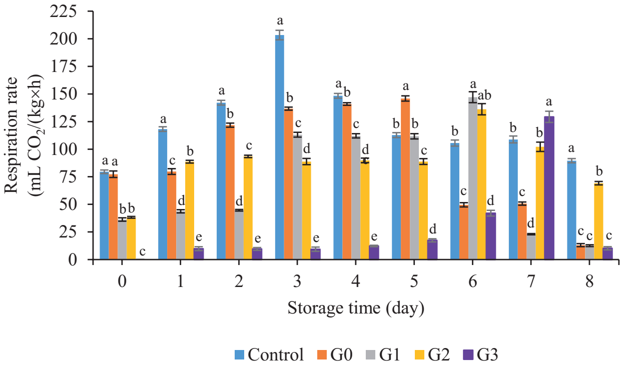

FIGURE 3. Respiration rate of bananas coated in solutions of electrolyzed cassava starch (G0), electrolyzed cassava starch with 1, 2 and 3% (*w/v*) gelatin (G1, G2 and G3, respectively) and uncoated fruits (control) stored for 8 days. Different letters above bars on the same day of storage indicate a statistically significant difference, $p<0.05$.

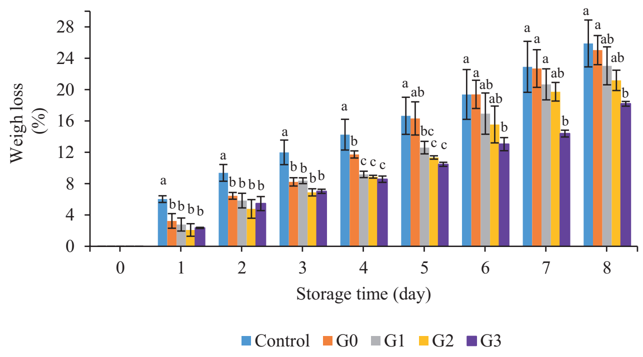

FIGURE 4. Weight loss of bananas coated by dipping in solutions of electrolyzed cassava starch (G0), electrolyzed cassava starch with 1, 2 and 3% (*w/v*) gelatin (G1, G2 and G3, respectively) and uncoated fruits (control) stored for 8 days. Different letters above bars on the same day of storage indicate a statistically significant difference, $p<0.05$.

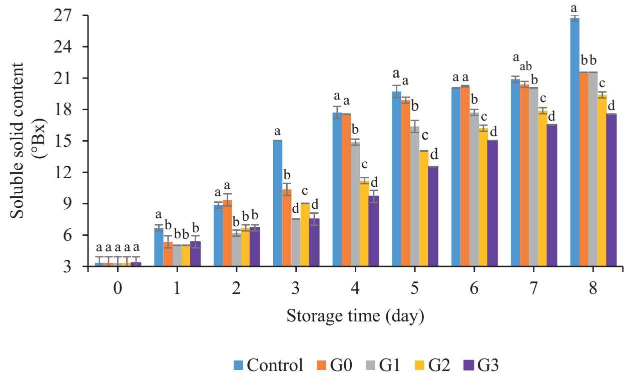

FIGURE 5. Soluble solid content of bananas coated by dipping in solutions of electrolyzed cassava starch (G0), electrolyzed cassava starch with 1, 2 and 3% (*w/v*) gelatin (G1, G2 and G3, respectively) and uncoated fruits (control) stored for 8 days. Different letters above bars on the same day of storage indicate a statistically significant difference, $p<0.05$.

If gelatin is added to the coating, it bonds together to form a gelatin network, reduces the holes for air to pass through, forms a denser polymeric matrix and increases the resistance to gas permeability [Fakhouri *et al.,* 2012].

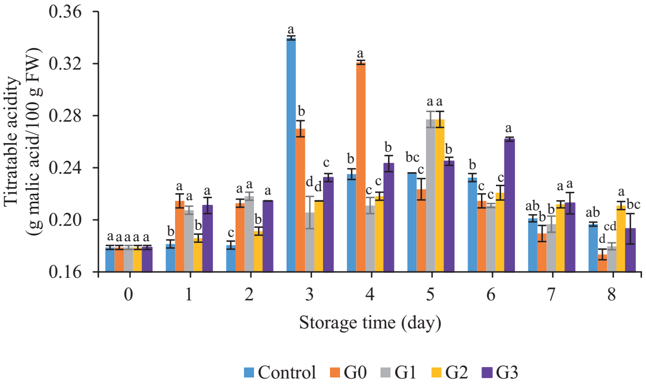

FIGURE 6. Titratable acidity of bananas coated by dipping in solutions of electrolyzed cassava starch (G0), electrolyzed cassava starch with 1, 2 and 3% (*w/v*) gelatin (G1, G2 and G3, respectively) and uncoated fruits (control) stored for 8 days. FW – fresh weight. Different letters above bars on the same day of storage indicate a statistically significant difference, $p<0.05$.

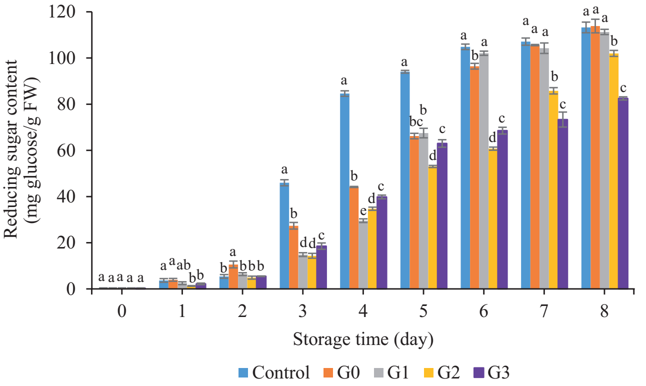

FIGURE 7. Reducing sugar content of bananas coated by dipping in solutions of electrolyzed cassava starch (G0), electrolyzed cassava starch with 1, 2 and 3% (*w/v*) gelatin (G1, G2 and G3, respectively) and uncoated fruits (control) stored for 8 days. FW – fresh weight. Different letters above bars on the same day of storage indicate a statistically significant difference, $p<0.05$.

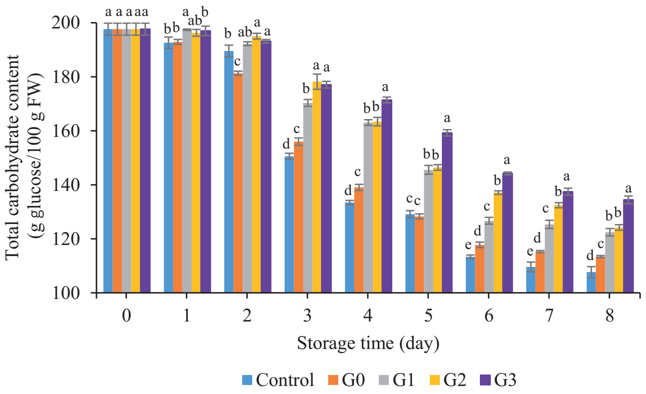

FIGURE 8. Total carbohydrate content of bananas coated by dipping in solutions of electrolyzed cassava starch (G0), electrolyzed cassava starch with 1, 2 and 3% (w/v) gelatin (G1, G2 and G3, respectively) and uncoated fruits (control) stored for 8 days. FW – fresh weight. Different letters above bars on the same day of storage indicate a statistically significant difference, $p<0.05$.

Reducing sugar and total carbohydrate contents

After harvesting, reducing sugar content of unripe banana fruit was very low (0.3 mg glucose/g FW). However, the content of reducing sugar raised to 80–111 mg glucose/g FW when the fruit ripened (Figure 7). Reducing sugars in ripened bananas were mainly glucose and fructose [Maduwanthi & Marapana, 2017]. The activity of amylase in banana led to the hydrolysis of starch into soluble sugars. In this study, reducing sugar contents were ordered as: control=G0=G1>G2>G3 after 8 day of storage. This result was due to the effect of the coating, which contributed to the reduction of the respiration rate and ethylene production, resulting in the starch hydrolysis taking place slowly [Thakur *et al.,* 2019]. Additionally, increasing the ratio of gelatin in coating composition was beneficial in reducing the content of reducing sugars and carbohydrates. This finding was supported by Gol & Rao [2014] study, which found that gelatin-based coatings were more effective at delaying ripening and maintaining fruit quality.

Total carbohydrate content in all samples tended to decrease gradually during 8 days of storage (Figure 8). The total carbohydrate contents at 8th-day storage were sorted as: control<G0<G1=G2<G3. Interestingly, in this study, the carbohydrate contents were negatively correlated to the maximal value of respiration rates. During ripening, starch and pectin were degraded. Especially, starch was hydrolyzed to simple sugars which are the main substrates for respiration [Gol & Rao, 2014]. A rapid increase in the respiration rate in banana fruits results from the loss of starch and sugar. Actually, the respiration process converted glucose into CO_2 gas [Elhadi *et al.,* 2019]. Thus, these phenomena were good explanations for the loss of total carbohydrates in our study. This result was consistent with the respiration rate results shown in Figure 3, where the coatings reduced the fruit respiratory rate, and the effect was enhanced with the addition of gelatin.

Starch content

The starch content of all banana samples was very high during the first days of storage (Figure 9). The persistence of a blue/black coloration after dyed with an iodine solution in the coated fruit compared to the control indicates delayed ripening. During the ripening, it sharply decreased until no starch was detected in the fruit. The rate of starch breakdown was much greater in control fruits ($p<0.05$) where 100% starch degradation was recorded at the end of day 6 (no blue/black color). However, at the same storage time, the values were, 16.1%, 38.9%, 44.3%, 88.6% for G0, G1, G2 and G3 sample, respectively. Interestingly, the coated samples (G1, G2, G3) still had the presence of starch in the banana pulp after 8 days of storage.

Most of the carbohydrates in unripe bananas were in the form of starch, which was hydrolyzed into sucrose then glucose and fructose during the short period of ripening [Gol & Rao, 2014]. The conversion of starch into sucrose during ripening was a complex process but the main pathway for starch degradation was described by Terra *et al.* [1983]. Starch content was extremely high in unripe fruit. It was rapidly reduced as a result of respiration, down to less than 1%. On the other hand, sucrose gradually increased until reaching its peak.

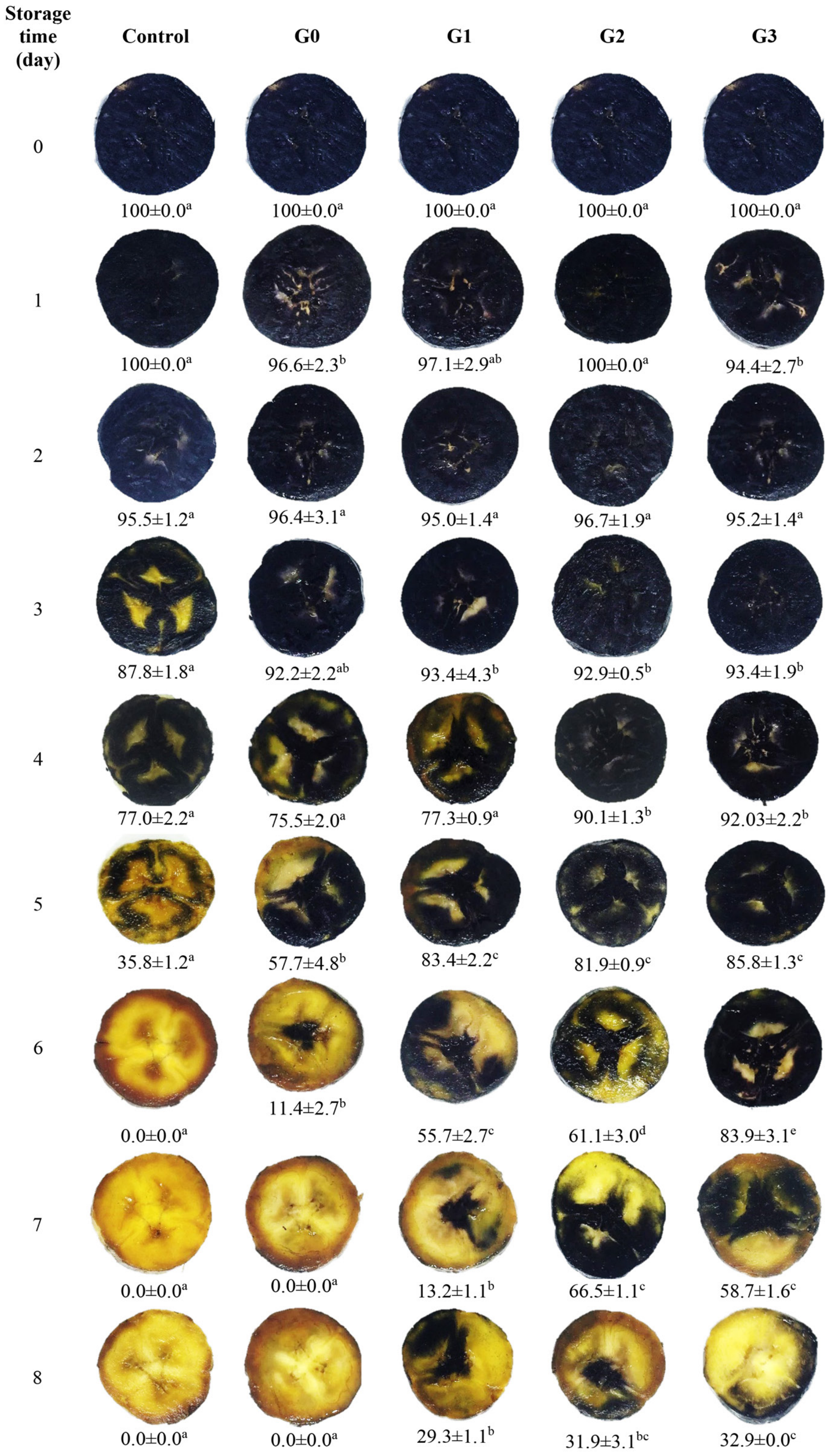

FIGURE 9. Images of the cross-section of the bananas after dyeing with an iodine solution and starch content in bananas (% of black-blue area (starch) to cross-section area). Bananas were coated by dipping in solutions of electrolyzed cassava starch (G0), electrolyzed cassava starch with 1, 2 and 3% (*w/v*) gelatin (G1, G2 and G3, respectively) and uncoated fruits (control) and stored for 8 days.

Data were shown as mean ± standard deviation; different letters in the same row indicate a statistically significant difference, $p<0.05$.

Moreover, the images showed that starch began to degrade in the central core of banana pulp and toward the outside during the ripening (Figure 9). It could be observed that the initial active enzyme area was not random due to the higher sensitivity of interior starch granule to degradation by enzyme [Terra *et al.,* 1983]. The breakdown of starch into sugar was more clearly observed at the cross-section of banana fruit. This was due to a sharp increase of ethylene on the pulp-peel interface [Yun *et al.,* 2019]. This finding demonstrated that the semi-anaerobic environment formed by surface coating decreased the activity of starch degrading enzyme and the effectiveness was enhanced with increasing concentration of gelatin.

CONCLUSION

In this study, the coating made from electrolyzed cassava starch and gelatin was effective in delaying banana ripening. The coating formulation showed good resistance to gas migration. The addition of gelatin in oxidized starch coating enhanced its ability to diminish respiratory intensity. Overall, the coating treatment with gelatin 3% (*w/v*) proved the most effective when it could prolong shelf life more than 2 times compared to the control sample. The electrolyzed cassava starch-gelatin coating could be a potential material to increase the shelf life of banana as well as other climacteric fruits.

RESEARCH FUNDING

The author(s) received no financial support for the research, authorship, and/or publication of this article.

ACKNOWLEDGMENTS

The authors acknowledge the Doctoral School of Food Science of the Hungarian University of Agriculture and Life Sciences for the support in this study. Special gratitude is given to HCMC University of Technology and Education for stimulating suggestions and encouragement that helped us to finish this study.

CONFLICTS OF INTERESTS

The authors declare that they have no conflicts of interest.

DATA AVAILABILITY STATEMENT

The data used to support the findings of this study are available from the corresponding author upon request.

ORCID IDs

T.T. Pham https://orcid.org/0000-0002-7911-6430
K.S. Trinh https://orcid.org/0000-0002-6365-2693

REFERENCES

1. Acosta, S., Jiménez, A., Cháfer, M., González-Martínez, C., Chiralt, A. (2015). Physical properties and stability of starch-gelatin based films as affected by the addition of esters of fatty acids. *Food Hydrocolloids*, *49*, 135–143. https://doi.org/10.1016/j.foodhyd.2015.03.015
2. Agarwal, S. (2021). Major factors affecting the characteristics of starch based biopolymer films. *European Polymer Journal*, *160*, art. no. 110788. https://doi.org/10.1016/j.eurpolymj.2021.110788
3. Aguilar-Méndez, M.A., Martín-Martínez, E.S., Tomás, S.A., Cruz-Orea, A., Jaime-Fonseca, M.R. (2008). Gelatine–starch films: Physicochemical properties and their application in extending the post-harvest shelf life of avocado (*Persea americana*). *Journal of the Science of Food and Agriculture*, *88*(2), 185–193. https://doi.org/10.1002/jsfa.3068
4. Al-Hassan, A.A., Norziah, M.H. (2012). Starch–gelatin edible films: Water vapor permeability and mechanical properties as affected by plasticizers. *Food Hydrocolloids*, *26*(1), 108–117. https://doi.org/10.1016/j.foodhyd.2011.04.015
5. Ávila-Martín, L., Beltrán-Osuna, Á.A., Perilla, J.E. (2020). Effect of the addition of citric acid and whey protein isolate in *Canna indica* L. starch films obtained by solvent casting. *Journal of Polymers and the Environment*, *28*, 871–883. https://doi.org/10.1007/s10924-019-01648-z
6. Bailey C.H. (1940). Respiration of cereal grains and flaxseed. *Plant Physiology*, *15*(2), 257–274. https://doi.org/10.1104/pp.15.2.257
7. Basiak, E., Lenart, A., Debeaufort, F. (2017). Effect of starch type on the physico-chemical properties of edible films. *International Journal of Biological Macromolecules*, *98*, 348–356. https://doi.org/10.1016/j.ijbiomac.2017.01.122
8. Basiak, E., Lenart, A., Debeaufort, F. (2018). How glycerol and water contents affect the structural and functional properties of starch-based edible films. *Polymers*, *10*(4), art. no. 412. https://doi.org/10.3390/polym10040412
9. Blankenship, S., Ellsworth, D.D., Powell, R.L. (1993). A ripening index for banana fruit based on starch content. *American Society for Horticultural Science*, *3*(3), 338–339. https://doi.org/10.21273/HORTTECH.3.3.338
10. Chiumarelli, M., Hubinger, M.D. (2014). Evaluation of edible films and coatings formulated with cassava starch, glycerol, carnauba wax and stearic acid. *Food Hydrocolloids*, *38*, 20–27. https://doi.org/10.1016/j.foodhyd.2013.11.013
11. Cisneros-Zevallos L., Krochta J.M. (2006). Dependence of coating thickness on viscosity of coating solution applied to fruits and vegetables by dipping method. *Food Science*, *68*(2), 503–510. https://doi.org/10.1111/j.1365-2621.2003.tb05702.x
12. Cortés-Rodríguez, M., Villegas-Yépez, C., González, J.H.G., Rodríguez, P.E., Ortega-Toro, R. (2020). Development and evaluation of edible films based on cassava starch, whey protein, and bees wax. *Heliyon*, *6*(9), art. no. e04884. https://doi.org/10.1016/j.heliyon.2020.e04884
13. De Carvalho, R.A., Grosso, C.R.F. (2004). Characterization of gelatin based films modified with transglutaminase, glyoxal and formaldehyde. *Food Hydrocolloids*, *18*(5), 717–726. https://doi.org/10.1016/j.foodhyd.2003.10.005
14. DuBois, M., Gilles, K.A., Hamilton, J.K., Rebers, P.A., Smith, F. (1956). Colorimetric method for determination of sugars and related substances. *Analytical Chemistry*, *28*(3), 350–356. https://doi.org/10.1021/ac60111a017

15. Dwivany, F.M., Aprilyandi, A.N., Suendo, V., Sukriandi, N. (2020). Carrageenan edible coating application prolongs cavendish banana shelf life. *International Journal of Food Science, 2020*, art. no. 8861610. https://doi.org/10.1155/2020/8861610
16. Elhadi M.Y., Carillo-Lopez, A., Bello-Perez, A.A. (2019). Carbohydrates. Chapter 9. In E. Yahia, A. Carrillo-Lopez (Eds.). *Postharvest Physiology and Biochemistry of Fruits and Vegetables*. 2nd edition, Woodhead Publishing: Elsevier Inc.
17. Emragi, E., Kalita, D., Jayanty, S.S. (2022). Effect of edible coating on physical and chemical properties of potato tubers under different storage conditions. *LWT – Food Science and Technology*, *153*, art. no. 112580. https://doi.org/10.1016/j.lwt.2021.112580
18. Fakhouri, F.M., Martelli, S.M., Caon, T., Velasco, J.I., Mei, L.H.I. (2015). Edible films and coatings based on starch/gelatin: Film properties and effect of coatings on quality of refrigerated Red Crimson grapes. *Postharvest Biology and Technology*, *109*, 57–64. https://doi.org/10.1016/j.postharvbio.2015.05.015
19. Fakhouri, F.M., Martelli, S.M., Bertan, L.C., Yamashita, F., Mei, L.H.I., Queiroz, F.P.C. (2012). Edible films made from blends of manioc starch and gelatin – Influence of different types of plasticizer and different levels of macromolecules on their properties. *LWT – Food Science and Technology*, *49*(1), 149–154. https://doi.org/10.1016/j.lwt.2012.04.017
20. FAO. (2021). *Banana Statistical Compendium 2020*. Rome.
21. Gol, N.B., Rao, T.R. (2014). Influence of zein and gelatin coatings on the postharvest quality and shelf life extension of mango (*Mangifera indica* L.). *Fruits*, *69*(2), 101–115. https://doi.org/10.1051/fruits/2014002
22. Horwitz, W. (1960). Use of dinitrosalicylic acid reagent for determination of reducing sugar. *Official Methods of Analysis of the Association of Official Analytical Chemists.* 9th ed. Washington DC: Association of Official Analytical Chemists.
23. Hossain, M.S., Iqbal, A. (2016). Effect of shrimp chitosan coating on postharvest quality of banana (*Musa sapientum* L.) fruits. *International Food Research Journal*, *23*(1), 277–283.
24. Jagannath, J.H., Nanjappa, C., Das Gupta, D.K., Bawa, A.S. (2003). Mechanical and barrier properties of edible starch–protein-based films. *Journal of Applied Polymer Science*, *88*(1), 64–71. https://doi.org/10.1002/app.11602
25. Kader, A.A. (2005). *Banana respiration, in Banana, Recommendations for Maintaining Postharvest Quality*. Postharvest Technology Research Information Centre, UCDAVIS: Davis, CA, USA.
26. Karaca, H., Pérez-Gago, M.B., Taberner, V., Palou, L. (2014). Evaluating food additives as antifungal agents against *Monilinia fructicola in vitro* and in hydroxypropyl methylcellulose-lipid composite edible coatings for plums. *International Journal of Food Microbiology*, *179*, 72–79. https://doi.org/10.1016/j.ijfoodmicro.2014.03.027
27. Khalil, H.A., Saurabh, C.K., Syakir, M.I., Fazita, M.N., Bhat, A., Banerjee, A., Fizreee, H.M., Rizal, S., Tahir, P.M. (2019). Barrier properties of biocomposites/hybrid films. In *Mechanical and Physical Testing of Biocomposites, Fibre-Reinforced Composites and Hybrid Composites*, Woodhead Publishing, pp. 241–258. https://doi.org/10.1016/B978-0-08-102292-4.00013-8
28. Kim, S.R.B., Choi, Y.G., Kim, J.Y., Lim, S.T. (2015). Improvement of water solubility and humidity stability of tapioca starch film by incorporating various gums. *LWT – Food Science and Technology*, *64*(1), 475–482. https://doi.org/10.1016/j.lwt.2015.05.009
29. Kokoszka, S., Lenart, A. (2007). Edible coatings-formation, characteristics and use-a review. *Polish Journal of Food and Nutrition Sciences*, *57*(4), 399–404.
30. Kudachikar, V.B., Kulkarni, S.G., Prakash, M.K. (2011). Effect of modified atmosphere packaging on quality and shelf life of ‘Robusta’ banana (*Musa* sp.) stored at low temperature. *Journal of Food Science and Technology*, *48*(3), 319–324. https://doi.org/10.1007/s13197-011-0238-y
31. Kumar, R., Ghoshal, G., Goyal, M. (2019). Synthesis and functional properties of gelatin/CA–starch composite film: excellent food packaging material. *Journal of Food Science and Technology*, *56*(4), 1954–1965. https://doi.org/10.1007/s13197-019-03662-4
32. Lawal, O.S., Adebowale, K.O., Ogunsanwo, B.M., Barba, L.L., Ilo, N.S. (2005). Oxidized and acid thinned starch derivatives of hybrid maize: functional characteristics wide-angle X-ray diffractometry and thermal properties. *International Journal of Biological Macromolecules*, *35*(1–2), 71–79. https://doi.org/10.1016/j.ijbiomac.2004.12.004
33. Le Nguyen, L.P., Visy, A., Baranyai, L. (2020). Application of hue spectra fingerprinting during cold storage and shelf-life of packaged sweet cherry. *Food Measure*, *14*, 2689–2702. https://doi.org/10.1007/s11694-020-00515-z
34. Maduwanthi, S.D.T., Marapana, R.A.U.J. (2017). Biochemical changes during ripening of banana: A review. *International Journal of Food Science and Nutrition*, *2*(5), 166–169.
35. Márquez Cardozo, C.J., Palacín Beltrán, J.R., Fuentes Berrio, L. (2015). Effect of cassava-starch coatings with ascorbic acidic and N-acetylcysteine on the quality of harton plantain (*Musa paradisiaca*). *Revista Facultad Nacional de Agronomía Medellín*, *68*(2), 7689–7701. https://doi.org/10.15446/rfnam.v68n2.50985
36. Mehdi, M., Asgar A., Peter, G.A., Noosheen, Z., Yasmeen, S. (2011). Effect of a novel edible composite coating based on gum arabic and chitosan on biochemical and physiological responses of banana fruits during cold storage. *Journal of Agricultural and Food Chemistry*, *59*(10), 5474–5482. https://doi.org/10.1021/jf200623m
37. Mohsen, R.E.F., Hamidreza, A., Sedigheh, A. (2017). Effect of gelatin-based edible coatings incorporated with *Aloe vera* and Black and Green tea extracts on the shelf life of fresh-cut oranges. *Journal of Food Quality, 2017*, art. no. 9764650. https://doi.org/10.1155/2017/9764650
38. Moreira, E.D.S., Silva, N.M.C.D., Brandão, M.R.S., Santos, H.C., Ferreira, T.A.P.D.C. (2021). Effect of modified starch and gelatin by-product based edible coating on the postharvest quality and shelf life of guava fruits. *Food Science and Technology, 42*, art. no. e26221. https://doi.org/10.1590/fst.26221
39. Moreno, O., Cárdenas, J., Atarés, L., Chiralt, A. (2017). Influence of starch oxidation on the functionality of starch-gelatin based active films. *Carbohydrate Polymers*, *178*, 147–158. https://doi.org/10.1016/j.carbpol.2017.08.128
40. Neelam, P., Mehar, H.A., Puneet, D., Manoj, K.S., Pravendra, N. (2003). Expression and activities of ethylene biosynthesis

enzymes during ripening of banana fruits and effect of 1-MCP treatment. *Plant Growth Regulation*, *40*(1), 11–19. https://doi.org/10.1023/A:1023040812205

41. Podshivalov, A., Toropova, A., Fokina, M., Uspenskaya, M. (2020). Surface morphology formation of edible holographic marker on potato starch with gelatin or agar thin coatings. *Polymers*, *12*(5), art. no. 1123. https://doi.org/10.3390/polym12051123
42. Podshivalov, A., Zakharova, M., Glazacheva, E., Uspenskaya, M. (2017). Gelatin/potato starch edible biocomposite films: Correlation between morphology and physical properties. *Carbohydrate Polymers*, *157*, 1162–1172. https://doi.org/10.1016/j.carbpol.2016.10.079
43. Pranoto, Y., Paramita, B.L., Cahyanto, M.N., Benjakul, S. (2021). Properties of ozone-oxidized tapioca starch and its use in coating of fried peanuts. *Molecules*, *26*(20), art. no. 6281. https://doi.org/10.3390/molecules26206281
44. Radziejewska-Kubzdela, E., Bieganska-Marecik, R., Czapski, J. (2007). Effect of composition of atmosphere inside packaging on quality of minimally processed vegetable salad based on white cabbage. *Polish Journal of Food and Nutrition Sciences*, *57*(4C), 461–465.
45. Salehi, F. (2020). Edible coating of fruits and vegetables using natural gums: A review. *International Journal of Fruit Science*, *20*(sup2), S570-S589. https://doi.org/10.1080/15538362.2020.1746730
46. Santi, R.B., Jung, C.P. (1992). Shelf-life of mature green tomatoes stored in controlled atmosphere and high humidity. *Journal of Food Science*, *57*(4), 948–953. https://doi.org/10.1111/j.1365-2621.1992.tb14331.x
47. Seymour G.B. (1993). Banana. *Biochemistry of Fruit Ripening*. Springer Netherlands, pp. 83–106. https://doi.org/10.1007/978-94-011-1584-1
48. Shen, X.L., Wu, J.M., Chen, Y., Zhao, G. (2010). Antimicrobial and physical properties of sweet potato starch films incorporated with potassium sorbate or chitosan. *Food Hydrocolloids*, *24*(4), 285–290. https://doi.org/10.1016/j.foodhyd.2009.10.003
49. Soradech, S., Nunthanid, J., Limmatvapirat, S., Luangtana-anan, M. (2017). Utilization of shellac and gelatin composite film for coating to extend the shelf life of banana. *Food Control*, *73*, 1310–1317. https://doi.org/10.1016/j.foodcont.2016.10.059
50. Terra, N.N., Garcia, E., Lajolo, F.M. (1983). Starch-sugar transformation during banana ripening: the behavior of UDP glucose pyrophosphorylase, sucrose synthetase and invertase. *Journal of Food Science*, *48*(4), 1097–1100. https://doi.org/10.1111/j.1365-2621.1983.tb09169.x
51. Thakur, R., Pristijono, P., Bowyer, M., Singh, S.P., Scarlett, C.J., Stathopoulos, C.E., Vuong, Q.V. (2019). A starch edible surface coating delays banana fruit ripening. *LWT – Food Science and Technology*, *100*, 341–347. https://doi.org/10.1016/j.lwt.2018.10.055
52. Trinh, K.S., Dang, T.B. (2019). Structural, physicochemical, and functional properties of electrolyzed cassava starch. *International Journal of Food Science, 2019,* art. no. 9290627. https://doi.org/10.1155/2019/9290627
53. Wills, R.B.H., John, B.G. (2016). Physiology and biochemistry. *Postharvest: An Introduction to the Physiology and Handling of Fruit and Vegetables*. 6th edition, NewSouth Publishing, pp. 34–63. https://doi.org/10.1079/9781786391483.0000
54. Yun, Z., Li, T., Gao, H., Zhu, H., Gupta, V.K., Jiang, Y., Duan, X. (2019). Integrated transcriptomic, proteomic, and metabolomics analysis reveals peel ripening of harvested banana under natural condition. *Biomolecules*, *9*(5), art. no. 167. https://doi.org/10.3390/biom9050167
55. Zsom, T., Strohmayer, E., Phuong Le Nguyen, L., Hitka, G., Zsom-Muha, V. (2018). Chilling injury investigation by non-destructive measuring methods during banana cold storage. *Progress in Agricultural Engineering Sciences*, *14*(S1), 147–158. https://doi.org/10.1556/446.14.2018.s1.14

Pol. J. Food Nutr. Sci., 2022, Vol. 72, No. 3, pp. 273–285
On-line ISSN: 2083-6007
Print ISSN: 1230-0322
DOI: 10.31883/pjfns/152070
http://journal.pan.olsztyn.pl

Original article
Section: Food Technology

Effect of Drying and Broccoli Leaves Incorporation on the Nutritional Quality of Durum Wheat Pasta

Natalia Drabińska[1,2]*, *Mariana Nogueira*[1,3], *Ewa Ciska*[1], *Henryk Jeleń*[2]

[1]*Department of Chemistry and Biodynamics of Food, Institute of Animal Reproduction and Food Research of Polish Academy of Sciences, Tuwima 10, 10–748 Olsztyn, Poland*
[2]*Food Volatilomics and Sensomics Group, Faculty of Food Science and Nutrition, Poznan University of Life Sciences, Wojska Polskiego 28, 60–637 Poznań, Poland*
[3]*Faculty of Biotechnology, Universidade Católica Portuguesa, Porto, Portugal*

Key words: pasta, by-products, valorisation, amino acids, fatty acids, sugars, broccoli leaves

Pasta is a great vehicle for the incorporation of vegetable-derived ingredients to increase the consumption of the health-beneficial components originating from vegetables. Notably, by-products of vegetable processing can also serve as a rich source of phytochemicals. An important step in pasta processing is drying which can affect the content of bioactive compounds in pasta. This study aimed to evaluate the effect of drying on the nutritional quality and cooking properties of durum wheat pasta fortified with broccoli leaves. Pasta enriched with broccoli leaf powder (BLP) at 2.5% (B2.5) and 5% (B5), and control pasta without BLP (C), which differed in drying conditions: fresh pasta without drying (F), pasta dried at 50°C for 8 h (L), and pasta dried at 80°C for 3 h (H) were formulated. The obtained pasta products were analysed for the cooking properties (optimal cooking time, cooking loss, water absorption and swelling capacity); colour parameters; proximate composition; and contents of free amino acids (FAA), fatty acids and sugars. BLP significantly improved the contents of ash by up to 35 g/100 g, FAA and fatty acids to up to 1298 nmol/g dry matter (DM) and 16741 μg/g DM, respectively, without compromising the cooking quality of pasta. Drying had a significant effect on fatty acids, which content in pasta processed at the highest temperature tested decreased. From the nutritional point of view, the low-temperature drying seems to be an interesting method for pasta preparation, with the highest content of FAA, fatty acids, especially unsaturated ones, and the lowest content of sugar. However, at the same time, the dried pasta products were characterised by greater cooking loss approximating 10%.

INTRODUCTION

The growing world's population demands an increase in the production of foodstuffs. The food industry generates a huge amount of waste and by-products during processing, which adversely impact the natural environment and whose utilization boosts production costs. At the same time, very often, the by-products from plant-derived food have a similar chemical composition to the edible parts and can still be a valuable source of phytochemicals. Therefore, a growing interest has been observed over the past few years in the utilization and valorisation of by-products [Gómez-García *et al.*, 2021]. Recent studies have shown that many of the so-called by-products of vegetable processing can be successfully deployed to develop novel, functional food products due to the high content of bioactive compounds [Dominguez-Perles *et al.*, 2011; Liu *et al.*, 2018; Michalak-Majewska *et al.*, 2020; O'Shea *et al.*, 2012; Reguengo *et al.*, 2022; Sedlar *et al.*, 2020]. An interesting example of a by-product, which showed very good nutraceutical potential in baked, gluten-free products, is the leaves of broccoli [Drabińska, 2022; Drabińska *et al.*, 2018; Krupa-Kozak *et al.*, 2021]. The gluten-free sponge cake and bread obtained in the aforementioned studies had improved nutritional quality, antioxidant capacity, and a more rich profile of bioactive compounds with their texture and sensory properties remained uncompromised. However, it is worth mentioning that these products were baked at a high temperature, which could lead to thermal degradation of phytochemicals.

In turn, pasta is not only willingly consumed worldwide by consumers of all age categories across all social groups [Nilusha *et al.*, 2019], but is also an example of a food product requiring milder temperatures during processing. Studies have shown that pasta is a good vehicle for incorporating potentially bioactive ingredients due to its capacity of maintaining acceptable physical and sensory properties despite the modification of its formula [Bruno *et al.*, 2019; Nilusha *et al.*, 2019]. Moreover, considering the low consumption of fruits and vegetables, especially in children, the incorporation of a vegetable-derived ingredient into the pasta could

---

* Corresponding Author:
E-mail: n.drabinska@pan.olsztyn.pl (N. Drabińska)

Submitted: 31 May 2022
Accepted: 13 July 2022
Published on-line: 26 July 2022

increase the intake of health-beneficial components originating from vegetables [Oliviero & Fogliano, 2016].

Durum wheat semolina is the most suitable material for the preparation of top-quality pasta [Fuad & Prabhasankar, 2010], characterised by high firmness and chewiness, low surface stickiness, and a bright and intense yellow colour. The most desirable cooking properties of top-quality pasta include a moderate water uptake at the optimal cooking time (OCT) and a low cooking loss [Bustos *et al.*, 2015; Cole, 1991]. Moreover, the nutritional properties of pasta have recently spurred a growing interest mainly due to the development of new, fortified products [Hoehnel *et al.*, 2020].

A pivotal stage in pasta production is drying which prolongs its shelf-life. Importantly, drying conditions significantly affect the quality, cooking behaviour and sensory properties of the final product [Piwińska *et al.*, 2016]. Different technologies of drying are applied and three main categories can be distinguished: drying at low temperature (<60°C), drying at high temperature (70–80°C) and drying at very high temperature (>110°C) [Giannetti *et al.*, 2021]. Higher temperatures are in general applied as they ensure an improvement in pasta colour and firmness, lower cooking loss, higher cooked weight and decreased stickiness [Anese *et al.*, 1999]. On the other hand, a higher temperature may result in the degradation of bioactive compounds and consequently reduction of the bioactive potential.

The effect of drying on the physical and aroma properties of gluten-free [D'Amico *et al.*, 2015] and durum wheat pasta was well established [Giannetti *et al.*, 2021; Piwińska *et al.*, 2016]. However, to the best of our knowledge, no studies have been performed to evaluate the effect of drying on the nutritional quality of the fortified pasta products. Therefore, the aim of this study was to evaluate the effect of drying on the nutritional quality and cooking properties of durum wheat pasta fortified with broccoli leaves. Its results were expected to help answer the arising question of whether the potential improvement in the nutritional quality caused by phytochemical-rich ingredients can be lost by drying.

MATERIALS AND METHODS

Broccoli leaf powder

Broccoli leaves were generously donated by GEMIX (Olsztyn, Poland). Broccoli leaf powder (BLP) was prepared from fresh, undamaged leaves of broccoli (*Brassica oleracea* L. var. *italica* cv. Sebastian), which were blanched in hot water for 1 min to inactivate enzymes, freeze-dried and ground into powder. Details of BLP preparation can be found in our previous work [Drabińska *et al.*, 2018].

Pasta preparation

Pasta formulation consisted of durum semolina flour, olive oil, salt (all purchased in local stores in Olsztyn, Poland) and tap water. The formulations were enriched with 2.5% (B2.5), and 5% (B5) of BLP as an additional ingredient to the optimal, control pasta formulation without BLP (C). The compositions of all formulations are presented in Table 1. To prepare the pasta, all ingredients were mixed for 5 min and then extruded through a penne-forming die in an electric pasta maker (Pastamatic 1581, Ariete, Florence, Italy).

TABLE 1. Composition of control and fortified pasta products (g/100 g).

	C	B2.5	B5
Semolina	71.8	70.5	69.3
Water	25.1	24.7	24.3
Olive oil	2.7	2.6	2.6
Salt	0.4	0.4	0.3
BLP	0.0	1.8	3.5

C – control pasta; B2.5 – pasta fortified with 2.5% of broccoli leaf powder (BLP); B5 – pasta fortified with 5% of BLP.

Three types of pasta were prepared for all formulations, differing in drying method: (F) fresh pasta without drying, (L) pasta dried at 50°C for 8 h, and (H) pasta dried at 80°C for 3 h. The images of the obtained pasta products are shown in Figure 1. Pasta products were cooked for the optimal cooking time (OCT) and then freeze-dried, ground into a fine powder (particle size <0.60 mm) and stored in tightly closed containers at –20°C until analyses.

Determination of cooking properties

The analysis of cooking loss (grams of solid material in cooking water per 100 g of pasta as is), OCT, water absorption and swelling capacity were performed according to the AACC approved method 66–50 [AACC, 2000].

Colour parameter analysis

The colour parameters of freeze-dried powders of BLP and pasta samples were evaluated using a HunterLab ColorFlex

FIGURE 1. The images of experimental pasta products. F – fresh pasta; L – pasta dried at low temperature (50°C, 8 h); H – pasta dried at high temperature (80°C, 3 h); C – control pasta; B2.5 – pasta fortified with 2.5% of broccoli leaf powder (BLP); B5 – pasta fortified with 5% of BLP.

spectrophotometer (Hunter Associates Laboratory, Inc, Reston, VA, USA). The colour was expressed in accordance with the CIELab system and the parameters determined were: lightness: L^* (0 (black) – 100 (white)) and chromatic components: a^* ($-a^*$ (greenness) – $+a^*$ (redness)) and b^* ($-b^*$ (blueness) – $+b^*$ (yellowness)). Each sample was measured in nine replicates. Moreover, a total colour difference (ΔE) in response to the F-C pasta was calculated using the following formula:

$$\Delta E = \sqrt{\Delta L^{*2} + \Delta a^{*2} + \Delta b^{*2}}$$

Proximate composition analysis

The proximate composition was established according to the AOAC approved methods: moisture content was analysed using the drying method (AOAC 925.10), protein content was determined with the Kjeldahl method (AOAC 979.09), and lipid content using Soxhlet extraction with hexane (AOAC 923.03); ash was determined using the gravimetric method (AOAC 923.03). [AOAC, 2005].

Amino acid analysis

Free amino acid (FAA) composition was analysed using the method described by Drabińska [2022]. Briefly, FAA were extracted from approx. 100 mg of freeze-dried powder with 3 mL of a 50% (*v/v*) methanol solution. The mixture was incubated for 20 min at 50°C with shaking at 500 rpm using a MultiTherm shaker (Benchmark Scientific, Edison, NJ, USA). Next, the mixture was centrifuged for 15 min at 11,200×*g*, and the supernatant was collected for analysis. A portion of 100 μL of the extract was analysed using the EZ: Faast™ kit for free amino acids (Phenomenex, Torrance, CA, USA) according to the protocol provided by the manufacturer. FAA were analysed in an Agilent 7890A gas chromatograph (GC) coupled with a 5975C mass selective detector (MSD) and 7683B autoinjector (Agilent Technologies, Santa Clara, CA, USA). The compounds were separated in a ZB-AAA EZ: Faast™ capillary column provided by the manufacturer (10 m × 0.25 mm, Phenomenex). The temperature gradient and GC and MS settings were according to the producer's protocol. Identification and calculation of individual FAA were performed using external standards provided by the manufacturer and normalised to the internal standard (norvaline). The results were expressed as nmol/g dry matter (DM).

Fatty acid analysis

Fatty acid methyl esters (FAME) were obtained and determined using a standard procedure with transesterification with sodium methylate (0.4 N methanolic solution). First, lipids were isolated from BLP and pasta samples. To 1 g of the sample, 3 mL of *n*-hexane were added and the mixture was vortexed vigorously and centrifuged for 15 min at 2268×*g*. The supernatant was collected and the extraction was performed three times. The collected *n*-hexane layer was dried in the flow of nitrogen. The remaining oil was then dissolved in 2 mL of *n*-hexane containing C19:0 internal standards (1 mg/mL), and 2 mL of derivatization agent were added. The mixture was vortexed and left at room temperature for 20 min. Afterwards, water was added and the upper *n*-hexane layer was collected to the GC vial. FAME were analysed using Agilent Technologies 6890 GC with a flame ionisation detector (FID) (Agilent Technologies). Separation of FAME was conducted in a Supelcowax-10 column (30 m × 0.32 mm × 0.5 μm, Supelco, Bellefonte, PA, USA) with hydrogen as a carrier gas with the flow rate of 1.5 mL/min. The injection volume was 1 μL at a split ratio of 50:1. The operating conditions were as follows: initial oven temperature 170°C (2 min) followed by 2°C/min increase to 230°C (held for 10 min). FAME were identified by comparison with the commercial standard, FAME Mix C4-C24 (Supelco, Bellefonte, PA), and quantified in response to the internal standard. Results were expressed in μg/g DM.

Sugar analysis

The extraction of sugars was performed following the method described by Wieczorek *et al.* [2022]. Approx. 1 g of BLP and pasta samples was extracted with water for 20 min at 60°C. Afterwards, the samples were centrifuged at 2268×*g* for 15 min. Supernatants were filtered through 0.45 μm cellulose acetate syringe filters (Lab Logistics Group GmbH, Meckenheim, Germany) and the extracts were directly analysed by high-performance liquid chromatography (HPLC).

Analysis of individual sugars was performed using an Agilent Technologies 1100 series HPLC system with a refractive index detector (Agilent Technologies), isocratically with water as a mobile phase at a flow rate of 0.6 mL/min at 80°C on the Rezex RPM-Monosaccharide Pb^{+2} 300×7.8 mm column (Phenomenex). Commercial standards of sugars purchased in Sigma Aldrich (Steinheim, Switzerland) were used for the identification and quantification of individual sugars. The results were expressed in mg/g DM.

Statistical analysis

Pasta was prepared with one batch of 700 g for each pasta type. All analyses were performed in triplicate unless differently stated, and the data are presented as mean ± standard deviation (SD). Differences between pasta samples were assessed using one-way analysis of variance (ANOVA) with the Fisher's least significant difference (LSD) post-hoc test. Moreover, two-way ANOVA was performed for contents of FAA, fatty acids and sugars to assess the effect of BLP addition and drying temperature (D), and interactions thereof (BLP×D) on the chemical composition of the experimental pasta samples. The differences were considered significant at $p<0.05$. All the statistical analyses were performed using STATISTICA version 13.3 (TIBCO Software Inc., Palo Alto, CA, USA) software.

RESULTS AND DISCUSSION

Cooking properties

Cooking properties are important drivers of the final quality and acceptance of pasta. The ideal pasta should feature high water absorption, low cooking loss and good texture [Bruneel *et al.*, 2010]. The results of determinations of the cooking properties of pasta with BLP dried under different conditions and control pasta (without BLP) are presented in Figure 2. Drying significantly prolonged the cooking time required to obtain *al dente* pasta. While in the F pasta,

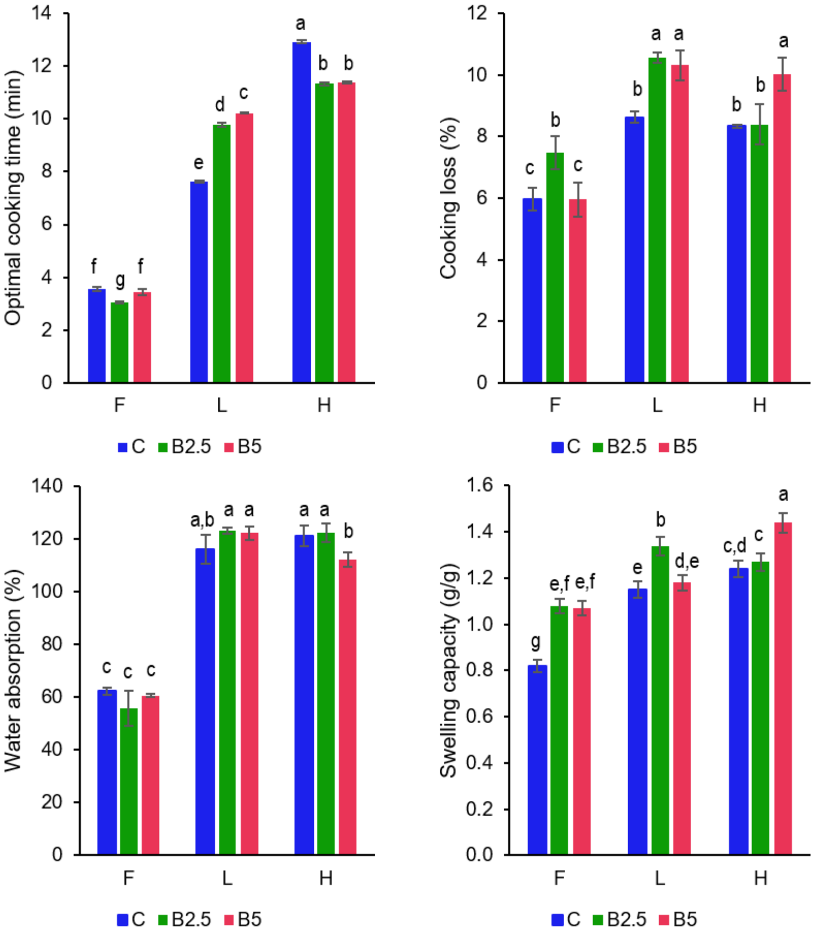

FIGURE 2. Cooking properties of the experimental pasta products. B2.5 – pasta fortified with 2.5% of broccoli leaf powder (BLP); B5 – pasta fortified with 5% of BLP; C – control pasta without BLP; F – fresh pasta; L –pasta dried at low temperature (50°C, 8 h); H – pasta dried at high temperature (80°C, 3 h). Different letters above bars indicate a significant difference ($p<0.05$).

the addition of BLP did not affect much the OCT, it caused differences in dried pasta samples. Interestingly, for L pasta, the OCT was significantly longer with a higher percentage of BLP, while an opposite phenomenon was observed for H pasta. The OCT of F pasta was definitely shorter due to a higher moisture content and faster rehydration compared to the dried pasta [Piwińska *et al.*, 2016].

Cooking loss should not exceed 8% for good-quality pasta [Piwińska *et al*., 2016; Desai *et al.*, 2018a]. All F pasta products were within this range (Figure 2). The cooking losses were greater after drying. The C and B2.5 pasta samples dried at the highest temperature tested were on the edge of the acceptance; whereas the cooking loss determined for H-B5 pasta approximated 10%. The greatest cooking loss was noted for L-B2.5 (10.55%) and L-B5 (10.31%). Similarly, Piwińska *et al.* [2016] reported that pasta dried for a longer time at a lower temperature was characterised by the greatest cooking loss.

Irrespectively of the drying method applied and BLP addition, the water absorption determined for the L and H samples was similar and much higher compared to F pasta (Figure 2). The high-temperature drying is believed to result in the best cooking quality of pasta, mainly due to the polymerisation of the protein network which entraps the starch granules and consequently reduces water absorption and prevents starch leaching [Lamacchia *et al.*, 2007]. Contrary, Bruneel *et al.* [2010] reported the highest cooking quality for pasta dried under mild conditions. The application of protein-rich ingredients was reported to increase cooking loss [Kaur *et al.*, 2013]. Raczyk *et al.* [2022] observed a high increase in the cooking loss after pasta fortification with spirulina, which was explained by solubilization and washing out of the protein fraction and gluten matrix weakening, which decreases the capacity for entrapping swollen starch granules during boiling.

The swelling capacity was significantly affected by BLP addition (Figure 2). For F pasta, it was higher in the BLP-enriched products, irrespective of BLP percentage. For L pasta, the highest swelling capacity was established for B2.5, which was the opposite for H pasta. In turn, F pasta had a lower swelling capacity compared to dried pasta products, likely due to shorter OCT. After BLP addition and drying, a stronger protein network might have been formed, which could have resulted in hampered starch swelling and lower water uptake [Piwińska *et al.*, 2016].

Colour parameters

The colour of pasta is affected by the quality of semolina and the addition of colour-containing ingredients [Piwińska *et al.*, 2016]. The results of the colour parameters analysis

TABLE 2. Colour parameters of experimental pasta products.

Pasta	L^*	a^*	b^*	ΔE
F-C	87.51 ± 0.01^{a}	-0.12 ± 0.01^{c}	14.05 ± 0.02^{g}	-
F-B2.5	76.05 ± 0.03^{d}	-6.25 ± 0.02^{h}	28.14 ± 0.03^{d}	19.17
F-B5	67.61 ± 0.02^{g}	-6.26 ± 0.02^{h}	31.48 ± 0.02^{a}	27.15
L-C	84.98 ± 0.01^{b}	-0.28 ± 0.01^{a}	14.56 ± 0.01^{f}	3.90
L-B2.5	68.88 ± 0.03^{f}	-3.67 ± 0.01^{d}	27.32 ± 0.02^{e}	12.92
L-B5	66.99 ± 0.04^{i}	-5.66 ± 0.01^{g}	28.69 ± 0.03^{c}	21.57
H-C	84.78 ± 0.02^{c}	-0.25 ± 0.01^{b}	12.63 ± 0.03^{h}	1.88
H-B2.5	72.10 ± 0.01^{e}	-4.23 ± 0.02^{f}	28.16 ± 0.03^{d}	15.38
H-B5	67.10 ± 0.05^{h}	-4.33 ± 0.01^{e}	29.52 ± 0.03^{b}	19.14

B2.5 – pasta fortified with 2.5% of broccoli leaf powder (BLP); B5 – pasta fortified with 5% of BLP; C – control pasta without BLP; F – fresh pasta; L – pasta dried at low temperature (50°C, 8 h); H – pasta dried at high temperature (80°C, 3 h). Different letters in superscript in the same column indicate a significant difference ($p<0.05$).

of pasta fortified with BLP and dried under different conditions are presented in Table 2. The highest lightness (L^*) value was determined for F-C pasta, which was observed to decrease in C pasta with an increasing drying temperature. In the case of pasta fortified with BLP, the L pasta was the darkest. As expected, the BLP-fortified pasta products were characterised by the highest greenness (a^*). Interestingly, for F and H pasta, the difference between the 2.5% and 5% BLP was very small, while for L pasta, the B5 pasta was almost twice more green compared to B2.5. The yellowness (b^*) value was observed to increase with an increasing BLP content in the formulation, irrespective of the drying conditions. A change in colour parameters of pasta was also reported by other authors who fortified pasta products [Duda *et al.*, 2019; Raczyk *et al.*, 2022]. Notably, the difference in sample colour (ΔE) differed between the drying methods (Table 2). As stated by Duda *et al.* [2019], the difference in ΔE of more than 3 is noticed by the eye without additional tools. The differences between F-C and H-C were lower than 3, while the difference between F-C and L-C which accounted for 3.90 could be perceived as noticeable. Similarly, for B2.5 pasta, the difference between the F and H samples was smaller as compared to L. The tendency was opposite at the highest BLP content, and compared to F-B5, the H pasta differed the most; however at the same time, the difference to F-C was the smallest. The green colour of BLP is due to chlorophylls, detected in Brassica leaves in high amounts [Drabińska *et al.*, 2021]. Notably, the loss of greenness was observed in B5 pasta products with the increasing drying temperature, which can be explained by the thermal degradation of chlorophylls. As reported by Van Loey *et al.* [1998] and Weemaes *et al.* [1999], degradation of chlorophylls in broccoli occurs when the temperature exceeds 50°C.

Proximate composition

The nutritional quality of pasta depends on the quality of ingredients used for its production. Semolina is the main component of pasta and is considered a relatively good source of protein with a low amount of minerals and lipids [Fuad & Prabhasankar, 2012; Pérez & Pérez, 2009]. Various ingredients, such as fish products, vegetables and crickets, were incorporated to improve the nutritional quality of pasta [Desai *et al.*, 2018a; Duda *et al.*, 2019; Michalak-Majewska *et al.*, 2020]. BLP was previously characterised as a rich source of protein and minerals [Drabińska *et al.*, 2018]. The proximate composition of cooked experimental pasta obtained in this study is shown in Figure 3. Except for F pasta, the addition of BLP resulted in the increased moisture content of cooked pasta compared to C, which can be associated with the high hygroscopic properties of freeze-dried BLP. The content of ash increased with an increasing percentage of BLP in all pasta products. However, as can be seen in Figure 3, the ash content decreased with increasing drying temperature. Similarly, Manthey & Hall [2007] reported that H pasta had a lower ash content compared to L. In our study, less pronounced changes were found for protein, the highest content of which was detected in H-B5. The insignificant changes in protein content can be explained by a relatively high protein content in semolina itself. No clear tendency was observed for lipid content in the analysed pasta samples. The lowest lipid content was noted for F-C pasta and the highest one for L-B5 pasta. For F and H pasta, the trend was similar (with the highest content of lipids in B2.5), whereas an opposite tendency was observed for L pasta. As summarised in the meta-analysis, the changes in the proximate composition of fortified pasta products vary depending on the type of additive and enrichment level [Mercier *et al.*, 2016]. And although the effect of drying on starch and protein digestibility and cooking properties of pasta was extensively studied [Bresciani *et al.*, 2022], the effect of drying on its proximate composition did not gain much scientific attention to date.

Free amino acid profile

Wheat flours used for pasta preparation are a source of protein in our diet. However, it has to be kept in mind that wheat proteins are of low quality with unbalanced amino acid composition, especially with lacking lysine and threonine [Filip & Vidrih, 2015; Hoehnel *et al.*, 2020]. Therefore, there have been many scientific attempts to incorporate the protein-rich ingredient into pasta formulations [Duda *et al.*, 2019; Hoehnel *et al.*, 2020; Raczyk *et al.*, 2022].

The contents of individual FAA in BLP and experimental pasta are presented in Table 3. BLP was found as a rich source of FAA with 15 individual FAA. The major FAA in BLP were aspartic and glutamic acids, alanine and glutamine followed by serine, valine and threonine. A similar profile of FAA in BLP was reported previously [Drabińska, 2022]. In control pasta, the presence of 11 FAA was detected, with dominant asparagine, aspartic acid and alanine, which is in agreement with the previous study with semolina-based pasta [Fois *et al.*, 2019]. The incorporation of BLP significantly affected the content of FAA in experimental pasta products, which increased upon all drying methods applied. Notably, threonine, tyrosine and glutamic acid were detected only in the BLP-enriched pasta and surprisingly also in the L-C pasta. The statistical analysis showed that BLP percentage influenced the total FAA content and the content of almost all individual FAA, except leucine. A similar effect of BLP was reported

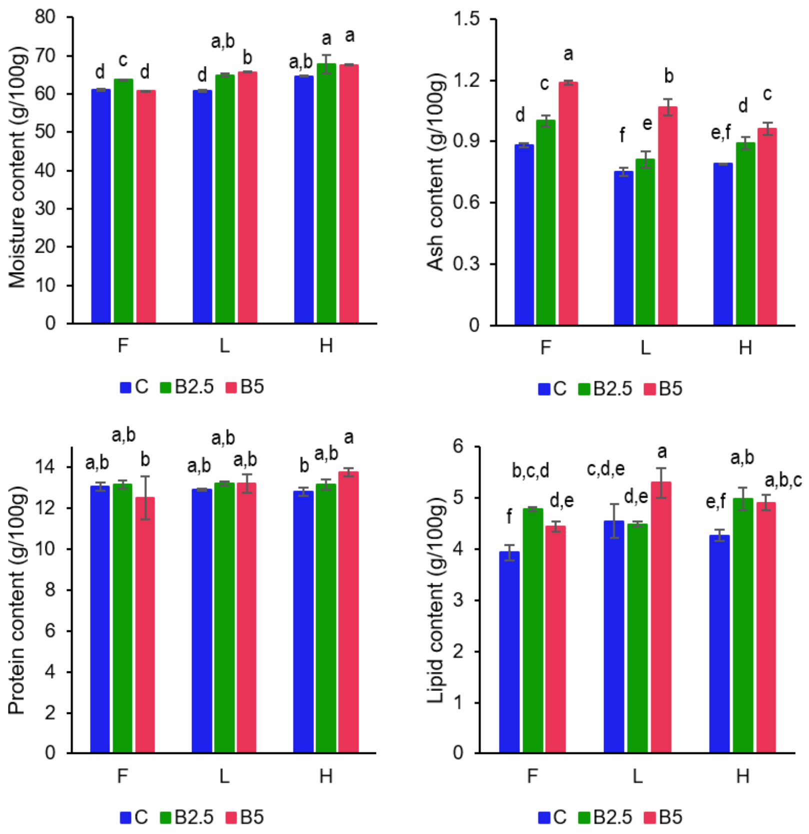

FIGURE 3. Proximate composition of the experimental pasta products. B2.5 – pasta fortified with 2.5% of broccoli leaf powder (BLP); B5 – pasta fortified with 5% of BLP; C – control pasta without BLP; F – fresh pasta; L – pasta dried at low temperature (50°C, 8 h); H – pasta dried at high temperature (80°C, 3 h). Different letters above bars indicate a significant difference ($p<0.05$).

by Drabińska [2022] in BLP-fortified gluten-free sponge cake muffins. Importantly, the semolina was previously reported to be lacking in lysine [Raczyk *et al.*, 2022]. In our study, lysine was not detected in experimental pasta although the BLP contained this amino acid. Maybe the incorporation of a higher level of BLP could result in products with excellent nutritional properties. Notably, the content of the second limiting amino acid in wheat, threonine, increased with increasing BLP fortification. After pasta enrichment with BLP, the content of polar FAA (aspartic and glutamic acids) increased with an increasing BLP content, which was suggested to increase protein solubility [Arise *et al.*, 2022].

The effect of drying on FAA content in pasta was much less prominent. The significant effect of drying was detected for alanine, valine, leucine, isoleucine, threonine, proline, phenylalanine, tyrosine and glutamic acid as well as total FAA (Table 3). A previous study showed that higher temperatures of drying negatively affected the content of lysine [Dexter *et al.*, 1984]. Although this amino acid was not reported in this study; similarly to the results reported by Dexter *et al.* [1984], a higher content of total FAA was found in L pasta compared to H. In another study [Manthey & Hall, 2007], drying conditions were considered as not influencing the content of individual amino acids. However, similarly to our study, significant changes were reported for valine and threonine.

The results of the two-way ANOVA showed that there was a clear interaction between the BLP percentage and drying temperature for individual compounds (leucine, isoleucine, threonine, phenylalanine, tyrosine and glutamic acid) and total FAA (Table 3).

Fatty acid profile

Brassica vegetables are one of the most important crops for the oil industry, mainly due to the high oil yield of rapeseed [Sharafi *et al.*, 2015]. Broccoli does not belong to oil crops; however, also contains fatty acids. Leaves of broccoli were found to have the highest compositional ratio of polyunsaturated fatty acid (PUFAs) among all its aerial parts, with linolenic (C18:3 *n*3), palmitic (C16:0) and linoleic (C18:2) acids being the most dominant, accounting for around 80% of total fatty acids [Bhandari *et al.*, 2013]. In our study, the content of fatty acids in BLP and experimental pasta products was evaluated and respective results are presented in Table 4. Eleven fatty acids were identified in BLP with γ-linoleic acid (C18:3 *n*6) and C16:0 being the major acids, followed by *trans*-heptadecenoic acid (C17:1 *trans*), C18:2 and C18:3 *n*3, which is in agreement with previous reports [Bhandari *et al.*, 2013; Joon Lee *et al.*, 2009]. Similarly to other authors, PUFA were found to dominate in the analysed BLP. The vast majority of fatty acids detected in experimental pasta products derived from olive oil used for pasta preparation. Nevertheless, also wheat contains a small amount of lipids (around 3%) with a profile of fatty acids consisting mainly of C18:2, C16:0, C18:1, C18:3, stearic acid (C18:0) and palmitoleic acid (C16:1) [Narducci

TABLE 3. Content of free amino acids (FAA) in broccoli leaf powder (BLP) and experimental pasta products (nmol/g dry matter).

Amino acid	BLP	F-C	F-B2.5	F-B5	L-C	L-B2.5	L-B5	H-C	H-B2.5	H-B5	*p*-Value$^{\#}$		
											BLP addition effect	Drying (D) effect	BLP×D effect
Alanine	1369.02±87.7	70.3±6.7^{d}	104±3.3^{c}	179.7±2.9^{b}	74.6±2.9^{d}	176.4±13.3^{b}	228.9±10.6^{a}	81.4±5.8^{d}	109.4±5.3^{c}	178.3±1.3^{b}	<0.001*	0.049*	0.432
Glycine	/	20.3±1.0^{c}	14.03±0.0^{c}	34.4±1.3^{a}	16.9±5.5^{c}	32.6±0.2^{a}	26.9±1.2^{a,b}	26.0±1.8^{b}	16.9±2.4^{c}	21.6±2.4^{b,c}	/	0.492	/
Valine	342.2±129.4	17.2±1.5^{b}	31.0±2.9^{b}	57.8±0.3^{a}	34.2±6.1^{b}	67.6±6.9^{a}	60.8±3.2^{a}	26.1±6.1^{b}	32.8±6.0^{b}	58.6±1.2^{a}	<0.001*	0.015*	0.158
Leucine	82.3±29.2	13.1±1.1^{c}	13.1±1.1^{c}	27.3±1.7^{b}	28.3±2.6^{b}	66.8±3.7^{a}	29.2±4.4^{b}	22.6±2.1^{b}	26.2±2.8^{b}	29.1±1.3^{b}	0.112	<0.001*	0.002*
Isoleucine	102.3±32.1	9.8±2.8^{d}	13.6±2.5^{d}	24.2±1.3^{b}	14.6±1.9^{d}	34.5±0.2^{a}	22.7±1.9^{b}	/	16.8±1.1^{c}	21.9±1.3^{b}	<0.001*	0.002*	0.002*
Threonine	325.3±111.3	/	/	26.5±2.2^{a}	/	33.5±1.4^{a}	35.8±1.1^{a}	/	22.6±0.7^{b}	34.7±2.7^{a}	<0.001*	0.002*	0.015*
Serine	569.0±192.4	16.8±0.0^{f}	32.1±6.3^{e}	67.3±8.4^{a,b,c}	/	56.9±3.9^{b,c}	73.6±1.4^{a,b}	27.8±4.6^{e}	41.3±7.6^{d}	76.9±5.4^{a}	<0.001*	0.055	0.233
Proline	243.3±82.9	19.6±3.0^{c}	23.9±1.9^{c}	49.9±0.1^{a}	24.0±2.1^{c}	55.0±4.1^{a}	52.0±1.1^{a}	24.7±2.9^{c}	35.5±3.9^{b}	48.7±0.9^{a}	<0.001*	0.046*	0.171
Aspatric acid	2055.7±633.8	87.9±13.3^{c}	121.0±12.2^{b}	301.9±0.1^{a}	79.7±7.2^{c}	168.4±3.9^{b}	341.8±12.8^{a}	78.5±26.5^{c}	213.8±10.2^{b}	296.0±20.2^{a}	<0.001*	0.164	0.628
Asparagine	/	103.7±7.2^{c}	76.4±3.5^{d}	233.1±5.0^{a}	63.6±3.0^{d}	128.3±19.5^{b,c}	186.8±19.9^{b}	124.7±15.3^{b,c}	139.3±9.9^{b,c}	156.8±2.6^{b}	/	0.126	/
Glutamine	1213.7±479.4	/	/	/	/	/	/	/	/	/	/	/	/
Phenylalanine	78.9±23.6	9.4±0.8^{c}	8.7±1.3^{c}	22.5±1.1^{b}	13.1±1.8^{c}	31.9±2.2^{a}	22.2±1.5^{b}	12.3±1.9^{c}	17.4±1.0^{b}	20.0±0.0^{b}	0.007*	0.037*	0.017*
Tyrosine	39.6±10.7	/	/	13.7±0.6^{a}	12.9±3.8^{a}	18.4±1.9^{a}	11.6±2.6^{a}	/	12.0±4.8^{a}	15.7±2.2^{a}	0.001*	0.003*	0.007*
Tryptophan	33.5±11.0	38.7±1.4^{b}	23.5±5.3^{c}	114.4±5.0^{a}	34.9±1.7^{b}	70.3±14.0^{a,b}	97.9±23.3^{a,b}	58.3±22.1^{b}	75.4±3.8^{a,b}	79.9±1.9^{a,b}	0.002*	0.215	0.224
Glutamic acid	1581.4±609.1	/	39.6±2.2^{c,d}	119.9±12.7^{a,b}	32.9±3.0^{d}	48.5±8.0^{c}	119.2±15.6^{a,b}	/	96.9±10.3^{b}	125.8±2.2^{a}	<0.001*	0.025*	0.040*
Lysine	52.0±9.4	/	/	/	/	/	/	/	/	/	/	/	/
Histidine	72.8±25.4	/	/	/	/	/	/	/	/	/	/	/	/
∑ FAA	8161.0±113.4	406.8±37.4^{d}	501.53±42.5^{d}	1262.4±42.8^{a}	429.6±41.5^{d}	989.0±83.1^{b,c}	1298.0±100.4^{a}	482.3±89.1^{d}	856.4±69.8^{c}	1164.0±45.0^{a,b}	<0.001*	<0.001*	<0.001*

B2.5 – pasta fortified with 2.5% of BLP; B5 – pasta fortified with 5% of BLP; C – control pasta without BLP; F – fresh pasta; L – pasta dried at low temperature (50°C, 8 h); H – pasta dried at high temperature (80°C, 3 h). Different letters in superscript in the same line indicate a significant difference ($p<0.05$) based on post-hoc Fisher's least significant difference (LSD) test. $^{\#}$Two-way analysis of variance. *Significant effect ($p<0.05$)

TABLE 4. Content of fatty acids in broccoli leaf powder (BLP) and experimental pasta products (μg/g dry matter).

Fatty acid	BLP	F-C	F-B2.5	F-B5	L-C	L-B2.5	L-B5	H-C	H-B2.5	H-B5	p-Value$^{\#}$		
											BLP addition effect	Drying (D) effect	BLP×D effect
C16:0	294.7±27.8	1625.2±49.1^{e}	2275.1±33.7^{a,b}	1951.5±101.4^{c}	1779.1±5.7^{d}	2302.3±10.9^{a,b}	2426.5±87.1^{a}	1852.5±40.6^{c,d}	2251.4±87.1^{b}	2240.4±103.1^{b}	<0.001*	<0.001*	0.007*
C16:1 *n*10	/	11.3±0.2^{d}	25.4±3.3^{a}	20.9±0.4^{b,c}	19.9±1.0^{c}	25.7±1.56^{a}	24.8±1.8^{a,b}	23.3±0.2^{a,b,c}	23.8±1.2^{a,b,c}	26.2±3.9^{a}	/	0.003*	/
C16:1 *n*7	/	97.5±2.9^{e}	133.8±1.5^{b}	113.5±5.2^{d}	112.1±0.8^{d}	128.2±3.6^{b,c}	144.8±2.5^{a}	128.0±7.5^{b,c}	120.8±5.3^{c,d}	136.9±0.6^{a,b}	/	<0.001*	/
C16:2	30.3±4.2	/	2.5±0.6^{d}	5.5±0.1^{b}	/	4.1±0.0^{c}	6.5±0.4^{a}	/	3.0±0.5^{d}	6.0±0.0^{a,b}	<0.001*	0.002*	0.037*
C16:3	35.3±4.8	/	1.4±0.0^{c}	2.0±0.2^{b}	/	1.4±0.0^{c}	2.6±0.3^{a}	/	1.3±0.0^{c}	2.9±0.2^{a}	<0.001*	0.016*	0.006*
C17:0	8.5±1.2	10.0±0.3^{d,e}	14.6±1.5^{c,d}	16.4±4.5^{b,c}	9.9±1.5^{e}	13.7±0.4^{c,d,e}	19.7±2.6^{a,b}	11.8±1.9^{c,d,e}	13.3±0.7^{c,d,e}	21.4±1.6^{a}	<0.001*	0.343	0.337
C17:1 *cis*	/	14.4±1.0^{d}	22.0±0.7^{b,c}	24.0±6.0^{b}	14.5±1.4^{d}	24.2±2.7^{b}	29.0±6.0^{a,b}	16.5±1.6^{c,d}	25.5±0.6^{b}	34.6±0.3^{a}	/	0.041*	/
C17:1 *trans*	192.4±20.7	/	4.1±0.6^{c}	6.3±0.6^{b}	/	1.8±0.2^{e}	8.4±0.1^{a}	/	3.1±0.0^{d}	9.3±0.9^{a}	<0.001*	0.019*	<0.001*
C18:0	46.1±3.0	263.3±12.9^{e}	366.8±20.4^{a,b}	321.2±16.2^{c}	275.0±0.2^{d,e}	382.1±0.2^{a,b}	393.2±8.4^{a}	302.2±16.9^{c,d}	387.1±13.4^{a,b}	360.7±18.0^{b}	<0.001*	0.003*	0.044*
C18:1 *cis*	69.3±3.9	7687.9±147.6^{c,d}	8897.5±30.4^{a,b}	7667.0±697.2^{c,d}	7621.1±14.1^{d}	8584.4±205.7^{b,c}	9508.9±468.7^{a}	8548.7±727.9^{b,c}	8134.9±127.0^{b,c,d}	8133.0±420.4^{b,c,d}	0.073	0.169	0.008*
C18:1 *trans*	21.8±3.0	785.7±230.1^{e}	1352.9±122.4^{a,b,c}	1118.0±18.6^{c,d,e}	933.2±204.2^{d,e}	1300.0±127.2^{a,b,c}	1496.4±127.3^{a,b}	1065.3±135.1^{c,d,e}	1211.6±37.1^{b,c,d}	1605.2±230.8^{a}	0.001*	0.103	0.140
C18:2	192.9±14.0	1668.5±4.8^{e,f}	2049.7±23.8^{b,c}	1785.9±196.7^{d,e,f}	1888.3±0.8^{c,d}	1850.7±2.8^{d,e}	2318.8±37.1^{a}	2119.8±149.1^{b}	1624.4±54.1^{f}	1930.7±45.6^{b,c,d}	0.021*	0.014*	<0.001*
C18:3 *n*6	697.5±83.0	113.2±510^{d}	153.4±19.8^{b}	159.4±22.5^{b}	121.5±0.3^{c,d}	146.6±0.6^{b,c}	207.6±1.3^{a}	139.8±8.0^{b,c,d}	119.0±17.2^{d}	201.6±6.6^{a}	<0.001*	0.104	0.009*
C18:3 *n*3	185.0±13.8	/	10.8±1.4^{c}	21.7±1.6^{b}	/	13.9±1.4^{c}	25.8±3.2^{a}	/	13.6±0.7^{c}	28.6±1.7^{a}	<0.001*	0.011*	0.083
C20:0	/	36.2±6.0^{d}	53.6±8.7^{b,c}	52.8±0.2^{c}	35.7±0.9^{d}	62.2±0.6^{a,b}	63.6±0.0^{a}	40.1±2.23^{d}	63.6±0.1^{a,b,c}	54.5±5.21^{a,b,c}	/	0.067	/
C20:1	/	29.0±4.7^{c}	52.7±12.4^{b}	52.6±5.7^{b}	31.8±0.6^{c}	59.0±2.1^{a,b}	64.6±1.6^{a}	35.4±0.6^{c}	56.4±0.6^{a,b}	57.0±5.8^{a,b}	/	0.106	/
∑ Fatty acids	1773.9±173.3	12341.9±291.8^{e}	15416.3±225.5^{b}	13318.7±1043.3^{d,e}	12842.1±193.8^{e}	14899.9±70.4^{b,c}	16741.2±477.9^{a}	14283.3±735.3^{c,d}	14050.1±126.8^{c,d}	14849.0±265.2^{b,c}	<0.001*	0.009*	<0.001*

B2.5 – pasta fortified with 2.5% of BLP; B5 – pasta fortified with 5% of BLP; C – control pasta without BLP; F – fresh pasta; L – pasta dried at low temperature (50°C, 8 h); H – pasta dried at high temperature (80°C, 3 h). Different letters in superscript in the same line indicate a significant difference ($p< 0.05$) based on post-hoc Fisher's least significant difference (LSD) test. $^{\#}$Two-way analysis of variance. *Significant effect ($p<0.05$).

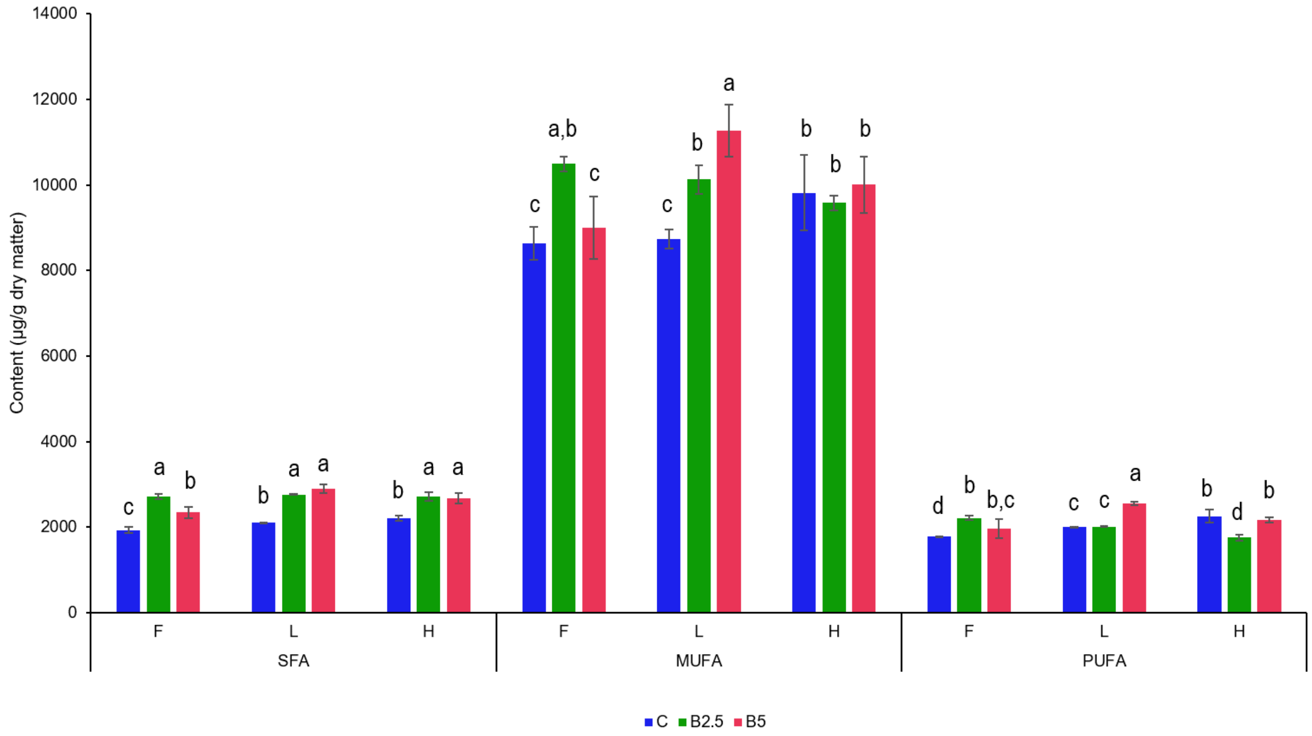

FIGURE 4. The summarized content of saturated (SFA), monounsaturated (MUFA) and polyunsaturated fatty acids (PUFA) in experimental pasta products. B2.5 – pasta fortified with 2.5% of broccoli leaf powder (BLP); B5 – pasta fortified with 5% of BLP; C – control pasta without BLP; F – fresh pasta; L – pasta dried at low temperature (50°C, 8 h); H – pasta dried at high temperature (80°C, 3 h). Different letters above bars indicate a significant difference ($p<0.05$), separately for SFA, MUFA and PUFA.

et al., 2019]. In control pasta, the presence of 11 fatty acids was detected with oleic acid (C18:1 *cis*), C18:2 and C16:0 as the major ones. The profile of fatty acids in control pasta is in agreement with the fatty acid profile of olive oil [Sánchez-Rodríguez *et al.*, 2019]. Although the percentage of BLP incorporation into pasta formulations was relatively low, changes were noticed in the fatty acid profile. Significant effects were detected for all fatty acids except for C18:1 *cis.* This resulted in a significant effect of BLP percentage on the total fatty acid content. Notably, in the fortified pasta products, hexadecadienoic acid (C16:2), hexadecatrienoic acid (C16:3), C17:1 *trans* and C18:3 *n*3 derived exclusively from BLP as they were not detected in C pasta. Notably, the high consumption of cereal-based products, rich in *n*6 fatty acids is considered to be responsible for the imbalance in the *n*6 to the *n*3 ratio [Fradique *et al.*, 2013]. BLP contained *n*3 fatty acids, which was reflected in the fatty acid profile of experimental pasta. C18:3 *n*3 was detected even in the pasta made with the minimum percentage of BLP (B2.5), which contributed to an important reduction in the *n*6:*n*3 ratio compared to C pasta. The consumption of BLP-enriched pasta may contribute to *n*6:*n*3 ratio normalisation in the diet, which is particularly imbalanced in the Western diet [Asefy *et al.*, 2021]. A summarised content of saturated fatty acids (SFA), monounsaturated fatty acids (MUFA) and PUFA is presented in Figure 4. The incorporation of BLP resulted in increased contents of all types of fatty acids. However, noteworthy increases in MUFA and PUFA were noted in L pasta. It is of a particular importance considering the recommendations of the European Food Safety Authority (EFSA), who underlined the importance of increasing the daily intake of PUFA [EFSA Panel on Dietetic Products, 2010]. An increase in fatty acid content in fortified pasta was previously reported by other authors; however, all these studies focused on the fortification of pasta with fish products [Ainsa *et al.*, 2021; Desai *et al.*, 2018b; Monteiro *et al.*, 2016].

The effect of drying on fatty acid contents could also be noticed, especially in the case of C16:0 and palmitoleic acid (C16:1 *n*7). The clear increasing trend of fatty acid content with increasing BLP percentage was observed only for L pasta products, with L-B5 pasta having the highest content of fatty acids among all analysed pasta products (Table 4). At the same time, this pasta was characterised by the highest proportion of MUFA and PUFA (Figure 4). Unsaturated fatty acids are particularly vulnerable to oxidation [Nawar, 1984], which can explain the lower content of fatty acids in the H pasta. In our study, the most thermally sensitive unsaturated fatty acids were C18:1 *cis*, C18:2 and C18:3 *n*6. Previously, C18:3 *n*3 was found to be particularly thermolabile in pasta fortified with flaxseed [Manthey *et al.*, 2002], which was not noted in our study. We observed an opposite phenomenon, and C18:3 *n*3 content was the highest in H pasta.

The results of the two-way ANOVA showed that there was a clear interaction between the BLP percentage and drying temperature for most individual fatty acids and total fatty acids (Table 4). The most significant interactions were noted for C17:1 *trans* and C18:2.

TABLE 5. Content of sugars in broccoli leaf powder (BLP) and experimental pasta products (mg/g dry matter).

Pasta	Fructose	Glucose	Sucrose	Stachyose	∑ Sugars
BLP	32.44 ± 1.53	17.56 ± 0.16	7.71 ± 5.94	55.38 ± 0.32	113.09 ± 6.99
F-C	0.62 ± 0.28^{e}	$0.81\pm0.21^{d,e}$	$18.05\pm1.06^{a,b}$	5.36 ± 0.25^{a}	$24.83\pm0.31^{a,b}$
F-B2.5	1.04 ± 0.08^{d}	$0.89\pm0.01^{c,d,e}$	$18.52\pm0.51^{a,b}$	4.51 ± 0.06^{b}	24.96 ± 0.61^{a}
F-B5	1.67 ± 0.23^{b}	$1.23\pm0.07^{b,c}$	$17.24\pm0.34^{a,b}$	4.60 ± 0.21^{b}	$24.74\pm0.78^{a,b}$
L-C	1.11 ± 0.16^{d}	1.32 ± 0.06^{b}	$17.46\pm0.17^{a,b}$	3.62 ± 0.16^{e}	$23.50\pm0.37^{a,b}$
L-B2.5	2.13 ± 0.51^{a}	2.31 ± 0.19^{a}	$17.03\pm0.66^{a,b}$	3.14 ± 0.05^{f}	$24.60\pm1.42^{a,b}$
L-B5	$1.58\pm0.11^{b,c}$	$1.18\pm0.11^{b,c,d}$	$16.43\pm0.88^{a,b}$	3.98 ± 0.11^{c}	$23.17\pm0.81^{a,b}$
H-C	0.58 ± 0.07^{e}	$0.97\pm0.52^{b,c,d,e}$	19.32 ± 7.06^{a}	$3.91\pm0.08^{c,d}$	24.78 ± 6.94^{a}
H-B2.5	$1.24\pm0.27^{c,d}$	0.76 ± 0.1^{e}	$16.26\pm0.98^{a,b}$	$3.67\pm0.18^{d,e}$	$21.94\pm1.21^{a,b}$
H-B5	1.20 ± 0.10^{d}	$0.84\pm0.07^{d,e}$	14.57 ± 0.85^{b}	$3.65\pm0.22^{d,e}$	20.26 ± 1.06^{b}
p-Value$^{\#}$					
BLP addition effect	<0.001*	0.033*	0.252	<0.001*	0.432
Drying (D) effect	<0.001*	<0.001*	0.615	<0.001*	0.169
BLP×D effect	0.006*	<0.001*	0.668	<0.001*	0.559

B2.5 – pasta fortified with 2.5% of BLP; B5 – pasta fortified with 5% of BLP; C – control pasta without BLP; F – fresh pasta; L – pasta dried at low temperature (50°C, 8 h); H – pasta dried at high temperature (80°C, 3 h). Different letters in superscript in the same column indicate a significant difference ($p<0.05$) based on post-hoc Fisher's least significant difference (LSD) test. $^{\#}$Two-way analysis of variance. *Significant effect ($p<0.05$).

Sugar profile

The main sugars detected in broccoli were glucose, fructose and sucrose, which are important contributors to its taste [Rosa *et al.*, 2001; Wieczorek *et al.*, 2022]. The content of individual sugars in BLP and experimental pasta is presented in Table 5. Four sugars were detected in BLP and experimental pasta, including fructose, glucose, sucrose and stachyose. The main sugar in BLP was stachyose. Contrary, sucrose was the main sugar in the experimental pasta products. The incorporation of BLP influenced the content of all sugars except for sucrose, which was purely derived from semolina. The most prominent effect of BLP addition was found for fructose; however, the increasing trend with increasing BLP percentage was observed only for F pasta. In the case of pasta products dried at low temperature, B2.5 pasta had a significantly higher content of fructose than B5. Similar tendencies were observed for glucose in F and L. For H pasta, incorporation of BLP resulted in insignificant changes in glucose content.

The effect of drying was found for fructose, glucose and stachyose. The content of stachyose was significantly lower in dried pasta compared to F. An increasing trend in glucose and fructose content was observed for F pasta with increasing BLP percentage, while no clear trend could be defined for dried pasta products. Notably, irrespective of BLP percentage, the content of glucose and fructose was higher in dried than in fresh pasta. It is in agreement with a previous study, which also reported a small increase in contents of these sugars [Gélinas *et al.*, 2016]. The authors reported also the difference in sucrose levels depending on drying temperature. In L products, sucrose content decreased, while in H products it was observed to increase. A similar tendency was observed also in our study, although statistical analysis did not highlight the effect of drying on sucrose content. In H pasta, the highest content of sucrose corresponded to the lowest content of glucose and fructose, which can suggest that a higher temperature of drying can inhibit sucrose hydrolysis. The lower content of sucrose observed with a higher content of glucose and fructose in L pasta can be explained by the most favourable conditions for possibly the enzymatic reaction.

The results of the two-way ANOVA showed that there was an interaction between the BLP percentage and drying temperature for individual sugars and total sugars (Table 5). The most significant interactions were noted for stachyose and glucose.

CONCLUSIONS

This study presented a successful attempt of incorporating BLP into pasta formulations. BLP significantly improved the contents of ash, FAA and fatty acids, without compromising the cooking quality of pasta. Drying temperature had a significant negative effect on the contents of fatty acids, which were probably partly oxidised at the highest temperature. From the nutritional point of view, the low-temperature drying seems to be an interesting method for pasta preparation, as the highest content of FAA, fatty acids, especially MUFA and PUFA, and the lowest sugar level were found in these pasta products. However, at the same time, dried pasta products were characterised by greater cooking loss approximating 10%, which is higher than the acceptable 8%.

ACKNOWLEDGEMENTS

The study was supported by the statutory research funds of the Institute of Animal Reproduction and Food Research of the Polish Academy of Sciences.

RESEARCH FUNDING

This research received no external funding. Mariana Nogueira's stay in IAR&FR PAS was financially supported by the EIT Food Fellowship program.

CONFLICT OF INTERESTS

The authors declare no conflict of interest.

ORCID IDs

E. Ciska https://orcid.org/0000-0002-8455-1429
N. Drabińska https://orcid.org/0000-0001-5324-5982
H. Jeleń https://orcid.org/0000-0002-6568-8155
M. Nogueira https://orcid.org/0000-0002-3463-3282

REFERENCES

1. AACC, A.M. (2000). American Association of Cereal Chemists. Method 66–50, 26–10A, 26.41, 66, 41.
2. Ainsa, A., Marquina, P.L., Roncalés, P., Beltrán, J.A., Calanche M.J.B. (2021). Enriched fresh pasta with a sea bass by-product, a novel food: Fatty acid stability and sensory properties throughout shelf life. *Foods*, *10*(2), art. no. 255. https://doi.org/10.3390/foods10020255
3. Anese, M., Nicoli, M.C., Massini, R., Lerici, C.R. (1999). Effects of drying processing on the Maillard reaction in pasta. *Food Research International*, *32*(3), 193–199. https://doi.org/10.1016/S0963-9969(99)00076-9
4. AOAC. (2005). Official Methods of Analysis, (18th edn). Association of Official Analytical Chemists, Gaithersburg, Maryland.
5. Arise, A.K., Oriade, K.F., Asogwa, T.N., Nwachukwu, I. (2022). Amino acid profile, physicochemical and sensory properties of noodles produced from wheat-Bambara protein isolate. *Measurement: Food*, *5*, art. no. 100020. https://doi.org/10.1016/j.meafoo.2021.100020
6. Asefy, Z., Tanomand, A., Hoseinnejhad, S., Ceferov, Z., Oshaghi, E.A., Rashidi, M. (2021). Unsaturated fatty acids as a co-therapeutic agents in cancer treatment. *Molecular Biology Reports*, *48*(3), 2909–2916. https://doi.org/10.1007/s11033-021-06319-8
7. Bhandari, S.R., Park, M.Y., Chae, W.B., Kim, D.Y., Kwak, J.H. (2013). Seasonal variation in fatty acid composition in various parts of broccoli cultivars. *Korean Journal of Agricultural Science*, *40*(4), 289–296. https://doi.org/10.7744/cnujas.2013.40.4.289
8. Bresciani, A., Pagani, M.A., Marti, A. (2022). Pasta-making process: a narrative review on the relation between process variables and pasta quality. *Foods 11*(3), art. no. 256. https://doi.org/10.3390/foods11030256
9. Bruneel, C., Pareyt, B., Brijs, K., Delcour, J.A. (2010). The impact of the protein network on the pasting and cooking properties of dry pasta products. *Food Chemistry*, *120*(2), 371–378. https://doi.org/https://doi.org/10.1016/j.foodchem.2009.09.069
10. Bruno, J.A., Konas, D.W., Matthews, E.L., Feldman, C.H., Pinsley, K.M., Kerrihard, A.L. (2019). Sprouted and non-sprouted chickpea flours: effects on sensory traits in pasta and antioxidant capacity. *Polish Journal of Food and Nutrition Sciences*, *69*(2), 203–209. https://doi.org/10.31883/pjfns/109280
11. Bustos, M.C., Perez, G.T., Leon, A.E. (2015). Structure and quality of pasta enriched with functional ingredients. *RSC Advances* *5*(39), 30780–30792. https://doi.org/10.1039/c4ra11857j
12. Cole, M.E. (1991). Prediction and measurement of pasta quality. *International Journal of Food Science & Technology*, *26*(2), 133–151. https://doi.org/https://doi.org/10.1111/j.1365-2621.1991.tb01149.x
13. D'Amico, S., Mäschle, J., Jekle, M., Tömösközi, S., Langó, B., Schoenlechner, R. (2015). Effect of high temperature drying on gluten-free pasta properties. *LWT – Food Science and Technology*, *63*(1), 391–399. https://doi.org/10.1016/j.lwt.2015.03.080
14. Desai, A.S., Brennan, M.A., Brennan, C.S. (2018a). Effect of fortification with fish (*Pseudophycis bachus*) powder on nutritional quality of durum wheat pasta. *Foods (Basel, Switzerland)*, *7*(4), art. no. 62. https://doi.org/10.3390/foods7040062
15. Desai, A.S., Brennan, M.A., Brennan, C.S. (2018b). Amino acid and fatty acid profile and digestible indispensable amino acid score of pasta fortified with salmon (*Oncorhynchus tshawytscha*) powder. *European Food Research and Technology*, *244*(10), 1729–1739. https://doi.org/10.1007/s00217-018-3085-5
16. Dexter, J.E., Tkachuk, R., Matuso, R.R. (1984). Amino acid composition of spaghetti: effect of drying conditions on total and available lysine. *Journal of Food Science*, *49*(1), 225–228. https://doi.org/https://doi.org/10.1111/j.1365-2621.1984.tb13713.x
17. Dominguez-Perles, R., Moreno, D.A., Carvajal, M., Garcia-Viguera, C. (2011). Composition and antioxidant capacity of a novel beverage produced with green tea and minimally-processed byproducts of broccoli. *Innovative Food Science & Emerging Technologies*, *12*(3), 361–368. https://doi.org/https://doi.org/10.1016/j.ifset.2011.04.005
18. Drabińska, N. (2022). The evaluation of amino acid profiles in gluten-free mini sponge cakes fortified with broccoli by-product. *Separations*, *9*(3), art. no. 81. https://doi.org/10.3390/separations9030081
19. Drabińska, N., Ciska, E., Szmatowicz, B., Krupa-Kozak, U. (2018). Broccoli by-products improve the nutraceutical potential of gluten-free mini sponge cakes. *Food Chemistry*, *267*, 170–177. https://doi.org/10.1016/j.foodchem.2017.08.119
20. Drabińska, N., Jeż, M., Nogueira, M. (2021). Variation in the accumulation of phytochemicals and their bioactive properties among the aerial parts of cauliflower. *Antioxidants*, *10*(10), art. no. 1597. https://doi.org/10.3390/antiox10101597
21. Duda, A., Adamczak, J., Chełmińska, P., Juszkiewicz, J., Kowalczewski, P. (2019). Quality and nutritional/textural properties

of durum wheat pasta enriched with cricket powder. *Foods (Basel, Switzerland)*, *8*(2), art. no. 46.
https://doi.org/10.3390/foods8020046

22. EFSA Panel on Dietetic Products, Nutrition and Allergies (NDA). (2010). Scientific Opinion on Dietary Reference Values for fats, including saturated fatty acids, polyunsaturated fatty acids, monounsaturated fatty acids, trans fatty acids, and cholesterol. *EFSA Journal*, *8*(3), art. no. 1461.
https://doi.org/10.2903/j.efsa.2010.1461
23. Filip, S., Vidrih, R. (2015). Amino acid composition of protein-enriched dried pasta: is it suitable for a low-carbohydrate diet? *Food Technology and Biotechnology*, *53*(3), 298–306.
https://doi.org/10.17113/ftb.53.03.15.4022
24. Fois, S., Campus, M., Piu, P.P., Siliani, S., Sanna, M., Roggio, T., Catzeddu, P. (2019). Fresh pasta manufactured with fermented whole wheat semolina: physicochemical, sensorial, and nutritional properties. *Foods*, *8*(9), art. no. 422.
https://doi.org/10.3390/FOODS8090422
25. Fradique, M., Batista, A.P., Nunes, M.C., Gouveia, L., Bandarra, N.M., Raymundo, A. (2013). *Isochrysis galbana* and *Diacronema vlkianum* biomass incorporation in pasta products as PUFA's source. *LWT – Food Science and Technology*, *50*(1), 312–319.
https://doi.org/10.1016/j.lwt.2012.05.006
26. Fuad, T., Prabhasankar, P. (2010). Role of ingredients in pasta product quality: a review on recent developments. *Critical Reviews in Food Science and Nutrition*, *50*(8), 787–798.
https://doi.org/10.1080/10408390903001693
27. Fuad, T., Prabhasankar, P. (2012). Influences of India's local wheat varieties and additives on quality of pasta. *Food and Bioprocess Technology*, *5*(5), 1743–1755.
https://doi.org/10.1007/s11947-011-0679-3
28. Gélinas, P., Mckinnon, C., Gagnon, F. (2016). Fructans, water-soluble fibre and fermentable sugars in bread and pasta made with ancient and modern wheat. *International Journal of Food Science and Technology*, *51*(3), 555–564.
https://doi.org/10.1111/ijfs.13022
29. Giannetti, V., Boccacci Mariani, M., Marini, F., Biancolillo, A. (2021). Effects of thermal treatments on durum wheat pasta flavour during production process: A modelling approach to provide added-value to pasta dried at low temperatures. *Talanta*, *225*, art. no. 121955.
https://doi.org/10.1016/j.talanta.2020.121955
30. Gómez-García, R., Campos, D.A., Aguilar, C.N., Madureira, A.R., Pintado, M. (2021). Valorisation of food agro-industrial by-products: From the past to the present and perspectives. *Journal of Environmental Management*, *299*, art.no. 113571.
https://doi.org/https://doi.org/10.1016/j.jenvman.2021.113571
31. Hoehnel, A., Bez, J., Petersen, I.L., Amarowicz, R., Juśkiewicz, J., Zannini, E., Arendt, E.K. (2020). Combining high-protein ingredients from pseudocereals and legumes for the development of fresh high-protein hybrid pasta: enhanced nutritional profile. *Journal of the Science of Food and Agriculture*.
https://doi.org/10.1002/jsfa.11015
32. Joon Lee, J., Mi Lee, Y., Ra Kim, A., Yul Lee, M. (2009). Physicochemical composition of broccoli sprouts. *Journal of Life Science*, *19*(2), 95–100.
https://doi.org/10.5352/JLS.2009.19.2.192
33. Kaur, G., Sharma, S., Nagi, H.P.S., Ranote, P.S. (2013). Enrichment of pasta with different plant proteins. *Journal of Food Science and Technology*, *50*(5), 1000–1005.
https://doi.org/10.1007/s13197-011-0404-2
34. Krupa-Kozak, U., Drabińska, N., Bączek, N., Šimková, K., Starowicz, M., Jeliński, T. (2021). Application of broccoli leaf powder in gluten-free bread: an innovative approach to improve its bioactive potential and technological quality. *Foods, (10)*4, art. no. 819.
https://doi.org/10.3390/foods10040819
35. Lamacchia, C., di Luccia, A., Baiano, A., Gambacorta, G., la Gatta, B., Pati, S., la Notte, E. (2007). Changes in pasta proteins induced by drying cycles and their relationship to cooking behaviour. *Journal of Cereal Science*, *46*(1), 58–63.
https://doi.org/https://doi.org/10.1016/j.jcs.2006.12.004
36. Liu, M., Zhang, L., Ser, S.L., Cumming, J.R., Ku, K.-M. (2018). Comparative phytonutrient analysis of broccoli by-products: the potentials for broccoli by-product utilization. *Molecules (Basel, Switzerland)*, *23*(4), art. no. 900.
https://doi.org/10.3390/molecules23040900
37. Manthey, F.A., Hall, C.A. (2007). Effect of processing and cooking on the content of minerals and protein in pasta containing buckwheat bran flour. *Journal of the Science of Food and Agriculture*, *87*(11), 2026–2033.
https://doi.org/10.1002/jsfa.2953
38. Manthey, F.A., Lee, R.E., Hall, C.A. (2002). Processing and cooking effects on lipid content and stability of α-linolenic acid in spaghetti containing ground flaxseed. *Journal of Agricultural and Food Chemistry*, *50*(6), 1668–1671.
https://doi.org/10.1021/jf011147s
39. Mercier, S., Moresoli, C., Mondor, M., Villeneuve, S., Marcos, B. (2016). A meta-analysis of enriched pasta: What are the effects of enrichment and process specifications on the quality attributes of pasta? *Comprehensive Reviews in Food Science and Food Safety*, *15*(4), 685–704.
https://doi.org/10.1111/1541-4337.12207
40. Michalak-Majewska, M., Teterycz, D., Muszyński, S., Radzki, W., Sykut-Domańska, E. (2020). Influence of onion skin powder on nutritional and quality attributes of wheat pasta. *PLoS ONE*, *15*(1), art. no. e0227942.
https://doi.org/10.1371/journal.pone.0227942
41. Monteiro, M.L.G., Mársico, E.T., Soares, M.S., Magalhães, A.O., Canto, A.C.V.C.S., Costa-Lima, B.R.C., Alvares, T.S., Conte, C.A. (2016). Nutritional profile and chemical stability of pasta fortified with tilapia (*Oreochromis niloticus*) flour. *PLoS ONE*, *11*(12), art. no. e0168270.
https://doi.org/10.1371/journal.pone.0168270
42. Narducci, V., Finotti, E., Galli, V., Carcea, M. (2019). Lipids and fatty acids in Italian durum wheat (*Triticum Durum Desf.)* cultivars. *Foods*, *8*(6), art. no. 223.
https://doi.org/10.3390/foods8060223
43. Nawar, W.W. (1984). Chemical changes in lipids produced by thermal processing. *Journal of Chemical Education*, *61*(4), 299–302.
https://pubs.acs.org/sharingguidelines
44. Nilusha, R.A.T., Jayasinghe, J.M.J.K., Perera, O.D.A.N., Perera, P.I.P. (2019). Development of pasta products with nonconventional ingredients and their effect on selected quality characteristics: A brief overview. *International Journal of Food Science*, *2019*, art. no. 6750726.
https://doi.org/10.1155/2019/6750726

45. Oliviero, T., Fogliano, V. (2016). Food design strategies to increase vegetable intake: The case of vegetable enriched pasta. *Trends in Food Science and Technology, 51*, 58–64. https://doi.org/10.1016/j.tifs.2016.03.008
46. O'Shea, N., Arendt, E.K., Gallagher, E. (2012). Dietary fibre and phytochemical characteristics of fruit and vegetable by-products and their recent applications as novel ingredients in food products. *Innovative Food Science and Emerging Technologies*, *16*, 1–10. https://doi.org/10.1016/j.ifset.2012.06.002
47. Pérez, E., Pérez, L. (2009). Effect of the addition of cassava flour and beetroot juice on the quality of fettuccine. *African Journal of Food Science*, *3*(11), 352–360. http://www.academicjournals.org/ajfs
48. Piwińska, M., Wyrwisz, J., Kurek, M.A., Wierzbicka, A. (2016). Effect of drying methods on the physical properties of durum wheat pasta. *CyTA – Journal of Food*, *14*(4), 523–528. https://doi.org/10.1080/19476337.2016.1149226
49. Raczyk, M., Polanowska, K., Kruszewski, B., Grygier, A., Michałowska, D. (2022). Effect of spirulina (*Arthrospira platensis*) supplementation on physical and chemical properties of semolina (*Triticum durum*) based fresh pasta. *Molecules*, *27*(2), art. no. 355. https://doi.org/10.3390/molecules27020355
50. Reguengo, L.M., Salgaço, M.K., Sivieri, K., Maróstica Júnior, M.R. (2022). Agro-industrial by-products: valuable sources of bioactive compounds. *Food Research International*, *152*, art. no. 110871. https://doi.org/https://doi.org/10.1016/j.foodres.2021.110871
51. Rosa, E., David, M., Gomes, M.H. (2001). Glucose, fructose and sucrose content in broccoli, white cabbage and Portuguese cabbage grown in early and late seasons. *Journal of the Science of Food and Agriculture*, *81*(12), 1145–1149. https://doi.org/10.1002/jsfa.919
52. Sánchez-Rodríguez, L., Kranjac, M., Marijanović, Z., Jerković, I., Corell, M., Moriana, A., Carbonell-Barrachina, Á.A., Sendra, E., Hernández, F. (2019). Quality attributes and fatty acid, volatile and sensory profiles of "Arbequina" hydrosostainable olive oil. *Molecules*, *24*(11), art. no. 2148. https://doi.org/10.3390/molecules24112148
53. Sedlar, T., Čakarević, J., Tomić, J., Popović, L. (2020). Vegetable by-products as new sources of functional proteins. *Plant Foods for Human Nutrition,* 76(1), 31–36. https://doi.org/10.1007/s11130-020-00870-8
54. Sharafi, Y., Majidi, M.M., Goli, S.A.H., Rashidi, F. (2015). Oil content and fatty acids composition in Brassica species. *International Journal of Food Properties*, *18*(10), 2145–2154. https://doi.org/10.1080/10942912.2014.968284
55. van Loey, A., Ooms, V., Weemaes, C., van den Broeck, I., Ludikhuyze, L., Indrawati, Denys, S., Hendrickx, M. (1998). Thermal and pressure-temperature degradation of chlorophyll in broccoli (*Brassica oleracea L. italica*) juice: a kinetic study. *Journal of Agricultural and Food Chemistry*, *46*(12), 5289–5294. https://doi.org/10.1021/jf980505x
56. Weemaes, C.A., Ooms, V., van Loey, A.M., Hendrickx, M.E. (1999). Kinetics of chlorophyll degradation and color loss in heated broccoli juice. *Journal of Agricultural and Food Chemistry*, *47*(6), 2404–2409. https://doi.org/10.1021/jf980663o
57. Wieczorek, M.N., Dunkel, A., Szwengiel, A., Czaczyk, K., Drożdżyńska, A., Zawirska-Wojtasiak, R., Jeleń, H.H. (2022). The relation between phytochemical composition and sensory traits of selected Brassica vegetables. *LWT– Food Science and Technology*, *156*, art. no. 113028. https://doi.org/https://doi.org/10.1016/j.lwt.2021.113028

Pol. J. Food Nutr. Sci., 2022, Vol. 72, No. 3, pp. 287–296
On-line ISSN: 2083-6007
Print ISSN: 1230-0322
DOI: 10.31883/pjfns/152432
http://journal.pan.olsztyn.pl

Original article
Section: Food Technology

Optimization of Ultrasound Treatment of Beverage from Mango and Carrot with Added Turmeric Using Response Surface Methodology

Leticia X. Lopez-Martinez[1], *Nill Campos-Gonzalez*[2], *Victor M. Zamora-Gasga*[3],
Jesús A. Domínguez-Avila[1], *Sunil Pareek*[4], *Mónica A. Villegas-Ochoa*[2],
Sonia G. Sáyago-Ayerdi[3], *Gustavo A. González-Aguilar*[2]*

[1]*CONACYT-Centro de Investigación en Alimentación y Desarrollo A.C. Carretera Gustavo Enrique Astiazarán Rosas No. 46, Col. La Victoria, Hermosillo, Sonora 83304, México*
[2]*Centro de Investigación en Alimentación y Desarrollo A.C. Carretera Gustavo Enrique Astiazarán Rosas No. 46, Col. La Victoria, Hermosillo, Sonora 83304, México*
[3]*Laboratorio Integral de Investigación en Alimentos, Tecnológico Nacional de México-Instituto Tecnológico de Tepic, Av. Tecnológico 255 Fracc. Lagos del Country, 63175 Tepic, Nayarit, Mexico*
[4]*Department of Agriculture and Environmental Sciences, National Institute of Food Technology Entrepreneurship and Management, Kundli, Sonipat, Haryana, 131 028, India*

Key words: antioxidant capacity, bioactive compounds, D-optimal design, response surface methodology, ultrasound

The effect of ultrasound treatment (UT) on a beverage from mango pulp and carrot juice with added turmeric powder on total soluble phenolic content (TSP), total carotenoid content (TC) and antioxidant capacity (AOC) was evaluated. Response surface methodology (RSM) was applied to obtain the optimal formulation of the beverage. The AOC was assigned as a response variable in addition to TSP and TC. Mathematical modeling showed that the formulation with 35% (*v/v*) of mango pulp, 10% (*v/v*) of carrot juice, and 0.7% (*w/v*) of turmeric powder, yielded the highest values of TSP, TC, and AOC. The beverages were subjected to different ultrasound conditions with varying exposure times (ET), sonication amplitudes (SA), and pulse cycles (PC) to obtain the highest values for response variables. Statistical modeling showed that a UT at 21 min ET, 100% SA, and 0.7 s PC, increased TSP, Trolox equivalent antioxidant capacity (TEAC), and ferric reducing antioxidant power (FRAP) by 15.5%, 45.1%, and 15.9%, respectively. Seven phenolic acids, three curcuminoids, five flavonoids, and a xanthonoid were identified in the beverages. The quantities of 3,4-dihydroxybenzoic acid, gallic acid, chlorogenic acids, (+)-catechin, quercetin, kaempferol, (–)-gallocatechin gallate, and mangiferin were higher in the UT beverage compared to the control, suggesting their release from cell-wall structures as a result of UT.

ABBREVIATIONS

UT, Ultrasound treatment; TSP, total soluble phenolic content; TC, total carotenoid content; AOC, antioxidant capacity, RSM, response surface methodology; ET, exposure time; SA, sonication amplitudes, PC, pulse cycles; TEAC, Trolox equivalent antioxidant capacity; ABTS, 2,2'-azino-bis-(3-ethylbenzothiazoline-6-sulfonic acid), FRAP, ferric reducing antioxidant power, TPTZ, 2,4,6-tripyridyl-s-triazine; GAE, gallic acid equivalent; TE, Trolox equivalent.

INTRODUCTION

Several epidemiological studies have demonstrated the relationship between consuming beverages from vegetable sources and the prevention of diseases related to oxidative stress, such as cardiovascular and neurodegenerative diseases and some types of cancer [Fujiki *et al.,* 2017; Wu *et al*., 2016; Zhou *et al*., 2015]. The main compounds to which these effects are attributed are phenolics and carotenoids. Consuming fruit and vegetable beverages can result in an increased intake of these compounds. Blending different fruit and vegetables increases the content and variety of bioactive compounds in beverages [Manna *et al*., 2017]. Furthermore, it has been reported that combining compounds of different chemical characteristics, such as phenolic compounds and carotenoids, can possibly enhance their antioxidant properties [Zhao *et al*., 2014]. To further maximize compound diversity and enhance organoleptic characteristics of beverages, the use of spices, like ginger or turmeric, and extracts thereof in their preparation has been investigated [Bhardwaj & Pandey, 2011]. In Mexico, mango and carrot are consumed

---

* Corresponding Author:
E-mail: gustavo@ciad.mx (G.A. Gonzalez-Aguilar)

Submitted: 10 February 2022
Accepted: 27 July 2022

by most of the population, consequently, their bioactive compound profile has been studied. Pacheco-Ordaz *et al*. [2018] established that mango contains chlorogenic acid, gallic acid, vanillic acid, protocatechuic acid, α- and β-carotene, lutein, and zeaxanthin. Flavonoids, like quercetin 3-isobutyrate, quercetin 4'-*O*-β-D-glucopyranoside-3,7-dimethyl ether, and quercetin, one gallotannin (theogallin) and 2 xanthones (mangiferin and mangiferin isomer) have also been identified in mango pulp [Barrón-García *et al*., 2022]. On the other hand, β-carotene, apigenin, rutin, chlorogenic acid, and protocatechuic acid have been reported in carrots [Šeregelj *et al*., 2020]. Bisdemethoxycurcumin, demethoxycurcumin, curcumin, (+)-catechin, quercetin, gallic acid, and *p*-coumaric acid have been identified in turmeric [Pal *et al*., 2020]. These molecules are known for their health benefits, which are related to the activation of different intracellular signaling pathways, immunomodulation, and cardioprotective properties [Palafox-Carlos *et al*., 2012]. Due to the reported properties of mango and carrot, in conjunction with the trend of adding spices to beverages, the use of powdered turmeric rhizomes is proposed due to their anti-inflammatory and antimutagenic properties [Deogade &Ghate, 2015].

Different investigations have been carried out where ultrasound treatments (UT) have been applied to fruits such as *Annona muricata* [Aguilar-Hernández *et al*., 2019, 2020; Nolasco-González *et al*., 2022]; juices like red and yellow watermelon juice [Yıkmış, 2020], black carrot juice [Hasheminya & Dehghannya, 2022], pear juice [Saeeduddin *et al*., 2016], Cape gooseberry juice [Ordóñez-Santos *et al*., 2017]; and beverages like grape-based beverage [Ahmad *et al*., 2020], carrot and grape beverage [Nadeem *et al*., 2018], and mango-based beverage [Mercado-Mercado *et al*., 2018]. These studies reported significant increases of bioactive compounds, like phenolics, carotenoids, anthocyanins or curcuminoids, in sonicated samples, as compared to the control, suggesting that UT is suitable to retain or enhance the content of bioactive compounds present in juices or beverages.

The aim of this study was to optimize UT parameters, like exposure time (ET), pulse cycle (PC) and sonication amplitude (SA), using response surface methodology (RSM), to obtain a beverage from mango, carrot and turmeric with the highest total soluble phenolic content (TSP), total carotenoid content (TC), and antioxidant capacity (AOC). Changes to the profile of antioxidants in the beverages as a result of UT were reported as well.

MATERIALS AND METHODS

Chemical and reagents

The Folin–Ciocalteu reagent, 2,2'-azino-bis-(3-ethylbenzothiazoline-6-sulfonic acid) (ABTS), Trolox (6-hydroxy-2,3,7,8-tetramethylchroman-2-carboxylic acid), TPTZ (2,4,6-tripyridyl-s-triazine), ferulic acid, as well as high-performance liquid chromatography (HPLC)-grade phenolic standards: *p*-coumaric acid, (+)-catechin hydrate, gallic acid, quercetin dihydrate, 3-hydroxybenzoic acid, and chlorogenic acid, were purchased from Sigma-Aldrich (St. Louis, MO, USA). The rest of the reagents used were obtained from J.T. Baker (Phillipsburg, NJ, USA). All solvents were of analytical grade.

Beverage preparation

Mango cv. Ataulfo and carrot cv. Early Gold, both of commercial ripeness, were acquired from local suppliers in Hermosillo, Mexico. Turmeric powder (food grade) was purchased from Proquimercy enterprise (Jalisco, Mexico). Mangoes and carrots were washed with tap water and disinfected with 0.05 mL/L sodium hypochlorite for 5 min. Mango peel was manually removed using a stainless-steel knife, and the flesh was cut into 3 mm cubes. Carrots were cut into sections about 3 to 5 mm thick and were subjected to a juice extraction process using a commercial juice extractor (Moulinex model 140–1–03, Naucalpan, State of Mexico, Mexico). Mango pulp, carrot juice, turmeric powder, and purified water were mixed at a 35:10:0.7:54.3 (*v/v/w/v*) ratio and blended using a commercial blender (Oster®, Milwaukee, WI, USA). Beverage formulation was based on previous experiments in the Laboratory of Antioxidants and Functional Foods, Center for Research in Food and Development, A.C. (Hermosillo, Sonora, Mexico). The contents of mango, carrots, and turmeric were based in reference to the Codex Alimentarius [2005] for the preparation of juices (≥45% fruit content) and for turmeric (≤0.7%). Experiments were performed in triplicate (3 separate beverages were made).

Ultrasound treatment of beverage

UT was carried out according to the method of Wei *et al*. [2014] with some modifications. An ultrasonic processor (UP400S, Hielscher, Teltow, Germany) was used for sonication. The beverage (50 mL) was processed at a constant frequency of 24 kHz. Energy input was controlled by setting the maximum amplitude at 175 μm and acoustic power density of 300 W/cm^2 of the sonicator probe (H7 Tip 7). Constant temperature of 25°C was maintained by circulating cold water through a jacketed vessel. The probe was immersed 2 cm into the beverage, and sonication started immediately. Exposure time (ET, 10–30 min), sonication amplitude (SA, 30–100%), and pulse cycles (PC, 0.4–0.8 s) varied. PC values were equal to acoustic power time in s, and the difference to 1 s as pause time (*e.g.*, 0.6 s indicates a power discharge of 0.6 s, and a pause of 0.4 s). Nine treatments (T1 to T9) were performed immediately after the beverage was prepared (Table 1). After UT, the beverages were filtered through filter paper (Whatman No. 1) under vacuum. In parallel, untreated beverages were also filtered. The filtrate was collected in a flask and used for the determination of TSP, TC, and AOC. Beverage samples (control and UT) were kept in sterilized airtight bottles and stored at 4°C until further analysis.

Experimental design

A fractional 3^{3-1} factorial design and RSM were used to establish the optimum conditions for UT. Factors were considered at different levels to determine which combination yielded the maximum TSP, TC, and AOC values. Exposure time (X_{ET}, min), pulse cycle (X_{PC}, s), and sonication amplitude (X_{SA}, %) were taken as design factors. The experimental design used, with three factors at three different levels: X_{ET} (10, 20 or 30 min), X_{PC} (0.4, 0.6 or 0.8 s), and X_{SA} (30, 65

TABLE 1. Levels of experimental design factors used to optimize ultrasound treatment of beverage from mango and carrot with added turmeric and levels of response variables: total soluble phenolic content (TSP), total carotenoid content (TC), Trolox equivalent antioxidant capacity (TEAC), and ferric reducing antioxidant power (FRAP).

Treatment	Factor			Response variable			
	X_{ET} (min)	X_{PC} (s)	X_{SA} (%)	TSP (mg GAE/mL)	TC (μg β-carotene E/mL)	TEAC (mmol TE/mL)	FRAP (mmol TE/mL)
Control	–	–	–	5.21 ± 0.11^{i}	26.78 ± 1.19^{f}	100.16 ± 1.19^{h}	0.59 ± 0.03^{g}
T 1	10	0.4	30	5.81 ± 0.06^{h}	42.87 ± 1.03^{c}	171.49 ± 3.02^{d}	0.68 ± 0.00^{e}
T 2	10	0.6	65	7.95 ± 0.03^{de}	42.09 ± 1.93^{c}	173.23 ± 2.13^{c}	0.83 ± 0.04^{cd}
T 3	10	0.8	100	8.04 ± 0.09^{d}	34.72 ± 0.69^{d}	173.85 ± 1.22^{bc}	0.90 ± 0.02^{b}
T 4	20	0.4	30	6.36 ± 0.05^{f}	43.25 ± 1.66^{c}	168.09 ± 1.31^{e}	0.62 ± 0.03^{fg}
T 5	20	0.6	65	6.17 ± 0.04^{g}	53.71 ± 1.54^{a}	161.25 ± 0.71^{g}	0.77 ± 0.03^{d}
T 6	20	0.8	100	8.79 ± 0.10^{a}	30.21 ± 0.04^{e}	195.84 ± 2.09^{a}	0.87 ± 0.01^{c}
T 7	30	0.4	30	7.41 ± 0.13^{e}	34.00 ± 1.97^{d}	176.09 ± 2.64^{b}	0.64 ± 0.02^{e}
T 8	30	0.6	65	8.28 ± 0.05^{bc}	48.87 ± 2.47^{b}	165.48 ± 2.21^{f}	0.82 ± 0.01^{cd}
T 9	30	0.8	100	8.43 ± 0.02^{b}	27.93 ± 0.84^{f}	172.32 ± 2.58^{d}	0.97 ± 0.02^{a}

Values are shown as mean ± standard deviation of three independent experiments. X_{ET}, exposure time; X_{PC}, pulse cycle; X_{SA}, sonication amplitude; GAE, gallic acid equivalents; TE, Trolox equivalents. Different letters in the same column indicate significant differences ($p<0.05$).

or 100%), is shown in Table 1. TSP (mg gallic acid equivalents (GAE)/mL), TC (μg β-carotene equivalents/mL) and AOC (mmol Trolox equivalents (TE)/mL) were defined as response variables.

To predict the behavior of response variables, the second-order polynomial equation used in the response surface was as described in equation (1) [Savasari *et al*., 2015; Yirsaw *et al*., 2016]:

$$Y = \beta_0 + \sum_{i+\Lambda}^{\mathbf{B}} \beta_i X_i + \sum_{i=\Lambda}^{B} \sum_{i=\Lambda \neq i}^{B} \beta_{ij} X_i + E \qquad (1)$$

where: Y is the predicted variable (TSP, TC or AOC), X_i represents coded values for the factors (X_{ET}, X_{PC}, and X_{SA}), β_0 is a constant, β_i is the main effect coefficient for each variable, and β_{ij} is the interaction effect coefficient. Model adequacy was evaluated using the F ratio. Lack of fit test was used to determine significant interactions in the model and the coefficient of determination (R^2 and R^2 adjusted) represented at a 5% level of significance.

Optimization and validation of conditions

The numerical optimization technique was adapted to optimize the process conditions to provide maximum TSP, TC, and AOC. The nature of the optimal condition (peak or saddle point response) was also evaluated by transforming the developed regression model into the conical form, and the values were computed using the statistical software Statistica 8.0 (StatSoft Inc., Tulsa, OK, USA). The experiment under optimal conditions was carried out in triplicate to determine the validity of the optimized parameters. The average values of the experiments were compared with the predicted values of the optimized conditions to determine the accuracy of the optimized conditions.

Extracts from the beverage preparation

An aliquot of 30 mL was taken from the beverages (control and UT), lyophilized (Labconco, model 77520 Series, Kansas City, KS, USA), and preserved at –20°C for future analyses. Extraction was performed using methanol solutions (80%, *v/v*). First, 1 g of the lyophilized material was placed in a tube and 20 mL of the solvent was added. Subsequently, it was placed for 30 min in a sonicator (Bransonic, model 2510R-DTH, Connecticut, CT, USA) and centrifuged at 18,407×*g* for 15 min at 4°C. The supernatant was recovered, the residue was washed twice with 10 mL of the same methanolic solution and centrifuged again. The combined supernatants were filtered through Whatman No. 1 paper and the volume of filtrate was adjusted to 30 mL with the 80% (*v/v*) methanolic solution. The extracts were kept at –35°C. They were later used to determine TSP, TC, Trolox equivalent antioxidant capacity (TEAC), and ferric reducing antioxidant power (FRAP).

Determination of total soluble phenolic content

The TSP was determined using the Folin-Ciocalteu method [Alvarez-Parrilla *et al*., 2011]. Briefly, 250 μL of the extract or standard solutions were mixed with 1 mL of a sodium carbonate solution (75 g/L) and 1250 μL of the Folin-Ciocalteu reagent (10%, *v/v*), and incubated for 30 min at 25°C. After reaction, the mixtures were moved to a 96-well microplate and absorbance was measured at 750 nm using a microplate reader (Synergy HT, Bio-Tek, Winooski, VT, USA). The results were calculated using a gallic acid standard curve (from 0.02 to 0.4 mg/mL), and the content of total soluble phenolics of beverage was expressed as mg of gallic acid equivalents per mL of beverage (mg GAE/mL).

Determination of total carotenoid content

The TC was measured as reported by Davis *et al*. [2007]. One milliliter of beverage was added to 5 mL of a tert-butylated hydroxytoluene solution in acetone (0.05%, *w/v*), 5 mL of 95% (*v/v*) ethanol, and 10 mL of *n*-hexane. The mixture was stirred at 180 rpm on an orbital shaker (ORBi-Shaker, Benchmark, Menlo Park, CA, USA) for 15 min; then, 3 mL of distilled water (5°C) were added to induce phase separation and recover the hydrophobic phase in which carotenoids are dissolved. The collected phase was centrifuged at 18,407×*g* for 15 min at 4°C and the absorbance of the supernatant was read at 450 nm. TC was expressed as μg β-carotene equivalents per mL of beverage (μg β-carotene E/mL) using the equation:

$$TC = \frac{(A \times V \times 10^4)}{(A_{1\,cm}^{1\%} \times w)} \tag{2}$$

where: TC is the content of total carotenoids, A is absorbance value, V is the recovered volume of the hydrophobic phase, $A_{1cm}^{1\%}$ is the specific absorbance of β-carotene (2500), and w is sample weight (g).

Determination of antioxidant capacity

The AOC of beverages was evaluated as TEAC determined by the ABTS assay and as FRAP. The method of Re *et al*. [1999] was used to carry out the ABTS assay. ABTS (7 mM) was dissolved in a 2.45 mM potassium persulfate solution and stored in the dark for 16 h to generate $ABTS^{\bullet+}$. Prior to use, the $ABTS^{\bullet+}$ solution was diluted with a phosphate buffer to an absorbance of 0.70±0.02 at 734 nm. The extract or a Trolox standard solution (20 μL) was mixed with 255 μL of the $ABTS^{\bullet+}$ solution and incubated (30°C for 7 min) in a 96-well microplate. The absorbance was measured at 734 nm using a microplate reader (Synergy HT, Bio-Tek). The Trolox curve from 0.05–1.00 mmol/g was used to calculate the results, which were expressed as mmol of Trolox equivalents per mL of beverage (mmol TE/mL).

The FRAP of beverages was determined according to the Benzie & Strain [1996] method. The FRAP solution contained 10:1:1 (*v/v/v*) sodium acetate buffer (0.3 M, pH 3.6), 10 mM TPTZ, and 20 mM ferric chloride hexahydrate. The solution was warmed to 37°C before mixing with the samples. For the reaction, 24 μL of the extract or Trolox standard were added to a 96-well microplate and mixed with 180 μL of a FRAP solution. Absorbance was measured at 595 nm after 30 min, a Trolox curve from 0.05–1.00 mmol/g was used to calculate the results, which were expressed as mmol of Trolox equivalents per mL of beverage (mmol TE/mL).

Phenolic profile analysis

The identification and quantification of phenolic compounds was carried out using HPLC with a diode array detector (DAD) and liquid chromatography-mass spectrometry (LC-MS) techniques. An Agilent 1260 series HPLC system (Agilent Technologies, Santa Clara, CA, USA) equipped with a DAD was employed for HPLC-DAD. After filtration, beverages were injected and separated using a Poroshell 120 EC-C18 column (4.6×150 mm, particle size 2.7 μm; Agilent Technologies). Injection volume was 10 μL. Mobile phase contained 0.1% (*v/v*) trifluoroacetic acid as a solvent A and acetonitrile as a solvent B, and was applied as follows: 0 min, 5% B; 10 min, 23% B; 15 min, 50% B; 20 min, 50% B; 23 min, 100% B; 25 min, 100% B; 27 min, 5% B, 30 min, 5% B. Flow rate was 0.4 mL/min. Detection was performed at 280–320 nm. In the case of curcuminoids, a range of 425––470 nm was used. For MS analysis, a 6120 Agilent Quadrupole LC/MS equipped with an electrospray ionization interface was used in a negative ionization mode. Nitrogen at a flow rate of 1.3 L/min was used as drying gas. Nebulizer pressure was 40 psi, gas drying temperature was 350°C, and capillary voltage was 3500 V. OpenLab CDS ChemStation Edition software (Agilent Technologies) was used for data analysis. The compounds were first detected using a single MS scan in the 100–1100 *m/z* range, followed by a targeted search based on the peaks showing major signals in the HPLC-DAD chromatograms. Tentative identification of the compounds was based on retention time (t_R) of HPLC-DAD separation and MS signal after comparison with the t_R of the standard and/or the literature data. The quantitative results were reported as peak areas (arbitrary units).

Statistical analysis

Data are reported as mean ± standard deviation (n=3). One-way analysis of variance (ANOVA) and Tukey's test were used to examine the differences between samples ($p<0.05$). All statistical analyses were done using the Statistica 8.0 software (Statsoft, Tulsa, OK, USA).

RESULTS AND DISCUSSION

Effect of ultrasound treatment on total soluble phenolic content

The TSP of ultrasound-treated (T1-T9) and untreated beverages are shown in Table 1. The highest TSP was noted for T6 (X_{ET} 20 min, X_{PC} 0.8 s, X_{SA} 100%), and the lowest TSP was determined for T1 (X_{ET} 10 min, X_{PC} 0.4 s, X_{SA} 30%), which were 8.79 and 5.81 mg GAE/mL, respectively. The highest value for 100% X_{SA} was in line with the literature. Nadeem *et al*. [2018] found that a sonication amplitude over 70% resulted in the highest TSP when applied to a carrot/grape beverage. Other authors reported similar relationship for different products, like blueberry, lime and mango juice, treated at high sonication amplitudes [Zou & Hou, 2017]. Statistically significant effects ($p<0.05$) and the regression coefficient of the experimental model (R^2=0.995, Table 2) suggest that the model adequately describes the functional relationship between the experimental factors and the response variable.

The determined TSP showed a high correlation with the predicted value (R^2 adjusted=0.993, Table 2). The correlation between predicted and experimental values suggests that the use of RSM allowed to accurately and reliably determine the optimum UT conditions for this variable.

Figure 1A shows the effects of beverage UT on TSP, which increased significantly at longer exposure time and higher sonication amplitudes. Thus, the highest TSP values were obtained when combining extended exposure time and maximum sonication amplitudes. On the other hand, X_{PC} was not a significant factor in the UT effect on TSP. Martinez-Guerra & Gude [2016] described a similar behavior of PC during the optimization of biodiesel production by UAE. The use of PC and continuous sonication

TABLE 2. Lineal and quadratic model equation coefficients and statistical parameters of experimental design for optimizing ultrasound treatment of beverage from mango and carrot with added turmeric. Response variables: total soluble phenolic content (TSP), total carotenoid content (TC), Trolox equivalent antioxidant capacity (TEAC) and ferric reducing antioxidant power (FRAP).

	TSP	TC	TEAC	FRAP
Intercept	-13.220*	81.633**	85.591*	0.747**
X_{ET}	2.013**	-5.803*	10.6343*	-0.026**
X_{ET}^2	-0.045**	0.095*	-0.228*	0.0005**
X_{SA}	0.820**	-2.060*	4.706**	0.005*
X_{SA}^2	-0.006**	0.017*	-0.045**	-0.00002
$X_{ET}X_{SA}$	-0.089**	0.307**	-0.597**	0.00008
$X_{ET}X_{SA}^2$	0.001**	-0.003**	0.006**	NSI
$X_{ET}^2X_{SA}$	0.002**	-0.006*	0.014**	NSI
$X_{ET}^2X_{SA}^2$	NSI	0.00005**	-0.0001**	NSI
R^2	0.995	0.975	0.965	0.972
R^2 adjusted	0.993	0.965	0.950	0.960

*$p<0.05$; **$p<0.001$; NSI, no significant interaction between factors; R^2, regression coefficient; X_{ET}, exposure time; X_{PC}, pulse cycle; X_{SA}, sonication amplitude.

for similar reaction conditions were compared. About 87% of biodiesel yield was obtained but was limited by the increase in temperature and the extraction time.

It is well-known that UT enhances the release of phenolics by collapsing the cell *via* cavitation in its surroundings [Nadeem *et al*., 2018]. Hence, higher amplitudes promote cavitation, which results in the maximum release of phenolic compounds [Maran & Priya, 2015]. In nature, phenolic compounds are bound to cellulose, hemicellulose, and pectin, which are part of the cell wall or are soluble in a vacuole. Cell walls expand with the enlargement of pores in cell membranes generated during the initial stages of cavitation, facilitating the higher diffusivity of water into the cell. Prolonged exposure of the sample to cavitation will lead to the collapse of cell walls, which results in the maximum diffusion of cell contents into the solvent, resulting in a higher extraction rate as the ultrasound amplitude increases [Maran & Priya, 2015].

Effect of ultrasound treatment on total carotenoid content

The TC of beverages treated in different conditions (T1--T9) ranged from 27.93 to 53.71 μg β-carotene E/mL (Table 1). The treatments with the highest TC were T5 (X_{ET} 20 min, X_{PC} 0.6 s, X_{SA} 65%) and T8 (X_{ET} 30 min, X_{PC} 0.6 s, X_{SA} 65%), while the lowest TC was found for T6 (X_{ET} 20 min, X_{PC} 0.8 s, X_{SA} 100%) and T9 (X_{ET} 30 min, X_{PC} 0.8 s, X_{SA} 100%). Lower values of X_{SA} (30% and 65%) resulted in a higher TC, *e.g.* X_{SA} of 30, 65, and 100% resulted in values of 42.87, 42.09, and 34.72 μg β-carotene E/mL, respectively. For TC, a high regression coefficient ($R^2=0.975$) and significant interactions (lack of fit, $p<0.05$) with the predicted model were determined (Table 2). The model showed that the significant parameters ($p<0.05$) were X_{ET} and X_{SA}, quadratic terms, linear-quadratic, and quadratic interaction. The effect of treatment parameters on TC was different to that on TSP, since applying high X_{SA} decreased TC in the treated beverages (Figure 1). This agrees with results reported by Mercado-Mercado *et al*. [2018], where UT led to decreased contents of lutein, β-carotene, and β-cryptoxanthin in mango-based beverages. Likewise, ultrasound-treated guava beverages showed a decrease in lycopene as ET and SA increased [Campoli *et al*., 2018]. The authors suggested that the decrease in TC could be explained by the effects of cavitation on their chemical structure, especially when dissolved in aqueous solutions [Campoli *et al*., 2018; Rojas *et al*., 2016]. High sonication amplitudes generate a greater number of cavitations

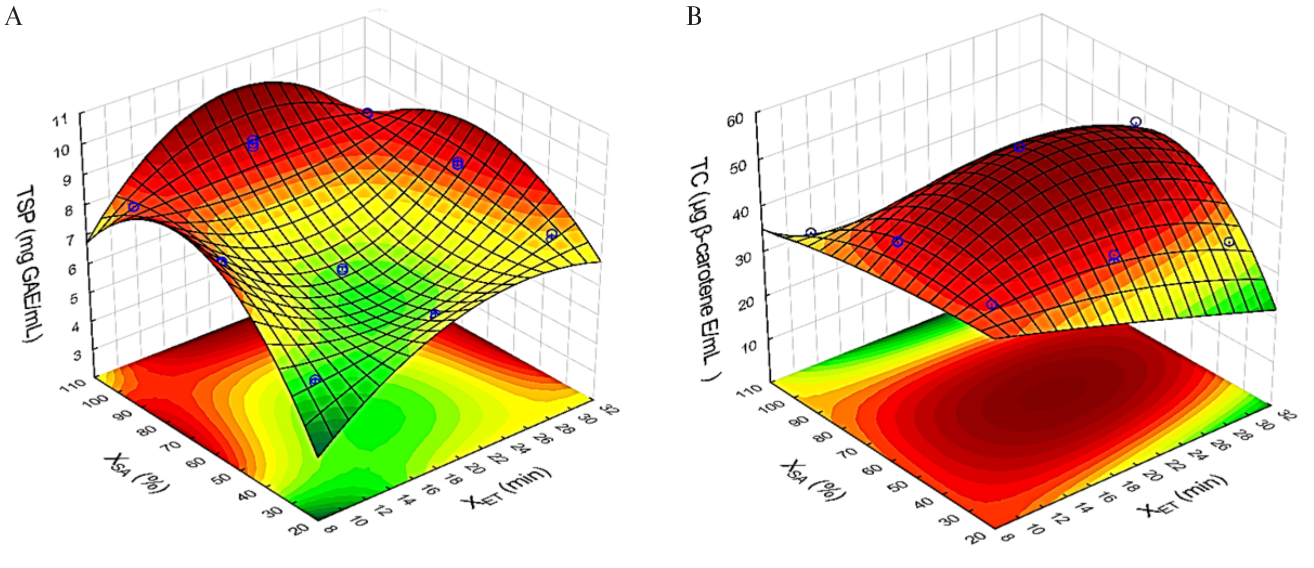

FIGURE 1. Response surface plots of optimization of ultrasound treatment of beverage from mango and carrot with added turmeric. Effect of exposure time (X_{ET}) and sonication amplitude (X_{SA}) on total soluble phenolic content (TSP) (A) and total carotenoid content (TC) (B).
Blue dots represent the experimental points. GAE, gallic acid equivalents.

TABLE 3. Predicted and experimental values of total soluble phenolic content (TSP), total carotenoid content (TC), Trolox equivalent antioxidant capacity (TEAC) and ferric reducing antioxidant power (FRAP) for optimized ultrasound treatment of beverage from mango and carrot with added turmeric.

Parameter	Predicted value	Experimental value
TSP (mg GAE/mL)*	8.81^{b}	11.48±0.33^{a}
TEAC (mmol TE/mL)*	195.31^{a}	199.38±5.10^{a}
FRAP (mmol TE/mL)*	0.87^{b}	1.5±0.06^{a}
TC (µg β-carotene E/mL)**	53.91^{a}	52.86±1.23^{a}

*For optimal ultrasound treatment parameters: 21 min of ultrasonication time at 100% sonication amplitude and 0.7 s pulse cycle. **For optimal ultrasound treatment parameters: 20 min of ultrasonication time at 65% sonication amplitude and 0.6s pulse cycle. Different letters in the same row indicate significant differences ($p<0.05$) between predicted and experimental values. GAE, gallic acid equivalent; TE, Trolox equivalent.

in the external environment, which then promote isomerization and oxidation reactions by the action of hydrogen peroxide; a highly reactive compound that is generated under UT conditions [Sun *et al*., 2017]. In contrast, treatments of medium X_{SA} conditions (65%) with intermediate and prolonged extraction times (20 or 30 min) showed the highest TC values (Table 1). The conditions in this study that maximized TC agree with the results reported by Jabbar *et al*. [2014] regarding the behavior of TC, lycopene, and β-carotene in carrot juice under different ultrasound conditions. The authors reported that when amplitudes of 70% were applied at 20 kHz, an increased content of these compounds was observed. This behavior is attributed to the fact that the sonication amplitude used does not promote isomerization reactions or any others that alter their molecular structure; consequently, the carotenoid content increased by mechanical disruption of the cell wall.

Effect of ultrasound treatment on antioxidant capacity

Figures 2A and 2B show the effects of UT on the AOC of beverage. For both, TEAC and FRAP, the maximum values were found when the operating conditions were applied at high X_{SA} (80–100%). This finding is consistent with the results shown in Table 1, which shows the highest TEAC for the beverage sonicated with an amplitude of 100% for 20 min (195.84 mmol TE/mL). On the other hand, the highest FRAP was obtained at X_{SA} of 100% and X_{ET} of 30 min (0.97 mmol TE/mL). In both cases, it is evident that exposure to 100% ultrasound amplitudes favors the increase of antioxidant capacity in the beverages subjected to ultrasound treatment. In the case of TEAC, the maximum values were obtained with exposure times close to 20 min, while two maxima are shown for FRAP, regardless of X_{ET} (Figure 2). This indicates that X_{SA} is the main parameter that governs AOC since both show proportional variation.

For TEAC, optimum operating conditions were similar to those reported by Yeoh & Ali *et al*. [2017], who applied UAE for 15 min at 70% sonication amplitude to slices of fresh pineapple, and found that these conditions yielded the highest values for this technique. Similarly, Ramírez-Moreno *et al*. [2018] reported that the optimum conditions to increase the AOC in blackberry juices were an exposure time of 15 min with a sonication amplitude of 80%, values that resemble those found in the present work. Regarding FRAP, it has been reported that substantial increases were found using amplitudes between 40 and 80% [Chaikham *et al*., 2016]. For example, an experiment performed on blackberry by-products showed that both SA and ET had a positive effect on AOC, as measured by FRAP [Romero & Yépez, 2014]. This can be explained by the fact that an increase in SA leads to more damage to the cell wall, causing compounds with antioxidant capacity to be released from the different cell structures [Hossain *et al*., 2012].

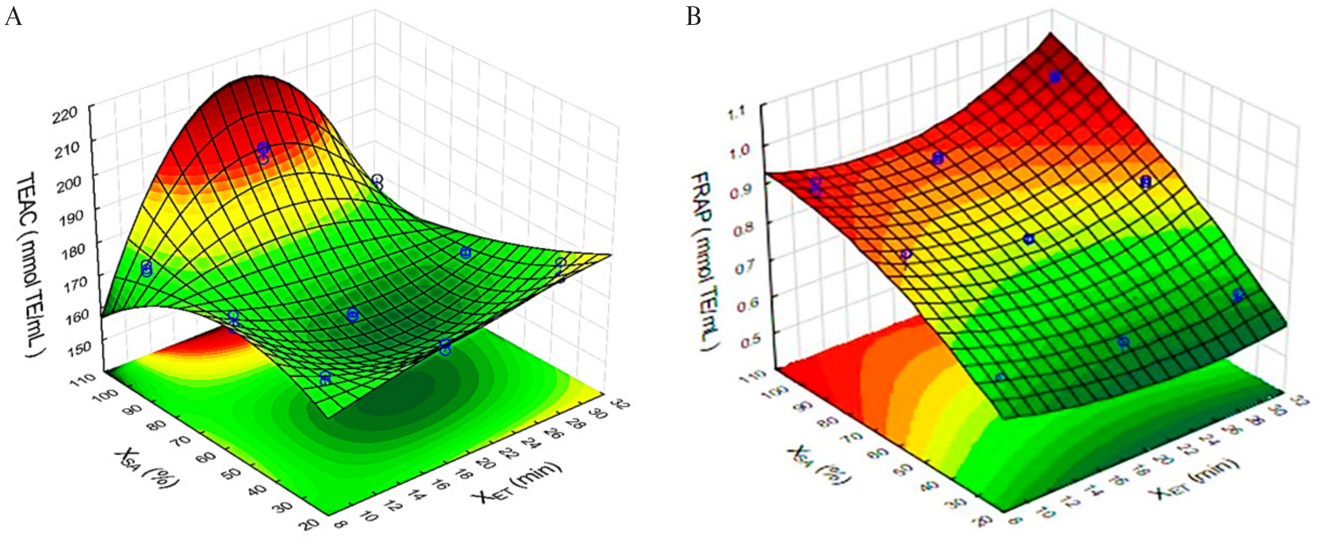

FIGURE 2. Response surface plots of optimization of ultrasound treated beverage from mango and carrot with added turmeric. Effect of exposure time (X_{ET}) and sonication amplitude (X_{SA}) on Trolox equivalent antioxidant capacity (TEAC) (A) and ferric reducing antioxidant power (FRAP) (B). Blue dots represent the experimental points. TE, Trolox equivalents.

TABLE 4. Chromatographic and mass spectrometric data, and quantification expressed as peak areas (arbitrary units) of phenolics in the control and the optimized ultrasound-treated (UT) beverages from mango and carrots with added turmeric.

Compound	Quantity		Retention time (min)	$[M-H]^-$ m/z
	Control beverage	UT beverage		
		Phenolic acids		
p-Hydroxybenzoic acid	21,626±1,399^{a}	6,041±1,347^{b}	11.99	137
3,4-Dihydroxybenzoic acid	2,492±506^{b}	7,221±487^{a}	10.23	153
Gallic acid	14,956±180^{b}	17,359±157^{a}	5.79	169
Vanillic acid	16,617±382^{a}	4,861±839^{b}	14.10	167
Chlorogenic acid	4,514,332±126,448^{b}	13,933,197±259,247^{a}	10.00	353
Ferulic acid	24,415±747^{a}	23,500±138^{a}	17.70	193
p-Coumaric acid	20,835±5,807^{a}	20,338±5,519^{a}	17.85	163
		Curcuminoids		
Curcumin	71,302±11,628^{a}	65,446±1,470^{a}	3.85	367
Demethoxycurcumin	232,359±32,115^{a}	83,260±4,260^{b}	4.23	337
Bisdemethoxycurcumin	112,036±14,018^{a}	86,724±6,911^{b}	4.19	307
		Flavonoids		
(–)-Gallocatechin	116,369±12,069^{a}	94,727±13,064^{b}	4.58	305
(–)-Gallocatechin gallate	4,712±315^{b}	7,403±447^{a}	1.20	457
(+)-Catechin	531,674±4,627^{b}	643,371±5,494^{a}	9.62	289
Kaempferol	6,683±729^{b}	22,135±2,771^{a}	21.37	285
Quercetin	20,197±4,384^{b}	84,501±1,707^{a}	20.63	301
		Xanthonoids		
Mangiferin	60,689±15,781^{b}	80,078±7,877^{a}	14.21	421

Values are expressed as mean ± standard deviation. Different letters in the same row denote significant differences ($p<0.05$).

Optimization of UT conditions and model validation

Optimization of UT conditions was performed by superimposing the contour graphs obtained from each dependent variable using the response surface. The present study performed two optimizations, one based on TSP and AOC (TEAC and FRAP) and the other based on TC. The predictive model showed that the optimal conditions for TSP and AOC were obtained by submitting the beverage to 21 min of ultrasonication at an amplitude and pulse of 100% and 0.7 s, respectively. For TC, the optimum values were 20 min at 65% amplitude and pulse of 0.6 s. The optimum values are shown in Table 3. The most favorable UT conditions were applied to the beverage to validate the proposed predictive model, and to confirm if the experimental values obtained coincide with those predicted by the mathematical model.

In the case of TSP and FRAP, it was found that the experimental values were higher than those predicted by the mathematical model. This phenomenon could be explained by the presence of other antioxidants not considered in the present work such as ascorbic acid or thiols, which were capable to disrupt the results. Nevertheless, for TC and TEAC, the predicted results matched with the experimental results obtained at optimal UT conditions, which were validated by the RSM model with a good correlation.

Identification of bioactive compounds by HPLC-DAD-MS

A total of 16 compounds (seven phenolic acids, three curcuminoids, five flavonoids and a xanthonoid) were identified in the control, as well as in the optimized UT beverages (Table 4). For phenolic acids, ultrasound treatment enhanced the quantity of 3,4-dihydroxybenzoic acid, gallic acid, and chlorogenic acid in the beverage. No significant differences were noted for the *p*-coumaric and ferulic acids between treated and control beverages, while abundance of vanillic acid and *p*-hydroxybenzoic acid decreased in the treated sample. Turmeric was the source of three curcuminoids (curcumin, demethoxycurcumin, and bisdemethoxycurcumin) detected in the control and UT beverages (Table 4). A lower quantity of curcumin, demethoxycurcumin, and bis-demethoxycurcumin was determined in the UT beverage, as compared to the control.

The five flavonoids in the UT beverage were found in the following order of quantity: (+)-catechin > (–)-gallocatechin > quercetin > kaempferol > (–)-gallocatechin gallate (Table 4). Furthermore, their contents increased with UT, except for (–)-gallocatechin, which decreased. A higher mangiferin quantity in the UT beverage than in control was also noted. The phenolic profile of the beverages agrees with those reported elsewhere for mango pulp, carrot juice, and turmeric. Gallic acid, *p*-coumaric acid, ferulic acid, vanillic acid, quercetin, (–)-gallocatechin, kaempherol, and mangiferin have been reported in mango pulp [Barrón-García *et al*., 2020; Lee *et al*., 2021; Quirós-Sauceda *et al*., 2017]. The presence of chlorogenic acid, (+)-catechin, *p*-coumaric acid, and ferulic acid was determined in carrots [Formica-Oliveira *et al*., 2017; Jabbar *et al*., 2015], while gallic acid, protocatechuic acid, (+)-catechin, chlorogenic acid, (–)-epicatechin, ferulic acid, curcumin, demethoxycurcumin, bisdemethoxycurcumin, and quercetin have been reported in turmeric [Ali *et al*., 2014; Pal *et al*., 2020].

It is known that ultrasound induces acoustic cavitation and the rupture of plant cells [Jing *et al*., 2015], which facilitates solvent penetration and increases the solubility of the solutes. Conversely, it is also possible that ultrasound treatment may degrade some compounds or promote reactions between others, which may result in a decrease in their content. Also, ruptured cells allow the release of various compounds into the solvent, such as insoluble and cytosolic substances, thereby limiting the solubility of the compounds of interest [Zhao *et al*., 2007].

CONCLUSION

In the present study, an ultrasound treatment was applied to increase contents of soluble phenolic compounds and carotenoids in a beverage from mango and carrot with added turmeric, using response surface methodology to optimize working parameters. Exposure time and sonication amplitude were shown to affect the dependent variables, while pulse cycle did not show any effect. Optimization and model validation data showed that TEAC and TC were accurately predicted by the model but TSP and FRAP were not. The data suggest that an adequately optimized ultrasound treatment of a beverage can improve its TSP. Contents of most of the individual phenolics of the beverage also increased in response to the optimized UT. Total carotenoid content changed by UT in a more variable manner; it was generally increased by the treatments, but with an evident decrease for more drastic conditions, such as longer exposure time and higher sonication amplitude.

RESEARCH FUNDING

This work was funded by Consejo Nacional de Ciencia y Tecnología (CONACYT), through Project number 563: ‘Un Enfoque Multidisciplinario de la Farmacocinética de Polifenoles de Mango Ataulfo: Interacciones Moleculares, Estudios Preclínicos y Clínicos’ and through project “De los subproductos alimenticios de vegetales a nuevos productos de valor agregado, el papel de la tecnología en la bioeconomía” (320351).

ACKNOWLEDGEMENTS

All authors thank the ALSUB-CYTED, “Red Iberoamericana de Alimentos Autóctonos Subutilizados”, network (118RT0543).

CONFLICT OF INTEREST

Authors declare no conflicts of interest.

ORCID IDs

N. Campos-Gonzalez https://orcid.org/0000-0001-9114-5800
J.A. Domínguez-Avila https://orcid.org/0000-0001-6220-1623
G.A. González-Aguilar https://orcid.org/0000-0002-7452-286X
L.X. Lopez-Martinez https://orcid.org/0000-0002-5572-5434
S. Pareek https://orcid.org/0000-0001-6873-6936
S.G. Sáyago-Ayerdi https://orcid.org/0000-0002-4430-1273
M.A. Villegas-Ochoa https://orcid.org/0000-0001-5559-1694
V.M. Zamora-Gasga https://orcid.org/0000-0002-3414-5860

REFERENCES

1. Aguilar-Hernández, G., García-Magaña, M.D.L., Vivar-Vera, M.D.L.Á., Sáyago-Ayerdi, S.G., Sánchez-Burgos, J.A., Morales-Castro, J., Anaya-Esparza, L.M., Montalvo González, E. (2019). Optimization of ultrasound-assisted extraction of phenolic compounds from *Annona muricata* by-products and pulp. *Molecules*, *24*(5), art. no. 904. https://doi.org/10.3390/molecules24050904
2. Aguilar-Hernández, G., Vivar-Vera, M.D.L.Á., García-Magaña, M.D.L., González-Silva, N., Pérez-Larios, A., Montalvo-González, E. (2020). Ultrasound-assisted extraction of total acetogenins from the soursop fruit by response surface methodology. *Molecules*, *25*(5), art. no. 1139. https://doi.org/10.3390/molecules25051139
3. Ahmad, K., Imran, M., Ahmad, T., Ahmad, M.H., Khan, M.K. (2020). Impact of ultrasound processing on physicochemical and bioactive attributes of grape based optimized fruit beverage. *Pakistan Journal of Agricultural Sciences*, *57*(4), 1117–1124. https://doi.org/10.21162/PAKJAS/20.8680
4. Ali, I., Haque, A., Saleem, K. (2014). Separation and identification of curcuminoids in turmeric powder by HPLC using phenyl column. *Analytical Methods*, *6*(8), 2526–2536. https://doi.org/10.1039/C3AY41987H
5. Alvarez-Parrilla, E., de la Rosa, L.A., Amarowicz, R., Shahidi, F. (2011). Antioxidant activity of fresh and processed Jalapeno and Serrano peppers. *Journal of Agricultural and Food Chemistry*, *59*(1), 163–173. https://doi.org/10.1021/jf103434u
6. Barrón-García, O.Y., Morales-Sánchez, E., Jiménez, A.R., Antunes-Ricardo, M., Luzardo-Ocampo, I., González-Jasso, E., Gaytán-Martínez, M. (2022). Phenolic compounds profile and antioxidant capacity of ‘Ataulfo’ mango pulp processed by ohmic heating at moderate electric field strength. *Food Research International*, *154*, art. no. 111032. https://doi.org/10.1016/j.foodres.2022.111032
7. Benzie, I.F., Strain, J.J. (1996). The ferric reducing ability of plasma (FRAP) as a measure of “antioxidant power”: The FRAP assay. *Analytical Biochemistry*, *239*(1), 70–76. https://doi.org/10.1006/abio.1996.0292
8. Bhardwaj, R.L., Pandey, S. (2011). Juice blends — a way of utilization of under-utilized fruits, vegetables, and spices a review. *Critical Reviews in Food Science and Nutrition*, *51*(6), 563–570. https://doi.org/10.1080/10408391003710654

9. Campoli, S.S., Rojas, M.L., do Amaral, J.E.P.G., Canniatti-Brazaca, S.G., Augusto, P.E.D. (2018). Ultrasound processing of guava juice: Effect on structure, physical properties and lycopene *in vitro* accessibility. *Food Chemistry*, *268*, 594–601. https://doi.org/10.1016/j.foodchem.2018.06.127
10. Chaikham, P., Kemsawasd, V., Apichartsrangkoon, A. (2016). Effects of conventional and ultrasound treatments on physicochemical properties and antioxidant capacity of floral honeys from Northern Thailand. *Food Bioscience*, *15*, 19–26. https://doi.org/10.1016/j.fbio.2016.04.002
11. Codex Alimentarius (2005). "Norma general del codex para zumos (jugos) y néctares de frutas." Codex Stan, *247*, 21.
12. Davis, A.R., Collins, J., Fish, W.W., Tadmor, Y., Webber III, C.L., Perkins-Veazie, P. (2007). Rapid method for total carotenoid detection in canary yellow-fleshed watermelon. *Journal of Food Science*, *72*(5), S319-S323. https://doi.org/10.1111/j.1750–3841.2007.00381.x
13. Deogade, S.C., Ghate, S. (2015). Curcumin: therapeutic applications in systemic and oral health. *International Journal of Biological and Pharmaceutical Research*, *6*(4), 281–90.
14. Formica-Oliveira, A.C., Martínez-Hernández, G.B., Díaz-López, V., Artés, F., Artés-Hernández, F. (2017). Effects of UV-B and UV-C combination on phenolic compounds biosynthesis in fresh-cut carrots. *Postharvest Biology and Technology*, *127*, 99–104. https://doi.org/10.1016/j.postharvbio.2016.12.010
15. Fujiki, H., Sueoka, E., Rawangkan, A., Suganuma, M. (2017). Human cancer stem cells are a target for cancer prevention using (−)-epigallocatechin gallate. *Journal of Cancer Research and Clinical Oncology*, *143*(12), 2401–2412. https://doi.org/10.1007/s00432–017–2515–2
16. Hasheminya, S.M., Dehghannya, J. (2022). Non-thermal processing of black carrot juice using ultrasound: Intensification of bioactive compounds and microbiological quality. *International Journal of Food Science & Technology*. https://doi.org/10.1111/ijfs.15901
17. Hossain, M.B., Brunton, N.P., Patras, A., Tiwari, B., O Donnell, C.P., Martin-Diana, A.B., Barry-Ryan, C. (2012). Optimization of ultrasound assisted extraction of antioxidant compounds from marjoram (*Origanum majorana* L.) using response surface methodology. *Ultrasonics Sonochemistry*, *19*(3), 582–590. https://doi.org/10.1016/j.ultsonch.2011.11.001
18. Jabbar, S., Abid, M., Hu, B., Muhammad Hashim, M., Saeeduddin, M., Lei, S., Wu, T., Zeng, X. (2014). Influence of sonication and high hydrostatic pressure on the quality of carrot juice. *Journal of Food Science & Technology*, *49*(11), 2449–2457. https://doi.org/10.1111/ijfs.12567
19. Jabbar, S., Abid, M., Wu, T., Hashim, M.M., Saeeduddin, M., Hu, B., Lei, S., Zeng, X. (2015). Ultrasound-assisted extraction of bioactive compounds and antioxidants from carrot pomace: A response surface approach. *Journal of Food Processing and Preservation*, *39*(6), 1878–1888. https://doi.org/10.1111/jfpp.12425
20. Jing, C.L., Dong, X.F., Tong, J.M. (2015). Optimization of ultrasonic-assisted extraction of flavonoid compounds and antioxidants from alfalfa using response surface method. *Molecules*, *20*(9), 15550–15571. https://doi.org/10.3390/molecules200915550
21. Lee, F.Y., Vo, G.T., Barrow, C.J., Dunshea, F.R., Suleria, H.A. (2021). Mango rejects and mango waste: Characterization and quantification of phenolic compounds and their antioxidant potential. *Journal of Food Processing and Preservation*, *45*(7), art. no. e15618. https://doi.org/10.1111/jfpp.15618
22. Manna, P., Gyasuddin, M., Manna, P. (2017). Development and quality evaluation of vegetable juice blend with coconut milk. *International Journal of Scientific & Engineering Research, 8*(7), 1871–1874.
23. Mercado-Mercado, G., López Teros, V., Montalvo-González, E., González-Aguilar, G.A., Álvarez-Parrilla, E., Sáyago-Ayerdi, S.G. (2018). Effect of ultrasound-assisted extraction on the release and *in vitro* bioaccessibility of carotenoids in mango (*Mangifera indica* L.) "Ataulfo"-based beverages. *Nova Scientia*, *10*(20), 100–132. https://doi.org/10.21640/ns.v10i20.1277
24. Martinez-Guerra, E., Gude, V.G. (2016). Determining optimum pulse mode for ultrasound enhanced biodiesel production. *Journal of Industrial and Engineering Chemistry*, *35*, 14–19. https://doi.org/10.1016/j.jiec.2016.01.004
25. Maran, J.P., Priya, B. (2015). Ultrasound-assisted extraction of pectin from sisal waste. *Carbohydrate Polymers*, *115*, 732–738. https://doi.org/10.1016/j.carbpol.2014.07.058
26. Nadeem, M., Ubaid, N., Qureshi, T.M., Munir, M., Mehmood, A. (2018). Effect of ultrasound and chemical treatment on total phenol, flavonoids and antioxidant properties on carrot-grape juice blend during storage. *Ultrasonics Sonochemistry*, *45*, 1–6. https://doi.org/10.1016/j.ultsonch.2018.02.034
27. Nolasco-González, Y., Chacón-López, M.A., Ortiz-Basurto, R.I., Aguilera-Aguirre, S., González-Aguilar, G.A., Rodríguez-Aguayo, C., Navarro-Cortez, M.C., Garcia-Galindo, H.S., Garcia-Magana de Lourdes, M., Meza-Espinoza, L., Montalvo-González, E. (2022). *Annona muricata* leaves as a source of bioactive compounds: Extraction and quantification using ultrasound. *Horticulturae*, *8*(7), art. no. 560. https://doi.org/10.3390/horticulturae8070560
28. Ordóñez-Santos, L.E., Martínez-Girón, J., Arias-Jaramillo, M.E. (2017). Effect of ultrasound treatment on visual color, vitamin C, total phenols, and carotenoids content in Cape gooseberry juice. *Food Chemistry*, *233*, 96–100. https://doi.org/10.1016/j.foodchem.2017.04.114
29. Pacheco-Ordaz, R., Antunes-Ricardo, M., Gutiérrez-Uribe, J.A., González-Aguilar, G.A. (2018). Intestinal permeability and cellular antioxidant activity of phenolic compounds from mango (*Mangifera indica* cv. Ataulfo) peels. *International Journal of Molecular Sciences*, *19*(2), art. no. 514. https://doi.org/10.3390/ijms19020514
30. Pal, K., Chowdhury, S., Dutta, S.K., Chakraborty, S., Chakraborty, M., Pandit, G.K., Dutta, S., Paul, P.K., Choudhury, A., Majumder, B., Sahana, N., Mandal, S. (2020). Analysis of rhizome colour content, bioactive compound profiling and ex-situ conservation of turmeric genotypes (*Curcuma longa* L.) from sub-Himalayan terai region of India. *Industrial Crops and Products*, *150*, art. no. 112401. https://doi.org/10.1016/j.indcrop.2020.112401
31. Palafox-Carlos, H., Yahia, E.M., González-Aguilar, G.A. (2012). Identification and quantification of major phenolic compounds from mango (*Mangifera indica*, cv. Ataulfo) fruit by HPLC-DAD-MS/MS-ESI and their individual contribution to the antioxidant activity during ripening. *Food Chemistry*, *135*(1), 105–111. https://doi.org/10.1016/j.foodchem.2012.04.103

32. Quirós-Sauceda, A.E., Chen, C.Y.O., Blumberg, J.B., Astiazaran-Garcia, H., Wall-Medrano, A., González-Aguilar, G.A. (2017). Processing 'ataulfo' mango into juice preserves the bioavailability and antioxidant capacity of its phenolic compounds. *Nutrients*, *9*(10), art. no. 1082.
https://doi.org/10.3390/nu9101082
33. Ramírez-Moreno, E., Zafra-Rojas, Q.Y., Arias-Rico, J., Ariza-Ortega, J.A., Alanís-García, E., Cruz-Cansino, N. (2018). Effect of ultrasound on microbiological load and antioxidant properties of blackberry juice. *Journal of Food Processing and Preservation*, *42*(2), art. no. e13489.
https://doi.org/10.1111/jfpp.13489
34. Re, R., Pellegrini, N., Proteggente, A., Pannala, A., Yang, M., Rice-Evans, C. (1999). Antioxidant activity applying an improved ABTS radical cation decolorization assay. *Free Radical Biology and Medicine*, *26*(9–10), 1231–1237.
https://doi.org/10.1016/S0891–5849(98)00315–3
35. Romero, J.C., Yépez, V.B. (2014). Ultrasound as pretreatment to convective drying of Andean blackberry (*Rubus glaucus* Benth). *Ultrasonics Sonochemistry*, *22*, 205–210.
https://doi.org/10.1016/j.ultsonch.2014.06.011
36. Rojas, M.L., Leite, T.S., Cristianini, M., Alvim, I.D., Augusto, P.E. (2016). Peach juice processed by the ultrasound technology: Changes in its microstructure improve its physical properties and stability. *Food Research International*, *82*, 22–33.
https://doi.org/10.1016/j.foodres.2016.01.011
37. Saeeduddin, M., Abid, M., Jabbar, S., Hu, B., Hashim, M.M., Khan, M.A., Xie, M., Wu, T., Zeng, X. (2016). Physicochemical parameters, bioactive compounds and microbial quality of sonicated pear juice. *International Journal of Food Science & Technology*, *51*(7), 1552–1559.
https://doi.org/10.1111/ijfs.13124
38. Savasari, M., Emadi, M., Bahmanyar, M.A., Biparva, P. (2015). Optimization of Cd (II) removal from aqueous solution by ascorbic acid-stabilized zero valent iron nanoparticles using response surface methodology. *Journal of Industrial and Engineering Chemistry*, *21*, 1403–1409.
https://doi.org/10.1016/j.jiec.2014.06.014
39. Šeregelj, V., Vulić, J., Ćetković, G., Čanadanović-Brunet, J., Šaponjac, V.T., Stajčić, S. (2020). Natural bioactive compounds in carrot waste for food applications and health benefits. *Studies in Natural Products Chemistry*, *67*, 307–344.
https://doi.org/10.1016/B978–0–12–819483–6.00009–6
40. Sun, J., Li, X., Lin, X., Mei, Z., Li, Y., Ding, L., Bai, W. (2017). Sonodegradation of cyanidin-3-glucosylrutinoside: degradation kinetic analysis and its impact on antioxidant capacity *in vitro. Journal of the Science of Food and Agriculture*, *97*(5), 1475–1481.
https://doi.org/10.1002/jsfa.7887
41. Wei, S.D., Chen, H., Yan, T., Lin, Y.M., Zhou, H.C. (2014). Identification of antioxidant components and fatty acid profiles of the leaves and fruits from *Averrhoa carambola*. *LWT – Food Science and Technology*, *55*(1), 278–285.
https://doi.org/10.1016/j.lwt.2013.08.013
42. Wu, T., Lv, H., Wang, F., Wang, Y. (2016). Characterization of polyphenols from *Lycium ruthenicum* fruit by UPLC-Q-TOF/MSE and their antioxidant activity in Caco-2 cells. *Journal of Agricultural and Food Chemistry*, *64*(11), 2280–2288.
https://doi.org/10.1021/acs.jafc.6b00035
43. Yeoh, W.K., Ali, A. (2017). Ultrasound treatment on phenolic metabolism and antioxidant capacity of fresh-cut pineapple during cold storage. *Food Chemistry*, *216*, 247–253.
https://doi.org/10.1016/j.foodchem.2016.07.074
44. Yıkmış, S. (2020). Sensory, physicochemical, microbiological and bioactive properties of red watermelon juice and yellow watermelon juice after ultrasound treatment. *Journal of Food Measurement and Characterization*, *14*(3), 1417–1426.
https://doi.org/10.1007/s11694-020-00391-7
45. Yirsaw, B.D., Megharaj, M., Chen, Z., Naidu, R. (2016). Reduction of hexavalent chromium by green synthesized nano zero valent iron and process optimization using response surface methodology. *Environmental Technology & Innovation*, *5*, 136–147.
https://doi.org/10.1016/j.eti.2016.01.005
46. Zhao, C.L., Chen, Z.J., Bai, X.S., Ding, C., Long, T.J., Wei, F.G., Miao, K.R. (2014). Structure-activity relationships of anthocyanidin glycosylation. *Molecular Diversity*, *18*(3), 687–700.
https://doi.org/10.1007/s11030-014-9520-z
47. Zhao, S., Kwok, K.C., Liang, H. (2007). Investigation on ultrasound assisted extraction of saikosaponins from *Radix Bupleuri*. *Separation and Purification Technology*, *55*(3), 307–312.
https://doi.org/10.1016/j.seppur.2006.12.002.
48. Zhou, B., Yi, H., Tan, J., Wu, Y., Liu, G., Qiu, Z. (2015). Anti-proliferative effects of polyphenols from pomegranate rind (*Punica granatum* L.) on EJ bladder cancer cells *via* regulation of p53/miR-34a Axis. *Phytotherapy Research*, *29*(3), 415–422.
https://doi.org/10.1002/ptr.5267
49. Zou, Y., Hou, X. (2017). Sonication enhances quality and antioxidant activity of blueberry juice. *Food Science and Technology*, 37(4), 599–603.
https://doi.org/10.1590/1678-457x.27816

Pol. J. Food Nutr. Sci., 2022, Vol. 72, No. 3, pp. 297–304
On-line ISSN: 2083-6007
Print ISSN: 1230-0322
DOI: 10.31883/pjfns/152677
http://journal.pan.olsztyn.pl

Original article
Section: Food Quality and Functionality

Characteristic and Antimicrobial Resistance of *Bacillus cereus* Group Isolated from Food in Poland

Joanna Kowalska, Elżbieta Maćkiw, Dorota Korsak, Jacek Postupolski*

*Laboratory of Food Microbiology, Department of Food Safety, National Institute of Public Health
NIH – National Research Institute, 24 Chocimska str, 00–791 Warsaw, Poland*

Key words: pastry, food safety, toxin, retail food, food control

Bacillus cereus is a foodborne pathogen causing food safety issues due to the formation of difficult to eliminate spores and biofilms. The objective of this study was to investigate the occurrence of *B. cereus* (conducted as part of monitoring in 2017–2018) and the presence of a toxin gene in strains isolated from retail products (pastries/cakes; vegetables, spices, delicatessen products) in Poland, and to determine the susceptibility of these microorganisms to different antimicrobial agents. A total of 267 *B. cereus* isolates from food products were examined, of which 95.51% were found positive for the presence of at least one toxin gene, with the highest frequency of the *nhe* gene (91.39%). The *hbl* and *cytK* genes were detected in 53.56% and 44.19% of *B. cereus* strains, respectively. The lowest frequency was found for the *ces* gene (2.62%). The susceptibility of *B. cereus* isolates to 16 antimicrobials was investigated. Ampicillin and penicillin resistance was the most common resistance phenotype and was identified in 100% of the *B. cereus* isolates. In addition, the tested isolates exhibited resistance to: amoxicillin-clavulanic acid (96.25%), cephalothin (67.79%), ceftriaxone (64.42%), rifampicin (46.82%), trimethoprim-sulfamethoxazole (5.62%), quinupristin/dalfopristin (4.87%), chloramphenicol (3.75%), clindamycin (2.62%), teicoplanin (1.87%), erythromycin (1.87%), ciprofloxacin (0.75%), imipenem (0.75%), tetracycline (0.37%), and gentamicin (0.37%). The study results contribute to characterizing the diversity of *B. cereus* isolated from various food products in Poland and their impact on food safety and public health. This study delivers practical information on antibiotic resistance and the frequency of toxin genes among strains isolated from food.

INTRODUCTION

Bacteria from the *Bacillus cereus* group (or *Bacillus cereus sensu lato*) are aerobic or facultative anaerobic rod-shaped Gram-positive, endospore forming bacteria widespread in the environment [Drobniewski, 1993; Messelhäußer & Ehling-Schulz, 2018]. The group includes at least nine species: *B. cereus sensu stricto, B. thuringiensis*, *B. weihenstephanensis*, *B. mycoides*, *B. pseudomycoides*, *B. anthracis*, *B. toyonensis*, *B. widmanni*, and *B. cytotoxicus* [Ehling-Schulz *et al.*, 2019]. The *Bacillus* species share similar rDNA, high degrees of DNA-DNA relatedness and 16S-23S rDNA intergenic spacers [Hansen *et al.,* 2001; Priest *et al.*, 1994]. The high prevalence of the *B. cereus* group in soil, air, and water, as well as spore production pose problems in the food processing industry [Faille *et al.*, 2007; Rossi *et al.*, 2018]. The primary source of contamination is the soil which contains from 10^2 to 10^7 colony-forming units (CFU) of vegetative cells and spores of *B. cereus* in 1 g [Raymond *et al.*, 2010; Brillard *et al.*, 2015].

The *B. cereus* group poses the risk of two types of gastrointestinal diseases – the diarrhoeal and the emetic syndrome [Carlin *et al.*, 2006; Gdoura-Ben *et al.,* 2018; Rodrigo *et al.*, 2021]. The diarrhoeal syndrome is caused by enterotoxin haemolysin BL (Hbl), non-hemolytic (Nhl) and protein cytotoxin K (CytK) produced after ingestion of viable cells or spores. The emetic syndrome is caused by cereulide produced in food before ingestion. In the case of the diarrheal syndrome, *B. cereus* produces toxins in the gastrointestinal tract, while in the case of the emetic toxin, the induction of disease symptoms is related to the presence of a toxin produced in food, and the presence of *B. cereus* cells is not required.

Hbl is a thermostable enterotoxin. Haemolysin consists of three components: binding protein B (37 kDa) encoded by the *hblA*, and lytic components: L1 (38 kDa) encoded by *hblC* and L2 (46 kDa) encoded by *hblD* [Ehling-Schulz *et al.*, 2006]. The non-haemolytic enterotoxin Nhe toxin comprises three components: NheA – 41 kDa, NheB – 39 kDa, NheC – 105 kDa coded, respectively, by the *nheA*, *nheB*, and *nheC* genes [Dietrich *et al.,* 2021; Lindbäck *et al.*, 2004]. Poisonings caused by *B. cereus* strains capable of producing Nhe and Hbl toxins are manifested by watery diarrhoea and abdominal pain, which appear from 8 to 16 h after ingestion of contaminated food [Ehling-Schulz *et al.*, 2019; Schoeni & Wong, 2005]. Protein CytK (34 kDa) has the capability to form pores in lipid bilayers. Moreover, it has been shown that CytK is highly toxic towards human intestinal

---

* Corresponding Author:
Tel.: +48 22 54 21 381; Fax: +48 22 54 21 392;
E-mail: jkowalska@pzh.gov.pl (J. Kowalska)

Submitted: 11 May 2022
Accepted: 8 August 2022
Published on-line: 2 September 2022

epithelial cells and can be responsible for severe food poisoning and also for necrotic enteritis [Hardy *et al.*, 2001]. The diarrhoea syndrome is frequently associated with the consumption of contaminated foods such as dairy products (*e.g.* puddings, raw and pasteurized milk) [EFSA, 2016; Gdoura-Ben *et al.*, 2018; Zhao *et al.*, 2020], soups, meat products [EFSA, 2016; Gdoura-Ben *et al.*, 2018], stews [Borge *et al.*, 2001; Shah *et al.,* 2019], sauces and vegetables [EFSA, 2016; Gdoura-Ben *et al.*, 2018]. The other sources of these bacteria include flour [EFSA, 2016; N'guessan *et al.*, 2019], pasta [EFSA, 2016; Gdoura-Ben *et al.*, 2018; Juneja *et al.*, 2019], confectionery (cakes) [EFSA, 2016], seafood [EFSA, 2016; Gdoura-Ben *et al.*, 2018], herbs and spices [EFSA, 2016; Gdoura-Ben *et al.*, 2018].

The emetic form of food poisoning involving *B. cereus* is the result of intoxication with emetic toxin (cereulide) [Marxen *et al.*, 2015]. Cereulide is one of the most resistant (heat-stable and acid-resistant) enterotoxins that stays active after being subjected to the temperature of 121°C for 90 min and at pH 2–11 for 2 h [Rajkovic *et al.*, 2008; Rouzeau-Szynalski *et al.,* 2020]. The amount of produced cereulide is related to the conditions of microbial growth, pH, temperature, and oxygen availability [Rouzeau-Szynalski *et al.,* 2020]. The optimal temperature for toxin formation is 21°C [Berthold & Doroszkiewicz, 2009]. However, significantly reduced cereulide production is observed at 8–10°C and above 35°C. The presence of oxygen in the environment significantly increases the amount of toxin formed. Characteristic symptoms of intoxication, *i.e.* nausea and vomiting, are observed 30 min to 6 h after ingestion of toxin-contaminated foodstuffs [Ehling-Schulz *et al.*, 2005; Glasset *et al.*, 2016]. Cereulide is found in food products, including pasta, rice, milk, and dairy products [Rouzeau-Szynalski *et al.,* 2020]. Symptoms may persist for about 24 h [Li *et al.,* 2021]. They often resemble poisoning with staphylococcal enterotoxin. Poisoning can lead to acute liver failure, haemolytic uremic syndrome, cerebral oedema or even death. The vomiting dose is 0.02–1.28 μg cereulide. The toxic dose for an adult human is 400–500 μg cereulide [Berthold & Doroszkiewicz, 2009]. Symptoms persist for 6 to 24 h after food intake, reminiscent of staphylococcal enterotoxin poisoning.

Most cases of foodborne outbreaks caused by the *B. cereus* group have been associated with concentrations exceeding 10^5 CFU/g. However, there have been cases of emetic and diarrhoeal illness reporting levels of *B. cereus* (10^3 and 10^5 CFU/g) [EFSA, 2016].

The objective of this study was to investigate the occurrence of *B. cereus* (conducted as part of monitoring in 2017–2018) and the presence of toxin genes in strains isolated from retail products (pastries/cakes; vegetables, spices, delicatessen products), and to determine the susceptibility of these microorganisms to different antimicrobial agents.

MATERIALS AND METHODS

Collection of samples and selection of isolates

The food samples were collected from 2004 to 2018 as part of the official control and monitoring program in Poland. The samples were examined at the microbiological laboratory of Provincial Sanitary and Epidemiological Stations using the method specified in PN EN ISO 7932:2005, accredited by the Polish Centre of Accreditation. In short, 10 g of each food sample was taken in an aseptic manner and homogenized in 90 mL of buffered peptone water (BPW, Biomaxima, Lublin, Poland). An aliquot of 0.1 mL of the initial suspension and further decimal dilution were transferred to mannitol egg yolk polymyxin agar plates (MYP Agar, Oxoid, Basingstoke, United Kingdom). After incubation for 24 – 48 h at 30°C, typical colonies were counted and then subjected to the haemolysis reaction test. In total, 267 *B. cereus* strains analysed in this study were collected in the years: 2004 – 11 strains; 2005 – 3; 2006 – 15; 2007 – 17; 2008 – 12; 2009 – 7; 2010 – 9; 2011 – 2; 2012 – 15; 2013 – 24; 2014 – 15; 2016 – 3; 2017 – 57; 2018 – 77. Strains isolated from the following food groups: heat-treated pastries, or non-heat-treated cream (240), delicatessen products (24), vegetables (2), and spices (1) (Supplementary Table S1), were sent to our laboratory, *i.e.*, the National Institute of Public Health NIH – National Research Institute, for further studies. Strains were recovered from −80°C brain heart infusion broth (BHI, Oxoid) with 20% glycerol (Merck, Darmstadt, Germany) into plate count agar (PCA, Biomaxima) and stored at 4°C.

Extraction of DNA from *B. cereus* group strains

The genomic DNA was extracted from *B. cereus* cells using the Chelex-100 resin-based technique (Bio-Rad, Hercules, CA, USA). Single colonies grown on plate count agar (PCA, Bio-Rad) were suspended in 100 μL of a 5% chelating resin solution. Bacterial cells were suspended with the use of a sterile loop in a Chelex solution, incubated at 99°C for 15 min. Suspensions were cooled on ice for 2 min and centrifuged at 16,162×*g* at room temperature for 2–3 min. The DNA-containing supernatant was used as a template for the molecular analysis.

PCR AMPLIFICATION OF 16S rDNA

PCR amplification of 16S rDNA for the detection of *B. cereus* strains was performed according to the procedure described by Hansen *et al.* [2001] with modifications. The following oligonucleotides were used: 5'-TCG AAA TTG AAA GGC GGC-3', 5'-GGT GCC AGC TTA TTC AAC-3' (Genomed, Warsaw, Poland). The final 25 μL of the PCR mixture contained a 2.5 μL DreamTaq buffer (10× concentrated, Thermo Fisher Scientific, Waltham, MA, USA), 3.75 μL of a dNTPs mix (2 mM, Thermo Fisher Scientific), 1 μL of $MgCl_2$ (1.25 mM, Thermo Fisher Scientific), 1 μL of each primer (10 μM), 0.25 μL of DreamTaq polymerase (1U, Thermo Fisher Scientific), 1 μL of DNA and water for molecular biology tests (Bio-Rad). The PCR was performed under the following conditions: 95°C–10 min, 30× (94°C–15 s, 63°C–45 s, 72°C–2 min), 72°C–2 min. Amplified PCR products were analysed on 1.5% (*w/v*) agarose gel (Prona, Narew, Poland) in a Tris-borate-ethylenediaminetetraacetic acid (TBE) buffer (1×) containing 0.15 μg/mL of Midori Green Advance DNA Stain (Genetics, Düren, Germany). Gels were run at 120 V for 1 h and photographed with a digital camera.

A GeneRuler™ 100 bp DNA Ladder (Thermo Fisher Scientific) was used as a molecular weight marker. The expected PCR product size was 288 bp. Affiliation to the *B. cereus* group by 16S rDNA amplification reaction was confirmed for all the analysed strains.

B. cereus toxin identification using multiplex PCR

The PCR amplification of *nhe*, *hbl*, *cytK* and *ces* toxin genes was carried out according to the procedure described by Ehling-Schultz *et al.* [2006] with modifications in primers and $MgCl_2$ concentration. Primers synthesized by Genomed (Poland) were used (Table 1). The final 25 μL reaction mixtures contained 0.6 μL of a mix of oligonucleotide primers: cesR (100 mM), cesF (100 mM), nheR (150 mM), nheF (150 mM), cytKF (200 mM), cytKR (200 mM), hblF (500 mM), hblR (500 mM); 2.5 μL of a DreamTaq buffer (10× concentrated, Thermo Fisher Scientific); 2.5 μL of a dNTP mix (2 mM, Thermo Fisher Scientific); 1 μL of $MgCl_2$ (1.25 mM, Thermo Fisher Scientific); 0.25 μL of the DreamTaq polymerase (5U, Thermo Fisher Scientific); 1 μL of template DNA; and water for molecular biology tests (Bio-Rad). Reaction conditions were as follows: 95°C–15 min, 30× (95°C–30 s, 49°C–30 s, 72°C–1 min), 72°C–2 min. Amplified PCR products were analysed on 1.5% (*w/v*) agarose gel (Prona) in a TBE buffer (1×) containing 0.15 μg/mL of Midori Green Advance DNA Stain (Genetics). A GeneRuler™ 1 kb DNA Ladder (Thermo Fisher Scientific) and GeneRuler™ 100 bp DNA Ladder (Thermo Fisher Scientific) were used as molecular weight markers. Gels were run at 120 V for 1 h and photographed with a digital camera. The expected PCR products size was: *ces* 1271 bp, *hbl* 1091 bp, *nhe* 766 bp, and *cytK* 421 bp (Table 1).

Antimicrobial susceptibility testing

Antibiotic susceptibility was assessed using the disc diffusion method. The test inoculum was prepared from colonies grown on PCA plates (Biomerieux, Marcy-l'Étoile, France) that had been incubated at 35°C for 18 h. Colonies were suspended in a 0.9% saline solution (Polpharma, Starogard Gdański, Poland) to obtain a suspension equivalent to the turbidity of a 0.5 McFarland standard. The cell suspension was used to swab the surface of a Mueller-Hinton agar plate (GRASO, Starogard Gdański, Poland). Discs with the following concentration of antibiotics (Oxoid) were used: penicillin G (10U), ampicillin (10 μg), cephalothin (30 μg), imipenem (10 μg), gentamicin (10 μg), chloramphenicol (30 μg), erythromycin (15 μg), tetracycline (30 μg), ciprofloxacin (5 μg), clindamycin (2 μg), sulfamethoxazole-trimethoprim (25 μg), rifampin (5 μg), ceftriaxone (30 μg), teicoplanin (30 μg), amoxicillin-clavulanic acid (30 μg), and quinupristin/dalfopristin (15 μg). The inhibition zones were measured after 20 h of incubation at 35°C. All strains were classified as sensitive, of intermediate susceptibility and resistant, following the recommendations for *Staphylococcus* spp. in the Clinical and Laboratory Standards Institute guideline M100-S22–2 [CLSI, 2012]. *Staphylococcus aureus* ATCC 25923 was used for quality control.

RESULTS AND DISCUSSION

B. cereus is mainly isolated from dairy-based and flour-based products. In Poland, the presence of the presumptive *B. cereus* group is officially monitored mainly in 2 categories of food products: (a) confectionery products and products with uncooked cream, and (b) confectionery products and products with heat-treated cream which are a milk-flour-based product. The remaining reporting cases concern food indicated in consumer notifications and potential sources related to the occurrence of food poisoning.

In the years 2017–2018, the microbiological laboratory of Provincial Sanitary and Epidemiological Stations tested a total of 21,200 food samples as part of a monitoring scheme and isolated 598 presumptive *B. cereus* strains. The percentage of samples in which presumptive *B. cereus* occurred was found to be low: 2.57% in the year 2017 and 3.07% in 2018. A high level of milk-based desserts contamination with *B. cereus* of was determined in a study by Amin *et al*. [2018], *i.e.* 45% of the 150 samples tested (pudding, custard, rice with milk). What is more, research conducted by Organji *et al*. [2015] showed a high percentage of contamination of raw milk. A total of 110 samples was screened for the presence of *B. cereus* and 31.8% of the samples yielded *Bacillus*-like growth. Among them, 54.28% of the samples were *B. cereus*-positive. In recent years, other research has been conducted in Poland on *B. cereus* prevalence in other food products. Berthold-Pluta

TABLE 1. Primers used in the multiplex PCR for the detection of virulence genes in *Bacillus cereus* group.

Targeted gene	Primer name	Sequence (5'–3')	Product size (bp)
hbl	hblF	GTA AAT TAI GAT GAI CAA TTTC	1091
	hblR	AGA ATA GGC ATT CAT AGA TT	
nhe	nheF	AAG CIG CTC TTC GIA TTC	766
	nheR	ITI GTT GAA ATA AGC TGT GG	
cytK	cytKF	ACA GAT ATC GGI CAA AAT GC	421
	cytKR	CAA GTI ACT TGA CCI GTT GC	
ces	cesF	GGT GAC ACA TTA TCA TAT AAG GTG	1271
	cesR	GTA AGC GAA CCT GTC RGR AAC AAC A	

et al. [2019] tested samples of herbs and spices, pasta, rice, breakfast cereals, infant formulas, pasteurized milk, fresh acid and acid/rennet cheeses, mould-ripened cheeses and ripening rennet cheeses. Test results of 585 samples showed that 38.8% were contaminated by *B. cereus*. Moreover, the study carried out in Tunisia revealed a high level of food contamination by *B. cereus* [Gdoura-Ben *et al.,* 2018], where 27.8% of the 687 food samples tested (spices, cereals, cooked food, fresh-cut vegetables, canned, seafood, raw and cooked poultry meats, pastry and dairy products) were found to be contaminated. When analysing 515 samples of dairy products, Proroga *et al.* [2019] found 26.8% of them to be contaminated with *B. cereus.* Similar results were obtained by Kong *et al*. [2021]. In this study, the contamination rate in the collected samples of meat and meat products was 26.37% (159/603). Our results indicate a lower frequency of contamination of samples collected as part of monitoring studies than the results obtained by other authors. Monitoring studies in this area conducted in Poland, due to the relatively high number of samples, are one of the few studies conducted in the field of detecting presumptive *B. cereus* at such a large scale in the world. Data on the occurrence of *B. cereus* in these areas is extremely limited.

The toxin gene profiles established with the use of a multiplex PCR were presented in Table 2. The *nhe* genes were present in 244 of the 267 (91.39%) isolates. The *hbl* genes were detected in 53.56% of the tested *B. cereus* strains, while the presence of the *cytK* gene was demonstrated in 44.19%. The lowest occurrence was found for the *ces* gene. Among the 267 isolates tested, the *ces* gene was found in 14 isolates only (2.62%). In 4.49% of the analysed *B. cereus* strains, no *hbl*, *nhe*, *cytK*, *ces* genes were found. Among the 267 tested strains, all groups were present (A–G) and the following profiles were identified: A (31.09%), B (0.37%), C (19.85%), D (8.99%), E (2.25%), F (28.84%), and G (1.5%). In 2.62% of the analysed isolates, toxin profiles consistent with the above-mentioned classification [Ehling-Schultz *et al.,* 2006] were not detected. With regard to the identified occurrence of two additional new patterns, their classification was proposed as group H (*hbl*) and group I (*hbl*, *cytK*). The new profile H was identified for 1 strain isolated from pastries, while the I profile was detected in 4 strains isolated from pastries and 1 strain from vegetables.

Almost all the strains isolated from food and food-poisoning samples carried the *nhe* genes, as was observed in previous works, which is consistent with the results obtained in our study [Hansen & Hendriksen, 2001]. The enterotoxigenic profiles of 51 *B. cereus* strains isolated from food prove that the *cytK* gene and *hbl-nhe-cytK* enterotoxin genes (group A according to Ehling-Schultz *et al.* [2006] classification) were isolated among foodborne samples in 37% of the strains [Guinebretière & Broussolle, 2002]. A study carried out in Germany also presented similar results – 91.2, 83.0, and 37.4% of the isolates were positive for the *hbl*, *nhe,* and *cytK* toxins genes, respectively. The *ces* gene was not detected [Fiedler *et al.*, 2019]. The *hbl*ACD gene cluster was found in 39% of the *B. cereus* strains isolated from ready-to-eat food in China, the *nhe* (A, B, C) genes were found in 89, 99, and 94% of the isolates, respectively, the *cytK* gene – in 68% of strains, while only 7% of them were identified as carrying the *cesB* gene [Yu *et al.*, 2020]. According to the toxin gene profile classification by Ehling-Schulz *et al.* [2006], the majority of strains isolated from cucumbers, carrots, herbs, salad leaves, and ready-to-eat mixed salad leaves (79 of 147; 53.7%) belong to the toxin gene profile C [Fiedler *et al.*, 2019]. In addition, about 25% were not defined as a toxin gene profile. The occurrence of other toxin gene profiles F and G in the study was, respectively at 9%, and 3%. According to the results for *B. cereus* strains isolated from milk powder (130 isolates) and Ras-cheese (70 isolates), the *nhe* gene was detected in all strains (both tested products) [Abdeen *et al.*, 2020]. For milk, *cytK*, *hbl*, *ces* genes were prevalent in 55.5%, 33.3%, and 22.2% of the strains, respectively. Whereas, to

TABLE 2. Toxin profile of *Bacillus cereus* isolated from retail food in Poland.

Profile		Gene				Source (number of isolates)			
		hbl	*nhe*	*cytK*	*ces*	Pastries (240)	Delicatessen products (24)	Vegetables (2)	Spices (1)
A		■	■	■		74	8	-	1
B			■	■	■	1	-	-	-
C		■	■			45	8	-	-
D			■	■		24	-	-	-
E			■		■	5	1	-	-
F			■			70	7	-	-
G				■		4	-	-	-
Unclassified	H*	■				1	-	-	-
	I*	■		■		4	-	2	-
None detected						12	-	-	-

*New classification groups; black boxes – gene presence. The source of strain isolation from food products and detailed results are described in Supplementary Table 1.

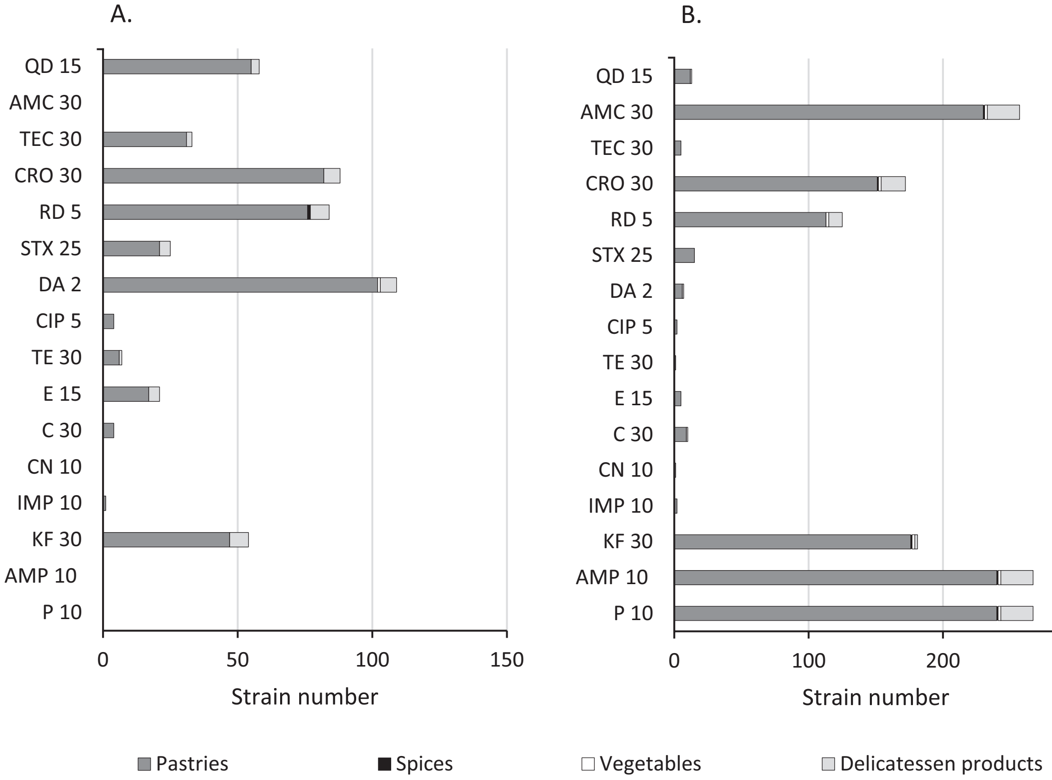

FIGURE 1. Susceptibility of *Bacillus cereus* stains isolated from food products to antimicrobials; A – number of intermediate strains, B – number of resistant strains; P 10 (penicillin G, 10U), AMP 10 (ampicillin, 10 µg), KF 30 (cephalothin, 30 µg), IMP 10 (imipenem,10 µg), CN 10 (gentamicin, 10 µg), C 30 (chloramphenicol, 30 µg), E 15 (erythromycin, 15 µg), TE 30 (tetracycline, 30 µg), CIP 5 (ciprofloxacin, 5 µg), DA 2 (clindamycin, 2 µg), STX 25 (trimethoprim-sulfamethoxazole, 25 µg), RD 5 (rifampicin, 5 µg), CRO 30 (ceftriaxone, 30 µg), TEC 30 (teicoplanin, 30 µg), AMC 30 (amoxicillin-clavulanic acid, 30 µg), QD 15 (quinupristin/dalfopristine, 15 µg).

the best of our knowledge, there is no data in the literature about *B. cereus* toxin profiles isolated from pastries or cakes.

The increase in drug resistance of strains isolated from food, including bacteria from the *B. cereus* group also gives rise to a serious problem. Antimicrobial resistance is a growing global threat that includes both human, animal and environmental issues. In our study, we investigated the susceptibility of *B. cereus* isolates to 16 antimicrobials. The antibiotic susceptibility of strains is presented in Figure 1. The conducted tests demonstrated the resistance of all analysed strains to penicillin G (100%) and ampicillin (100%). In addition, the tested isolates were resistant to: amoxicillin-clavulanic acid (96.25%), cephalothin (67.79%), ceftriaxone (64.42%), rifampicin (46.82%), trimethoprim-sulfamethoxazole (5.62%), quinupristin/dalfopristin (4.87%), chloramphenicol (3.75%), clindamycin (2.62%), teicoplanin (1.87%), erythromycin (1.87%), ciprofloxacin (0.75%), imipenem (0.75%), tetracycline (0.37%), and gentamicin (0.37%). The study confirmed intermediate susceptibility of the strains to: clindamycin (40.82%), ceftriaxone (32.96%), rifampicin (31.46%), quinupristin/dalfopristin (21.72%), cephalothin (20.22%), teicoplanin (12.36%), trimethoprim-sulfamethoxazole (9.36%), erythromycin (7.87%), tetracycline (2.62%), chloramphenicol (1.5%), ciprofloxacin (1.5%), and imipenem (0.37%).

According to the antibiotic susceptibility tests, most of the *B. cereus* group strains isolated from food in Poland were resistant to β-lactam antibiotics including penicillin ampicillin, and cephalothin, which is consistent with previous studies on the antibiotic resistance of *B. cereus* in food products [Gao *et al*., 2018; György *et al*., 2021; Yibar *et al*., 2017]. Yu *et al.* [2020] found that most isolates were resistant to penicillin (99.7%), ampicillin (99.7%), and amoxicillin-clavulanic (97.6%), which is compliant with our results. Additionally, Yu *et al.* [2020] revealed that strains were resistant to rifampicin (83%), cephalothin (86.7%), quinupristin/dalfopristin (19.57%), tetracycline (15.49%), and trimethoprim-sulfamethoxazole (12.5%), while the results of our study indicate lower rates of resistance to these antibiotics (rifampicin (46.82%), cephalothin (67.79%), quinupristin/dalfopristin (4.87%), tetracycline (0.37%), and trimethoprim-sulfamethoxazole (5.62%). Most isolates were sensitive to: gentamycin (97.6%), imipenem (99.7%), ciprofloxacin (92.9%), chloramphenicol (94.6%), and teicoplanin (81%). Isolates also showed intermediate resistance to quinupristin (61.9%) and clindamycin (74.8%). In this study, *B. cereus* strains showed similar susceptibility to the above-mentioned antibiotics. Owusu-Kwarteng *et al.* [2017] reported resistance to penicillin (100%), amoxicillin (100%), ampicillin (98%), trimethoprim/sulfamethoxazole (80% with 20% intermediate resistant strains), and susceptibility to other antimicrobials such as chloramphenicol (99%), ciprofloxacin (100%), clindamycin (100%), erythromycin (92%), gentamicin (100%), quinupristin/dalfopristin (100%), rifampin (100%), tetracycline (97%), and vancomycin (100%) for *B. cereus* isolated from soil, milk or milk-based products. Similarly to the previous study and our results, the isolates demonstrated 100% resistance to penicillin and were mostly sensitive to gentamycin, imipenem, ciprofloxacin, erythromycin, and chloramphenicol [Park *et al.*, 2020]. The presented result is consistent with findings of other authors demonstrating that *B. cereus* is susceptible to chloramphenicol, ciprofloxacin, erythromycin, gentamicin, and imipenem [Al-Khatib *et al.*, 2007; Zhao *et al.*, 2020].

Bacteria from the *B. cereus* group, in addition to food poisoning, are sometimes associated with infections, including among others, those of the central nervous system, bacteraemia, respiratory tract infections, and endocarditis [Bianco *et al.,* 2021; De Medts *et al*., 2018; Ribeiro *et al.,* 2022]. The incidence for this type of infection is low, although the mortality rate is high. The spread of antimicrobial-resistant bacteria in the environment is a major public health concern and is associated with increasing mortality and costs of treatment. Therefore, it is important to assess the antimicrobial susceptibility of bacteria isolated from food.

CONCLUSIONS

The obtained results contribute to characterizing the diversity of *B. cereus* isolated from various products and their impact on food safety and public health. Our study revealed that 95.51% of *B. cereus* strains isolated from food products in Poland were positive for the presence of at least one or more toxin genes, with the highest occurrence of the *nhe* gene. Additionally, the tested strains were resistant to a wide spectrum of antibiotics tested. Due to the high prevalence of toxin genes and the occurrence of antibiotic resistance among the isolates, continuous monitoring of presumptive *B. cereus* is strongly recommended based on the 'One Health' approach in order to evaluate the risk posed to human health by food consumption.

RESEARCH FUNDING

This work was supported financially by NIPH-NIH (1/ZŚ/2017; 1/ZŚ/2018; BŻ-5/2019; 1FBBW/2021).

CONFLICTS OF INTERESTS

The authors declare that they have no known competing financial interests or personal relationships that could have appeared to influence the work reported in this paper.

ORCID IDs

D. Korsak https://orcid.org/0000-0002-4432-3712
J. Kowalska https://orcid.org/0000-0001-9798-1068
E. Maćkiw https://orcid.org/0000-0001-5147-487X
J. Postupolski https://orcid.org/0000-0001-7961-9188

SUPPLEMENTARY MATERIALS

The following are available online at http://journal.pan.olsztyn.pl/Characteristic-and-Antimicrobial-Resistance-of-Bacillus-cereus-Group-Isolated-from,152677,0,2.html; Detailed information about strains and antimicrobial susceptibility.

REFERENCES

1. Abdeen, E.E., Hussien, H., Hadad, G.A.E., Mousa, W.S. (2020). Prevalence of virulence determinants among *Bacillus cereus* isolated from milk products with potential public health concern. *Pakistan Journal of Biological Sciences: PJBS*, *23*(3), 206–212. https://doi.org/10.3923/pjbs.2020.206.212
2. Amin, W.F. (2018). Occurrence of *Bacillus cereus* in some milk-based desserts. *Assiut Veterinary Medical Journal*, *64*(156), 41–46. https://doi.org/10.21608/avmj.2018.168685
3. Berthold, A., Doroszkiewicz, B. (2009). Characteristics of *Bacillus cereus* emetic toxin. *Medycyna Weterynaryjna, 65*(1), 15–19 (in Polish; English abstract).
4. Berthold-Pluta, A., Pluta, A., Garbowska, M., Stefańska, I. (2019). Prevalence and toxicity characterization of *Bacillus cereus* in food products from Poland. *Foods*, *8*(7), art. no. 269. https://doi.org/10.3390/foods8070269
5. Bianco, A., Capozzi, L., Monno, M.R., Del Sambro, L., Manzulli, V., Pesole, G., Loconsole, D., Parisi, A. (2021). Characterization of *Bacillus cereus* group isolates from human bacteremia by whole-genome sequencing. *Frontiers in Microbiology*, *11*, art. no. 599524. https://doi.org/10.3389/fmicb.2020.599524
6. Borge, G.I.A., Skeie, M., Sørhaug, T., Langsrud, T., Granum, P.E. (2001). Growth and toxin profiles of *Bacillus cereus* isolated from different food sources. *International Journal of Food Microbiology*, *69*(3), 237–246. https://doi.org/10.1016/S0168-1605(01)00500-1
7. Brillard, J., Dupont, C., Berge, O., Dargaignaratz, C., Oriol-Gagnier, S., Doussan, C., Broussolle, V., Gillon, M., Clavel, T., Berard, A. (2015). The water cycle, a potential source of the bacterial pathogen *Bacillus cereus*. *BioMed Research International*, *2015*(SI), art. no. 356928. https://doi.org/10.1155/2015/356928
8. Carlin, F., Fricker, M., Pielaat, A., Heisterkamp, S., Shaheen, R., Salonen, M.S., Svensson, B., Nguyen-The, C., Ehling-Schulz, M. (2006). Emetic toxin-producing strains of *Bacillus cereus* show distinct characteristics within the *Bacillus cereus* group. *International Journal of Food Microbiology*, *109*(1–2), 132–138. https://doi.org/10.1016/j.ijfoodmicro.2006.01.022
9. CLSI. (2012) Clinical and Laboratory Standards Institute Performance standards for antimicrobial susceptibility testing: twenty-second informational supplement M100-S22. Clinical and Laboratory Standards Institute, Wayne, PA, USA.
10. De Medts, R., Kolwijck, E., Corsten, M.F., Gòraj, B., Schouten, J. (2018). *Bacillus cereus* bacteraemia and cerebral lesions in two patients with haematological malignancies. *Netherlands Journal of Critical Care*, *26(6)*, 230–233.
11. Dietrich, R., Jessberger, N., Ehling-Schulz, M., Märtlbauer, E., Granum, P.E. (2021). The food poisoning toxins of *Bacillus cereus*. *Toxins, 13*(2), art. no. 98. https://doi.org/10.3390/toxins13020098
12. Drobniewski, F.A. (1993). *Bacillus cereus* and related species. *Clinical Microbiology Reviews*, *6*(4), 324–338. https://doi.org/10.1128/CMR.6.4.324
13. EFSA Panel on Contaminants in the Food Chain. (2016). Scientific opinion on the risks for public health related to the presence of *Bacillus cereus* and other *Bacillus* spp. including *Bacillus thuringiensis* in foodstuffs. *EFSA Journal, 14*(7), art. no. e04524. https://doi.org/10.2903/j.efsa.2016.4524

14. Ehling-Schulz, M., Guinebretiere, M.-H., Monthán, A., Berge, O., Fricker, M., Svensson, B. (2006). Toxin gene profiling of enterotoxic and emetic *Bacillus cereus*. *FEMS Microbiology Letters*, *260*(2), 232–240. https://doi.org/10.1111/j.1574-6968.2006.00320.x
15. Ehling-Schulz, M., Lereclus, D., Koehler, T.M. (2019). The *Bacillus cereus* group: *Bacillus* species with pathogenic potential. Chapter 55, In: V.A. Fischetti, R.P. Novick, J.J. Ferretti, D.A. Portnoy, M. Braunstein, J.I. Rood (Eds). *Gram-Positive Pathogens*, 3rd edition, ASM Press, Washington, DC, USA, pp. 875–902. https://doi.org/10.1128/9781683670131.ch55
16. Ehling-Schulz, M., Vukov, N., Schulz, A., Shaheen, R., Andersson, M., Märtlbauer, E., Scherer, S. (2005). Identification and partial characterization of the nonribosomal peptide synthetase gene responsible for cereulide production in emetic *Bacillus cereus*. *Applied and Environmental Microbiology*, *71*(1), 105–113. https://doi.org/10.1128/AEM.71.1.105-113.2005
17. Faille, C., Tauveron, G., Le Gentil-Lelièvre, C., Slomianny, C. (2007). Occurrence of *Bacillus cereus* spores with a damaged exosporium: consequences on the spore adhesion on surfaces of food processing lines. *Journal of Food Protection*, *70*(10), 2346–2353. https://doi.org/10.4315/0362-028X-70.10.2346
18. Fiedler, G., Schneider, C., Igbinosa, E.O., Kabisch, J., Brinks, E., Becker, B., Stoll, D.A., Cho, G.-S., Huch, M., Franz, C.M.A.P. (2019). Antibiotics resistance and toxin profiles of *Bacillus cereus*-group isolates from fresh vegetables from German retail markets. *BMC Microbiology*, *19*, art. no. 250. https://doi.org/10.1186/s12866-019-1632-2
19. Gao, T., Ding, Y., Wu, Q., Wang, J., Zhang, J., Yu, S., Wu, H. (2018). Prevalence, virulence genes, antimicrobial susceptibility, and genetic diversity of *Bacillus cereus* isolated from pasteurized milk in China. *Frontiers in Microbiology*, *9*, art. no. 533. https://doi.org/10.3389/fmicb.2018.00533
20. Gdoura-Ben Amor, M., Siala, M., Zayani, M., Grosset, N., Smaoui, S., Messadi-Akrout, F., Baron, F., Jan, S., Gautier, M., Gdoura, R. (2018). Isolation, identification, prevalence, and genetic diversity of *Bacillus cereus* group bacteria from different foodstuffs in Tunisia. *Frontiers in Microbiology*, *9*, art. no. 447. https://doi.org/10.3389/fmicb.2018.00447
21. Glasset, B., Herbin, S., Guillier, L., Cadel-Six, S., Vignaud, M.-L., Grout, J., Pairaud, S., Michel, V., Hennekinne, J.-A., Ramarao, N., Brisabois, A. (2016). *Bacillus cereus*-induced food-borne outbreaks in France, 2007 to 2014: epidemiology and genetic characterisation. *Eurosurveillance*, *21*(48), art. no. 30413. https://doi.org/10.2807/1560-7917.ES.2016.21.48.30413
22. Guinebretière, M.-H., Broussolle, V., Nguyen-The, Ch. (2002). Enterotoxigenic profiles of food-poisoning and food-borne *Bacillus cereus* strains. *Journal of Clinical Microbiology*, *40*(8), 3053–3056. https://doi.org/10.1128/JCM.40.8.3053-3056.2002
23. György, É., Laslo, É., Antal, M., András, C.D. (2021). Antibiotic resistance pattern of the allochthonous bacteria isolated from commercially available spices. *Food Science Nutrition*, *9*(8), 4550–4560. https://doi.org/10.1002/fsn3.2433
24. Hansen, B.M., Hendriksen, N.B. (2001). Detection of enterotoxic *Bacillus cereus* and *Bacillus thuringiensis* strains by PCR analysis. *Applied and Environmental Microbiology*, *67*(1), 185–189. https://doi.org/10.1128/AEM.67.1.185-189.2001
25. Hansen, B.M., Leser, T.D., Hendriksen, N.B. (2001). Polymerase chain reaction assay for the detection of *Bacillus cereus* group cells. *FEMS Microbiology Letters*, *202*(2), 209–213. https://doi.org/10.1111/j.1574-6968.2001.tb10805.x
26. Hardy, S.P., Lund, T., Granum, P.E. (2001). CytK toxin of *Bacillus cereus* forms pores in planar lipid bilayers and is cytotoxic to intestinal epithelia. *FEMS Microbiology Letters*, *197*(1), 47–51. https://doi.org/10.1111/j.1574-6968.2001.tb10581.x
27. Juneja, V.K., Golden, C.E., Mishra, A., Harrison, M.A., Mohr, T.B. (2019). Predictive model for growth of *Bacillus cereus* at temperatures applicable to cooling of cooked pasta. *Journal of Food Science*, *84*(3), 590–598. https://doi.org/10.1111/1750-3841.14448
28. Kong, L., Yu, S., Yuan, X., Li, C., Yu, P., Wang, J., Guo, H., Wu, S., Ye. Q., Lei, T., Yang, X., Zhang, Y., Wei, X., Zeng, H., Zhang, J., Wu, Q., Ding, Y. (2021). An investigation on the occurrence and molecular characterization of *Bacillus cereus* in meat and meat products in China. *Foodborne Pathogens and Disease*, *18*(5), 306–314. https://doi.org/10.1089/fpd.2020.2885
29. Li, D., Lin, R., Xu, Y., Chen, Q., Deng, F., Deng, Y., Wen, J. (2021). Cereulide exposure caused cytopathogenic damages of liver and kidney in mice. *International Journal of Molecular Sciences*, *22*(17), art. no. 9148. https://doi.org/10.3390/ijms22179148
30. Lindbäck, T., Fagerlund, A., Rødland, M.S., Granum, P.E. (2004). Characterization of the *Bacillus cereus* Nhe enterotoxin. *Microbiology*, *150*(12), 3959–3967. https://doi.org/10.1099/mic.0.27359-0
31. Marxen, S., Stark, T.D., Rütschle, A., Lücking, G., Frenzel, E., Scherer, S., Ehling-Schulz, M., Hofmann, T. (2015). Depsipeptide intermediates interrogate proposed biosynthesis of cereulide, the emetic toxin of *Bacillus cereus*. *Scientific Reports*, *5*, art. no. 10637. https://doi.org/10.1038/srep10637
32. Messelhäußer, U., Ehling-Schulz, M. (2018). *Bacillus cereus* — a multifaceted opportunistic pathogen. *Current Clinical Microbiology Reports, 5*, 120–125. https://doi.org/10.1007/s40588-018-0095-9
33. N'guessan, E., Bakayoko, S., Cisse, M., Dalie, W., Sindic, M. (2019). Prevalence of *Bacillus cereus* and emetic strains detection from Ivory Coast local flours. *Agronomie Africaine*, *8*(1), 151–159.
34. Organji, S.R., Abulreesh, H.H., Elbanna, K., Osman, G.E.H., Khider, M. (2015). Occurrence and characterization of toxigenic *Bacillus cereus* in food and infant feces. *Asian Pacific Journal of Tropical Biomedicine*, *5*(7), 515–520. https://doi.org/10.1016/j.apjtb.2015.04.004
35. Owusu-Kwarteng, J., Wuni, A., Akabanda, F., Tano-Debrah, K., Jespersen, L. (2017). Prevalence, virulence factor genes and antibiotic resistance of *Bacillus cereus sensu lato* isolated from dairy farms and traditional dairy products. *BMC Microbiology*, *17*, art. no. 65. https://doi.org/10.1186/s12866-017-0975-9
36. Park, K.M., Kim, H.J., Jeong, M., Koo, M. (2020). Enterotoxin genes, antibiotic susceptibility, and biofilm formation of low-temperature-tolerant *Bacillus cereus* isolated from green leaf lettuce in the cold chain. *Foods*, *9*(3), art. no. 249. https://doi.org/10.3390/foods9030249

37. PN EN ISO 7932:2005 (2005). Food and feed microbiology – Horizontal method for the enumeration of presumptive *Bacillus cereus* – Colony enumeration method at 30°C.
38. Priest, F.G., Kaji, D.A., Rosato, Y.B., Canhos, V.P. (1994). Characterization of *Bacillus thuringiensis* and related bacteria by ribosomal RNA gene restriction fragment length polymorphisms. *Microbiology*, *140*(5), 1015–1022. https://doi.org/10.1099/13500872-140-5-1015
39. Proroga, Y.T.R., Capuano, F., Castellano, S., Giordano, A., Mancusi, A., Delibato, E., Dumontet, S., Pasquale, V. (2019). Occurrence and toxin gene profile of *Bacillus cereus* in dairy products. *Journal of Microbiology, Biotechnology and Food Sciences*, *9*(1), 58–62. https://doi.org/10.15414/jmbfs.2019.9.1.58-62
40. Rajkovic, A., Uyttendaele, M., Vermeulen, A., Andjelkovic, M., Fitz-James, I., In 't Veld, P., Denon, Q., Verhe, R., Debevere, J. (2008). Heat resistance of *Bacillus cereus* emetic toxin, cereulide. *Letters in Applied Microbiology*, *46*(5), 536–541. https://doi.org/10.1111/j.1472-765X.2008.02350.x
41. Raymond, B., Wyres, K.L., Sheppard, S.K., Ellis, R.J., Bonsall, M.B. (2010). Environmental factors determining the epidemiology and population genetic structure of the *Bacillus cereus* group in the field. *PLoS Pathogens*, *6*(5), art. no. e1000905. https://doi.org/10.1371/journal.ppat.1000905
42. Ribeiro, R.L., Bastos, M.O., Blanz, A.M., da Rocha, J.A., de Oliveira Velasco, N.A., de Oliveira Marre, A.T., Martins, I.S. (2022). Subacute infective endocarditis caused by *Bacillus cereus* in a patient with Systemic Lupus Erythematosus. *The Journal of Infection in Developing Countries, 16*(4), 733–736. https://doi.org/10.3855/jidc.15685
43. Rossi, G.A.M., Aguilar, C.E.G., Silva, H.O., Vidal, A.M.C. (2018). *Bacillus cereus* group: genetic aspects related to food safety and dairy processing. *Arquivos Do Instituto Biológico*, *85*(1–7), art no. e0232017. https://doi.org/10.1590/1808-1657000232017
44. Rodrigo, D., Rosell, C.M., Martinez, A. (2021). Risk of *Bacillus cereus* in relation to rice and derivatives. *Foods, 10*(2), art. no. 302. https://doi.org/10.3390/foods10020302
45. Rouzeau-Szynalski, K., Stollewerk, K., Messelhaeusser, U., Ehling-Schulz, M. (2020). Why be serious about emetic *Bacillus cereus*: Cereulide production and industrial challenges. *Food Microbiology*, *85*, art. no. 103279. https://doi.org/10.1016/j.fm.2019.103279
46. Schoeni, J.L., Lee Wong, A.C. (2005). *Bacillus cereus* food poisoning and its toxins. *Journal of Food Protection*, *68*(3), 636–648. https://doi.org/10.4315/0362-028X-68.3.636
47. Shah, M.M., Miringu, G., Wada, A., Kaneko, S., Ichinose, Y. (2019). Case report: *Bacillus pumilus*–caused bacteremia in a patient with food poisoning. *The American Journal of Tropical Medicine and Hygiene, 100*(3), 688–690. https://doi.org/10.4269/ajtmh.18-0593
48. Yibar, A., Cetinkaya, F., Soyutemiz, E., Yaman, G. (2017). Prevalence, enterotoxin production and antibiotic resistance of *Bacillus cereus* isolated from milk and cheese. *Kafkas Universitesi Veteriner Fakultesi Dergisi Journal, 23*(4), 635–642. https://doi.org/10.9775/kvfd.2017.17480
49. Yu, S., Yu, P., Wang, J., Li, C., Guo, H., Liu, C., Kong, L., Yu, L., Wu, S., Lei, T., Chen, M., Zeng, H., Pang, R., Zhang, Y., Wei, X., Zhang, J., Wu, Q., Ding, Y. (2020). A study on prevalence and characterization of *Bacillus cereus* in ready-to-eat foods in China. *Frontiers in Microbiology*, *10*, art. no. 3043. https://doi.org/10.3389/fmicb.2019.03043
50. Zhao, S., Chen, J., Fei, P., Feng, H., Wang, Y., Ali, M.A., Li, S., Jing, H., Yang, W. (2020). Prevalence, molecular characterization, and antibiotic susceptibility of *Bacillus cereus* isolated from dairy products in China. *Journal of Dairy Science*, *103*(5), 3994–4001. https://doi.org/10.3168/jds.2019-17541

Pol. J. Food Nutr. Sci., 2022, Vol. 72, No. 3, pp. 305–317
On-line ISSN: 2083-6007
Print ISSN: 1230-0322
DOI: 10.31883/pjfns/151750
http://journal.pan.olsztyn.pl

Original article
Section: Food Technology

Enantioselective HS-SPME-GC-MS for Authentication of Natural and Synthetic Strawberry Flavour in Syrups

Karolína Průchová, Adéla Grégrová, Hana Helísková, Vojtěch Kružík, Helena Čížková*

Department of Food Preservation, Faculty of Food and Biochemical Technology,
University of Chemistry and Technology Prague, Technicka 3, 16628 Prague 6, Czech Republic

Key words: strawberry, syrup, chiral gas chromatography, volatiles, synthetic flavour, natural flavour

Demand for a reliable distinction of the strawberry flavour naturalness stood in the beginning of this research. An efficient chiral column with CP-Chirasil-Dex CB stationary phase was involved in headspace solid-phase microextraction-gas chromatography-mass spectrometry analysis of strawberry flavour in 6 strawberry cultivars, 7 samples of strawberry flavourings and 14 samples of strawberry syrups to evaluate the authenticity of flavour naturalness and reveal adulteration. Enantiomeric ratios of 8 selected chiral volatiles (methyl 2-methylbutanoate, ethyl 2-methylbutanoate, 2-methylbutanoic acid, linalool, α-ionone, γ-decalactone, γ-undecalactone, δ-dodecalactone) were evaluated. Seven chiral volatiles contributed to the revelation of synthetic origin. γ-Decalactone (enantiomeric ratios: 100⁄0, 100⁄0, 99⁄1, 99⁄1, 100⁄0, and 99⁄1 in strawberries; 100⁄0 in 3 natural flavourings; 100⁄0 in syrup with natural flavour) was the most contributive indicator of synthetic and natural strawberry flavour, followed by ethyl 2-methylbutanoate (enantiomeric ratios: 0⁄100, 5⁄95, 5⁄95 in 3 natural flavourings, 0⁄100 in syrup with natural flavour). The best chiral resolution was observed for α-ionone (R_S>4). One syrup supposed to contain only natural strawberry flavouring was suspected to be adulterated regarding nearly racemic ratios of its four crucial chiral volatiles. Investigation of enantiomeric ratios of the unique selection of chiral volatiles and strawberry samples using the CP-Chirasil-Dex CB chiral column wider revealed possibilities for reliable recognition of strawberry flavour naturalness in complex matrices and in food samples in general.

INTRODUCTION

In recent years, findings on different sensory properties [Werkhoff *et al.*, 1993] or different biological activities [da Silva Rivas *et al.*, 2012] of flavour compounds' enantiomers have appeared, as well as the studies demonstrating unlike enantiomeric composition of natural and synthetic flavours [Ravid *et al.*, 2010]. Therefore, some consumers can prefer products with natural flavours and a credible flavour declaration on the label. The expression 'flavourings' is usually found without any additional description on food products. The probability of the synthetic origin in the case of 'flavourings' declaration is high, and even the declaration of natural flavouring can be misleading. Large assortment of strawberry products in local markets as well as the effort of producers to reduce expenses are among the factors that often lead to adulteration in the form of replacing the natural flavour declared on the product package with a synthetic one. The appropriate analytical testing to reveal flavour origin can be therefore very helpful.

Regarding limited possibilities for authentication of strawberry flavour (*e.g.* stable isotope ratio mass spectrometry which should be used as a set of values [Nitz *et al.*, 1991; Schipilliti *et al.*, 2011] considering the overlapping isotopic ranges for γ-decalactone of synthetic and natural origin [Nitz *et al.*, 1991]), there is a crucial focus on the scope of possibilities in chiral gas chromatography (GC). To the best of our knowledge, there is paucity of literature dealing with the chiral GC for authentication of natural strawberry flavour and the available works focus mainly on fruit (Table 1), while even fewer studies have investigated synthetic strawberry flavour in commercial products [Cagliero *et al.*, 2012; Kreck *et al.*, 2001; Nitz *et al.*, 1991; Ravid *et al.*, 2010; Schipilliti *et al.*, 2011]. In one study only [Kreck *et al.*, 2001], chiral GC was used to authenticate strawberry flavour in syrup, a matrix that is different and can be more complicated, and moreover, just one syrup sample was researched therein. Besides that, to the best of found knowledge, there is a lack of studies investigating a rather wide range of chiral volatiles in commercial food products for the purposes of strawberry flavour authentication, despite its crucial importance. Kreck *et al.* [2001] investigated seven chiral volatiles, Cagliero *et al.* [2012] compared four chiral volatiles in strawberry yogurt, Schipilliti *et al.* [2011] two in yoghurt and candies, and Nitz *et al.* [1991] detected six γ-lactones in strawberry wines of which only two

---

* Corresponding Author:
E-mail: Pruchovk@vscht.cz (K. Průchová)

Submitted: 30 May 2022
Accepted: 20 July 2022

TABLE 1. Enantiomeric characterisation of selected volatiles of strawberries obtained by analysis on cyclodextrin stationary phases.

Elution order	Compound	t_{RI} (min)		t_{RII} (s)		LRI		Elution order of enantiomers		Enantiomeric comparison	Enantiomeric ratio	Chiral stationary phase[a]	Literature
		1.	2.	1.	2.	1.	2.	1.	2.				
1	Methyl 2-methylbutanoate							*R*	*S*	*S*>>*R*	97/3–99/1[e]	DIME-β-CD[i]	Kreck *et al.* [2001]
		9.7	10.2	1.11	1.13							EtTBS-β-CD[i] and CycloSil B[i]	Williams *et al.* [2005]
2	Ethyl 2-methylbutanoate							(-)-	(+)-	(+)>>(-)	95/5; 100/0; 99/1[bf]	Chirasil-β-Dex[i]	de la Peña Moreno *et al.* [2010]
								R	*S*	*S*>>*R*	97/3–99/1[e]	DIME-β-CD[i]	Kreck *et al.* [2001]
		11.6	12.1	1.30	1.30							EtTBS-CD[i] and CycloSil B[i]	Williams *et al.* [2005]
3	2-Methylbutanoic acid							*S*	*R*	*S*>>*R*	99/1[e]	DIME-β-CD[i]	Kreck *et al.* [2001]
		35.5 (*S*)		1.43 (*S*)								EtTBS-CD[i] and CycloSil B[i]	Williams *et al.*, [2005]
4	(β)-Linalool									*S*>>*R*	97/3–99/1[f]	Lipodex C[i]	Bernreuther&Schreier, [1991]
								(-)-	(+)-	*(+)>(-)*	57/43; 62/38; 60/40[bf]	Chirasil-β-Dex[i]	de la Peña Moreno *et al.* [2010]
						1226[d]	1233[d]	*R*(-)[d]	*S*(+)[d]			Rtβ-DEXsm[i]	Ravid *et al.* [2010]
						1296[d]	1298[d]	*S*(+)[d]	*R*(-)[d]			Rtγ-DEXsa	Ravid *et al.* [2010]
										S>>*R*	97/3–99/1[e]	Megadex DETTBS-β[i]	Schipilliti *et al.* [2011]
		37.8	38.5	2.05	2.00							EtTBS-CD[i] and CycloSil B[i]	Williams *et al.* [2005]
5	(*E*)-α-Ionon							*S*	*R*	*R*>>*S*	99/1[e]	DIME-β-CD[i]	Kreck *et al.* [2001]
						1502[d]	1512[d]	*S*(-)[d]	*R*(+)[d]			Rtβ-DEXsm[i]	Ravid *et al.* [2010]
6	γ-decalacton							*R*	*S*	*R*>>*S*	98/2[f]	Lipodex B	Bernreuther *et al.* [1989]
										R>>*S*	97/3–99/1[e]	DIME-β-CD[i]	Kreck *et al.* [2001]
								R	*S*	*R*>>*S*	>99% *R*[bf]	Lipodex D[i]	Mosandl *et al.* [1989]
										R>>*S*	99/1[f]	Lipodex B	Nitz *et al.* [1991]
						1680[d]	1688[d]	*R*(+)[d]	*S*(-)[d]	*R*>>*S*	90/10–100/0[eg]	Rtβ-DEXsm[i]	Ravid *et al.* [2010]
										R>>*S*	89/11–95/5[e]	Megadex DETTBS-β[i]	Schipilliti *et al.* [2011]
7	γ-undecalacton							*R*	S		traces[cf]	Lipodex B	Bernreuther *et al.* [1989]
						1745[d]	1748[cd]	*R*(+)[d]	*S*(-)[d]			Rtβ-DEXsm[i]	Ravid *et al.* [2010]
8	δ-dodecalacton							*S*(-)	*R*(+)	*R*>*S*	30.10/69.10[f]	Lipodex D[i]	Bernreuther *et al.* [1991]
								S(-)	*R*(+)	*R*>*S*	33/67–35.8/64.2[h]	Hydrodex β analogue[i]	Krammer *et al.* [2006]

Elution order – elution order of the compounds based on literature data; t_{RI} – retention time of enantiomer standards on EtTBS-CD column; t_{RII} – retention time of enanciomer standards on CycloSil B column; LRI – linear retention index; Enantiomeric comparison – comparison of enantiomers *R* and *S* according to their percentage proportion; Enantiomeric ratio – ratios between enantiomers *R* and *S*.

[a] For detailed composition see Table S3 in supplementary materials. [b] Data from literature were recalculated to enantiomeric ratios for the purposes of our study as: [(predominant enantiomer–minor t-enantiomer)/(predominant enantiomer+minor enantiomer)×100]. [c] Enantiomeric discrimination not possible. [d] Measured for standards. [e] Obtained from strawberries. [f] Obtained from strawberry extract. [g] Obtained from supernatan after lyophilization of strawberries. [h] Obtained from condensate strawberry water phase after lyophilization of strawberries. [i] β-cyclodextrin (β-CD) is the chiral selector of chiral stationary phase.

were functional. γ-Decalactone was a substance investigated wider than the others in strawberries (Table 1), but even this substance has been rarely studied in the literature in commercial products, just once in syrup and only in a single sample [Kreck *et al*., 2001]. The urgent need for a reliable authentication of the natural and synthetic origin of strawberry flavour by chiral gas chromatography-mass spectrometry (chiral GC-MS) based on the results of a wider range of substances as well as its application in strawberry syrups for revealing their adulteration stood in the beginning of our research.

The condition for such a determination was to find a chiral column allowing good separation of the enantiomers of the investigated substances. Modified forms of cyclodextrin are gaining in popularity as the bases of chiral stationary phases in GC enabling enantiomeric separation of almost all classes of volatile chiral compounds, highly effective in the flavour and fragrance field [Betzenbitcher *et al*., 2022; Cagliero *et al*., 2015, 2017; Engel, 2020]. For a specific case – a molecule of permethylated β-cyclodextrin separating enantiomers of selected flavours in GC – Lipkowitz's group described a lot of aspects of the separation mechanisms [Lipkowitz *et al*., 1997a,b; 1998]. Instead of different number of bondings ("three-point interaction model" – [Easson & Stedman, 1933; Fanali *et al.*, 2019]), the authors pointed out the same interactions of both enantiomers but their greater or lesser extent [Lipkowitz *et al*., 1997b]. Simultaneously, the authors concluded that permethylated β-cyclodextrin displayed its enhanced chiral discriminating capacity because of the spatial congruence of its domain of greatest enantiodifferentiation, found to be inside its macrocyclic cavity, with the analyte's preferred binding site [Lipkowitz *et al.,* 1998]. Later, the question arose, whether the formation of inclusion complexes was really a prerequisite for enantiorecognition. On the one hand, external complexes of selected enantiomers with β-cyclodextrine derivatives were observed in some other separation techniques, such as capillary electrophoresis [Servais *et al.*, 2012]; on the other hand, selected racemic compounds were enantioseparated also on the acyclic analogue ('acyclodextrin') of a specific β-cyclodextrin derivative in GC conditions [Sicoli *et al.*, 2005, 2007]. However, the enantioseparation factors α of compounds separated on the acyclic form were found mostly lower than those separated on their cyclic counterpart. Moreover, there was no study for GC conditions demonstrating the enantioseparations of similar compounds on the acyclic analogue of permethylated β-cyclodextrin studied by Lipkowitz's group. Current literature usually mentions the formation of inclusion complexes [Betzenbichler *et al*., 2022; Cagliero *et al.,* 2015; Scriba, 2016; Uccello-Barreta *et al*., 2010], but is more cautious about explaining the origins and mechanism of enantiorecognition, rather discussing factors enhancing the recognition efficiency or contributing to enantioselective process [Menestrina *et al.,* 2018; Uccello-Barreta *et al*., 2010; Wu *et al*., 2022]. Anyway, even nowadays there are studies considering inclusion interactions as a factor that can play an important role in enantioseparation [Betzenbichler *et al*., 2022]. The need for more explicit clarification of the enantioseparation mechanisms is often mentioned, as this would make it possible to prepare even a more universal enantioselector [Cagliero *et al.,* 2015; Engel, 2020]. Therefore, testing the functionality of chiral selectors by their direct application in the chromatographic analysis of real samples is a significant support in the field of enantioselectivity research. The CP-Chirasil-Dex CB column was chosen for our investigation due to its possible efficiency in separating enantiomers of the investigated enantiomeric pairs, due to the popularity of similar enantioseparating columns in relevant literature [Betzenbichler *et al*., 2022; Cagliero *et al*., 2017; de la Peña Moreno *et al.*, 2010; Schmalzing *et al.*, 1992], as well as because of the results achieved on β-cyclodextrin phases in the analysis of strawberries (Table 1).

The knowledge about enantioselective recognition of synthetic and natural strawberry flavour has been gathered since the 20th century. Some volatiles provide specific distribution of enantiomers in their natural forms in different matrices, as it is obvious from the study by Nitz *et al.* [1991], providing several key findings. The authors assumed that chiral substances with one of the enantiomers significantly predominant in natural form, as they observed in the case of γ-decalactone and γ-dodecalactone, should be suitable for the evaluation of strawberry flavour naturalness, as they differ sufficiently from the racemic enantiomeric ratio (racemate) of their synthetic forms. At the same time, however, it depended on the lactones involved. The study showed almost pure *R*-enantiomer of γ-decalactone and γ-dodecalactone in strawberries and its absolute predominance in strawberry wines. In contrast, Nitz *et al.* [1991] found nearly racemic ratios of γ-hexa- and γ-heptalactone in strawberries and racemic γ-decalactone in deep frozen raspberries. Similarly, Bernreuther *et al*. [1991] noticed nearly racemic ratios for δ-octalactone in strawberries. Nitz *et al*. [1991] also discussed the potential effect of processing, microbial fermentation, and flavouring additives on the enantiomeric ratios, resulting in racemization. The authors [Nitz *et al*., 1991] noted that *R*-enantiomer of γ-decalactone observed in strawberry wines might be present due to an additive of microbiological origin, thus could not be reliably considered as a proof of natural flavour content. The following research extended these conclusions. In the study by Ravid *et al*. [2010], the authors focused closer on γ-decalactone in strawberries and strawberry products and similarly concluded that (*R*)-(+)-γ-decalactone was typical for the natural flavour (the enantiomeric purity ranged between 90 and 100% in 11 varieties of strawberries), for the synthetic flavour the enantiomeric ratio was equivalent to or close to the racemate. The authors highlighted the headspace-solid phase microextraction (HS-SPME) technique as the procedure without racemization. In turn, Kreck *et al*. [2001] explored various strawberry varieties and strawberry products to evaluate the influence of strawberry processing on enantiomeric composition of investigated volatiles. The results provided pure enantiomers for (*S*)-methyl 2-methylbutanoate, (*S*)-ethyl 2-methylbutanoate, (*R*)-γ-octalactone, (*R*)-α-ionone, (*R*)-γ-decalactone and (*R*)-γ-dodecalactone in strawberry flavour of natural origin, no racemization or creation of artefacts during sample processing was documented. Enantiomeric ratios close to the racemates were revealed in synthetic flavour. The authors explained that synthetic compounds are often racemic due to their nonselective chemical synthesis.

This present study focuses on eight chiral substances. Simultaneously, to the best of our knowledge, it is the first study focusing in detail on authentication of strawberry flavour in syrups and applying the CP-chirasil-Dex CB chiral column for strawberry flavour authentication. It is also the first study which compares enantiomeric ratios in 6 strawberry cultivars, 9 strawberry flavourings, and 14 strawberry syrups together in one research to evaluate functionality of the investigated chiral volatiles for authentication of strawberry flavour in complex matrices with variable composition. Analysis of a rather wide range of chiral volatiles, large number and unique selection of samples and the easily achievable technique of HS-SPME GC-MS providing no racemization [Ravid *et al*., 2010] in combination with the CP-chirasil-Dex CB chiral column are expected to enable more reliable authentication of strawberry flavour and extend the possibilities to recognize synthetic or natural strawberry flavour in strawberry syrups and strawberry products.

MATERIALS AND METHODS

Samples

Strawberry cultivars of Viva (S1), Dart Select (S2), Korona (S3), Evie 2 (S4), Malvina (S5), and Elsanta (S6) were purchased in the Czech Republic in local Prague markets; 7 strawberry flavourings (A to F, where B, C, F were natural, see Table S1 – supplementary materials) were obtained from Darmstadt, Germany; and 14 syrups with strawberry flavour (1–14, syrup 1 and 3 with natural strawberry flavour, see Table S2 – supplementary materials) were bought in the Czech Republic in Prague shops. Strawberries were homogenized by T18 basic ULTRA-TURAX (IKA® group, Staufen, Germany) and stored for 6 months in a freezer at –24°C. Flavouring samples were kept in originally closed packages and stored at 4°C in a fridge, while syrups were kept at room temperature of 20°C.

Chemicals

Butyl acetate (≥98%), ethyl butyrate (≥98%), hexanal (98%), (*E*)-hex-2-enal (≥95%), hexyl acetate (99%), 3-methylbutyl acetate (≥97%), (–)-linalool (95%) and (+)-γ-decalactone (≥97%) were provided in analytical quality; the mixture of alkane standards C8-C20 (40 mg/L, in *n*-hexane) was of analytical standard grade. The substances were purchased from Sigma Aldrich (St. Louis, Missouri, USA), subsidiary company of Merck KGaA (Darmstadt, Germany). Sodium chloride (p.a.) was obtained from Penta (Prague, Czech Republic). Helium (purity 99.998%) was supplied by Linde Gas (Prague, Czech Republic).

Sample preparation and isolation of volatiles

Preparation procedure and the main isolation steps (as well as chromatographic conditions described later) were inspired by Schipilliti *et al*. [2011] and adjusted to our conditions of measurements. Approximately 2 g of each homogenized defrosted strawberry sample as well as 2 g of each syrup sample were separately placed into vials (10 mL glass vial, Supelco, Bellefonte, Pensylvania, USA) with 2 mL of saturated NaCl solution. Two microlitres of each flavouring were mixed with 100 mL of NaCl solution (mixture of 20 g of NaCl and 100 mL of distilled water), and 4 mL were placed into a vial. The mixture of butyl acetate, ethyl butyrate, hexanal, (*E*)-hex-2-enal, hexyl acetate, 3-methylbutyl acetate, linalool, γ-decalactone served as a quality control sample. One microliter of each substance was transferred by 1 μL microsyringe (Hamilton, Giarmata, Romania) into the same vessel containing 1 L of distilled water. The mixture was ultrasonicated for 30 s, 10 times diluted with distilled water, the final concentrations of substances were approximately in the range of 0.08–0.1 mg/L. Four millilitres were placed into a vial with 1.5 g of NaCl. The mixture was always measured no later than 2–3 days after its preparation. In the case of alkane standards, 5 μL of the mixture were analysed immediately after being placed into vials, blanks were prepared as 4 mL of distilled water. All vials with the analysed solutions were sealed with 1.3 mm thick PTFE/silicone septum and 18 mm thread magnetic stainless steel screw cap (Supelco). HS-SPME extraction of volatiles was performed with 50/30 μm divinylbenzene/carboxen/polydimethylsiloxane fibre (Supelco) and Autosampler Combi Pall (Agilent Technologies, Santa Clara, CA, USA). Samples were incubated for extraction for 15 min at 50°C. Afterwards, the fibre was held for 15 min at the temperature of 50°C in the head space. Samples were exposed to agitation (8 Hz) during both procedures, incubation as well as extraction.

Analysis of volatiles

The gas chromatograph System 7890A coupled to an inert mass selective detector with a triple-axis detector 5975C (Agilent Technologies) was used. Enantiomeric separation was enabled by the CP-Chirasil-Dex CB chiral column (β-cyclodextrin directly bonded to dimethylpolysiloxane) of 25 m × 250 μm × 0.25 μm (Agilent Technologies) using helium as the carrier gas at a flow rate of 0.82 mL/min. Volatile compounds were thermally desorbed for 2 min at the temperature of 220°C in the GC injector port. The sample was injected in a split mode at the split ratio of 1:1. The GC oven initial temperature of 50°C was held for 2 min and subsequently increased up to 200°C with a ramp rate of 2°C/min. The complete analysis took 79 min. The mass spectrometer was operating in the scan range (*m*/*z*) between 40 and 550 amu, temperature of the ion source of 230°C and temperature of quadrupole of 150°C. Identification of volatile compounds was performed by comparing their mass spectra with Mass Spectral Library NIST 11 (National Institute of Standards and Technology, Gaithersburg, MD, USA) included in GC-MS data analysis software MSD ChemStation (version G1701EA E.02.02.1431, Agilent Technologies). The order of identified volatiles, their retention time (t_R) and linear retention indices (LRIs, calculation based on H. van den Dool and D. J. Kratz equation [Zellner *et al*., 2008] using retention time of selected alkane standards and eluted substances) were compared with literature data (Table 1). Calculation of the chiral resolution (R_S) was based on the equation (1).

$$R_S = [(t_{R2} - t_{R1})]/[(W_1 + W_2)/2] \quad (1)$$

where: t_{R1} and t_{R2} are retention times of enantiomers 1 and 2 and W_1 and W_2 baseline widths of chromatographic peaks of enantiomers 1 and 2.

The (enantio)separation factor α has been calculated according to the equation (2).

$$\alpha = k_2/k_1 \qquad (2)$$

where: $k_1 = (t_{R1} - t_{R0})/t_{R0}$, $k_2 = (t_{R2} - t_{R0})/t_{R0}$ and t_{R0} is the dead time.

Enantiomeric ratios (E ratio) were expressed based on peak areas of enantiomers (*R* and *S*) as:

$$E_{ratio} = [R/(R + S) \times 100] / \{100 - [R/(R + S) \times 100]\} \qquad (3)$$

or

$$E_{ratio} = [S/(S + R) \times 100] / \{100 - [S/(S + R) \times 100]\} \qquad (4)$$

Two equivalent aliquots of each sample of strawberry cultivar, flavouring and syrup were analysed. Reliability was evaluated as part of the verification of the method as relative standard deviation (RSD) from at least 2 determinations of the total area of the quality control sample during 1 series of measurements (1.5–12.5% within all monitored series). Repeatability was calculated for the γ-decalactone enantiomers as RSD from two equivalent aliquots for all samples, in 64% of cases it was 0–6% (in strawberries in 89% of cases), in 28% it was 7–11%, and in 8% of cases (in flavours A, D, G) it was up to 15%.

RESULTS AND DISCUSSION

The condition for authentication of strawberry flavour was based on two main suppositions. The first one, the efficiency of the chiral column, was met. As can be seen in Figure 1, the enantiomers were well distinguishable thanks to the CP-Chirasil-Dex CB stationary phase. 2-Methylbutanoic acid, linalool, α-ionone, γ-decalactone and γ-undecalactone achieved chiral resolution in the baseline level (except for γ-decalactone, all of them in all samples with their paired enantiomers). The best resolution of enantiomers was obtained for α-ionone (R_S>4), their least differentiation for methyl 2-methylbutanoate. Elution order of these volatiles was in agreement with their elution order on chiral columns in studies by Williams *et al.* [2005] and Ravid *et al.* [2010] with LRIs values very close to those reported in literature (see t_R and LRIs in Table 1 and Table 2). The second supposition – selection of volatiles having enantiomeric composition in natural strawberry flavour different from the composition in its synthetic form – achieved gratifying results. An absolute predominance of one enantiomeric form was characteristic for all positively detected investigated volatiles in our strawberries (Table 2; the results were comparable to those found for strawberries, reported for each substance mostly in only one or two studies so far, as can be seen in Table 1). Moreover, such predominance was observed even on our flavourings of natural origin subjected to processing during production, while the near-racemates in flavourings with the expected synthetic origin were obtained (Table 3). It was an important finding supporting reliable application of these volatiles for authentication of strawberry flavour in syrups. Thanks to the fulfilled suppositions, it was possible to focus on the authentication of strawberry flavour in syrups. The exception for linalool in strawberries reported in one study [de la Peña Moreno *et al.*, 2010] and shown in Table 1 was supposed to be due to processing to strawberry extract, as the racemization during specific processing conditions was noticed for this substance [Bernreuther & Schreier, 1991; Marchelli *et al.*, 1996] and created one more incentive to test this substance in our samples and conditions.

As can be seen in Table 2, Table 3, and Table 4, the tested samples of strawberries and flavourings were clearly poorer in volatile contents than syrup samples. Ethyl 2-methylbutanoate was missing in strawberries, methyl 2-methylbutanoate and 2-methylbutanoic acid in strawberry flavourings, α-ionone, γ-undecalactone, δ-dodecalactone in both. Single peak predominance of ethyl-2-methylbutanoate and α-ionone in strawberries was considered based on the study by Kreck *et al.* [2001], which is – to the best of our knowledge – the only source providing it in pure strawberries (Table 1). The deficit of the substances could lie in the selection of cultivars. The absolute predominance of one of the paired enantiomers required for natural flavour as a condition enabling distinguishing the synthetic flavour [Nitz *et al.*, 1991], was found in the case of methyl 2-methylbutanoate, 2-methylbutanoic acid and linalool (also called β-linalool) in strawberries in which they were detected, and in the case of γ-decalactone even in all strawberries. Moreover, the condition was fulfilled also for linalool, ethyl 2-methylbutanoate and γ-decalactone in the samples of strawberry flavourings declared as natural. Pure *R*-peak of γ-decalactone was again present in all of them (Table 3, samples B, C, F), the effect of processing steps on its enantiomeric ratio in the natural form was not noticeable at all. It already highlighted the great ability of γ-decalactone to indicate the natural strawberry flavour. Slight differences from 100% one-peak predominance observed for linalool in strawberries S4, S5, and S6; and for γ-decalactone in S3, S4, and S6 could be caused by cultivar selection, for ethyl 2-methylbutanoate in naturally declared strawberry flavourings C and F also by processing, the complication described for several other chiral substances in literature [Nitz *et al.*, 1991; Ravid *et al.*, 2010]. Unfortunately, there is a lack of comparable findings in literature to suppose other reasons for negligible racemization (up to 5%) of ethyl 2-methylbutanoate in flavourings or to consider the presence of its *R*-enantiomer due to the material of different natural origin (up to 5% allowed by legislation [Guidance Document, 2019]). The reason for linalool's enantiomeric reverse order (*S*>>*R* with *S* eluted first) in strawberry cultivars S1 and S2 (Table 2) and in naturally declared strawberry flavourings B and F (Table 3), contrary to the order reported in literature (*S*>>*R*, *R* eluted first, Table 1), could be similar to the one discussed in studies by Cagliero *et al.* [2017] and Mosandl *et al.* [1990]. Cagliero *et al.* [2017] mentioned that changes of elution order of enantiomers from members of homologous series on the same column could be related to the strength of interactions between enantiomer and cyclodextrin stationary phase; therefore, it was unreliable to correlate the absolute configuration (*R* or *S*) with the elution order. Moreover, Mosandl *et al.* [1990] demonstrated changes in the elution order

TABLE 2. Enantiomeric ratios and characterization of selected chiral volatiles in strawberries (S1–S6)

Elution order	Compound	E order		t_R (min)	LRI (calc.)	α	Peak area (×10³, Abundance×second)**					
							S1	S2	S3	S4	S5	S6
1	Methyl 2-methylbutanoate	1.	*R*	7.0	821	1.03	nd	nd	nd	nd	nd	nd
		2.	*S*	7.1–7.5	823–833		1542	nd	nd	580	163	nd
				E ratio			0/100	na	na	0/100	0/100	na
2	Ethyl 2-methybutanoate	1.		8.7–9.4	860–877	1.03	nd	nd	nd	nd	nd	nd
		2.		8.9–9.6	865–881		nd	nd	nd	nd	nd	nd
				E ratio			na	na	na	na	na	na
3	2-Methylbutanoic acid	1.	*S*	28.6–29	1198–1205	1.02	nd	nd	nd	255	42	1122
		2.	*R*	29.2–29.4	1208–1212		nd	nd	nd	nd	nd	nd
				E ratio			na	na	na	100/0	100/0	100/0
4	(β)-Linalool	1.	*S, R*	31.1–31.2	1241–1242	1.00	1419	2815	nd	459	710	540
		2.	*S*	31.3–31.4	1244–1246		nd	nd	nd	10542	12060	5720
				E ratio			100/0	100/0	na	4/96	6/94	9/91
5	(*E*)-α-Ionone	1.		42.8–42.9	1450–1452	1.02	nd	nd	nd	nd	nd	nd
		2.		43.8	1469		nd	nd	nd	nd	nd	nd
				E ratio			na	na	na	na	na	na
6	γ-Decalactone	1.	*R*	49.9–50.6	1589–1604	1.01	438	26741	16806	5571	626	8013
		2.	*S*	50.3–50.7	1597–1606		nd	nd	188	43	nd	78
				E ratio			100/0	100/0	99/1	99/1	100/0	99/1
7	γ-Undecalactone	1.		55.0–55.1	1696–1698	1.00	nd	nd	nd	nd	nd	nd
		2.		55.3	1702		nd	nd	nd	nd	nd	nd
				E ratio			na	na	na	na	na	na
8	δ-Dodecalactone	1.		60.7–60.8	1822–1824	1.00	nd	nd	nd	nd	nd	nd
		2.		60.9	1826		nd	nd	nd	nd	nd	nd
				E ratio			na	na	na	na	na	na

nd – not detected; na – not available; Elution order – elution order of the substances monitored in our study; E order – enantiomeric order – elution order of enantiomers *R* and *S* obtained by comparison of their percentage proportions in literature (column E comparison, Table 1) with their peak areas in tested samples; t_R – retention time of the enantiomers in strawberries, flavourins, syrups; LRI (calc.) – calculated linear retention index, calculation is based on H. van den Dool and D. J. Kratz equation [Zellner *et al*., 2008]; α – calculated separation factor; E ratio – enantiomeric ratio – percentage ratio of the peak areas of the substance's enantiomers *R* and *S* (for the calculation equation see the section Materials and Methods); **Results of enantiomers (source data from GS-MS chromatogram) represent the measured peak areas integrated by RTE integrator of the software used.

TABLE 3. Enantiomeric ratios and characterization of selected chiral volatiles in strawberry flavourings (A–G)

Elution order	Compound	E order		Peak area (×10^3, Abundance×second)**						
				A	B	C	D	E	F	G
1	Methyl 2-methylbutanoate	1		nd	nd	nd	nd	nd	nd	nd
		2		nd	nd	nd	nd	nd	nd	nd
		E ratio		na	na	na	na	na	na	na
2	Ethyl 2-methylbutanoate	1	*R*	13923	0	185	14638	5067	11686	9089
		2	*S*	21405	4572	3194	28128	9612	215517	20390
		E ratio		39/61	0/100	5/95	*34/66*	*35/65*	5/95	*31/69*
3	2-Methylbutanoic acid	1		nd	nd	nd	nd	nd	nd	nd
		2		nd	nd	nd	nd	nd	nd	nd
		E ratio		na	na	na	na	na	na	na
4	(β)-Linalool	1	*S*	nd.	155	nd	nd	nd	569	nd
		2	*R*	nd	nd	nd	nd	nd	nd	nd
		E ratio		na	100/0	na	na	na	100/0	na
5	(E)-α-Ionone	1		nd	nd	nd	nd	nd	nd	nd
		2		nd	nd	nd	nd	nd	nd	nd
		E ratio		na	na	na	na	na	na	na
6	γ-Decalactone	1	*R*	1573	548	236	3363	493	761	1319
		2	*S*	888	nd	nd	3182	483	nd	549
		E ratio		64/36	100/0	100/0	51/49	51/49	100/0	71/29
7	γ-Undecalactone	1		nd	nd	nd	nd	nd	nd	nd
		2		nd	nd	nd	nd	nd	nd	nd
		E ratio		na	na	na	na	na	na	na
8	δ-Dodecalactone	1		nd	nd	nd	nd	nd	nd	nd
		2		nd	nd	nd	nd	nd	nd	nd
		E ratio		na	na	na	na	na	na	na

** See the legend below Table 2 for details. Coelutions were noticed for the results in italics.

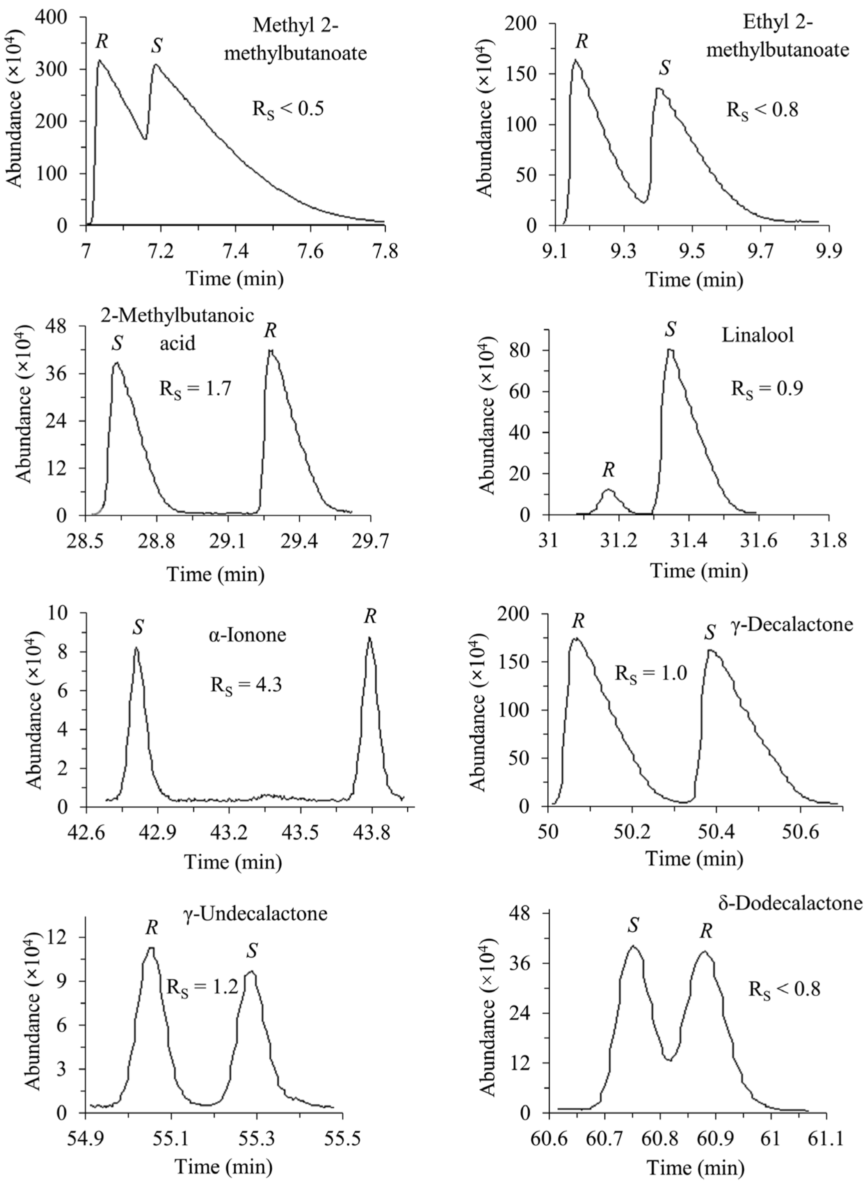

FIGURE 1. The enantiomeric separations on CP-Chirasil-Dex CB in selected syrups (methyl 2-methylbutanoate, ethyl 2-methylbutanoate, 2-methylbutanoic acid, α-ionone, γ-decalactone, γ-undecalactone, δ-dodecalactone) and in strawberry sample (linalool). R_S – chiral resolution.

of enantiomers in homologous series of selected volatiles directly on permethylated β-cyclodextrin phase. Possible influence of processing or addition of acidic additives on the enantiomeric ratios of linalool in strawberry products resulting in enantiomeric size reverse order (*R*>>*S*, *R* eluted first) was also conceivable. Anyhow, regarding literature discussing such influence [Bernreuther & Schreier, 1991; Cagliero *et al*., 2012; Marchelli *et al*., 1996; Nitz *et al*., 1991], including mentions of possible impact of acidic conditions on linalool [Bernreuther & Schreier, 1991; Marchelli *et al*., 1996], or alternatively observing nearly racemic ratios of linalool in strawberry extracts [de la Peňa Moreno *et al*., 2010], the triggered ratio changes did not lead to absolute predominance of opposite enantiomer there; instead racemization or partial racemization is rather discussed. A shift in retention time seemed as an unlikely reason. Although slight shifts in retention times were observed for some substances, in the case of linalool the retention time values of each enantiomer were in a stable range (Table 2). Therefore, both alternatives of *R* and *S* enantiomeric order are considered in Table 2. Nearly racemic ratios of dominant γ-decalactone and ethyl 2-methylbutanoate in the rest of flavourings indicated the presence of synthetic flavours in accordance with our supposition. The coelution of ethyl 3-methylbutanoate with ethyl 2-methylbutanoate in strawberry flavourings of D, E, and G finally did not have any significant impact on the possibility to distinguish between natural and synthetic forms, as the ratios would be indicative of synthetic flavour in both cases, with coverage by ethyl 3-methylbutanoate or without it. Based on visual estimation, exclusion of ethyl 3-methylbutanoate from the second eluted peak could lead to ratios close to the racemates.

By closer focusing on syrups (Table 4), it is evident that the possibility to distinguish between synthetic and natural flavour for investigated chiral volatiles in syrups is more

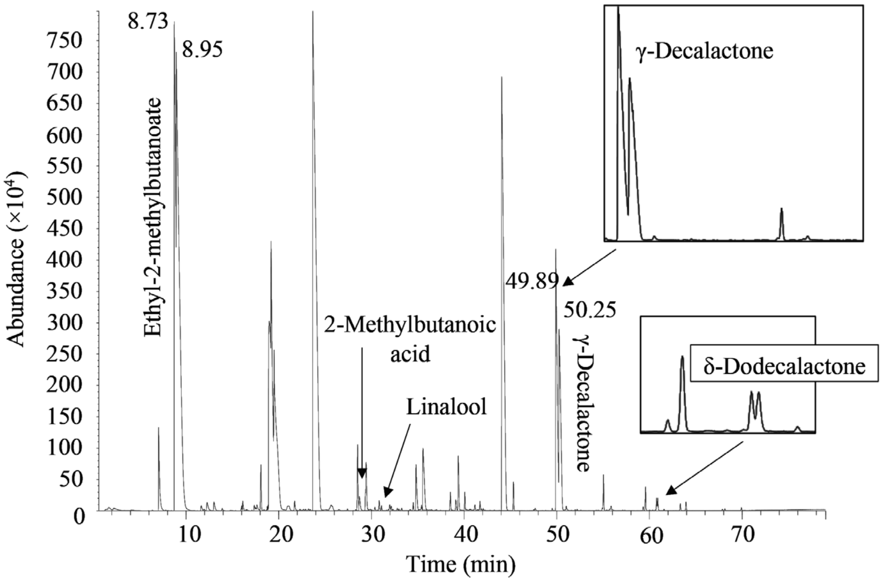

FIGURE 2. Chiral GC-MS spectrum of syrup 1 suspected of adulteration.

evaluable due to their higher presence and overall larger spectrum of results than in the samples of strawberry flavourings and strawberries. Exceptions were observed for methyl 2-methylbutanoate in syrup 9 and 12 and for linalool in syrups 2, 5, 6, 9, and 10. For these samples with strawberry flavour not declared as 100% natural, only their dominant single peaks were recorded. Accordingly, in addition to the declared flavourings or strawberry flavouring indicating possible content of synthetic flavourings, the samples contained strawberry fruit juice, a supposed source of natural strawberry flavour. Therefore, the single peaks of linalool and methyl-2-methylbutanoate could be of natural origin, similar situation as in the peach flavour mixture of synthetic and natural origin in the study by Ravid *et al.* [2010]. For the named samples, these two substances could not be included in the authentication of synthetic flavour. Thus, linalool did not contribute to such authentication in any of the cases. Despite the susceptibility of linalool to racemization under specific processing conditions [Bernreuther & Schreier, 1991; Marchelli *et al.*, 1996], no racemates were observed in our conditions.

More contributive results were obtained for other crucial substances in syrups. Ethyl 2-methylbutanoate was found in syrup 3 as a single enantiomeric peak consistent with the supposition for syrup's natural flavour. No racemization due to processing was observed. According to its label, syrup 1 should contain only strawberry flavouring of natural origin, similarly to syrup 3. However, the enantiomeric ratio (31/69) of ethyl 2-methylbutanoate indicated a very high probability of synthetic flavour addition, even by considering the nearly racemic ratios of other 3 chiral volatiles in this syrup including γ-decalactone (57/43) – see Table 4 and Figure 2, and a range of the enantiomeric ratios of ethyl 2-methylbutanoate in other syrups without natural flavour declaration (Table 4). It could be assumed that ethyl 2-methylbutanoate might be a useful indicator for distinguishing between natural and synthetic flavour. Coelution of *S*-enantiomer in five syrups (Table 4) was similar to those observed in the flavourings with the same insignificant impact as it was described above.

The problematic coelution was noticed for another monitored volatile, namely the 2-methylbutanoic acid. Its second eluted enantiomer coeluting with methyl salicylate (calculated LRI 1213) in syrup samples 1, 2, and 8, with phenylethyl acetate (calculated LRI 1212) in samples 9 and 12 or its first eluted enantiomer with cyclohexasiloxane derivative (calculated LRI 1197) in syrup 4, were responsible for the impossibility to accurately determine its enantiomeric ratio in the named syrups. The ability of the substance to distinguish between natural and synthetic flavour was not judged in the case of flavour deficit (syrup 3, syrup 6 with only one detected enantiomer instead of two expected). In the case of coelution in syrups 1 and 8, substances' near racemates could be estimated after visual recognition of the substances' overlapped areas or from extracted ion chromatograms, whereas only the latter was possible in the case of syrups 2 and 12. For syrups 4 and 9, the estimation was problematic due to the extensive overlap with the enantiomer. In five syrups without observed coelutions, ratios were similar to those of γ-decalactone or ethyl 2-methylbutanoate, confirming potential for synthetic flavour recognition. Enantiomeric reverse order observed among them and among the extracted ion chromatograms of 2-methylbutanoic acid in coeluting samples might have the same reason as the one described for linalool in strawberry flavourings.

In the case of α-ionone, almost exact racemic ratios were observed in syrups 5, 9, 11 and 12 (Table 4). Moreover, results of γ-decalactone and ethyl 2-methylbutanoate in the same syrups as well as the result of δ-dodecalactone in syrup 5 supported the supposition of synthetic flavour origin due to the racemic ratios found. Despite the low content, the enantiomeric separation of α-ionone was perfect (Figure 1).

By closer focus on γ-decalactone in syrups, benefits of this substance for recognition of flavour origin are evident even in this matrix. The substance was again present in all

TABLE 4. Enantiomeric ratios and characterization of selected chiral volatiles in strawberry syrups (1–14)

Elution order	Compound	E order		Peak area ($\times 10^3$, Abundance×second)**													
				1	2	3	4	5	6	7	8	9	10	11	12	13	14
1	Methyl 2-methyl butanoate	1	*R*	nd	nd	nd	25779	nd	nd	nd	nd	nd	nd	20492	nd	nd	nd
		2	*S*	nd	nd	nd	51606	nd	nd	nd	nd	3529	nd	43164	2732	nd	nd
		E ratio		na	na	na	33/67	na	na	na	na	0/100	na	32/68	0/100	na	na
2	Ethyl 2-methylbutanoate	1	*R*	76682	17069	nd	30346	17775	7477	18405	11723	21799	10296	28476	19635	25895	12877
		2	*S*	168455	25417	122	122636	22863	8555	46036	20885	47454	11725	48487	42222	80916	15237
		E ratio		31/69	40/60	0/100	20/80	44/56	47/53	*29/71*	*36/64*	*31/69*	47/53	37/63	*32/68*	*24/76*	46/54
3	2-Methylbutanoic acid	1	*S, R*	1935	585	nd	14366	1316	59	850	1376	1147	2884	4145	1281	1097	206
		2	*R, S*	5434	988	nd	8404	1765	nd	1149	3356	2597	3351	5318	2558	898	594
		E ratio		*26/74*	*37/63*	na	*63/37*	43/57	100/0	43/57	*29/71*	*31/69*	46/54	44/56	*33/67*	55/45	26/74
4	(β)-Linalool	1	*S*	806	106	nd	nd	277	128	nd	nd	474	165	nd	nd	nd	nd
		2	*R*	nd	nd	nd	nd	nd	nd	nd	nd	nd	nd	nd	nd	nd	nd
		E ratio		100/0	100/0	na	na	100/0	100/0	na	na	100/0	100/0	na	na	na	na
5	(*E*)-α-Ionone	1	*S, R*	nd	nd	nd	nd	381	nd	nd	nd	96	nd	176	119	nd	nd
		2	*R, S*	nd	nd	nd	nd	415	nd	nd	nd	104	nd	175	126	nd	nd
		E ratio		na	na	na	na	48/52	na	na	na	48/52	na	50/50	49/51	na	na
6	γ-Decalactone	1	*R*	46393	24578	1003	40184	21575	10944	16493	15991	29372	12693	6096	25569	14431	14344
		2	*S*	35524	21053	nd	17137	15568	7722	15514	15226	22950	9951	5406	25200	14383	11858
		E ratio		57/43	54/46	100/0	70/30	58/42	59/41	52/48	51/49	56/44	56/44	53/47	50/50	50/50	55/45
7	γ-Undecalactone	1	*R*	nd	nj	nd	nd	nd	nd	nd	859	1700	nj	nd	1794	559	nd
		2	*S*	nd	387	nd	nd	nd	nd	nd	650	1506	367	nd	1676	507	nd
		E ratio		na	100/0	na	na	na	na	na	57/43	53/47	100/0	na	52/48	52/48	na
8	δ-Dodecalactone	1	*S*	871	46	nd	nd	1664	296	126	226	nd	nd	nd	nd	nd	nd
		2	*R*	944	57	nd	nd	1883	323	134	259	nd	nd	nd	nd	nd	nd
		E ratio		48/52	45/55	na	na	47/53	48/52	48/52	47/53	na	na	na	na	na	na

** See the legend below Table 2 for other details. Coelutions were noticed for the results in italics; nj – not judgeable due to coelution.

the samples tested (Table 4). Regarding pure *R*-enantiomer found in syrup 3 declared with only natural strawberry flavouring, the absolute predominance of *R*-enantiomer in our (Table 2) and previously analysed strawberries (Table 1), as well as in strawberry flavourings of natural origin (Table 3), processing steps did not seem to affect the enantiomeric ratio of γ-decalactone in its natural form, not even in the case of syrups. However, other factors, as *R*-enantiomer of unwanted microbial origin [Hidalgo *et al*., 2013; Nitz *et al*., 1991; Rong *et al*., 2017; Silva *et al*., 2021; Vandamme & Soetaert, 2002], might be considered as a possibility of uncertainty. Nearly racemic enantiomeric ratios in the samples were comparable with the ratios of other investigated substances, namely the ethyl 2-methylbutanoate, α-ionone, γ-undecalactone, δ-dodecalactone, evaluable ratios of 2-methylbutanoic acid and two ratios of methyl 2-methylbutanoate (Table 4). Findings of nearly racemic ratios of γ-decalactone in syrups containing flavour of supposedly synthetic origin were similar to those of flavourings of synthetic origin (Table 3) and they are comparable with results of γ-decalactone in synthetic strawberry flavour of other previously analysed commercial products [Kreck *et al*., 2001; Ravid *et al*., 2010; Schipilliti *et al.,* 2011]. These findings document its unified character in strawberry flavour. With regards to all results and conclusions, γ-decalactone seemed to be the most reliable indicator of synthetic and natural strawberry flavour. Nevertheless, the uncertainty had to be taken into consideration.

Nearly racemic ratios strengthening the supposition of synthetic flavourings in syrups 8, 9, 12, and 13 were observed also for γ-undecalactone (Table 4). The single enantiomer in syrups 2 and 10 was supposed to be found due to full coverage of the first enantiomer by larger peak of coeluting nonadecane. Absence of γ-undecalactone in syrup 3 assumed to contain only natural flavour was in this case in accordance with our expectations. With the exception of Bernreuther *et al*. [1989], who demonstrated traces of γ-undecalactone in strawberries, the presence of this volatile in natural strawberry flavour was not discussed in other literature works dealing with strawberry flavour authentication (probably due to the awareness of the volatile's absence), while in the same works the substance's racemates were related to synthetic flavours of other fruits [Cagliero *et al*., 2012; Ravid *et al*., 2010]. Our observations could be explained as a potential of this volatile to distinguish between synthetic and natural strawberry flavour. Nonetheless, more literature sources dedicated to γ-undecalactone enantiomers in natural strawberry flavour exposed to various processing techniques in different matrices could help clarify this issue more.

The last substance of interest was represented by δ-dodecalactone. Enantiomeric pairs with ratios close to the racemate were found in 6 samples including syrup 1 that was declared as natural (Table 4). Regarding enantiomeric ratio of δ-dodecalactone in the processed strawberry extract (*S*(-)30.1%/*R*(+)69.1%) [Bernreuther *et al*., 1991] and concentrated strawberry water phase (*S*(-)33%/*R*(+)67% – *S*(-)36%/*R*(+)64%) [Krammer *et al.*, 2006] known from literature as well as any information recorded for the tested syrup 3, expected to contain natural flavouring in accordance with information on the label, there was too little information to consider the enantiomeric ratio in the natural form. Anyhow, the near-racemates of the substance in our other syrup samples and consistency with observations for dominant γ-decalactone and ethyl-2-methyl butanoate, including syrup 1 declared with strawberry flavour of natural origin, were obvious (Table 4). Considering the whole complex of our results on the investigated volatiles, the accusation of adulteration was made in case of syrup 1.

Regarding the issue of coelutions, it is recommended to implement a second GC column, if possible [Gomes da Silva *et al*., 2008]. Anyway, the contained strawberry flavour is often a complicated mixture of compounds with variable composition, therefore the coelution in individual cases can be observed in any conditions. Also in this regard, authentication based on the evaluation of a large number of functional chiral volatiles is crucial.

CONCLUSIONS

The implemented CP-Chirasil-Dex CB chiral column simultaneously with adjusted measurement conditions enabled determining enantiomeric ratios of the monitored chiral volatiles in the studied strawberries, strawberry flavourings, and syrups; and evaluating the strawberry flavour authenticity with contribution of seven chiral volatiles. Especially due to γ-decalactone and ethyl 2-methylbutanoate, supported by observations on 2-methylbutanoic acid and γ-dodecalactone, it was possible to make accusation of adulteration concerning one syrup sample. In the case of γ-decalactone, results were available for all tested samples and in all cases indicated natural or synthetic form in accordance with the corresponding enantiomeric ratios. Ethyl 2-methylbutanoate was similarly contributive, detected in all syrups and flavourings. Racemates of α-ionone and γ-undecalactone from positively detected samples supported the observed results as well as 2-methylbutanoic acid in the case of evaluable values. Methyl-2-methylbutanoate contributed to the evaluation in two cases. The results found for strawberries, natural flavourings, and one natural syrup gave evidence that there was no or negligible racemization during processing in strawberry flavour, which is an important condition for reliable authentication. However, for the practical purposes, it is recommended to evaluate the strawberry flavour authenticity in syrups on the basis of the enantiomeric ratios obtained for a rather wide range of chiral volatiles considered for each syrup individually. The CP-Chirasil-Dex CB column was efficient in enantiomeric separations (five of the eight volatiles investigated achieved baseline resolution, while the resolution value was even greater than 4 for α-ionone) and represents an easily accessible technique together with the method described above.

RESEARCH FUNDING

This research was supported from Specific university research – grant No A1_FPBT_2021_004.

CONFLICT OF INTEREST

Authors declare no conflicts of interest.

ORCID IDs

H. Čížková https://orcid.org/0000-0001-9666-7261
A. Grégrová https://orcid.org/0000-0002-5397-6985
V. Kružík https://orcid.org/0000-0002-8213-1738
K. Průchová https://orcid.org/0000-0002-6608-5866

SUPPLEMENTARY MATERIAL

Supplementary data related to this article can be found at http://journal.pan.olsztyn.pl/Enantioselective-HS-SPME-GC-MS-for-Authentication-of-Natural-and-Synthetic-Strawberry,152237,0,2.html. Strawberry flavourings and syrups used in the study. Composition of chiral stationary phases.

REFERENCES

1. Bernreuther, A., Bank, J., Krammer, G., Schreier, P. (1991). Multidimensional gas chromatography/mass spectrometry: A powerful tool for the direct chiral evaluation of aroma compounds in plant tissues I. 5-alkanolides in fruits. *Phytochemical Analysis, 2*(1), 43–47. https://doi.org/10.1002/pca.2800020109
2. Bernreuther, A., Christoph, N., Schreier, P. (1989). Determination of the enantiomeric composition of γ-lactones in complex natural matrices using multidimensional capillary gas chromatography. *Journal of Chromatography A, 481*, 363–367. https://doi.org/10.1016/S0021-9673(01)96780-9
3. Bernreuther, A., Schreier, P. (1991). Multidimensional gas chromatography/mass spectrometry: A powerful tool for the direct chiral evaluation of aroma compounds in plant tissues. II. Linalool in essential oils and fruits. *Phytochemical Analysis, 2*(4), 167–170. https://doi.org/10.1002/pca.2800020405
4. Betzenbichler, G., Huber L., Kräh, S., Morkos, M.-L.K., Siegle, A.F., Trapp, O. (2022). Chiral stationary phases and applications in gas chromatography. *Chirality*, *34*(5), 732–759. https://doi.org/10.1002/chir.23427
5. Cagliero, C., Bicchi, C., Cordero, C., Rubiolo, P., Sgorbini, B., Liberto, E. (2012). Fast headspace-enantioselective GC–mass spectrometric-multivariate statistical method for routine authentication of flavoured fruit foods. *Food Chemistry*, *132*(2), 1071–1079. https://doi.org/10.1016/j.foodchem.2011.10.106
6. Cagliero, C., Sgorbini, B., Cordero, C., Liberto, E., Rubiolo, P., Bicchi, C. (2015). Cyclodextrin derivatives as stationary phases for the GC separation of enantiomers in the flavor and fragrance field. In: K.H. Engel, G. Takeoka (Eds.), *Importance of Chirality to Flavor Compounds, American Chemical Society*, Chapter 2, *ACS Symposium Series, 1212*, 15–34. https://doi.org/10.1021/bk-2015-1212.ch002
7. Cagliero, C., Sgorbini, B., Cordero, C., Liberto, E., Rubiolo, P., Bicchi, C. (2017). Enantioselective gas chromatography with cyclodextrin in odorant analysis. In: A. Buettner (Ed.), *Springer Handbook of Odor*, Springer, Cham, Switzerland, pp. 409–438. https://doi.org/10.1007/978-3-319-26932-0_19
8. da Silva Rivas, A.C., Lopes, P.M., de Azevedo Barros, M.M., Costa Machado, D.C., Alviano, C.S., Alviano, D.S. (2012). Biological activities of α-pinene and β-pinene enantiomers. *Molecules*, *17*(6), 6305–6316. https://doi.org/10.3390/molecules17066305
9. de la Peňa Moreno, F., Blanch, G.P., Flores, G., del Castillo, M.L.R. (2010). Development of a method based on on-line reversed phase liquid chromatography and gas chromatography coupled by means of an adsorption–desorption interface for the analysis of selected chiral volatile compounds in methyl jasmonate treated strawberries. *Journal of Chromatography A, 1217*(7), 1083–1088. https://doi.org/10.1016/j.chroma.2009.10.037
10. Easson, L.H., Stedman, E. (1933). Studies on the relationship between chemical constitution and physiological action: Molecular dissymmetry and physiological activity. *Biochemical Journal*, *27*(4), 1257–1266. https://doi.org/10.1042/bj0271257
11. Engel, K.H. (2020). Chirality: An important phenomenon regarding biosynthesis, perception, and authenticity of flavor compounds. *Journal of Agricultural and Food Chemistry*, *68*(38), 10265–10274. https://doi.org/10.1021/acs.jafc.0c01512
12. Fanali, Ch., D'Orazio, G., Gentili, A., Fanali, S. (2019). Analysis of enantiomers in products of food interest. *Molecules*, *24*(6), art. no. 1119. https://doi.org/10.3390/molecules24061119
13. Gomes da Silva, M.D.R., Cardeal, Z., Marriott, P.J. (2008). Comprehensive two-dimensional gas chromatography: Application to aroma and essential oil analysis. In: H. Tamura, S.E. Ebeler, K.K. Gary, R. Takeoka (Eds.). *Food Flavour*, American Chemical Society, Washington, DC, pp. 3–24. https://doi.org/10.1021/bk-2008-0988.ch001
14. Guidance Document on EC Regulation on Flavourings (2019). *European Flavour Association.* Brussels, Belgium [accessed: 14 February 2022]. https://cdn2.assets-servd.host/aggressive-shelduck/production/Documents/Guidance/effa-guidance-document-on-the-ec-regulation-on-flavourings-updated-july-2019.pdf
15. Hidalgo, C., Torija, M., Mas, A., Mateo, E. (2013). Effect of inoculation on strawberry fermentation and acetification processes using native strains of yeast and acetic acid bacteria. *Food Microbiology*, *34*(1), 88–94. https://doi.org/10.1016/j.fm.2012.11.019
16. Krammer, G.E., Weckerle, B., Brennecke, S., Weber, B., Kindel, G., Ley, J., Hilmer, J.M., Reinders, G., Stöckigt, D., Hammerschmidt, F.J., Ott, F., Gatfield, I., Schmidt, C.O., Bertram, H.J. (2006). Product-oriented flavor research: Learnings from the past, visions for the future. *Molecular Nutrition & Food Research*, *50*(4–5), 345–350. https://doi.org/10.1002/mnfr.200500204
17. Kreck, M., Scharrer, A., Bilke, S., Mosandl, A. (2001). Stir bar sorptive extraction (SBSE)-enantio-MDGC-MS–a rapid method for the enantioselective analysis of chiral flavour compounds in strawberries. *European Food Research and Technology*, *213*(4), 389–394. https://doi.org/10.1007/s002170100397
18. Lipkowitz, K.B., Coner, B., Peterson, M.A., Morreale, A. (1997a). Enantioselective binding in gas chromatography: A computational study of chiral selection bypermethyl-β-cyclodextrin. *Journal of Physical Organic Chemistry, 10*(5), 311–322. https://doi.org/10.1002/(SICI)1099-1395(199705)10:5<311::AID-POC871>3.0.CO;2-P
19. Lipkowitz, K.B., Coner, R., Peterson, M., Morreale, A., Shackelford, J. (1998). The principle of maximum chiral discrimination:

chiral recognition in permethyl-β-cyclodextrin. *Journal of Organic Chemistry, 63*(3), 732–745.
https://doi.org/10.1021/jo9717090

20. Lipkowitz, K.B., Pearl, G., Coner, B., Peterson, M.A. (1997b). Explanation of where and how enantioselective binding takes place on permethylated β-cyclodextrin, a chiral stationary phase used in gas chromatography. *Journal of the American Chemical Society*, *119*(3), 600–610.
https://doi.org/10.1021/ja963076x
21. Marchelli, R., Dossena, A., Palla, G. (1996). The potential of enantioselective analysis as a quality control tool. *Trends in Food Science & Technology, 7*(4), 113–119.
https://doi.org/10.1016/0924-2244(96)10011-X
22. Menestrina, F., Ronco, N.R., Romero L.M., Castells, C.B. (2018). Enantioseparation of polar pesticides on chiral capillary columns based on permethyl-β-cyclodextrin in matrices of different polarities. *Microchemical Journal*, *140*, 52–59.
https://doi.org/10.1016/j.microc.2018.03.037
23. Mosandl, A., Hener, U., Hagenauer-Hener, U., Kustermann, A. (1989). Direct enantiomer separation of chiral γ-lactones from food and beverages by multidimensional gas chromatography. *Journal of High Resolution Chromatography, 12*(8), 532–536.
https://doi.org/10.1002/jhrc.1240120807
24. Mosandl, A., Rettinger, K., Fischer, K., Schubert, V., Schmarr, H.G., Maas, B. (1990). Stereoisometric flavor compounds XLI: New applications of permathylated β-cyclodextrin phasse in chiral CGC analysis. *Journal of High Resolution Chromatography*, *13*(5), 382–385.
https://doi.org/10.1002/jhrc.1240130522
25. Nitz, S., Kollmannsberger, H., Weinreich, B., Drawert, F. (1991). Enantiomeric distribution and 13C/12C isotope ratio determination of γ-lactones: appropriate methods for the difterentiation between natural and non-natural flavours? *Journal of Chromatography A*, *557*, 187–197.
https://doi.org/10.1016/S0021-9673(01)87132-6
26. Ravid, U., Elkabetz, M., Zamir, C., Cohen, K., Larkov, O., Aly, R. (2010). Authenticity assessment of natural fruit flavour compounds in foods and beverages by auto-HS–SPME stereoselective GC–MS. *Flavour and Fragrance Journal, 25*(1), 20–27.
https://doi.org/10.1002/ffj.1953
27. Rong, S., Yang, S., Li, Q., Cai, B., Guan, S., Wang, J., Zhou, Y., Chen, Y. (2017). Improvement of γ-decalactone production by stimulating the import of ricinoleic acid and suppressing the degradation of γ-decalactone in *Saccharomyces cerevisiae*. *Biocatalysis and Biotransformation, 35*(2), 96–102.
https://doi.org/10.1080/10242422.2017.1289182
28. Schipilliti, L., Dugo, P., Bonaccorsi, I., Mondello, L. (2011). Headspace-solid phase microextraction coupled to gas chromatography–combustion-isotope ratio mass spectrometer and to enantioselective gas chromatography for strawberry flavoured food quality control. *Journal of Chromatography A, 1218*(42), 7481–7486.
https://doi.org/10.1016/j.chroma.2011.07.072
29. Schmalzing, D., Jung, M., Mayer, S., Rickert, J., Schurig, V. (1992). Extending the scope of enantiomer separations on Chirasil-Dex by GLC: Comparison with permethylated β-cyclodextrin dissolved in OV-1701. *Journal of High Resolution Chromatography, 15*(11), 723–729.
https://doi.org/10.1002/jhrc.1240151106
30. Scriba, G.K. (2016). Chiral recognition in separation science – an update. *Journal of Chromatography A*, *1467*, 56–78.
https://doi.org/10.1016/j.chroma.2016.05.061
31. Servais, A.C., Rousseau, A., Dive, G., Frederich, M., Crommen, J., Fillet, M. (2012). Combination of capillary electrophoresis, molecular modelling and nuclear magnetic resonance to study the interaction mechanisms between single-isomer anionic cyclodextrin derivatives and basic drug enantiomers in a methanolic background electrolyte. *Journal of Chromatography A*, *1232*, 59–64.
https://doi.org/10.1016/j.chroma.2011.10.010
32. Sicoli, G., Jiang, Z., Jicsinsky, L., Schurig, V. (2005). Modified linear dextrins (“acyclodextrins”) as new chiral selectors for the gas-chromatographic separation of enantiomers. *Angewandte Chemie International Edition*, *44*(26), 4092–4095.
https://doi.org/10.1002/anie.200500509
33. Sicoli, G., Pertici, F., Jiang, Z., Jicsinszky, L., Schurig, V. (2007). Gas-chromatographic approach to probe the absence of molecular inclusion in enantioseparations by carbohydrates. Investigation of linear dextrins (“acyclodextrins”) as novel chiral stationary phases. *Chirality: The Pharmacological, Biological, and Chemical Consequences of Molecular Asymmetry*, *19*(5), 391–400.
https://doi.org/10.1002/chir.20383
34. Silva, R., Coelho, E., Aguiar, T.Q., Domingues, L. (2021). Microbial biosynthesis of lactones: Gaps and opportunities towards sustainable production. *Applied Sciences, 11*(18), art. no. 8500.
https://doi.org/10.3390/app11188500
35. Uccello-Barretta, G., Vanni, L., Balzano, F. (2010). Nuclear magnetic resonance approaches to the rationalization of chromatographic enantiorecognition processes. *Journal of Chromatography A*, *1217*(7), 928–940.
https://doi.org/10.1016/j.chroma.2009.10.070
36. Vandamme, E.J., Soetaert, W. (2002). Bioflavours and fragrances via fermentation and biocatalysis. *Journal of Chemical Technology & Biotechnology: International Research in Process, Environmental & Clean Technology*, *77*(12), 1323–1332.
https://doi.org/10.1002/jctb.722
37. Werkhoff, P., Brennecke, S., Bretschneider, W., Güntert, M., Hopp, R., Surburg, H. (1993). Chirospecific analysis in essential oil, fragrance and flavor research. *Zeitschrift für Lebensmittel-Untersuchung und Forschung*, *196*(4), 307–328.
https://doi.org/10.1007/BF01197930
38. Williams, A., Ryan, D., Guasca, A.O., Marriott, P., Pang, E. (2005). Analysis of strawberry volatiles using comprehensive two-dimensional gas chromatography with headspace solid--phase microextraction. *Journal of Chromatography B, 817*(1), 97–107.
https://doi.org/10.1016/j.jchromb.2004.05.021
39. Wu, D., Ma, C., Fan, G.C., Pan, F., Tao, Y., Kong, Y. (2022). Recent advances of the ionic chiral selectors for chiral resolution by chromatography, spectroscopy and electrochemistry. *Journal of Separation Science*, *45*(1), 325–337.
https://doi.org/10.1002/jssc.202100334
40. Zellner, B., Bicchi, C., Dugo, P., Rubiolo, P., Dugo, G., Mondello, L. (2008). Linear retention indices in gas chromatographic analysis: a review. *Flavour and Fragrance Journal, 23*(5), 297–314.
https://doi.org/10.1002/ffj.1887

Pol. J. Food Nutr. Sci., 2022, Vol. 72, No. 3, pp. 319–321
http://journal.pan.olsztyn.pl

Instruction for Authors
Section: Editorial News

INSTRUCTIONS FOR AUTHORS

SUBMISSION. Original contributions relevant to food and nutrition sciences are accepted on the understanding that the material has not been, nor is being, considered for publication elsewhere. **All papers should be submitted and will be processed electronically via Editorial Manager system (available from PJFNS web site: http://journal.pan.olsztyn.pl). On submission, a corresponding author will be asked to provide: Cover letter; Files with Manuscripts, Tables, Figures/Photos; and Names of two potential reviewers (one from the author's homeland – but outside author's Institution, and the other from abroad).** All papers which have been qualified as relevant with the scope of our Journal are reviewed. All contributions, except the invited reviews are charged. Proofs will be sent to the corresponding author or to the first author and should be returned within one week since receipt. No new material may be inserted in the text at proof stage. It is the author's duty to proofread proofs for errors.

Authors should very carefully consider the preparation of papers to ensure that they communicate efficiently, because it permits the reader to gain the greatest return for the time invested in reading. Thus, we are more likely to accept those that are carefully designed and conform the instruction. Otherwise, papers will be rejected and removed from the on-line submission system.

SCOPE. The Polish Journal of Food and Nutrition Sciences publishes original, basic and applied papers, and reviews on fundamental and applied food research, preferably these based on a research hypothesis, in the following Sections:

Food Technology:
- Innovative technology of food development including biotechnological and microbiological aspects
- Effects of processing on food composition and nutritional value

Food Chemistry:
- Bioactive constituents of foods
- Chemistry relating to major and minor components of food
- Analytical methods

Food Quality and Functionality:
- Sensory methodologies
- Functional properties of food
- Food physics
- Quality, storage and safety of food

Nutritional Research Section:
- Nutritional studies relating to major and minor components of food (excluding works related to questionnaire surveys)

"News" section:
- Announcements of congresses
- Miscellanea

OUT OF THE SCOPE OF THE JOURNAL ARE:
- Works which do not have a substantial impact on food and nutrition sciences
- Works which are of only local significance i.e. concern indigenous foods, without wider applicability or exceptional nutritional or health related properties
- Works which comprise merely data collections, based on the use of routine analytical or bacteriological methods (i.e. standard methods, determination of mineral content or proximate analysis)
- Works concerning biological activities of foods but do not provide the chemical characteristics of compounds responsible for these properties
- Nutritional questionnaire surveys
- Works related to the characteristics of foods purchased at local markets
- Works related to food law
- Works emphasizing effects of farming / agricultural conditions / weather conditions on the quality of food constituents
- Works which address plants for non-food uses (i.e. plants exhibiting therapeutic and/or medicinal effects)

TYPES OF CONTRIBUTIONS. *Reviews:* (at least: 30 pages and 70 references) these are critical and conclusive accounts on trends in food and nutrition sciences; *Original papers:* (maximally: 30 pages and 40 references) these are reports of substantial research; *Reports on post and forthcoming scientific events, and letters to the Editor* (all up to three pages) are also invited (free of charge).

REVIEW PROCESS. All scientific contributions will be peer-reviewed on the criteria of originality and quality. Submitted manuscripts will be pre-evaluated by Editor-in-Chief and Statistical Editor (except for review articles), and when meeting PJFNS' scope and formal requirements, they will be sent to a section Editor who upon positive pre-evaluation will assign at least two reviewers from Advisory Board Members, reviewers suggested by the author or other experts in the field. Based on the reviews achieved, Section Editor and Editor-in-Chief will make a decision on whether a manuscript will be accepted for publication, sent back to the corresponding author for revision, or rejected. Once a manuscript is sent back to the corresponding author for revision, all points of the reviews should be answered or rebuttal should be provided in the Explanation letter. The revised manuscripts will be checked by Section Editor and by the original reviewers (if necessary), and a final decision will be made on acceptance or rejection by both Section Editor and Editor-in-Chief.

Polish Journal of Food and Nutrition Sciences uses CrossCheck's iThenticate software to detect instances of similarity in submitted manuscripts. In publishing only original research, PJFNS is committed to deterring plagiarism, including self-plagiarism. Your manuscript may be screened for similarity to published materials.

COPYRIGHT LICENSE AGREEMENT referring to Authorship Responsibility and Acknowledgement, Conflict of Interest and Financial Disclosure, Copyright Transfer, are required for all authors, i.e. *Authorship Responsibility and Acknowledgement*: Everyone who has made substantial intellectual contributions to the study on which the article is based (for example, to the research question, design, analysis, interpretation, and written description) should be an author. It is dishonest to omit mention of someone who has participated in writing the manuscript ("ghost authorship") and unfair to omit investigator who have had important engagement with other aspects of the work. All contributors who do not meet the criteria for authorship should be listed in an Acknowledgments section. Examples of those who might be acknowledged include a person who provided purely technical help, writing assistance, or a department chairperson who provided only general support. Any financial and material support should also be acknowledged. *Conflict of Interest and Financial Disclosure*: Authors are responsible for disclosing financial support from the industry or other conflicts of interest that might bias the interpretation of results. *Copyright License Agreement*: Authors agree that papers accepted become the copyright of the Institute of Animal Reproduction and Food Research of the Polish Academy of Sciences in Olsztyn, Poland, and may not be published elsewhere without the Editor's permission in writing.

A manuscript will not be published once the signed form has not been submitted to the Editor with the manuscript revised after positive reviews.

ETHICAL APPROVAL OF STUDIES AND INFORMED CONSENT. For all manuscripts reporting data from studies involving human participants or animals, formal approval by an appropriate institutional review board or ethics committee is required and should be described in the Methods section. For those investigators who do not have formal ethics review committees, the principles outlined in the Declaration of Helsinki should be followed. For investigations of humans, state in the Methods section the manner in which informed consent was obtained from the study participants (i.e., oral or written). Editors may request that authors provide documentation of the formal review and recommendation from the institutional review board or ethics committee responsible for oversight of the study.

UNAUTHORIZED USE AND COPYRIGHT AGREEMENT. Published manuscripts become the property of the Institute of Animal Reproduction and Food Research of the Polish Academy of Sciences (IAR&FR PAS) and may not be published elsewhere without written permission. Unauthorized use of the PJFNS name, logo, or any content for commercial purposes or to promote commercial goods and services (in any format, including print, video, audio, and digital) is not permitted by IAR&FR PAS.

MANUSCRIPTS. A manuscript in English must be single-sided, preferably in Times New Roman (12) with 1.5-point spacing, without numbers of lines. The Editor reserves the right to make literary corrections and to make suggestions to improve brevity. English is the official language. The English version of the paper will be checked by Language Editor. Unclear and unintelligible version will be sent to the author(s) for correction.

Every paper should be divided under the following headings in this order: a **Title** (possibly below 150 spaces), **Running title** (up to 50 spaces, submitted under the Title); the Names(s) of the author(s) in full. In paper with more than one author, the asterisk indicates the name of the author to whom correspondence and inquiries should be addressed, otherwise the first author is considered for the correspondence. Current full postal address of the indicated corresponding author or the first author must be given in a footnote on the title page; the Place(s) where the work was done including the institution name, city, country if not Poland. In papers originated from several institutions the names of the authors should be marked with respective superscripts; the **Key words** (up to 6 words or phrases) for the main topics of the paper; an **Abstract** (up to 250 words for regular papers and reviews and 100 words for Short Reports) summarizing briefly main results of the paper, no literature references; an **Introduction** giving essential background by saying why the research is important, how it relates to previous works and stating clearly the objectives at the end; **Materials and Methods** with sufficient experimental details permitting to repeat or extend the experiments. Literature references to the methods, sources of material, company names and location (city, country) for specific instruments must be given. Describe how the data were evaluated, including selection criteria used; **Results and Discussion** presented together (in one chapter). Results should be presented concisely and organized to supplement, but not repeat, data in tables and figures. Do not display the data in both tabular and graphic form. Use narrative form to present the data for which tables or figures are unnecessary. Discussion should cover the implications and consequences, not merely recapitulating the results, and it must be accomplished with concise **Conclusions**; **Acknowledgements** should be made to persons who do not fill the authorship criteria (see: Authorship forms); **Research funding** should include financial and material support; and **References** as shown below.

REFERENCES each must be listed alphabetically at the end of the paper (each should have an Arabic number in the list) in the form as follows: **Periodicals** – names and initials of all the authors, year of publication, title of the paper, journal title as in Chemical Abstracts, year of publication, volume, issue, inclusive page numbers; **Books** – names and initials of all the authors, names of editors, chapter title, year of publication, publishing company, place of publication, inclusive page numbers; **Patents** – the name of the application, the title, the country, patent number or application number, the year of publication.

For papers published in language other than English, manuscript title should be provided in English, whereas a note on the original language and English abstract should be given in parentheses at the end.

The reference list should only include peer-reviewed full-text works that have been published or accepted for publication. Citations of MSc/PhD theses and works unavailable to international Editors, Reviewers, and Readers should be limited as much as possible.

References in the text must be cited by name and year in square parentheses (e.g.: one author – [Tokarz, 1994]; two authors – [Słonimski & Campbell, 1987]; more than two authors – [Amarowicz *et al*., 1994]). If more than one paper is published in the same year by the same author or group of authors use [Tokarz, 1994a, b]. Unpublished work must only be cited where necessary and only in the text by giving the person's name.

Examples:

Article in a journal:

Słonimski, B.A., Campbell, L.D., Batista, E., Howard B. (2008). Gas chromatographic determination of indole glucosinolates. *Journal of Science and Food Agriculture*, *40*(5), 131–143.

Book:

Weber, W., Ashton, L., Milton, C. (2012). *Antioxidants – Friends or Foes?* 2nd editition. PBD Publishing, Birmingham, UK. pp. 218–223.

Chapter in a book:

Uden, C., Gambino, A., Lamar, K. (2016). Gas chromatography. In M. Queresi, W. Bolton (Eds.), *CRC Handbook of Chromatography*, CRC Press Inc., Boca Raton, Florida, USA, pp. 44–46.

ABBREVIATIONS AND UNITS. Abbreviations should only be used when long or unwieldy names occur frequently, and never in the title; they should be given at the first mention of the name. Metric SI units should be used. The capital letter L should be used for liters. Avoid the use of percentages (% g/g,% w/w; Mol-%; vol-%), ppm, ppb. Instead, the expression such as g/kg, g/L, mg/kg, mg/mL should be used. A space must be left between a number and a symbol (e.g. 50 mL not 50mL). A small x must be used as multiplication sign between numeric values (e.g. 5×10^2 g/mL). Statistics and measurements should be given in figures, except when the number begins a sentence. Chemical formulae and solutions must specify the form used. Chemical abbreviations, unless they are internationally known, Greek symbols and unusual symbols for the first time should be defined by name. Common species names should be followed by the Latin at the first mention, with contracting it to a single letter or word for subsequent use.

FIGURES should be submitted in separate files. Each must have an Arabic number and a caption. Captions of all Figures should be provided on a separate page "Figure Captions". Figures should be comprehensible without reference to the text. Self-explanatory legend to all figures should be provided under the heading "Legends to figures"; all abbreviations appearing on figures should be explained in figure footnotes. Three-dimensional graphs should only be used to illustrate real 3-D relationships. Start the scale of axes and bars or columns at zero, do not interrupt them or omit missing data on them. Figures must be cited in Arabic numbers in the text.

TABLES should be submitted in separate files. They should be as few in number and as simple as possible (like figures, they are expensive and space consuming), and include only essential data with appropriate statistical values. Each must have an Arabic number and a caption. Captions of all Tables should be provided on a separate page "Table Captions". Tables should be self-explanatory; all abbreviations appearing in tables should be explained in table footnotes. Tables must be cited in Arabic numbers in the text.

PAGE CHARGES. A standard publication fee has been established at the rate of 450 EUR + tax (if applicable) irrespective of the number of pages and tables/figures. For Polish Authors an equivalent fee was set at 1950 PLN + VAT. Payment instructions will be sent to Authors via e-mail with acceptance letter.

Information on publishing and subscription is available from:

Ms. Joanna Molga
Editorial Office of Pol. J. Food Nutr. Sci.
Institute of Animal Reproduction and Food Research
Tuwima 10 Str., 10–748 Olsztyn 5, Poland
phone (48 89) 523–46–70, fax (48 89) 523–46–70;
e-mail: pjfns@pan.olsztyn.pl; http://journal.pan.olsztyn.pl

Nutrition